Modeling and Production of Bioethanol from Mixtures of Cotton Gin Waste and Recycled Paper Sludge

Jiacheng Shen

Dissertation submitted to the faculty of the Virginia Polytechnic Institute and State University in partial fulfillment of the requirements for the degree of Doctor of Philosophy in Biological System Engineering

Committee Chair Dr. Foster Aryi Agblevor
Dr. Chenming Zhang
Dr. Zhiyou Wen
Dr. Richard Helm
Dr. William Barbeau

Dec. 19, 2008
Blacksburg, Virginia

Keywords: Cotton gin waste; Recycled paper sludge; Cellulose; Ethanol; Enzymatic hydrolysis; Simultaneous saccharification and fermentation; Kinetic model; Operating mode; Deactivation; Profit rate; Diffusivity.

Modeling and Production of Bioethanol from Mixtures of Cotton Gin Waste and Recycled Paper Sludge

Jiacheng Shen

(ABSTRACT)

In this study, the hydrolytic kinetics of mixtures of cotton gin waste (CGW) and recycled paper sludge (RPS) at various initial enzyme concentrations of Spezyme AO3117 and Novozymes NS50052 was investigated. The experiments showed that the concentrations of reducing sugars and the conversions of the mixtures increased with increasing initial enzyme concentration. The reducing sugar concentration and conversion of the mixture of 75wt% CGW and 25wt% RPS were higher than those of the mixture of 80% CGW and 20% RPS. The conversion of the former could reach 73.8% after a 72-hour hydrolysis at the initial enzyme loading of 17.4 Filter Paper Unit (FPU)/g substrate. A three-parameter kinetic model with convergent property based on enzyme deactivation and its analytical expression were derived. Using nonlinear regression, the parameters of the model were determined from the experimental data of hydrolytic kinetics of the mixtures. Based on this kinetic model of hydrolysis, two profit rate models, representing two kinds of operating modes with and without substrate recycling, were developed. Using the profit rate models, the optimal enzyme loading and hydrolytic time could be predicted for the maximum profit rate in ethanol production according to the costs of enzyme and operation, enzyme loading, and ethanol market price. Simulated results from the models based on the experimental data of hydrolysis of the mixture of 75% CGW and 25% RPS showed that use of a high substrate concentration and an operating mode with feedstock recycling could greatly increase the profit rate of ethanol production. The results also demonstrated that the hydrolysis at a low enzyme loading was economically

required for systematic optimization of ethanol production. The development of profit rate model points out a way to optimize a monotonic function with variables, such as enzyme loading and hydrolytic time for the maximum profit rate.

The study also investigated the ethanol production from the steam-exploded mixture of 75% CGW and 25% RPS at various influencing factors, such as enzyme concentration, substrate concentration, and severity factor, by a novel operating mode: semi-simultaneous saccharification and fermentation (SSSF) consisting of a pre-hydrolysis and a simultaneous saccharification and fermentation (SSF). Four cases were studied: 24-hour pre-hydrolysis + 48-hour SSF (SSSF 24), 12-hour pre-hydrolysis + 60-hour SSF (SSSF 12), 72-hour SSF, and 48-hour hydrolysis + 12-hour fermentation (SHF). SSSF 24 produced higher ethanol concentration, yield, and productivity than the other operating modes. The higher temperature of steam explosion favored ethanol production, but the higher initial enzyme concentration could not increase the final ethanol concentration though the hydrolytic rate of the substrate was increased. A mathematical model of SSSF, which consisted of an enzymatic hydrolysis model and a SSF model including four ordinary differential equations that describe the changes of cellobiose, glucose, yeast, and ethanol concentrations with respect to residence time, was developed, and was used to simulate the data for the four components in the SSSF processes of ethanol production from the mixture. The model parameters were determined by a MATLAB program based on the batch experimental data of the SSSF. The analysis to the reaction rates of cellobiose, glucose, cell, and ethanol using the model and the parameters from the experiments showed that the conversion of cellulose to cellobiose was a rate-controlling step in the SSSF process of ethanol production from cellulose.

Contents

List of Figures

List of Tables

Nomenclature

Symbols

A acetic acid concentration (g/l)

A_{ave} an average dimensionless activity of the enzyme at hydrolytic time t

a dimensionless activity of enzyme

a_1 constant in Eq. (4.15) (l/g)

a_2 constant in Eq. (4.15) (dimensionless)

B cellobiose concentration (g/l)

B_1 cellobiose concentration entering the fermenter R_2 (g/l)

b constant in Eq. (4.15) (dimensionless $b = \frac{k_2^{'}}{K_e k_3^{'}}$)

$b^{'}$ constant in Eq. (3.18) (g/l)

C cellulose concentration in the insoluble substrate (g/l)

C_c carbohydrate concentration (g/l)

Ce^* effective complex concentration (g/l)

Ce_{in}^* ineffective complex concentration (g/l)

Ce_{ein}^* ineffective complex formed by the enzymes and substrate (g/l)

C_s reducing sugar concentration in the filtrate by DNS method (g/l)

C_0 initial cellulose concentration (g/l)

C_1 cellulose concentration in the feed (g/l) or entering the fermenter R_2 (g/l)

c_e enzyme cost in a sugar production process ($/g enzyme)

c_g sugar market price in unit sugar weight ($/g sugars)

$c_{f,}$ cost of feedstock per treated unit weight of substrate ($/g substrate)

c_f cost of feedstock based on liter ethanol ($/l ethanol)

$c_{h,}$ cost of hydrolysis per treated unit weight of substrate ($/g substrate)

c_h cost of hydrolysis based on liter ethanol ($/l ethanol)

c_p cost of operation including feedstock handling, pretreatment, and steam production per treated unit weight of substrate ($/g substrate)

$c_p^{'}$ cost of operation including feedstock handling, pretreatment, and steam production based on liter ethanol ($/l ethanol)

$c_{s,}$ market price of a unit of sugar ($/g sugars)

$c_s^{'}$ market price of sugar based on liter ethanol ($/l ethanol)

D dilution rate (= F/V h^{-1}) or apparent diffusivity of enzyme in insoluble substrate in Eq. (3.30) (m^2/h)

e free enzyme concentration (g/l)

e_d enzyme loading based on the dried substrate (FPU/g)

e_e endo-β-1,4-glucanase and exo-β-1,4-cellobiohydrolase concentration (g/l)

e_0 initial enzyme concentration (g/l)

e_1 enzyme concentration entering the fermenter R_2 (g/l)

F feed rate (l/h)

f proportionality constant in Eq. (5.12)

G reducing sugar or glucose concentration (g/l)

G_r glucan fraction in raw biomass (dimensionless)

G_1 glucose concentration entering the fermenter R_2 (g/l)

K half-saturation constant (g/l)

K_e equilibrium constant (g/l)
K_G glucose saturation constant for the microbial growth (g/l)
K_{1B} inhibitory constant of cellobiose to the endo-β-1,4-glucanase and exo-β-1,4-cellobiohydrolase (g/l)
K_{1G} inhibitory constant of glucose to the endo-β-1,4-glucanase and exo-β-1,4-cellobiohydrolase (g/l)
K_{2G} inhibitory constant of glucose to the glycosidase (g/l)
$K_{e,ave}$ average value of K_e in Eq. (21) (g/l)
k_1, specific rate constant of cellulose hydrolysis to cellobiose (l(g.h))
k_1" forward reaction rate constant during adsorption (l(g.h))
k_1"' variable associated with enzyme deactivation (h^{-1})
k_{-1}' backward reaction rate constant during desorption (h^{-1})
k_2, specific rate constant of cellobiose hydrolysis to glucose (h^{-1})
k_2' rate constant of product formation (h^{-1}).
k_3 specific rate constant of enzyme deactivation (l/(g.h))
$k_{3,ave}$ average value of k_2 in Eq. (21) (/h)
k_3' constant (= $k_3 f$) in Eq. (5.13)
k_4, product formation coefficient associated with cell growth (= k_4'$Y_{G/E}$ dimensionless)
k_4,, product formation coefficient associated with cell growth (dimensionless)
k_4' product formation coefficient associated with cell growth (=$k_4/Y_{X/G}$ dimensionless)
k_5 coefficient of growth associated with glycerol formation (dimensionless)
k_6 coefficient of growth associated with acetic acid formation (dimensionless)
k_7 coefficients of growth associated with lactic acid formation (dimensionless)
L lactic acid concentration (g/l)
log(R_0) severity factor
M initial quantity of insoluble substrate in the suspension (g)
m maintenance coefficient for endogenous metabolism of the microorganisms (h^{-1}) or total number of initial enzyme concentration
m_b sample weight of the autoclaved suspension in ASTM E1721-95
m_c contents of the carbohydrate in the mixtures (wt%)
n total number of experimental points for an initial enzyme concentrations
P product (sugar) concentration (g/l)
p_s ratio of profit rate and sugar production cost for recycle (/h)
p_{sn} ratio of profit rate and sugar production cost for no-recycle (/h)
p_r, profit per unit reactor volume for the sugar production ($/l hydrolytic volume)
p_r' profit rate with substrate recycle ($/l hydrolytic volume and time)
p_{rn} profit rate without substrate recycle ($/l hydrolytic volume and time)
p_s market price of sugar ($/l hydrolytic volume)
q uptake of enzyme at time t (g/g)
q_∞ uptake of enzyme at equilibrium (g/g)
R_0 reaction ordinate (dimensionless)
R_1 conversion factor from substrate to ethanol (l ethanol/g substrate)
R_2 inverse fraction of cellulose in biomass (g substrate/g cellulose)
R_3 fraction of sugar market price in ethanol market price
r constant of average conversion factor from cellulose and hemicellulose to sugars (g cellulose/g sugars) or radius of fiber (m)

r_A rate of change of acetic acid concentration (g/(l.h))
r_E rate of change of ethanol concentration (g/(l.h))
r_G actual rate of substrate conversion by enzyme or rate of change of glucose concentration (g/(l.h))
r_{Gl} rate of change of glycerol concentration (g/(l.h))
r_{G0} rate of substrate conversion without enzyme inhibition (g/(l.h))
r_L rate of change of lactic acid concentration (g/(l.h))
r_X rate of change of cell concentration (g/(l.h))
r_1 rate of change of cellulose concentration to cellobiose (g/(l.h))
r_2 rate of change of cellobiose concentration to glucose (g/(l.h))
s_{pc} sugar production cost per unit reactor volume ($/l hydrolytic volume)
T_b base temperature (100^{o}C)
T_r explosion temperature (^{o}C)
t residence time (h) or residence time (minutes)
t_s residence time in steam explosion (minute)
t_0 time of the pre-hydrolysis phase (h)
V liquid volume in reactor or actual culture volume in Eq. (5.40) (l)
V_m maximum hydrolytic rate (g/(l.h))
V_2 liquid volume in fermenter R_2 (l)
v hydrolytic rate in Eq. (3.26) (g/(l.h)) or volume of liquid (liter)
v_f final volume of the filtrate after pH adjustment (l)
v_i initial volume of the filtrate before pH adjustment (l)
W substrate mass in the culture in Eq. (7.2) (g).
w weight determined by variance in Eq. (4.17)
w_{gd} glucan concentration in the liquid fraction (g/l)
w_{glw} glucan concentration in the wet steam-exploded mixture (g/l)
w_i i composition content in dried mixture in Eq. (7.1)
w_{il} i composition content of liquid fraction held by the dried mixture in Eq. (7.1)
w_{it} ratio of i composition content in the wet steam-exploded mixture to the content of dry mixture in Eq. (7.1)
w_{xd} xylan concentration in the liquid fraction (g/l)
w_{xlw} xylan concentration in the wet steam-exploded mixture (g/l)
X cell concentration (g/l)
X_0 initial cell concentration (g/l)
x experimental conversion in Eq. (4.17)
x_c predicted conversion in Eq.(4.20)
Y yield in Eq. (7.2) (g ethanol/g dried substrate)
$Y_{G/E}$ conversion factor of ethanol from glucose
Y_{th} theoretical yield (g/g)
$Y_{X/E}$ yield coefficient of cell from ethanol
$Y_{X/G}$ yield coefficient of cell mass on the glucose (g/g)

Greek Symbols

α ratio of the mass of the free enzyme in the suspension to the mass of the adsorbed enzyme on the insoluble substrate under equilibrium conditions
μ specific cell growth rate constant (h^{-1})

μ_c constant calculated from Monod model at initial glucose concentration in Eq. (6.40)
μ_m maximum specific cell growth rate constant (h^{-1})

Subscripts

i index number of initial enzyme concentration in Eq. (4.20)
j index number of the experimental points in Eq. (4.20)
m total number of initial enzyme concentration in Eq. (4.20)
n total number of experimental points for an initial enzyme concentration subscripts Eq. (4.20)
op optimal condition

Dissertation Organization

This dissertation includes nine chapters. Chapter one introduces raw materials and basic processes of bioethanol production, and the project objectives. Chapter two reviews bioethanol production from cotton gin waste (CGW) and recycled paper sludge (RPS), and hydrolysis and fermentation models. Chapters three to seven are the main parts of the dissertation, including kinetics of enzymatic hydrolysis of cotton gin waste (Chapter 3), optimization of enzyme loading and hydrolytic time (Chapter 4), development of simultaneous saccharification and fermentation (SSF) model (chapter 5), operating mode development of semi-simultaneous saccharification and fermentation (SSSF) (Chapter 6), and application of SSSF to bioethanol production from CGW and RPS. These fives chapters have individual objectives, experimental methods, results, and conclusions. Chapter eight is the dissertation summary. The last chapter (Chapter nine) proposes a project for further work.

Acknowledgments

I would like to express my sincere gratitude to Dr. Foster A. Agblevor, for his support, guidance, and financial assistance throughout this project. I also would like to express my gratitude to my other committee members: Drs. Chenming Zhang, Zhiyou Wen, Richard Helm, and William Barbeau for their support and advice.

My sincere thanks to bioprocess laboratory specialist Ms. Amy Egan and computer systems engineer Mr. Denton Yoder of Biological Engineering Department for their technical assistance during the experiments.

Finally, I acknowledge the National Science Foundation (NSF) under contract No. 0420577 and Xethanol Inc. for providing financial support for this project.

Publications

Published and Submitted Refereed Journal Articles

1. Jiacheng Shen and Foster A. Agblevor. Optimization of enzyme loading and hydrolytic time in the hydrolysis of the mixtures of cotton gin waste and recycled paper sludge for the maximum profit rate. Biochemical Engineering Journal. 41: 241-250 2008.

2. Jiacheng Shen and Foster A. Agblevor. Kinetics of enzymatic hydrolysis of steam exploded cotton gin waste. Chemical Engineering Communications. 195:9: 1107-1121, 2008.

3. Jiacheng Shen and Foster A. Agblevor. The operable modeling of simultaneous saccharification and fermentation of ethanol production from cellulose. Submitted to Applied Biochemistry and Biotechnology.

4. Jiacheng Shen and Foster A. Agblevor. Modeling semi-simultaneous saccharification and fermentation of ethanol production from cellulose. Submitted to Biomass & Bioenergy.

5. Jiacheng Shen and Foster A. Agblevor. Ethanol production from the mixture of cotton gin west and recycled paper sludge using semi-simultaneous saccharification and fermentation. Submitted to Applied Biochemistry and Biotechnology.

Refereed Conference Article

1. Jiacheng Shen and Foster A. Agblevor. Ethanol production from the mixture of cotton gin west and recycled paper sludge by simultaneous saccharification and fermentation. National beltwide cotton conference, Nashville, TN, Jan. 9-11, 2008.

Conference Oral and Poster Presentations

1. Jiacheng Shen and Foster A. Agblevor. Effect of microbial inoculation time in hydrolysis and fermentation on ethanol production from mixture of cotton gin waste and recycled paper sludge. Accepted by ASABE annual meeting, Reno, Nevada, June 21-24, 2009.

2. Jiacheng Shen and Foster A. Agblevor. Effect of pre-hydrolysis prior to simultaneous saccharification and fermentation on ethanol production from cellulose. ASABE annual meeting, Providence, Rhode Island, June 29-July 2, 2008.

3. Jiacheng Shen and Foster A. Agblevor. Simulation of simultaneous saccharification and fermentation of ethanol production from cellulose by an operable model. Spring National AIChE Meeting, New Orleans, LA. April 6-10, 2008.

4. Jiacheng Shen and Foster A. Agblevor. Ethanol production from the mixture of cotton gin west and recycled paper sludge by simultaneous saccharification and fermentation. National beltwide cotton conference, Nashville, TN, Jan. 9-11, 2008.

5. Jiacheng Shen and Foster A. Agblevor. A two-parameter model of hydrolysis of insoluble substrate based on deactivation of enzyme and its application for hydrolysis of cotton gin waste. ASABE annual meeting, Minneapolis, MN. June 17-20, 2007.

6. Jiacheng Shen and Foster A. Agblevor. The hydrolytic kinetics of the mixtures of cotton gin waste and recycled paper sludge. ASABE annual meeting, Minneapolis, MN. June 17-20, 2007.

Chapter One

Introduction

Currently, bioethanol production from lignocellulosic materials has been given attention because of the potential depletion of the world's petroleum resources. Ethanol can be used in automobiles as a fuel additive at 10%, which can decrease emission of carbon monoxide, and greenhouse gases. Ethanol can also replace methyl tertiary butyl ether (MTBE), an additive of gasoline, which is potentially toxic to human health. Furthermore, ethanol produced from lignocellulosic material is a domestic and renewable energy source, which will reduce our petroleum imports.

Ethanol is colorless clear liquid. It has molecular formula of CH_3CH_2OH, and its structure is shown in Fig. 1.1. The physical properties of ethanol are listed in Table 1.1.

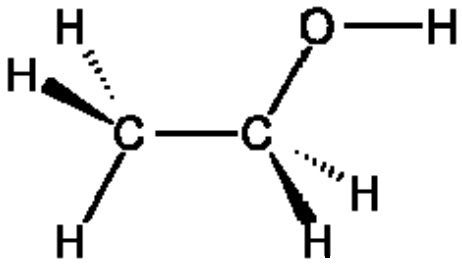

Fig. 1.1 Ethanol structure [http://en.wikipedia.org/wiki/Ethanol]

Table 1.1 Physical properties of ethanol [http://en.wikipedia.org/wiki/Ethanol]

Property	MW g/mol	Melting point	Boiling point	Density	Viscosity 20°C
Value	46.07	−114.3 °C	78.4 °C	0.789 g/cm^3	1.2 cP
Property	Dipole moment	Miscible activity (pK_a)	Solubility in water	Appearance	
Value	1.69 D (gas)	15.9	Full	Colorless	

Generally, three kinds of carbohydrate materials: sucrose, starch, and cellulose can be used for ethanol production. Sucrose is chemically termed α-glucose-1,2-β-fructose (Fig. 1.2), commonly used for human consumption as a sweetener. Most sucrose comes from sugar cane and sugar beet containing 20% sucrose by weight, about 74% water, 5% cellulose, and 1% inorganic salts. The sucrose substrate for fermentation can be obtained mechanically by crushing sugar cane or stripping and pulping the sugar beet. The sucrose is a particularly favorable substrate for the production of ethanol by yeast fermentation. Yeast produces the enzyme invertase in both the cytoplasm and a secreted form, and this enzyme hydrolyzes sucrose to glucose and fructose, which are then fermented by the yeast cells to form ethanol. This process is often called the Brazilian approach. Natural *Saccharomyces cerevisiae* and related yeasts can take up and metabolize many sugars, including glucose, fructose, galactose, mannose, maltose (glucose-α-1,4-glucose), and maltotriose. However, natural yeast cannot utilize pentose.

Starch is mainly comprised of amylose and amylopectin. Amylose consists of long, unbranched chains of D-glucose units connected by (α1-4) linkages (Fig. 1.3). Such chains vary in molecular weight from a few thousand to 500,000. Amylopectin has a high molecular weight (up to 1 million), but is highly branched (Fig. 1.4). The glycosidic linkages joining successive glucose residues in amylopectin main chains are (α1-4), but the branch points, occurring in every 24 to 30 residues, connected with the main chains are (α1-6) linkages. Most starch used in the United State is from cornstarch, a major feedstock for the production of fuel ethanol. Corn starch consists of 20 wt% water-soluble amylose fraction and a 80 wt% water-insoluble higher-molecular-weight amylopectin fraction. To obtain corn starch, dry corn is

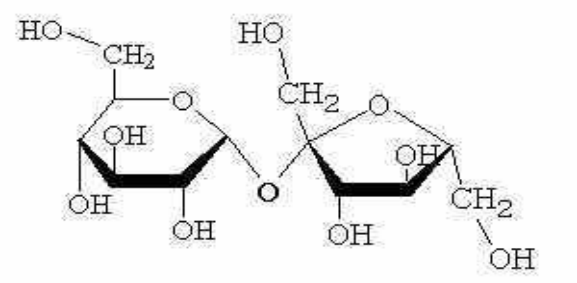

Fig. 1.2 Sucrose structure [http://en.wikipedia.org/wiki/Sucrose]

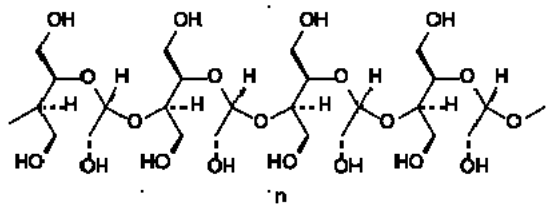

Fig. 1.3 Amylose structure [http://en.wikipedia.org/wiki/Amylose]

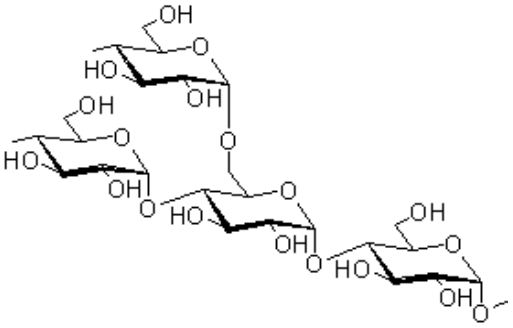

Fig. 1.4 Amylopectin structure [http://en.wikipedia.org/wiki/Amylopectin]

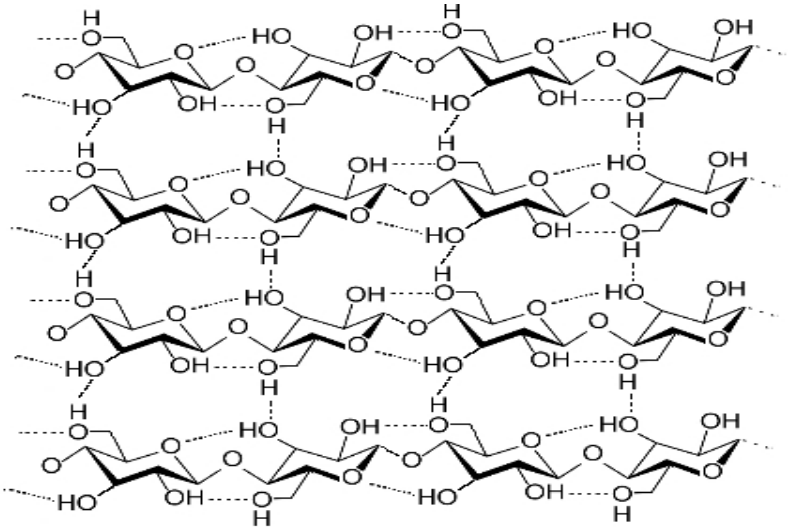

Fig. 1.5 Cellulose structure [http://en.wikipedia.org/wiki/Cellulose]

milled, and the corn particles are slurred with water. The starch slurry is solubilized by heating, which makes the starch amenable to enzymatic hydrolysis for conversion of reducing sugars.

Cellulose is a linear, unbranched homopolysaccharide of 10,000 to 15,000 D-glucose units. In cellulose the glucose residues have the β configuration: the glucose residues in cellulose are linked by (β1-4) glycosidic bonds (Fig. 1.5). Cellulose is found in lignocellulosic materials. Lignocellulosic materials must be pretreated to disrupt, at least in part, the highly crystalline structure of the cellulose fibers so that the cellulose becomes more accessible to hydrolytic enzymes. Several pretreatment processes for raw materials, such as steam explosion hot water treatment, dilute acid treatment, and ammonia fiber/freeze explosion (AFEX) [Mosier et al., 2005], have been designed to achieve these objectives.

The ethanol production process from biomass includes two stages. The first stage is to convert the carbohydrates in the raw materials into sugars. The complication of conversion process depends on the carbohydrate types in the raw materials. The sucrose conversion is the easiest, while the lignocellulose is the most difficult among the three carbohydrates. The second stage is to convert the sugars into ethanol by microorganism fermentation, *i.e*., the monomeric sugars released from polysaccharides in stage one as substrates are used to produce ethanol in microbial fermentations. Many types of yeast and a few bacteria can convert glucose to ethanol. The most common yeast used in industrial processes is the genus *Saccharomyces*. Although yeasts have many of the attributes as an ideal ethanol producer, they have significant limitations, such as narrow substrate range (not taking up pentoses) and limited tolerance to ethanol.

1.1 Lignocellulosic Materials

Although the ethanol production processes from sucrose and starch sources are simpler than that from lignocellulosic materials, their applications are limited because some sucrose plants, such as sugar cane, require hot climate and the starches are major food sources for people and animals. Lignocellulosic materials are composed of three major biopolymers: cellulose, hemicelluloses, and lignin. Cellulose is a glucose polysaccharide, hemicelluloses are polysaccharides with a backbone of different hexoses (glucose, mannose, galactose) and pentoses (xylose, arabinose), and lignin is a complex network of different phenyl propane units (p-coumaryl alcohol, coniferyl alcohol, and sinapyl alcohol). In general, cellulose gives rigidity to materials, hemicelluloses provide stickiness, and lignin acts as glue to hold polysaccharides together to confer rigidity, for example, in a tree stem.

The compositions of lignocellulosic materials depend not only on the plant varieties, but also on the growth conditions of plants, the part of the plants, and the age at plant harvesting. The average composition of plants is about 40-45% cellulose, 20-30% hemicelluloses, and 15-25% lignin. In general, wood has a higher content of cellulose and lignin, which makes wood more rigid than straw. In contrast, straw has more flexibility because of its relatively high content of hemicelluloses. The cellulose contents of softwood and hardwood are almost similar, but softwood contains more lignin and less hemicellulose. The hemicellulose composition is also different in various plants.

1.2 Hydrolysis of Lignocellulosic Materials

The first stage for ethanol production from biomass is to convert polysaccharides in biomass into monosaccharides by acid or enzymatic hydrolysis. Over the years, a number of different methods have been proposed for the hydrolysis of the lignocellulosic material. During the first step of all of these methods, the lignocellulosic material is mechanically chipped, granulated, or milled to increase the surface area. After the materials are treated mechanically, two routes: acid or enzymatic hydrolysis, are employed to hydrolyze the lignocellulosic materials. However, for enzymatic hydrolysis, a pretreatment process, such as steam explosion, hot water treatment, dilute acid treatment, and ammonia fiber/freeze explosion (AFEX), is required before hydrolysis to achieve five objectives: increase in the accessible surface area, cellulose decrystalization, hemicellulose removal, lignin removal, and alteration of lignin structure. This is because cellulose crystalline structure, linkage between hemicellulose and cellulose, and linkage between hemicellulose and lignin reduce enzyme accessibility to cellulose. In a pretreatment of steam explosion, biomass is conveyed into large vessels, and high-pressure steam is applied for a few minutes with or without addition of chemicals, such as acids. At a set time, the steam is rapidly vented from the reactor to reduce the pressure, and the contents are flashily discharged into a large vessel to cool the biomass. In a pretreatment of hot water, the biomass is washed by hot liquid maintained by pressure at elevated temperatures. In a pretreatment using dilute sulfuric acid, the biomass is contacted with acid, and the mixture is held at temperatures of 160-220°C for periods ranging from minutes to seconds. In a pretreatment of ammonia fiber/freeze explosion (AFEX), the biomass is contacted with aqueous ammonia (ammonia solution 5-15%) in a

column reactor packed with the following typically operating conditions: temperatures of 160-180°C, a fluid velocity of 1 cm/min, and residence times of 14 min. The steam explosion, hot water treatment, and dilute acid treatment can increase the accessible surface of lignocellulosic biomass, and remove hemicelluloses from biomass. Moreover, dilute acid treatment can alter lignin structure in biomass. The most effective pretreatment is AFEX, which can increase accessible surface, alter lignin structure, remove lignin, and decrystalize cellulose in biomass [Mosier et al., 2005].

Compared to acid hydrolysis, enzymatic hydrolysis is considered the most promising method for commercial production of ethanol because of its potential for reducing the overall cost of ethanol production. Cellulase, which is a complex of endo-β-1,4-glucanase, exo-β-1,4-cellobiohydrolase, and glycosidase, is usually produced by microorganisms, such as *Trichoderma reesei*. These enzymes play different roles in cellulose hydrolysis: endo-β-1,4-glucanase hydrolyzes internal β-1,4-glucosidic bonds randomly in the cellulose chain, and exo-β-1,4-cellobiohydrolase cleaves off cellobiose units from the ends of the cellulose chains. Both enzymes act on the solid substrate. Glycosidase, which is active with fluid phase, hydrolyzes cellobiose to glucose.

1.3 Fermentation

The second stage for ethanol production from biomass is conversion of monosaccharides into ethanol by fermentation. The hydrolysis and fermentation can be performed in two separate units, which is referred to as separate hydrolysis and fermentation (SHF), or a combined unit, which is referred to as simultaneous saccharification and fermentation (SSF). Two principal approaches for SSF can be taken:

(1) The process can take place with one microorganism. This approach is often referred to as consolidated bioprocessing (CBP);

(2) The process can take place with an enzyme for hydrolysis of lignocellulosic material in combination with a microorganism to produce ethanol from different sugar monomers.

In a batch SHF operation, the feedstock is hydrolyzed by enzyme for 3-4 days, and the solid in the slurry is separated from the hydrolysate. The hydrolysate is fermented by microorganisms for 1-2days to produce ethanol. In a batch SSF operation, the enzyme and microorganism are added to the slurry to start hydrolysis and fermentation simultaneously. The SSF process is shorter, usually 3-4 days, compared to the SHF process, which is usually 5-6 days. The advantage of the SHF is that two units can be operated in their optimal conditions because hydrolysis and fermentation have different optimal parameters, typically temperature 50^{o}C for enzymatic hydrolysis, and 36^{o}C for fermentation. The main advantages of the SSF are 1) the sugar monomers can be utilized directly to form ethanol after they are depolymerized by the enzymatic action. Since ethanol is less inhibitory on enzymes than reducing sugars, the SSF process reduces the inhibitory effect of glucose and cellobiose on the enzymatic activities [Holtzapple et al., 1990]. Therefore, SSF enables a more effective enzymatic hydrolysis than SHF; 2) the capital cost of SSF is expected to be less than that of SHF because only one process unit is required; 3) the productivity (product per time per volume) of SSF is higher than that of SHF; and 4) when the simultaneous saccharfication and co-fermentation (SSCF) to ferment glucose and xylose are conducted, the slower pentose fermentation than hextose fermentation is not rate controlling of SSCF because the enzymatic hydrolysis usually is

a slower reaction than the pentose fermentation. However, in SHF the slower pentose fermentation controls the fermentation rate.

On the other hand, it was found that inhibition occurred during fermentation due to some toxic chemicals generated from steam explosion of the feedstock. The main cause producing various inhibitory chemicals to fermentable sugars is degradation of the hemicellulose, lignin, extractives, and cellulose during steam explosion. The degradation products are complex mixtures of monomeric and oligomeric compounds that are inhibitory to microbial growth. The toxic compounds include furans, aromatic aldehydes, aromatic carboxylic acids, aliphatic acids, macromolecules, and other unidentified degradation products. In order to ferment the reducing sugars in the hydrolysates, the substrate must be detoxified using suitable methods such as overliming. An alternative to overliming is adding recycled paper sludge containing the calcium carbonate, an effective component in overliming process, to feedstock, and the mixtures are pretreated by steam explosion to reduce the inhibitory chemical production.

1.4 Objectives

The overall goals of this study were 1) to develop simple models of enzymatic hydrolysis for bioreactor scale up and industrial applications; 2) to develop the profit rate model for the optimization of process parameters in enzymatic hydrolysis of ethanol production; 3) to develop an operable simultaneous saccharification and fermentation model for the description of the variations in the concentrations of main component and by products in ethanol production; and 4) to develop a novel operating mode: semi-simultaneous saccharification and fermentation, consisting of a pretreatment and a SSF,

for bioethanol production from the mixture of cotton gin waste and recycled paper sludge. The project not only solves the disposal problems of two wastes from the cotton and paper industries, and reduces greenhouse gas and particle emission and dependence on petroleum, but also provides a basis of process scale up.

References

Holtzapple, M., Cognata, M., Shu, Y., and Hendrickson, C. Inhibition of Trichoderma reesei cellulase by sugars and solvents. Biotechnol. Bioeng. 36: 275-287 1990.

Mosier, N., Wyman, C., Dale, B., Elander, R., Lee, Y. Y., Holtzapple, M., and Ladisch, M. Features of promising technologies for pretreatment of lignocellulosic biomass. Bioresource Technology 96(6): 673-686, 2005.

http://en.wikipedia.org/wiki/Amylose

http://en.wikipedia.org/wiki/Amylopectin

http://en.wikipedia.org/wiki/Cellulose

http://en.wikipedia.org/wiki/Ethanol

http://en.wikipedia.org/wiki/Sucrose

Chapter Two

Literature Review

2.1 Ethanol Production from Cotton Gin Waste

Lignocellulosic materials, such as wheat straw, rice straw, hardwood, and softwood, have been extensively studied for bio-fuel production. In the southern areas of USA, cotton industry produces a large mass of cotton gin waste (CGW). About 40–147 kg of cotton gin waste per bale of cotton (227 kg) is produced, depending on the cotton harvest method. It was estimated that about 2.04 million tons of cotton gin waste were produced annually by the USA cotton industry [Holt, et al. 2000]. Therefore, CGW is a great problem in the warm regions of the USA as it serves as an overwintering site for insect pests, and thus must be destroyed. The traditional disposal methods for this waste are land filling, incorporation into the soil, and incineration [Thomasson, 1990]. These methods have some disadvantages. The first and second methods cause the contamination of groundwater and surface water and soil detriment. When cotton gin waste is filled in soil, the organic and inorganic compounds are leached into the soil, which causes contamination of underwater and the environment. Some pollutant gases, such as ammonia, methane, and carbon dioxide, are generated by soil microorganisms. Furthermore, most field operations used to bury the residue are energy intensive, and tend to destroy soil structure, thereby increasing the potential for erosion. The incineration causes air pollution from particle and gaseous pollutants during combustion. With stricter regulation on air pollutants due to the Clean Air Act, companies are looking for alternative methods for disposal. Cotton gin waste, which comprises of broken cotton fibers, stems, cotton stalks, upper portion of the taproot, and leaves [Pessarakli, 1990],

contains cellulose and hemicellulose. These biopolymers can be converted into monomeric sugars through hydrolysis, and these sugars can be used to produce ethanol and other high-value chemicals through the fermentation process. In addition to the common advantages of other biomass, such as low cost and abundant resources, cotton gin waste has some unique advantages for ethanol production: 1) it is concentrated at processing sites; and 2) it has already been collected from fields and transported to factories, thus the transportation costs could be considerably low.

Due to the government regulations of clean air act in 1990, methyl tertiary butyl ether (MTBE) in 1998, and renewable fuels standard (RFS) in 2006, it was estimated that the ethanol production in USA would reach about 19,000 million liters by 2010 (Fig. 2.1) [Berg, 2004]. The amount of cotton gin waste produced in USA cotton industry has decreased slightly from about 2.26 million tons in 1990 [Thomasson, 1990] to about 2.04 million tons in 2000 [Holt et al. 2000]. The waste based on the amount in 2000 can produce 383 million liters of ethanol, which is about 2.02 % of the projection of USA ethanol production by 2010.

The conversion of cotton gin waste to bio-fuel has been investigated by some researchers. Agblevor et al. [2005] investigated storage and characterization of cotton gin waste for bioethanol production. The storage time of CGW obviously affected its physical properties. The bulk densities of the fresh wet and dry CGW were 210.2±59.9 kg/m^3 and 183.3±52.2 kg/m^3, respectively. After six-months of storage, the volumes of

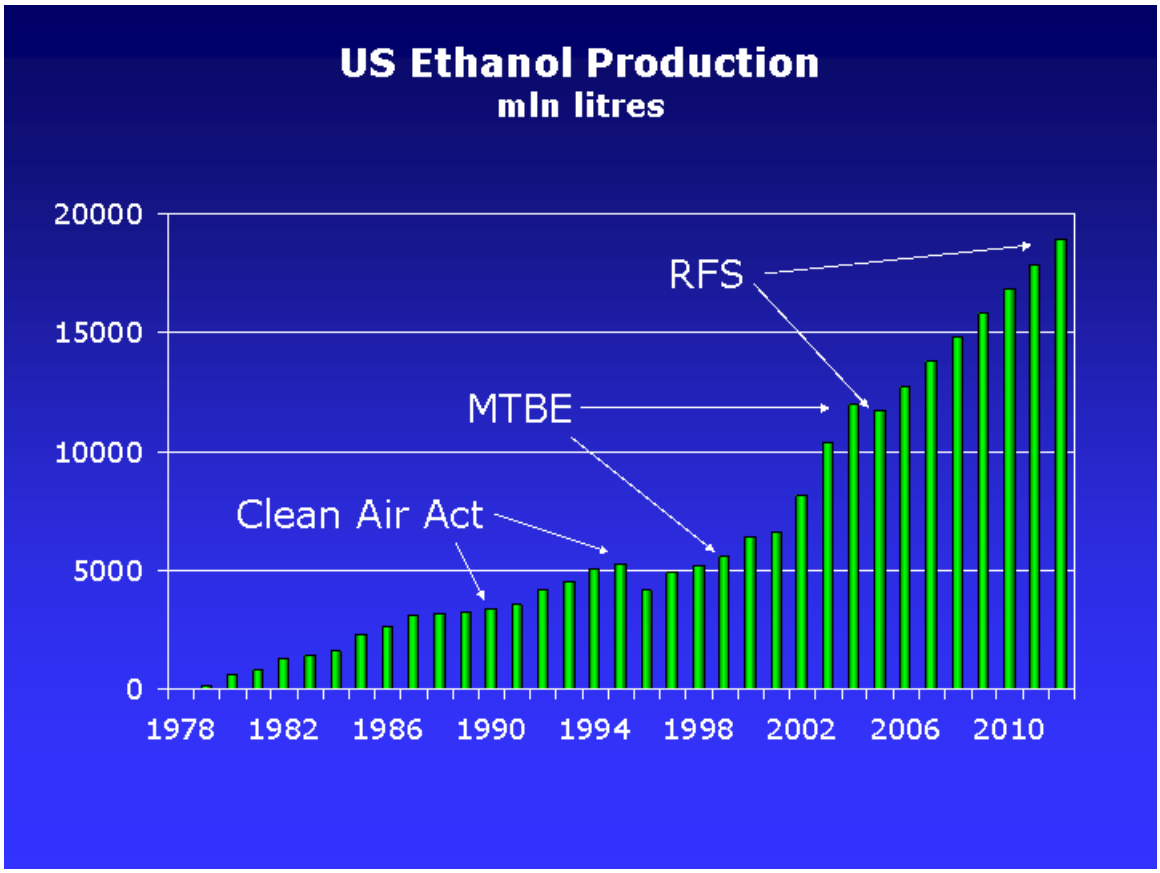

Fig. 2.1 USA ethanol production [Berg, 2004]. MTBE: methyl tertiary butyl ether, and RFS: renewable fuels standard.

three piles from different locations decreased by 38.7%, 41.5%, and 33.3%, respectively, relative to the volume of the pile at the start of the storage. The ash content of the CGW was very high ranging from 10% to 21% and the acid insoluble fraction was high (21% to 24%). The total carbohydrate content was very low and ranged from 34% to 49%. The total carbohydrate was highest due to moisture loss in CGW after three months storage. However, it was found the loss of total carbohydrates was as high as 25% after six months.

Generally, there are three routs to convert CGW into bio-fuel: gasification, pyrolysis and fermentation. The gasification of CGW produces synthesis gas, the pyrolysis mainly produces bio-oil, and fermentation produces ethanol. Kosstrin et al [1979] first used a dense phase fluidized-bed to gasify cotton gin waste to synthesis gas. The heating valves of gas, oil, and char produced were approximately 11,250 kJ/m^3, 23,000-30,000 kJ/kg, and 23,000-27,000 kJ/kg, respectively. Product yields and synthesis gas components vary widely, primarily as a function of temperature and residence time. LePori et al. [1980] also used fluidized bed technology to evaluate the combustion and gasification of cotton gin waste. The primary products of gasification were H_2 and CO with heating value of 7.45-7.91 MJ/kg CGW. LePori et al. [1981] further converted raw cotton gin trash to synthesis gas in fluidized-bed combustion reactor. The reaction was carried out at 404-436°C and the synthesis gas had a heating value of 3.66-5.30 MJ/m^3. Equipment for on-site energy production from cotton gin waste was developed by Hiler [1982]. Gasification experiments were carried out in a 51-mm diameter fluidized bed using cotton gin trash as feedstocks. The predominant products of gasification suitable for combustion were CO, H_2, and CH_4. The quality of gas produced at these conditions was

a function of the fuel-to-air ratio. A typical heating value of gases produced by gasification of cotton gin trash was 6.26 MJ/m^3. Parnell et al. [1991] investigated the gasification of cotton gin waste in a fluidized bed reactor. The process was not economical because of a low heating value of the gas. Zabaniotou et al. [2000] studied pyrolysis of cotton gin waste. The heating rate of the reactor was 80-100°C/s and the temperature range studied was 350-850°C. The pyrolysis mainly yielded char and gaseous products, and liquids and tar were produced in very small quantities. The yield of gaseous products increased with temperature in contrast to the yield of char. The peak temperature at which the percentage of gaseous products was equal to the percentage of char was 550°C; above this temperature, the percentage of gaseous products was higher than that of the char. The percentages of CO and H_2 in the gases increased with temperature. Experimental data about total weight loss of CGW and the yield of CO, CH_4 and H_2 followed a first-order kinetic model. Recently, Capareda et al. [2007] evaluated the feasibility of producing high value liquid fuels from fluidized bed gasification of cotton gin trash. They used a 305 mm diameter laboratory scale fluidized bed to produce the synthesis gas for liquid fuel production. Novel zeolite catalysts would be used for the reforming process in addition to using steam at high temperature and pressure.

The third route for utilization of CGW is production of ethanol. Brink [1981], and Beck and Clements [1982] reported that they obtained 157-liter ethanol per ton of cotton gin waste. Jeoh and Agblevor [2001] found that efficiency of enzymatic hydrolysis of cotton gin waste could be increased 42-67% after the waste was treated by steam explosion, and finally obtained the maximum ethanol yield of 83% using *E. coli* KO11

fermentation. Agblevor et al. [2003] further found that ethanol yield could be increased up to 92.5% by overliming the steam exploded cotton gin waste before the substrate was hydrolyzed. Ethanol yields ranging from 58 to 92.5% of the theoretical yields depended on feedstock and severity factor of steam explosion. The highest ethanol yield was 191 l/t, and the lowest was 120 l/t.

2.2 Ethanol Production from Recycled Paper Sludge

Recycled paper sludge (RPS) is another waste from paper industry. Currently, about 48% of paper used in the U. S. is manufactured by the recycling process, and this paper contains 37.7% of the recycled fibers. Generally, the recycling process creates more sludge (about 440 to 500 kg of sludge per metric ton paper) than the virgin paper process (190 kg of sludge per metric ton of paper) [Frederick et al., 1996, Gregg et al., 1997]. About 4 billion dry kilograms of sludge every year were produced from the papermaking industry [Glen, 1997]. Disposal methods of recycled paper sludge include land-filling, land application, and incineration. The disadvantages of these methods were mentioned in Chapter 2.1. In addition, the third method of combustion of recycled paper sludge is not efficient because the RPS contains significant amounts of ash, hence it has a low heating value.

Ethanol production from RPS through cellulase hydrolysis and yeast fermentation has been investigated by some investigators. Kerstetter et al [1996] analyzed chemical characteristics of RPS, including solids content, alkali, ash, glucose, hemicellulose, and acid insoluble organics. SSF ethanol productions were performed for selected samples from the eleven mills. Kraft mill sludges had moderately high ash contents (25-50%),

and the 7-day hydrolysis yields were 90 to 96% of theoretical ethanol based on cellulose content. Old corrugated container sludges had low ash (2-13%), and greater than 50 percent cellulose content. The hydrolysis yields were less than 90%. Sludge from the sulfite mill was highly susceptible to SSF. The 4-day SSF achieved a 93% yield, and the 7-day SSF did a 98% yield. Lark et al. [1997] also studied ethanol production from RPS. Their study showed that at a low cellulase loading of 8 FPU/g dry RPS, about 32 and 35 g/l of ethanol were produced from 180 and 190 g/l dry materials, respectively, after 72 hours of incubation. Fan at al. [2003] analyzed major components of the bleached Kraft sludge: glucan (62 wt. %, dry basis), xylan (11.5%), and minerals (17%). They also converted RPS to ethanol in a semicontinuous solids-fed reactor using SSF and *Saccharomyces cerevisiae*. Cellulase loading was 15 to 20 FPU/g cellulose. SSF was carried out for a period of 4 month in a first-generation system, resulting in an average ethanol concentration of 35 g/L. Run 1 produced 50 g/L ethanol at a cellulose conversion of 74%. Run 2 produced 42 g/L ethanol at a conversion of 92%. For run 2, the ethanol yield was 0.466 g ethanol/g glucose and more than 94% of the xylan fed to the reactor was solubilized. Zhang and Lynd [2007] also applied recombinant xylose-fermenting microbes in simultaneous saccharification and cofermentation to ethanol production of RPS. Experimental work was conducted using two promising recombinant microbes engineered to be able to utilize xylose: *Z .mobilis* 8b and *S. cerevisiae* RWB222. Simultaneous saccharification and co-fermentation (SSCF) of paper sludge produced more than 40 g/L ethanol at 30^{o}C and 37^{o}C. The process SSCF from RPS increased ethanol yields by about 20%. Viruthagiri and Sasikumar [2007] produced ethanol from RPS using SSF. *Trichoderma viride* and thermotolerant yeast *Kluyveromyces marxianus*

var. marxianus were used. The effects of substrate concentration, initial pH, and temperature on ethanol production from RPS were examined by conducting batch experiments using *Trichoderma viride* and thermotolerant yeast. At SSF conditions, a maximum yield of about 16.5 g/L of ethanol was obtained from 50 g/L of dry RPS after 144 h of fermentation. Marques et al. [2008] compared the effects of ethanol production from RPS on SHF and SSF using *Pichia stipitis*, which can co-ferment cellulose and xylan into ethanol in SSF or SHF. In the enzymatic hydrolysis step using Celluclast 1.5 L supplemented with Novozym 188, 100% saccharification was achieved. A slightly higher conversion yield was attained on SHF, corresponding to an ethanol concentration of 19.6 g/l, but 179 h were needed. The SSF process was completed after 48 hours, which produced 18.6 g/l of ethanol from 178.6 g/l of dried RPS, corresponding to an overall conversion yield of 51% of the available carbohydrates on the initial substrate. These results demonstrated that the conversion of RPS to ethanol was efficient even with no pre-treatment or substrate supplementation. However, there is no publication on the hydrolysis and ethanol production from the mixture of CGW and RPS.

On the other hand, recycled paper sludge contains about 50-70% low quality short fiber, which is composed of mostly cellulose, low lignin and hemicellulose contents, and 30-50% inorganic ash, which contains calcium carbonate and titanium dioxide. It is noted that the calcium carbonate in RPS can replace that used in overliming. Therefore, if RPS is combined with CGW for steam explosion, the toxic components in the steam-exploded CGW could be eliminated, and the feedstock could be directly hydrolyzed and fermented to ethanol without any further pretreatment.

2.3 Hydrolytic Mechanism of Insoluble Substrate

Generally, enzymatic hydrolysis of insoluble substrate undergoes five steps in sequence to convert the insoluble carbohydrate polymers into reducing sugars:

(1) The external mass transfer of enzyme from the bulk fluid to the surface of insoluble substrate through the liquid boundary layer surrounding the solid substrate. Here we assume that the mixing in the bulk fluid is perfect so that there is no concentration gradient in the bulk fluid;

(2) Enzymatic adsorption (for example, adsorption of endo-β-1,4-glucanase, exo-β-1,4-cellobiohydrolase) on the active sites of the external surface of insoluble substrate, and the internal surface of insoluble substrate if the pores in the substrate are big enough to admit the protein molecules. If the latter case takes place, the internal mass transfer in insoluble substrate is one of the considering mechanisms because the internal surface area of the substrate is generally much greater than the external surface area;

(3) Occurrence of the catalytic enzyme reaction at the adsorbed sites of the insoluble substrate to form sugars (such as cellobiose);

(4) The product (cellobiose) desorption from the surface of the insoluble substrate;

(5) The external mass transfer of cellobiose from the surface of the insoluble substrate to the bulk fluid through the liquid boundary layer, and occurrence of the catalytic reaction of enzyme (glycosidase) in the liquid phase to form glucose.

Among these steps, the slowest step, or the rate-controlling step, will determine the overall hydrolytic rate of the entire process. According to this mechanism, in principle, models based on any of the three types: external mass transfer, internal mass transfer, and

surface reaction models can describe the phenomenon of enzymatic hydrolysis of insoluble substrate. However, only the model that represents the rate-controlling step is intrinsic; the others are apparent.

2.4 Enzymatic Hydrolytic Model of Insoluble Substrate

In order to design an effective reactor for enzymatic hydrolysis of insoluble substrates, mathematical models are often used to describe the basic characteristics of the enzymatic hydrolysis. Historically, two types of empirical and mechanistic models have been developed and used to describe the enzymatic hydrolytic process. These mechanistic models can be classified according to their mechanisms. Compared to the mechanistic models, the empirical methods have few parameters, usually 2-3 parameters [Ghose, 1969; Holtzapple et al., 1984]. Hence, they are easily mastered by engineers, but they do not reflect intrinsic phenomena of mass transfer and reaction mechanism occurring in the reactor. In contrast, the mechanistic models overcome this disadvantage.

For enzymatic hydrolysis of insoluble substrate, the external mass transfer models have not been adopted by most researchers because the external mass transfer rate is considered fast compared to the slow catalytic reaction rate of the enzyme. This means that the external mass transfer is not the rate-controlling step during hydrolysis. The internal mass transfer models have been used by several investigators. Etters [1980], and Chrastil and Wilson [1981] developed, respectively, two three-parameter models based on internal mass diffusion. Most researchers focused on the surface reaction models because the slow surface reaction of enzyme is assumed to be the rate-controlling step. Howell and Mangat [1978] developed a four-parameter model and obtained its analytical

solution in which they accounted for enzyme deactivation, and assumed a homogeneous substrate and a single effect of enzymes for hydrolysis. Gan et al. [2003] and Fan and Lee [1983] developed more complicated models whose solutions cannot be solved analytically. In Gan et al.'s model [2003] they accounted for two different regions in the substrate: amorphous and crystalline regions. Fan and Lee further distinguished the functions of the three kinds of enzymes in the cellulase system: endo-β-1,4-glucanase, exo-β-1,4-cellobiohydrolase, and glycosidase. Endo-β-1,4-glucanase hydrolyzes internal β-1,4-glucosidic bonds randomly in the cellulose chain, and exo-β-1,4-cellobiohydrolase cleaves off cellobiose units from the ends of cellulose chains. Both enzymes act on the solid substrate. In contrast, glycosidase reacts in the liquid phase to convert cellobiose into glucose.

It was realized that the enzyme is deactivated during the hydrolysis of the insoluble substrates, resulting in a decrease in hydrolytic rate and no reuse of the enzymes. The deactivation was attributed to various factors, such as the shear force, temperature, pH [Ganesh et al., 2000; Azevedo et al., 2002], and ineffective adsorption of cellulase on the surface of the insoluble substrate and product inhibition [Fan and Lee, 1983]. Some investigators developed mathematical models that included the enzyme deactivation during the hydrolysis of the insoluble substrate [Fan and Lee, 1983; Gan et al., 2003]. However, these models are complicated because 1) the models consist of several ordinary differential equations; 2) analytical solutions cannot be obtained for these equations so that using them is not convenient; 3) there are too many parameters in these ordinary differential equations, and these parameters cannot be uniquely determined; and 4) the values of some parameters in these models were often chosen from other experiments

rather than from a fitting process based on real experimental data. Thus, the chosen values were arbitrary. Therefore, for industrial application, it is necessary to develop models with the following characteristics: models with analytical solutions, few parameters, easy determination of the values of these parameters, and these parameters must have physical meaning rather than empirical.

The adsorption of cellulase on insoluble substrate is an important mechanism in the hydrolytic process. The diffusion rate of cellulase in the solution and in the pore of the insoluble substrate may significantly affect the hydrolytic rate. Hence, diffusivities are the basic data for the reactor design. Generally, the diffusivity of cellulase in the solution and in the pore of insoluble substrate can be estimated by fitting the data of adsorbed cellulase on the adsorbent with the analytical solutions of the corresponding partial differential equations of diffusion derived from Fick's second law [Fournier, 2007; Chen et al., 2003]. Although several investigators have studied adsorption of cellulase on insoluble substrate, there is little information about the diffusivity of cellulase on insoluble substrate.

2.5 Optimization of Enzyme Loading and Hydrolytic Time

The ethanol production from lignocellulosic materials has not been commercialized because the process is not economical compared to the other processes from sucrose and starch materials. The optimization of the process parameters has focused on improving the economic feasibility of the process. These parameters include hydrolytic temperature, pH, time, and enzyme loading. The optimal hydrolytic temperature and pH can be obtained by determining the maximum conversion or sugar concentration within

the fixed temperature and pH ranges using the experimental method or experimental plus model method. However, how to determine the optimal enzyme loading and hydrolytic time is still a challenge for researchers since the conversion often increases with increasing enzyme loading and hydrolytic time. Thus, the conversion cannot be an objective function for optimization of enzyme loading and hydrolytic time. Rather, the objective function should be profit or profit rate produced by the hydrolytic process. Another barrier to the commercial production of bio-ethanol from lignocellulosic materials is the high cost of enzyme. Therefore, many investigations have been conducted on low enzyme loading for hydrolysis to decrease the enzyme consumption. However, the low enzyme loading often results in a low conversion of lignocellulosic materials during hydrolysis, particularly for feedstocks with high lignin and ash contents. It was reported that a high lignin content of feedstock required a high enzyme loading for effective hydrolysis [Pan et al., 2005]. Thus, the low enzyme loading will result in more feedstock consumption and a higher raw material cost. For low hydrolytic conversion, using a recycle process can improve on the overall conversion efficiency, but it may increase the operating cost. Thus, a quantitative method that can take the advantage of both the low enzyme loading and the recycle operation is required.

Economic evaluations of bio-ethanol production from some lignocellulosic materials using enzymatic hydrolysis have been reported [Galbe et al., 1997; Holt et al., 2000]. These studies included the general economic aspects of commercial bio-ethanol production from the lignocellulosic materials, but do not show the quantitative relationship among several parameters, such as operating cost, enzyme cost, ethanol market price, and enzyme loading. The results from these studies cannot be used to adjust

enzyme dosage and hydrolytic time when the other factors change in order to maximize profit in ethanol production. For such an objective, a mathematical model combined with hydrolytic and profit factors is required. The first step of this combined model is to establish a kinetic model of the enzymatic hydrolysis. Although a lot of kinetic models of enzymatic hydrolysis, including the empirical and mechanistic models, have been proposed in literature, they cannot be applied to such an objective because of some limitations. The empirical models are simple, usually 2-3 parameters [Ghose, 1969; Holtzapple et al., 1984], but their parameters are not physically meaningful. A particular drawback is that the models often do not possess a convergent property, *i. e.* if the residence time of the substrate is increased, the conversion will approach infinity rather than one. Another drawback is that they do not include the enzyme concentration parameter, which makes it impossible to correlate all the experimental data for different enzyme concentrations with a set of parameters. On the contrary, the mechanistic models are complicated, and often have no analytical solutions, and have too many parameters in the ordinary differential equations [Gan et al., 2003; Fan and Lee, 1983]. The estimation of these parameters is often difficult. Thus, their applications to industrial processes are not convenient. Therefore, for an optimal enzymatic hydrolysis with potential industrial application, it is necessary to develop a model with the following characteristics: analytical solution obtained for the model, a good convergence for the conversion, few number of parameters, easy determination of the parametric values, and the parameters must have physical meaning rather than empirical. The second step of this combined model is to develop a profit rate model which relates the profit rate with various factors influencing the hydrolysis such as operating cost, enzyme cost, and conversion rate *etc*.

Using such a profit rate model, the maximum profit rate can be predicted for a set of optimal initial enzyme loading and hydrolytic time. Furthermore, the enzyme loading and hydrolytic time can be adjusted to obtain the maximum profit rate according to the changes in enzyme cost and other factors such as ethanol market price. There is no such study in literature in which the hydrolytic and profit rate factors are combined in a model, and the model is applied to a dynamic process to derive the optimal enzyme loading and hydrolytic time for the maximum profit rate in ethanol production.

2.6 Simultaneous Saccharification and Fermentation

As discussed in Chapter 1.3, in SSF, an enzyme degrades the polymeric material and a microorganism converts the soluble sugars to ethanol. Since each process has its optimal conditions, it is necessary to find a compromise for the conditions used in SSF. These conditions generally include temperature and pH.

Ruiz et al [2006] reported ethanol production from pretreated olive tree wood and sunflower stalks using the SSF process. The olive tree wood was pretreated by steam at 230^{o}C for 5 minutes and after 72-h SSF, ethanol concentration was 30 g/l. For sunflower stalks, ethanol concentration was 21 g/l under similar pretreatment conditions but temperature 220°C. Kim and Lee [2005] investigated ethanol production from corn stover pretreated with aqueous ammonia using the SSF process and *S. cerevisiae* (D_5A). The ethanol yield was 73% of the theoretical maximum on the basis of the glucan content in the treated corn stover. The accumulation of xylose in the SSF appeared to inhibit the cellulase activity during glucan hydrolysis, which reduced the yield of ethanol. In the simultaneous saccharification and co-fermentation (SSCF) test, using recombinant *E. coli*

(KO11), both the glucan and xylose were effectively utilized, resulting in on overall ethanol yield of 77% based on the glucan and xylan content of the substrate. Soderstrom et al. [2005] used the two-step steam pretreated softwood for ethanol production. When SSF and SHF were performed at the same dry matter content and enzyme loading, the ethanol yield in SSF exceeded the yield obtained from SHF in both pretreatment cases. Thus, SSF is a better process than SHF if yield is the main priority.

The operating temperature of SSF is of concern because the optimal temperature of enzymatic hydrolysis is about 47-52°C, which is higher than those (about 36°C) for microbial fermentation [Kadam and Schmidt, 1997]. For example, *S. cerevisiae* strain, which is often used in simultaneous saccharification and fermentation, has a suitable temperature around 36°C at which the yeast has the highest activity. If temperature is above 40°C, the yeast activity will quickly decrease. Another study found that SSF using *S. cerevisiae* on steam-pretreated spruce resulted in 82% of the theoretical ethanol yield [Stenberg et al., 2000]. However, since the enzymatic hydrolysis is considered a rate-limiting step, a thermotolerant microorganism will be expected to perform SSF better [Sun and Cheng, 2002]. It was found that the strain of thermotolerant *Klyveromyces marxianus* had the optimal temperature 42°C for SSF of steam-pretreated spruce instead of 37°C for *S. cerevisiae* [Bollok et al., 2000]. But the investigation also found that *K. marxianus* was sensitive to the inhibitors present in the steam-pretreated spruce, and after 10 hours of fermentation, the ethanol production ceased. However, another investigation found that *K. marxianus* was not inhibited by the hot water pretreated olive pulp, and SSF resulted in 80 % of the theoretical ethanol yield [Ballesteros et al., 2002].

Another approach to improve the performance of SSF is to use an optimal temperature profile throughout the process to satisfy the optima of both the enzymatic hydrolysis and the fermentation. Huang and Chen [1988] investigated the SSF of Solka Floc cellulose using temperature profiling. They used *Zymomonas mobilis* as the fermenting microorganism, and *Trichoderma reesei* cellulases for hydrolysis. During the initial phase of the experiments, the temperature was controlled between 30°C and 37°C for the optimal propagation of the cells. After the cells entered the active ethanol production phase, and the hydrolysis reaction became the rate-limiting step of SSF process, the temperature was increased to 40°C. The results showed that the ethanol yield of 0.32 g/g was significantly higher than that obtained with isothermal SSF. Unfortunately, the productivity, 0.32 g/(l.h), was reduced due to the increased processing time required for the prehydrolysis. Oh et al. [2000] investigated SSF of purified cellulose using cellulase from *Brettanomyces custerii* H_1-55 (Cellulast 1.5L) and β-glucosidase (Novozym 188). Based on a model of the process, an optimal temperature profile was designed. The optimized temperature profile yielded up to 21% more ethanol than an isothermal SSF. However, the results of Kadar et al [2004] on ethanol production from various lignocellulosic substrates (Solka Floc, OCC waste cardboard, and paper sludge) in temperature-profiling SSF and SSF with two yeast strains (*S. cerevisiae* and a thermotolerant *K. marxianus*) showed that SSF had a higher ethanol yield than the non-isothermal SSF (NSSF). Their results also showed that there was no significant difference between *S. cerevisiae* and *K. marxianus*. The ethanol yields were 0.31-0.34 g/g for both strains. It should be pointed out that in Kadar et al.'s experiments the fermentation temperature during SSF was 40°C and the temperature for starting fermentation in NSSF

was 30°C, and they also did not control the pH (pH range was 4.4-5.3, the enzymatic activity is sensitive to pH). In addition, they used a longer hydrolytic time (24 hours), resulting in a relatively short fermentation time (72 hours) in NSSF compared to 96 hours in SSF. The above reasons may explain the conflicting results with Huang and Chen [1988].

A novel equipment design is also expected to improve the SSF process. Wu and Lee [1998] designed a nonisothermal simultaneous saccharification and fermentation process (NSSF), where the hydrolysis and fermentation were carried out simultaneously, but in two separate zones at their optimal temperatures. This concept could be operated under stable conditions, and the experiments showed that the initial hydrolytic rate was increased by a factor 2-3 when the hydrolytic temperature was raised from 30°C to 50°C. They concluded that the NSSF reduced the enzyme requirement by 30-40%. At an enzyme loading of 10 FPU on dilute-acid pretreated switchgrass, the final yield (50% of the theoretical) of the NSSF process was reached after 40 hours, while it took 4 days for the SSF process to reach the same yield [Wu and Lee, 1998]. At higher enzyme loadings, no increased ethanol productivity could be found by using the NSSF process compared to the SSF process.

2.7 Simultaneous Saccharifucation and Fermentation Model

As discussed in Chapter 1.3, SSF has several advantages over the traditional SHF process. Many investigations of SSF for ethanol production from lingocellulosic materials have been reported, and some mathematical models of SSF have also been proposed [Philippidis et al., 1992; Philippidis et al., 1993; South et al., 1995; Philippidis

and Hatzis, 1997; Shin et al., 2006]. The SSF model developed by Philippidis and Hatzis [1997; 1993] included four differential equations to describe changes in corresponding concentrations of cellulose, cellobiose, glucose and microorganism with respect to time, and an algebraic equation for ethanol concentration. Philippidis et al.'s model [1993] was used by Moon et al. [2001] and Pettersson et al. [2002] to describe the SSF processes of steam-exploded hardwood and softwood, respectively. However, a common shortcoming of these studies is that only three (cellobiose, glucose, and ethanol) or two (glucose and ethanol) components in the SSF processes were simulated. The changes in microorganism concentration over time were not simulated. Hence, the models could not be completely verified because the simulation of four sets of data was more difficult than that of three sets of data. In addition, the cellulose concentrations over time in Philippidis and Hatzis's [1997] model were required for the model to work. However, cellulose is a solid, and measuring its concentration in a suspension is often tedious, particularly when cellulose is in biomass using the standard procedures ASTM E1721-95 [1997] and ASTM E1755-95 [1997]. This shortcoming makes the model inoperable. Furthermore, since ethanol is the main product of the SSF process, to investigate the dynamics of ethanol in the SSF process, it will be more convenient if variations in ethanol concentration are expressed as differential equation rather than as an algebraic equation.

The batch experiment is the main experimental method used in the SSF of lignocellulosic materials. However, the commercial production of ethanol, as a low value and large volume product, must be a continuous operation to be economical. Thus, one of the main tasks of process engineers is to use the data from batch experiments to predict the effect of continuous process on reducing the production cost relative to the batch

process. Philippidis and Hatzis [1997] extended their batch model to the continuous model. Unfortunately, their continuous model was not complete because the model does not include enzyme addition. In a continuous operation, the enzyme is gradually lost in the outflow. Furthermore, the enzyme deactivation, which was expressed as an exponential function in Philippidis and Hatzis's model [1997], also causes a decrease in effective enzyme concentration. Therefore, adding enzyme during continuous operation is necessary. Otherwise, the reaction rate of enzymatic hydrolysis approaches zero with time, and steady state of the process cannot be achieved.

In these models, there were more than seventeen parameters. Some of these parameters, such as enzyme inhibitory constants, were determined from independent enzyme experiments that were not part of the SSF experiments. For industrial applications, the SSF models with fewer parameters would be more suitable than those with detailed fundamental mechanisms because the parameters in a simple model can be determined through an SSF experiment without other additional experiments.

The fed-batch operating mode is a middle operation between batch and continuous modes. It has some unique advantages for biochemical experiments and production. For example, to enhance the ethanol concentration in a broth in order to save energy during distillation, a high substrate concentration (*e.g.* 10 % (w/v)) is often used in the batch process. However, it was found that in such a high substrate concentration, the concentrations of components toxic to fermentable microorganisms also were greatly increased. To reduce the inhibitory effect, a fed-batch process is superior to batch processes due to the incremental substrate concentration [Zhu et al., 2006; Rudolf et al., 2005]. Another reason against using the batch process is that in a high substrate

concentration, the mass transfer between enzyme and substrate is reduced due to the imperfect mixing, resulting in a low rate of enzymatic hydrolysis. On the other hand, in a fed-batch process, both the culture volume and the dilution rate change with respect to time. Hence, modeling and analysis of fed-batch processes are more complicated. There is no published literature on SSF model of fed-batch operation in ethanol production.

2.8 Semi-simultaneous Saccharification and Fermentation and its Model

As discussed in Chapter 1.3, the carbohydrate fraction in biomass can be converted to ethanol using two operating modes. The operating modes affect the ethanol productivity and yield, both of which can be used to estimate the efficiency of the processes. SSF is generally considered to have a higher productivity than SHF, because SSF processing time is shorter. However, for ethanol yield, there is no consensus conclusion on which process is better. For example, Ohgren et al. [2007] compared the yields for three cases of SSF and SHF using steam-pretreated corn stover. The two-case studies of SSF were better than SHF. Mishima et al. [2008] observed that SSF produced higher yield and concentration of ethanol from water hyacinth and water lettuce than SHF. However, the experiments of Marques et al. [2008] showed that the conversion for SHF was higher than that for SSF when they used RPS, *Pichia stipitis*, and Celluclast 1.5 L supplemented with Novozym 188 for ethanol production.

The advantages of SSF can be attributed to less inhibition of enzymes, and a longer enzymatic time than SHF in which the substrate is separated from the hydrolysate after hydrolysis. In contrast, the advantages of SHF can be attributed to its faster hydrolytic rate in optimal operating conditions than that of SSF. If a pre-hydrolysis prior to

fermentation is applied in which the hydrolytic rate is faster under the optimal conditions, and the substrate in the hydrolysate after hydrolysis is not removed to start SSF, the process has the advantages of both SSF and SHF. There is an optimal time to start the fermentation for such a combined process, which is a balance point between the inhibitory and rate-controlling factors. This process can be referred to as semi-simultaneous saccharification and fermentation (SSSF), which includes a pre-hydrolytic phase and a SSF phase. Because SSSF is a process between SSF and SHF, it is expected that SSSF will have both higher productivity and yield than SSF and SHF if the suitable pre-hydrolytic time is selected.

On the other hand, Shen and Agblevor [2008] developed SSF model which describes the rates of change of cellobiose, glucose, cell, and ethanol concentrations at the initial glucose and cellobiose concentrations equal to zero. In principle, the proposed SSF model will also simulate the second phase of SSSF process with the different initial conditions (non-zero glucose and cellobiose concentrations). However, the proposed model did not include some by-products, such as glycerol, acetic acid, and lactic acid, during ethanol production. These by-product reactions from microbial metabolism occur in ethanol production, and should be considered in a detailed mass balance.

References

Agblevor, F. A., Batz, S., and Trumbo, J. Composition and ethanol production potential of cotton gin residues. Applied Biochemistry and Biotechnology 105-108: 219-230 2003.

Agblevor, F. A., Cundiff, J. S., Mingle, C., and Li, W. Storage and characterization of cotton gin waste for bioethanol production. Proceedings - Beltwide Cotton Conferences 2829/1-2829/16. Publisher: National Cotton Council, 2005.

ASTM E1721-95. Standard test method for determination of acid insoluble residues. In: Annual book of ASTM standards, American Society for Testing and Materials, West Conshohocken, PA. Vol. 11.05, p. 1238-1240, 1997.

ASTM E1755-95. Standard test method for determination of acid insoluble residues. In: Annual book of ASTM standards, American Society for Testing and Materials, West Conshohocken, PA. Vol. 11.05, p. 1252-1254, 1997.

Azevedo, H., Bishop, D., and Cavaco-Paulo, A. Possibilities for recycling cellulases after use in cotton processing. Applied Biochemistry and Biotechnology, 101: 61-74 2002.

Ballesteros, I., Oliva, J. M., Negro, M. J., Manzanares, P., and Ballesteros, M. Ethanol production from olive oil extraction residue pretreated with hot water. Appl. Biochem. Biotechnol. 98-100: 717-732 2002.

Beck, R. S., and Clements, D. L. Ethanol production from cotton gin trash. Proceedings of the symposium on: Cotton gin trash utilization alternatives, Texas Agricultural Experiment Service, Lubock, TX, p163–81 1982.

Berg, Christoph. World fuel ethanol analysis and outlook. http://www.distill.com/World-Fuel-Ethanol-A&O-2004.html, 2004.

Bollok, M., Réczey, K., and Zacchi, G. Simultaneous saccharification and fermentation of steam-pretreated spruce to ethanol. Appl. Biochem. Biotechnol. 84-86: 69-80 2000.

Brink, D. L. Making alcohol from cotton gin waste and cotton stalks. Proceedings of the symposium on: Cotton gin trash utilization alternatives, University of California Cooperative Extension, Hanford, CA, p.20-27 1981.

Capareda, Sergio, and Parnell, Calvin. Fluidized bed gasification of cotton gin trash for liquid fuel production. Proceedings - Beltwide Cotton Conferences 2097-2105. Publisher: National Cotton Council, 2007.

Chen, W. D., Dong, X. Y., Bai, S., and Sun, Y. Dependence of pore diffusivity of protein on adsorption density in anion-exchange adsorbent. *Biochemical Engineering Journal*, 14 (1), 45-50, 2003.

Chrastil, J., and Wilson, J. T. The effect of chemical and physiological factors on the kinetics for product formation as it relates to enzyme-activity and concentration, reaction-time and to substrate adsorption and affinity. International Journal of Biochemistry 14 (1): 1-17, 1982.

Etters, J. N. Diffusion equations made easy. Textile Chemist Colorist. 12: 140-145 1980.

Fan, L. T., and Lee, Y. H. Kinetic studies of enzymatic hydrolysis of insoluble cellulose: derivation of a mechanistic kinetic model. Biotechnology and Bioengineering, 25 (11): 2707-2733 1983.

Fan, Z. L., South, C., Lyford, K., Munsie, J., van Walsum, P., and Lynd, L. R. Conversion of paper sludge to ethanol in a semicontinuous solids-fed reactor. Bioprocess and Biosystems Engineering, 26(2), 93-101, 2003.

Fournier, R. L. *Basic Transport Phenomena in Biomedical Engineering,* 2nd Taylor & Francis Group, LLC, New York. p. 182-192, 2007.

Frederick, W. J., Iisa, K., Lundy, J. R., OConnor, W. K., Reis, K., Scott, A. T., Sinquefield, S. A., Sricharoenchaikul, V., and Van Vooren, C. A. Energy and materials recovery from recycled paper sludge. TAPPI Journal 79 (6): 123-131 1996.

Galbe, M., Larsson, M., Stenberg, K., Tengborg, T., and Zacch, G. Ethanolfrom wood: design and operation of a process development unit for technoeconomic process evaluation. Fules and Chemicals from Biomass edited by Saha BC, Woodward J. ACS symposium series 666. p. 110-129, 1997.

Gan, Q., Allen, S. J., and Taylor, G. Kinetic dynamics in heterogeneous enzymatic hydrolysis of cellulose: an overview, an experimental study and mathematical modeling. Process Biochemistry, 38 (7), 1003-1018, 2003.

Ganesh, K., Joshi J. B., and Sawant, S. B. Cellulase deactivation in a stirred reactor. Biochemical Engineering Journal 4 (2): 137-141, 2000.

Ghose, T. K. Continuous enzymatic saccharification of gellulose with culture filtrates of *Trichoderma viride* QM 6a. Biotechnology and Bioengineering 11: 239-261 1969.

Glen, J. Paper mill sludge: feedstock for tomorrow. BioCycle, 38 (11): 30-36 1997.

Gregg, J. J, Zander, G. K., and Theis, T. L. Fate of trace elements in energy recovery from recycled paper sludge. TAPPI Journal 80 (9): 157-162 1997.

Hiler, E. A. On-site energy production from agricultural residues. Avail. NTIS. Report (1982), (TENRAC/EDF-074; Order No. DE83900814), 83 pp. From: Energy Res. Abstr. 8(6), Abstr. No. 12104, 1983.

Holt, G. A., Simonton, J. L., Beruvides, M. G., and Canto, A. Utilization of cotton gin by-products for the manufacturing of fuel pellets: An economic perspective. Applied Engineering in Agriculture 20 (4), 423-430, 2004.

Holtzapple, M. T., Caram, H. S., and Humphrey, A. E. A comparison of two empirical models for the enzymatic hydrolysis of pretreated poplar wood. Biotechnology and Bioengineering. 26: 936-941 1984.

Howell, J. A. and Mangat, M. Enzyme deactivation during cellulose hydrolysis. Biotechnology and Bioengineering 20: 847-863 1978.

Huang, S.Y., and Chen, J. C. J. Ethanol production in simultaneous saccharification and fermentation of cellulose with temperature profiling. Ferment. Technol. 66: 509–516 1988.

Jeoh, T. and Agblevor, F. A. Characterization and fermentation of steam exploded cotton gin waste. Biomass and Bioenergy. 21 (2): 109-120 2001.

Kadam, K. L. and Schmidt, S. L. Evaluation of Candida acid othermophi/um in ethanol production from lignocellulosic biomass. Appl. Microbiol. Biotechnol. 48 (6): 709-713 1997.

Kadar, Z., Szengyel, Z., and Reczey, K. Simultaneous saccharification and fermentation (SSF) of industrial wastes for the production of ethanol. Industrial Crops and Products 20 (1): 103-110 2004.

Kerstetter, J. D., Lyford, K., and Lynd, L. Assessment of pulp and paper sludge for conversion to ethanol. Editor(s): Cundiff, John S. Liquid Fuel and Industrial Products from Renewable Resources, Proceedings of the Liquid Fuel Conference, 3rd, Nashville, Sept. 15 -17, 260-267, 1996.

Kim, T. H., and Lee, Y. Y. Pretreatment of corn stover by soaking in aqueous ammonia. Applied Biochemistry and Biotechnology 121: 1119-1131 2005.

Kosstrin, H. M., Himmelblau, D. A., and Traxler, D. Fluidized-bed gasification of solid wastes. Energy and the Environment (Dayton) 6 480-486, 1979.

Lark, N., Xia, Y. K., Qin, C. G., Gong, C. S., and Tsao, G. T. Production of ethanol from recycled paper sludge using cellulase and yeast, Kluveromyces marxianus. Biomass & Bioenergy. 12 (2) 135-143, 1997.

LePori, W. A., Anthony, R. G., Lalk, T. R., Craig, J., and Groves, J. Fluidized-bed energy technology for biomass conversion. Technical Bulletin - Texas Engineering Experiment Station 80-2 32-40, 1980.

LePori, W. A., Anthony, R. G., Lalk, T. R., and Craig, J. D. Fluidized-bed combustion and gasification of biomass. ASAE Publication (4-81, Agric. Energy, v2), 330-334, 1981.

Marques, S., Alves, L., Roseiro, J. C., and Girio, F. M. Conversion of recycled paper sludge to ethanol by SHF and SSF using *Pichia stipitis*. Biomass and Bioenergy, 32(5), 400-406, 2008.

Mishima, D., Kuniki, M., Sel, K., Soda, S., Ike, M., and Fujita, M. Ethanol production from candidate energy crops: Water hyacinth (*Eichhornia crassipes*) and water lettuce (*Pistia stratiotes L.*). *Bioresource Technology* 99(7): 2495-2500, 2008.

Moon, H., Kim, J. S., Oh, K. K., Kim, S. W., and Hong, S. I. Kinetic modeling of simultaneous saccharification and fermentation for ethanol production using steam-exploded wood with glucose- and cellobiose-fermenting yeast, *Brettanomyces custersii*. Journal of Microbiology and Biotechnology. 4, 598-606, 2001.

Oh, K. K., Kim, S. W., Jeong, Y.S., and Hong, S. I. Bioconver sian of cellulose into ethanol by nonisothermal simulta neous saccharification and fermentation. Appl. Biochem. Biotechnol. 89: 15-30 2000.

Ohgren, K., Bura, R., Lesnicki, G., Saddler, J., and Zacchi, G. A comparison between simultaneous saccharification and fermentation and separate hydrolysis and fermentation using steam-pretreated corn stover. Process Biochemistry. 42 (5), 834-839, 2007.

Pan, X.J., Arato, C., Gilkes, N., Gregg, D., Mabee, W., Pye, K., Xiao, Z.Z., Zhang, X., and Saddler, J. Biorefining of softwoods using ethanol organosolv pulping: Preliminary evaluation of process streams for manufacture of fuel-grade ethanol and co-products. Biotechnology and Bioengineering. 90 (4), 473-481, 2005.

Parnell C. B, Lepori W. A, and Capareda, S. C. Converting cotton gin trash into useable energy-technical and economic considerations. Proceedings Beltwide Cotton Conference, National Cotton Council of America, Memphis, TN, Vol. 2: p969-972 1991.

Pessarakli, M. Composting gin trash reduces waste-disposal and pollution problems. J. Environ. Sci. Health Part A Environ Sci. Eng., 25(8): 237-1047, 1990.

Pettersson, P. O., Eklund, R., and Zacchi, G. Modeling simultaneous saccharification and fermentation of softwood. Applied Biochemistry and Biotechnology. 98, 733-746, 2002.

Philippidis G. P., Hatzis C. Biochemical engineering analysis of critical process factors in the biomass to ethanol technology. Biotechnology Progress 13 (3): 222-231, 1997.

Philippidis G. P., Spindler, D. D. and Wyman, C. E. Mathematical modeling of cellulose conversion to ethanol by the simultaneous saccharification and fermentation process. Applied Biochemistry and Biotechnology. 34-5: 543-556, 1992.

Philippidis G. P., Smith, T. K., and Wyman, C. E. Study of the enzymatic hydrolysis of cellulose for production of fuel ethanol by simultaneous saccharification and fermentation process. Biot4echnology and Bioengineering 41 (9): 846-853, 1993.

Rudolf, A., Alkasrawi, M., Zacchi, G., and Liden, G. A comparison between batch and fed-batch simultaneous saccharification and fermentation of steam pretreated spruce. Enzyme and Microbial Technology. 37 (2), 195-204, 2005.

Ruiz, E., Cara, C., Ballesteros, M. Manzanares, Paloma; Ballesteros, Ignacio; and Castro, Eulogio. Ethanol production from pretreated olive tree wood and sunflower stalks by an SSF process. Applied Biochemistry and Biotechnology. 29-132: 631-643 2006.
Shen, J., and Agblevor, F.A. The operable modeling of simultaneous saccharification and fermentation of ethanol production from cellulose. Submitted. 2008.

Shin, D., Yoo, A., Kim, S. W., and Yang, D. R. Cybernetic modeling of simultaneous saccharification and fermentation for ethanol production from steam-exploded wood with Brettanomyces custersii. Journal of Microbiology and Biotechnology. 16 (9), 1355-1361, 2006.

Soderstrom, J., Galbe, M., and Zacchi, G. Separate versus simultaneous saccharification and fermentation of two-step steam pretreated softwood for ethanol production. Journal of Wood Chemistry and Technology 25 (3): 187-202 2005.

South, C. R., Hogsett, D. A. L., and Lynd, L. R. Modeling simultaneous saccarification and fermentation of lignocellulose to ethanol in batch and continuous reactors. Enzyme and Microbial Technology. 17 (9), 797-803, 1995.

Stenberg, K., Bollok, M., Reczei, K., Galbe, M., and Zacchi, G. Effect of substrate and cellulase concentration on simultaneous saccharification and fermentation of steam-pretreated softwood for ethanol production. Biotechnol. Bioeng. 68: 205-210 2000.

Sun, Y., and Cheng, J. Y. Hydrolysis of lignocellulosic materials for ethanol production: a review. Bioresour. Technol. 83 (1): 1-11 2002.

Thomasson, J. A. A review of cotton gin trash disposal and utilization. Proceedings Beltwide Cotton Production and Research Conference, National Cotton Council of America, Memphis, TN, p689-705 1990.

Viruthagiri, T., and Sasikumar, E. Simultaneous saccharification and fermentation of recycled paper sludge for ethanol production. Asian Journal of Microbiology, Biotechnology & Environmental Sciences, 9(3), 587-590, 2007.

Wu, Z. W., and Lee, Y. Y. Nonisothermal simultaneous saccharification and fermentation for direct conversion of lignocellulosic biomass to ethanol. Applied Biochemistry and Biotechnology 70-72: 479-492 1998.

Zabaniotou, A. A., Roussos, A. I., and Koroneos, C. J. A laboratory study of cotton gin waste pyrolysis. Journal of Analytical and Applied Pyrolysis 56(1), 47-59, 2000.

Zhang, J., and Lynd, L. Simultaneous saccharification and cofermentation of paper sludge to ethanol by recombinant xylose-fermenting microbes. Preprints of Symposia - American Chemical Society, Division of Fuel Chemistry. 52(2), 431-432, 2007.

Zhu, S. D., Wu, Y. X., Zhao, Y. F., Tu, S. Y., and Xue, Y. P. Fed-batch simultaneous saccharification and fermentation of microwave/acid/alkali/H2O2 pretreated rice straw for production of ethanol. Chemical Engineering Communications. 193 (5), 639-648, 2006.

Chapter Three

Kinetics of Enzymatic Hydrolysis of Steam-exploded Cotton Gin Waste*

3.1 Introduction

Cotton gin waste (CGW) is a massive residue from USA cotton industry. Cotton gin waste consists of broken cotton fibers, stems, and leaves [Pessarakli, 1990]. It contains cellulose and hemicellulose, both of which can be converted into monomeric sugars through hydrolysis, and these sugars can be used to produce ethanol and other high-value chemicals through fermentation process. As discussed in Chapter Two, some investigations about conversion of CGW into bio-fuel have been conducted by Brink [1981], Beck and Clements [1982], Parnell et al. [1991], Jeoh and Agblevor [2001], Agblevor et al. [2003]. However, an enzymatic hydrolysis kinetics of CGW has been not reported in literature. In this chapter, the kinetics of enzymatic hydrolysis of steam-exploded cotton gin waste is reported.

3.2 Objectives

The objectives of this study were

(1) To investigate the hydrolytic kinetics of cotton gin waste using two commercial enzymes;

(2) To develop a simple model of enzymatic hydrolysis based on enzyme deactivation;

* Jiacheng Shen and Foster A. Agblevor. Optimization of enzyme loading and hydrolytic time in the hydrolysis of the mixtures of cotton gin waste and recycled paper sludge for the maximum profit rate. Biochemical Engineering Journal. 41: 241-250 2008.

(3) To apply this model to the hydrolytic kinetics of cotton gin waste and determine the values of the model parameters;

(4) To estimate the diffusivities of the two enzymes on cotton gin waste.

3.3 Development of Enzymatic Hydrolysis Model

Assumptions of the model were

(1) The cellulase enzyme containing endo-β-1,4-glucanase, exo-β-1,4-cellobiohydrolase, and glycosidase was assumed to be a single enzyme that hydrolyzes insoluble substrate to produce reducing sugars;

(2) The structure of the insoluble substrate fiber were considered homogeneous, *i.e.* there is no distinction between amorphous and crystalline regions. In fact, this assumption is in agreement with the requirement of the Langmuir adsorption model;

(3) The enzyme deactivation was assumed to be a second order reaction and the main factor influencing the hydrolytic rate.

The free enzymes (e) (g/l) in a suspension are adsorbed on the active sites on the surface of the insoluble substrate (C) (g/l) to form complexes (Ce^*) (g/l), which is expressed in the following reaction.

$$C + e \Leftrightarrow Ce^* \tag{3.1}$$

where the forward reaction represents an adsorption, whose rate constant is k_1' (l/(g.h), and the backward reaction represents a desorption, whose rate constant is k_{-1}' (l/(g.h)). These complexes will produce reducing sugars (G) (g/l) and free enzymes (Eq. (3.2)).

$$Ce^* \xrightarrow{k_2'} G + e \tag{3.2}$$

where $k_2^{'}$ (h^{-1}) is the rate constant of the sugar formation. These complexes include the effective complexes that will produce the reducing sugars, and the ineffective complexes that make the enzymes lose their activities, and do not take part in the hydrolysis.

According to the law of mass action, the reaction rate should be a product of the n^{th} power of the reactants. Thus, the complex-forming rate from reactions (3.1) and (3.2) is

$$\frac{dCe^*}{dt} = k_1^{'}C \times e - k_{-1}^{'}Ce^* - k_2^{'}Ce^* \tag{3.3}$$

Considering the substrate mass balance, the un-reacting substrate concentration, C, is given by

$$C = C_0 - Ce^* - G \tag{3.4}$$

where C_0 (g/l) is the initial substrate concentration. Substituting Eq. (3.4) into Eq. (3.3) yields

$$\frac{dCe^*}{dt} = k_1^{'}\left(C_0 - Ce^* - G\right)e - k_{-1}^{'}Ce^* - k_2^{'}Ce^* \tag{3.5}$$

Applying the quasi-steady state condition to Eq. (3.5), the complex concentration is

$$Ce^* = \frac{(C_0 - G)e}{K_e + e} \tag{3.6}$$

$$K_e = \frac{k_{-1}^{'} + k_2^{'}}{k_1^{'}} \tag{3.7}$$

where K_e (g/l) is the equilibrium constant.

At any time during the hydrolysis, the sugar-forming rate from reaction (3.2) is

$$\frac{dG}{dt} = k_2^{'}Ce^* \tag{3.8}$$

At the initial time, Eq. (3.8) becomes

$$\left(\frac{dG}{dt}\right)_{G0} = k_2^{'} Ce_0^* \tag{3.9}$$

where $\left(\frac{dG}{dt}\right)_{G0}$ denotes the sugar-forming rate at the initial time. Substituting Eq. (3.6) in Eqs. (3.8) and (3.9) at t = 0, and t = t, respectively, Eqs. (3.8) and (3.9) become

$$\frac{dG}{dt} = \frac{k_2^{'} e(C_0 - G)}{K_e + e} \tag{3.10}$$

$$\left(\frac{dG}{dt}\right)_{G0} = \frac{k_2^{'} C_0 e_0}{K_e + e_0}. \tag{3.11}$$

Similarly with a definition of the activation of a catalyst pellet [Levenspiel, 1972], the activation of an enzyme on the insoluble substrate is defined as follows:

$$a = \frac{actual\ rate\ of\ substrate\ conversion\ by\ enzyme}{rate\ of\ substrate\ conversion\ by\ enzyme\ without\ adsorption} = \frac{r_G}{r_{G0}} = \frac{\left(\frac{dG}{dt}\right)}{\left(\frac{dG}{dt}\right)_{G0}} \tag{3.12}$$

According to this definition, the dimensionless activity, a, of an enzyme should be less or equal to one. Hence, Eq. (3.10) becomes

$$\frac{dG}{dt} = \frac{k_2^{'} a C_0 e_0}{K_e + e_0} \tag{3.13}$$

Assuming that the enzyme deactivation by the insoluble substrate is independent, and follows assumption 3, the deactivation rate can be expressed in equation (3.14) [Levenspiel, 1972],

$$\frac{da}{dt} = -k_3^{'} a^2 \tag{3.14}$$

where $k_3^{'}$ (h^{-1}) is the enzyme deactivation rate constant. Integrating Eq. (3.14) with the boundary conditions a = 1 at t = 0, and a = a at t = t produces

$$a = \frac{1}{1 + k_3' t} \tag{3.15}$$

Substituting Eq. (3.15) into Eq. (3.13) produces

$$\frac{dG}{dt} = \frac{k_2' Ce^*}{1 + k_3' t} = \frac{k_2' C_0 e_0}{\left(1 + k_3' t\right)\left(K_e + e_0\right)} \tag{3.16}$$

Since k_2', C_0, e_0, k_3', and K_e are constants, Eq. (3.16) can be integrated with the boundary conditions G = 0 at t = 0, and G = G at t = t, which produces

$$G = b' \ln\left(1 + k_3' t\right) \tag{3.17}$$

$$b' = \frac{k_2' Ce_0^*}{k_3'} = \frac{k_2' C_0 e_0}{k_3'\left(K_e + e_0\right)} \tag{3.18}$$

where the constant b' has a unit of g/l. Eq. (3.17) is a two-parameter model. Because Eq. (3.17) expresses the natural logarithm relationship between the product concentration and time, it is expected that the model can describe the wide ranges of product concentration and time. However, since the production concentration increases with increase in time, and product concentration approaches infinity when time approaches infinity, the model is not suitable for extrapolating the product concentration beyond the experimental time range.

To evaluate the overall effect of the enzyme, and to compare the activities of various enzymes during the hydrolysis period, an average dimensionless activity of the enzyme in a hydrolytic time t is defined as follows:

$$A_{ave} = \frac{1}{t}\int_0^t a\,dt \tag{3.19}$$

If the enzyme deactivation follows the second order kinetics, the average dimensionless activity of the enzyme should be

$$A_{ave} = \frac{\ln\left(1 + k_3' t\right)}{t k_3'} \tag{3.20}$$

Eq. (3.20) indicates that the average dimensionless activity of A_{ave} is a function of both the residence time t and the rate constant k_3' of the enzyme deactivation. To evaluate the efficiency of the enzyme, both factors k_3' and t should be considered.

3.4 Materials and Methods

3.4.1 Materials

Cotton gin waste was obtained from MidAtlantic Cotton Gin, Inc. (Emporia, VA). The two enzymes used in the experiments were Novozymes NS50052 (Novozymes, North America, Inc. Franklinton, NC), and Spezyme AO3117 (Genencor International, Rochester, NY, USA). The actual activities were 97 Filter Paper Unit (FPU)/ml for the Novozymes enzyme and 29 FPU/ml for the Spezyme enzyme using Ghose's method [1987].

3.4.2 Methods

3.4.2.1 Pretreatment of materials

The raw cotton gin waste was pretreated by steam explosion for 2 minutes at 220°C in a 25-l batch reactor located at the Thomas M. Brooks Forest Products Center, Blacksburg, Virginia. The severity factor ($\log(R_0)$) for the residence time and temperature was calculated to be 3.83 according to the concept of the reaction ordinate [Overend and Chornet, 1987].

$$\log\left(R_0\right) = \log\left[\int_0^t \exp\left(\frac{T_r - T_b}{14.75}\right) dt\right] = \log\left[t \exp\left(\frac{T_r - T_b}{14.75}\right)\right] \tag{3.21}$$

where log is the common logarithm based on 10, R_0 (dimensionless) is the reaction ordinate, t (minutes) is the residence time, T_r (^oC) is the explosion temperature, and T_b is the base temperature (100^oC). The constant 14.75 is the activation energy, assuming that the overall process is hydrolytic and obeys first order kinetic law. In Eq. (3.21) it is assumed that the explosion temperature T_r is constant (*i.e.* the time for preheating can be ignored). The steam-exploded cotton gin waste contained about 65% water.

3.4.2.2 Enzymatic hydrolysis and analytical method

The steam-exploded cotton gin waste of 10.5 g (dry basis) was added to 500 ml flasks, and these flasks were sterilized in an autoclave at 121^oC for 1 hour. After sterilization, 0.3 liter sodium acetate buffer (0.1 M) at pH 5.0 and various quantities of the enzyme were added to the flasks. The initial enzyme concentrations were from 0.593 g/l (1.54 FPU/g of enzyme loading on dry substrate) to 4.73 g/l (12.3 FPU/g) for Novozymes, and from 0.641 g/l (0.460 FPU/g) to 5.11 g/l (3.68 FPU/g) for Spezyme. The suspensions in the flasks were hydrolyzed for 7 hours in a reciprocating shaker bath (Versa-Baths, Fisher Scientific) at 50°C and 80 rpm. Aliquots of 1 ml were taken from the suspension at various intervals, and centrifuged at 6000 rpm for 5 minutes (Marathon26km, Fisher Scientific). DNS method was used to determine the reducing sugar contents in the supernatants [Miller, 1959].

3.5 Results and Discussion

3.5.1 The effect of the initial enzyme concentrations on the hydrolysis of steam-exploded cotton gin waste

The effect of the initial enzyme concentrations of Novozymes and Spezyme on the hydrolysis of steam-exploded cotton gin waste is shown in Figs. 3.1 and 3.2, respectively. With increase in residence time and initial enzyme concentration (or enzyme loading), reducing sugar concentrations increased. For example, the reducing sugar concentration increased from 2.33 g/l to 6.41 g/l when the initial Novozymes enzyme concentration was increased from 0.593 g/l to 4.73 g/l. Similarly, in the corresponding initial concentration range of Spezyme enzyme, the reducing sugar concentration increased from 1.65 g/l to 4.92 g/l. Although an increase in the initial enzyme concentration can enhance the reducing sugar concentration, it is necessary to compare the reducing sugar yields per gram of enzyme and per FPU of enzyme from an economic point of view. Figs. 3.3 and 3.4 show two such comparisons for the two enzymes. The highest yields of reducing sugar were obtained at the lowest initial enzyme concentrations, and the yields of Novozymes were higher than those of Spezyme (Fig. 3.3). However, the yields per FPU of Novozymes were lower than those of Spezyme (Fig. 3.4). These results suggest that the optimal dosages of the initial enzymes should be determined on the basis of the enzyme cost, yield per gram enzyme, and yield per FPU enzyme.

The data from the variation of the reducing sugar concentrations with time were fitted into Eq. (3.17) using nonlinear regression, and the constants k_3' and b' were determined and are shown in Tables 3.1 and 3.2. For both enzymes, enzyme deactivation decreased with increase in the initial enzyme concentration as shown by the decrease in the constant k_3' in Tables 3.1 and 3.2. However, this enzyme deactivation was not inversely proportional to the increase in initial enzyme concentration because the ratios (Tables 3.1 and 3.2) of k_3' and the initial enzyme concentration e_0 greatly decreased, from 14.8 (l/h.g)

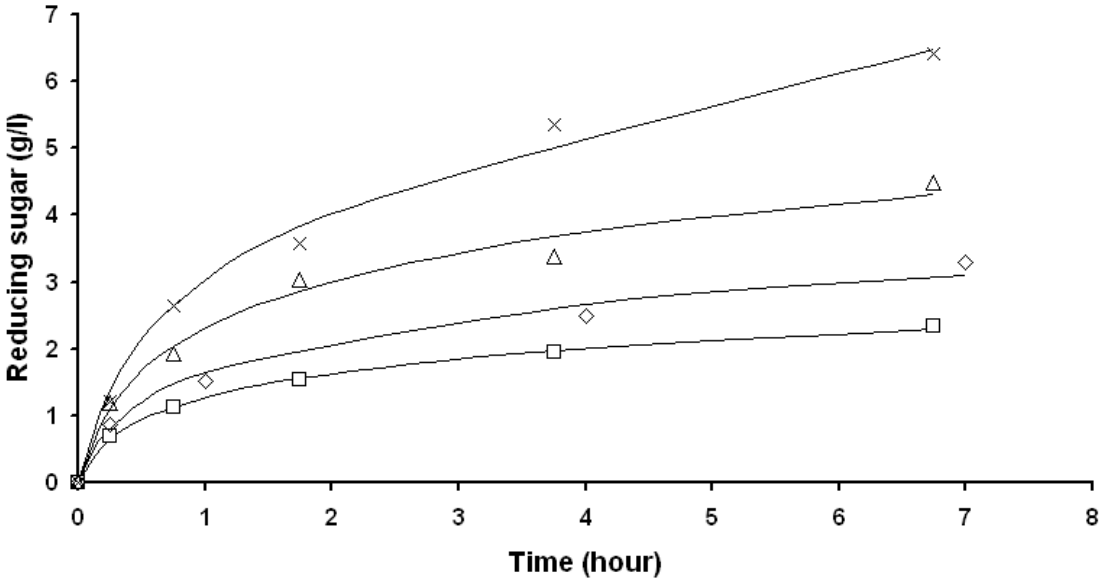

Fig. 3.1 Hydrolytic kinetics of cotton gin waste using Novozymes NS50052. Experimental conditions: cotton gin waste concentration 35 g(dry)/l, temperature 50°C, and 80 rpm. Initial enzyme concentrations (g/l): □ 0.593, ◊ 1.18, Δ 2.36, and × 4.73. Solid lines represent the model values (Eq. 3.17) of the corresponding enzyme concentrations.

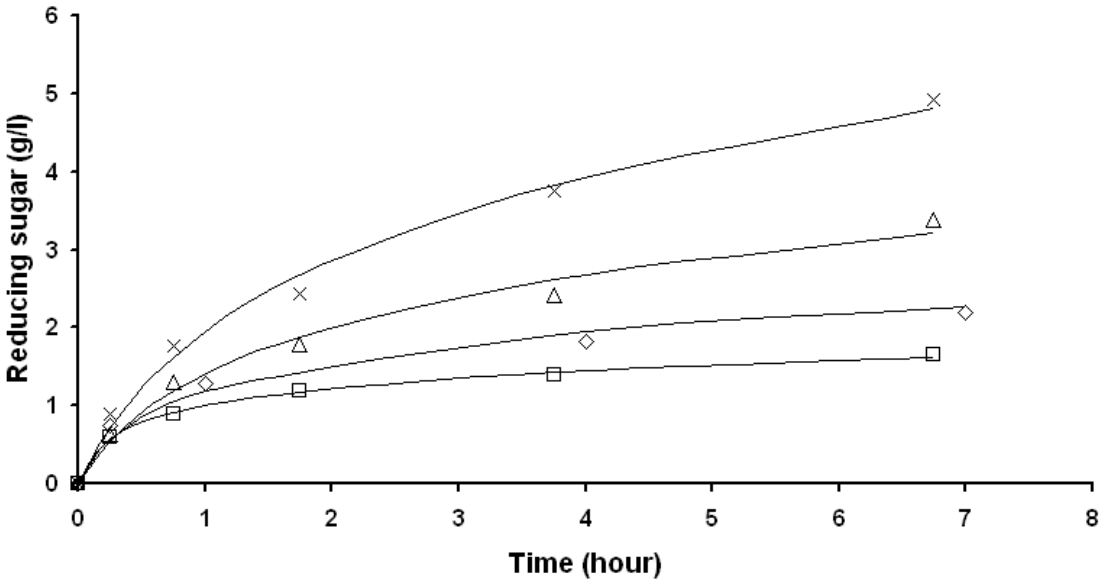

Fig. 3.2 Hydrolytic kinetics of cotton gin waste using Spezyme AO3117. Experimental conditions: cotton gin waste concentration 35 g(dry)/l, temperature 50°C, and 80 rpm. Initial enzyme concentrations (g/l): □ 0.641, ◊ 1.28, Δ 2.55, and × 5.11. Solid lines represent the model values (Eq. 3.17) of the corresponding enzyme concentrations.

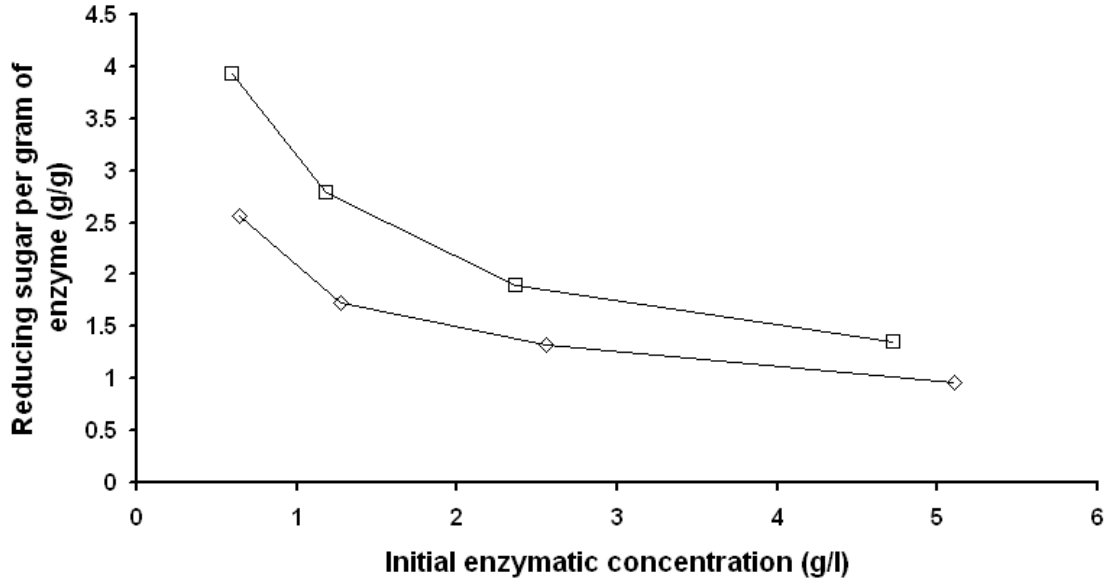

Fig. 3.3 A comparison of the reducing sugar yields per gram enzyme (g/g). □ Novozymes; ◊ Spezyme.

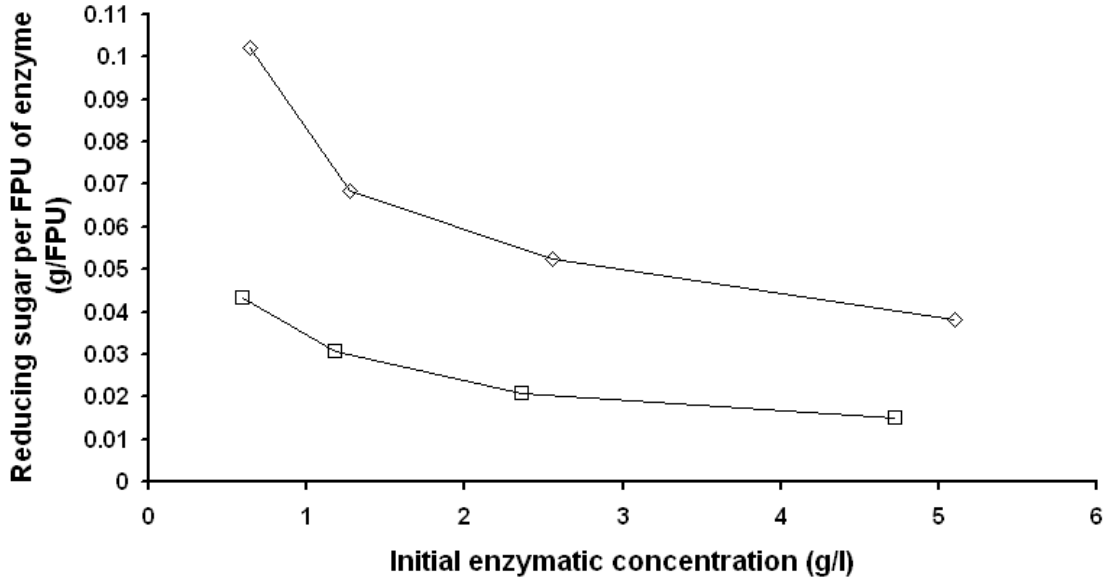

Fig. 3.4 A comparison of the reducing sugar yields per FPU of enzyme (g/FPU). □ Novozymes; ◊ Spezyme.

to 1.12 (l/h.g) for Novozymes and from 28.7 (l/h.g) to 0.374 (l/h.g) for Spezyme instead of being constant with increase in initial enzyme concentration. The k_3' values of Novozymes were lower than those of Spezyme at the lower initial enzyme concentrations ($\leq$ 1.28 g/l); but at a higher initial enzyme concentrations ($\geq$2.36 g/l), the k_3' values of Novozymes were greater than those of Spezyme.

The average dimensionless activities of the two enzymes from Eq. (3.20) are shown in Tables 3.1 and 3.2. The average dimensionless activities for the two enzymes increased with increasing initial enzyme concentration. At the lower initial enzyme concentrations ($\leq$ 1.28 g/l), the average dimensionless activities of Novozymes were greater than those of Spezyme. At the higher initial enzyme concentrations ($\geq$ 2.36 g/l), the average activities of Novozymes were lower than those of Spezyme. These phenomena can be explained by the fact that the Novozymes enzyme has a higher activity (FPU/ml) than that of the Spezyme enzyme. At a high initial enzyme concentration, the Novozymes enzyme quickly hydrolyzed the most accessible substrate. Towards the end of the hydrolysis period, the hydrolytic rate dropped because the most accessible substrate had been consumed. In contrast, the Spezyme enzyme had a lower activity, hence, it could maintain relatively high hydrolytic rate for a longer period because there was accessible substrate to be consumed. These results may suggest that using the Spezyme enzyme in a high initial concentration would be more effective.

The average dimensionless activity of the enzyme during a hydrolytic process is related to the residence time, and it can be shown by the following method that the longer the residence time, the lower the average dimensionless activity. Differentiating Eq. (3.20) with respect to tk_3 produces

Table 3.1 Model parameters (Eq. 3.17), average dimensionless activity (Eq. 3.20), and diffusivities ((Eq. 3.30) for Novozymes

e_0 (g/L)	e_d (FPU/g)	b' (g/l)	k_3' (h^{-1})	k_3'/e_0 (l/h.g)	A_{ave}	D (m^2/s)
0.593	1.54	0.561	8.77	14.8	0.0629	7.54E-17
1.18	3.08	0.791	7.01	5.93	0.0819	7.09E-17
2.36	6.16	1.12	6.79	2.87	0.0839	6.60E-17
4.73	12.3	1.65	5.28	1.12	0.101	7.34E-17

e_d The enzyme loading based on the dry substrate (FPU/g)

Table 3.2 Model parameters (Eq. 3.17), average dimensionless activity (Eq. 3.20), and diffusivities (Eq. 3.30) for Spezyme

e_0 (g/L)	e_d (FPU/g)	b' (g/l)	k_3' (h^{-1})	k_3'/e_0 (l/h.g)	A_{ave}	D (m^2/s)
0.641	0.460	0.336	18.4	28.7	0.0389	4.89E-17
1.28	0.920	0.458	15.3	12.0	0.0450	4.58E-17
2.55	1.84	1.11	2.56	1.00	0.168	6.80E-17
5.11	3.68	1.81	1.91	0.374	0.204	6.05E-17

e_d The enzyme loading based on the dry substrate (FPU/g)

Table 3.3 Constants $k_2'C_0$ (V_m), k_2' and K_e (K) for the two enzymes

Enzyme Name	$k_2'C_0$ (V_m) g/(l.h))	k_2' (/h)	K_e (K) (g/l)	SOSE
Novozymes (linear)	1.41	0.0403	0.642	8.68E-3
Novozymes (nonlinear)	1.42	0.0406	0.655	8.60E-3
Spezyme (linear)	0.944	0.0270	0.378	1.06E-4
Spezyme (nonlinear)	0.951	0.0272	0.390	1.02E-4

SOSE Sum of square errors

$$\frac{da_{ave}}{d\left(tk_3^{'}\right)} = \frac{tk_3^{'} - \left(1+tk_3^{'}\right)\ln\left(1+tk_3^{'}\right)}{\left(tk_3^{'}\right)^2\left(1+tk_3^{'}\right)} \tag{3.22}$$

Equating Eq. (3.22) to zero,

$$tk_3^{'} - \left(1+tk_3^{'}\right)\ln\left(1+tk_3^{'}\right) = 0 \tag{3.23}$$

it produces

$$tk_3^{'} = 0.00026 \tag{3.24}$$

Eq. (3.24) indicates that when t is smaller than $0.00026/k_3^{'}$, the derivative $da_{ave}/d(tk_3^{'})$ (Eq. (3.22)) is negative. Therefore, the average dimensionless activity of the enzyme will decrease with increasing time because the residence time of the substrate in a hydrolytic process is almost always greater than the critical residence time $t_c = 0.00026/k_3^{'}$. For example, the critical residence times are only 0.107 second and 0.0509 second for the initial enzyme concentrations 0.593 g/l ($k_3^{'} = 8.77\ h^{-1}$) of Novozymes and 0.641 g/l ($k_3^{'} = 18.4\ h^{-1}$) of Spezyme, respectively. Furthermore, it is also concluded that a comparison of the average dimensionless activities of the two enzymes should be done for the same residence time.

3.5.2 Determination of constants K_e and $k_2^{'}$ in Eq. (3.10) using the initial product-formation rates at various initial enzyme concentrations

Fig. 3.5 shows the initial sugar-formation rates (sugar concentration change in the initial 15 minutes) versus various initial concentrations for the two enzymes. Both curves in Fig. 3.5 have shapes similar to the Langmuir adsorption curve: the initial product-formation rates increased and approached the maximum values with increasing initial concentrations for the two enzymes. The initial rates for Novozymes were greater than those for Spezyme.

The constants K_e and $k_2^{'}$ of Eq. (3.18) can be estimated by linear and nonlinear regressions from the initial sugar-formation rates. Eq. (3.11) can be linearized as follows:

$$\frac{1}{(dG/dt)_{G0}} = \frac{K_e}{k_2^{'} C_0 e_0} + \frac{1}{k_2^{'} C_0} \tag{3.25}$$

The plots of the initial sugar-formation rates versus various initial enzyme concentrations for the two enzymes were linear (Fig. 3.6). The intersections and slopes of two straight lines represented the constants $k_2^{'}C_0$ and K_e shown in Table 3.3. The correlation coefficients of the two lines in Fig. 3.6 for Novozymes and Spezyme were 0.987 and 0.999, respectively. The constants K_e and $k_2^{'}$ in Eq. (3.18) can also be obtained directly by fitting the initial rates in Eq. (3.11) (nonlinear method). The fitted results are also shown in Table 3.3. Because the nonlinear method has a smaller sum of square errors (8.60E-3 and 1.02E-4 for Novozymes and Spezyme, respectively) than those of the linear method (8.68E-3 and 1.06E-4 for Novozymes and Spezyme, respectively), the nonlinear method is more precise. The equilibrium constant K_e and the product formation rate constant $k_2^{'}$ of Novozymes in Table 3.3 were greater than those of Spezyme. The constant K_e represents the ratio of the rate constant of complex-consuming and the rate constant of complex-forming (Eq. (3.7)). The greater the equilibrium constant K_e, the faster the complex consumption or the slower the complex formation. Therefore, the complexes from Novozymes were consumed faster than those from Spezyme, which explains the higher activity of the Novozymes enzyme.

On the other hand, Bailey [1989] proposed an enzymatic kinetic model of cellulose hydrolysis using the free enzyme concentration:

$$v = \frac{V_m e}{K + e} \tag{3.26}$$

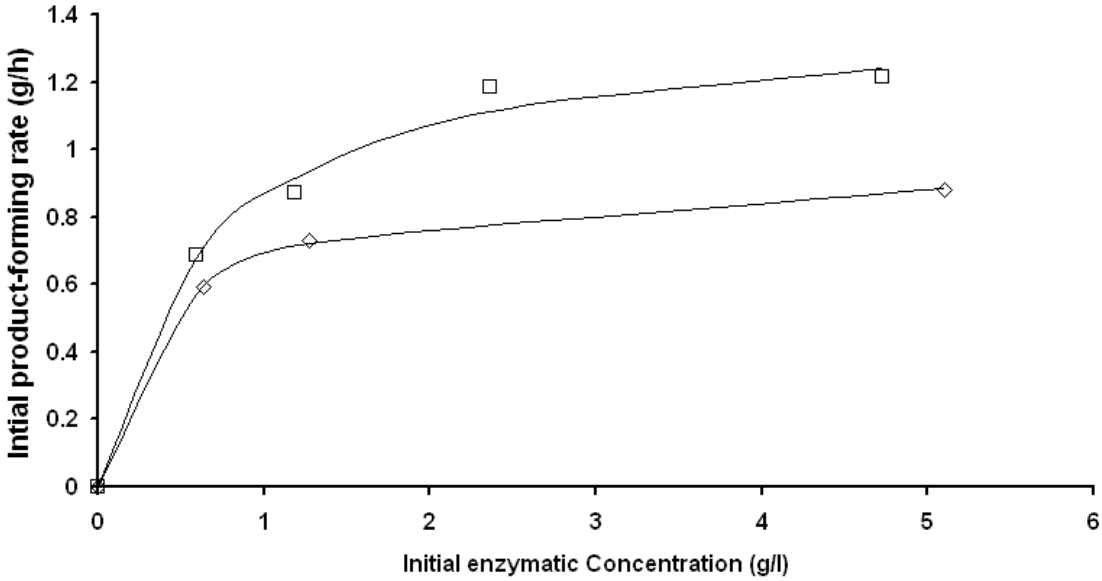

Fig. 3.5 Initial product-forming rates versus initial enzyme concentrations. □ Novozymes, ◊ Spezyme. Solid lines represent model values (Eq. 3.11) of the corresponding enzymes.

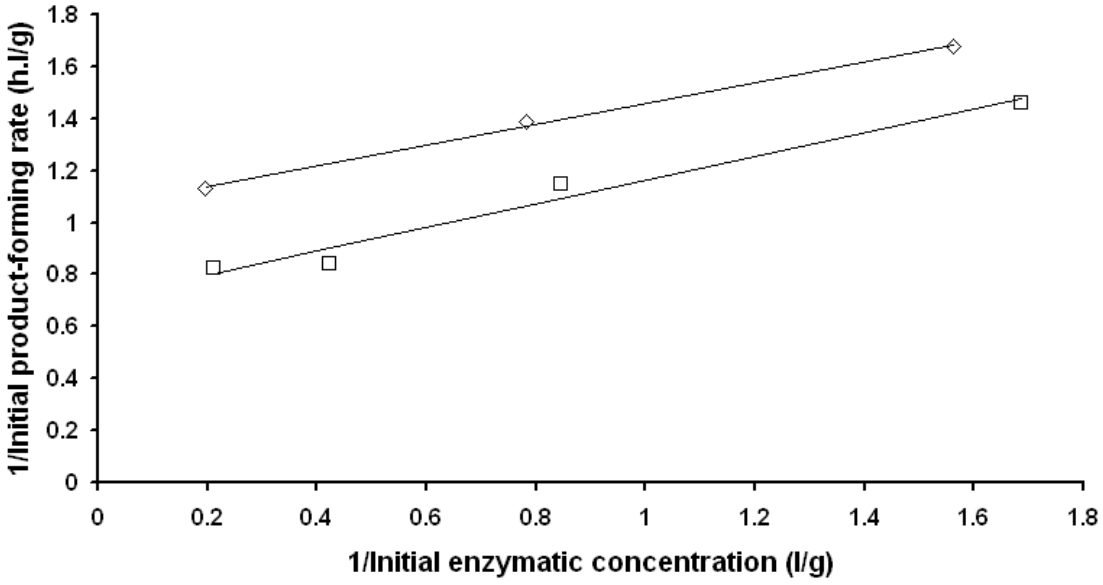

Fig. 3.6 Constants $k_2' C_0$ (V_m) and K_e (K) determined from initial product-forming rates. □ Novozymes, ◊ Spezyme. Solid lines represent model values (Eq. 3.25) of the corresponding enzymes.

where v (g/(l.h)) is the hydrolytic rate, V_m (g/(l.h)) is the maximum hydrolytic rate, and K (g/l) is the half-saturation constant. Comparing Eq. (3.26) at the initial time with Eq. (3.11), the relationships between V_m and $k_2' C_0$, and K and K_e can be obtained.

$$V_m = k_2' C_0 \tag{3.27}$$

$$K = K_e \tag{3.28}$$

Thus, the maximum hydrolytic rate of Novozymes was greater than that of Spezyme (Table 3.3).

3.5.3 Estimation of apparent diffusivities of enzymes on cotton gin waste

Equating Eq. (3.10) to Eq. (3.16) and solving this equal equation for e produces

$$e = \frac{C_0 K_e e_0}{\left(1 + k_3' t\right)\left(K_e + e_0\right)\left(C_0 - G\right) - C_0 e_0} \tag{3.29}$$

Substituting the constants k_3', and K_e in Tables 3.1, 3.2, and 3.3, and the sugar concentrations and initial enzyme concentrations in the experiments into Eq. (3.29), the free enzyme concentrations at various initial enzyme concentrations with time course can be obtained. Once the free enzyme concentrations are known, the adsorbed enzyme on the cotton gin waste can be calculated from the enzyme mass balance. Thus, the diffusivity of the enzyme on the cotton gin waste can be estimated using Fick's second law. Assuming 1) that a homogenous cylinder (*e. g.* fibers of CGW) is placed in a well-stirred solution of limited volume (*e. g.* a hydrolytic reactor with agitation), 2) that the solute (enzyme) concentration in the solution is always uniform and the initial solute concentration is equal to zero, and 3) that the cylinder is initially free from solute, a series expression for the adsorbed solute fraction and diffusivity of solute on solid at a high uptake fraction is given [Crank, 1975]:

$$\frac{q}{q_\infty} = \frac{1+\alpha}{1+1/4\alpha}\left[1 - \frac{\alpha\left(Dt/r^2\right)^{-1/2}}{2\pi^{1/2}\left(1+1/4\alpha\right)} + \frac{\alpha^3\left(Dt/r^2\right)^{-3/2}}{16\pi^{1/2}\left(1+1/4\alpha\right)^3} - \frac{3\alpha^5\left(Dt/r^2\right)^{-5/2}}{128\pi^{1/2}\left(1+1/4\alpha\right)^5} + ...\right] \quad (3.30)$$

$$\alpha = \frac{E_0 v - q_\infty M}{q_\infty M} \quad (3.31)$$

where e_0 is the initial enzyme concentration (g/l) in the suspension, D is the apparent diffusivity (m^2/h) of enzyme in insoluble substrate, M is the initial quantity (gram) of insoluble substrate in the suspension, q is the uptakes (g/g) of enzyme at time t, q_∞ is the uptakes (g/g) of enzyme at equilibrium time, r is the radius (m) of fiber, t is the residence time (h), V is the volume (liter) of liquid, and α is the ratio of the mass of the free enzyme in the suspension to the mass of the adsorbed enzyme in the insoluble substrate under equilibrium conditions. Therefore, if the function of the enzyme uptake fraction q/q_∞ with time t is known, the diffusivity of the enzyme can be estimated by a fitting process of Eq. (3.30). Figs. 3.7 and 3.8 show the adsorptive complex fractions with time course and the simulated curves using Eq. (3.30). The diffusivities of the enzymes on the steam-exploded CGW were between 6.60E-17 - 7.54E-17 m^2/s for Novozymes, and 4.58E-17 - 6.80E-17 m^2/s for Spezyme (Tables 3.1 and 3.2). It appears that the change in diffusivities was not monotonous with changing enzyme concentration. The average diffusivities were 7.14E-17 m^2/s for Novozymes, and 5.58E-17 m^2/s for Spezyme, assuming that the diffusivities did not change in the experimental enzyme concentration ranges. The results were somewhat smaller than those (9.0E-17-11.2E-17 m^2/s) for dye Disperse Yellow 23 on Polyester Fiber derived from the internal diffusion model [Etters, 1980]. The difference could be attributed to the cellulase (protein) molecular weight,

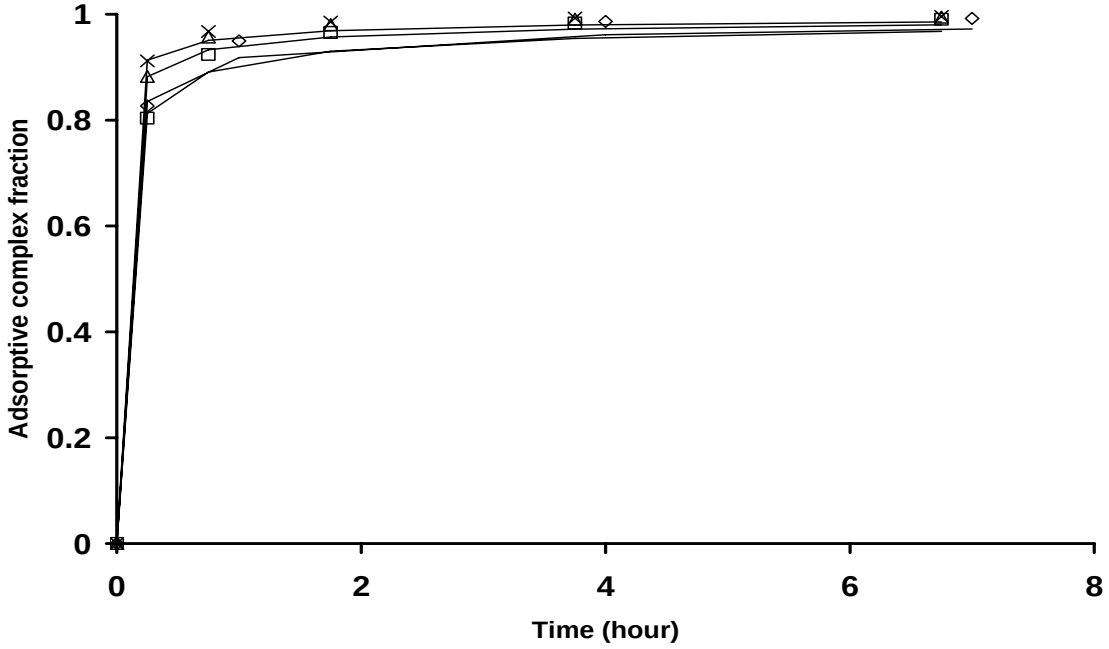

Fig. 3.7 Simulated enzyme complex uptake fraction of Novozymes with time. Initial enzyme concentrations (g/l): □ 0.593, ◊ 1.18, Δ 2.36, and × 4.73. Solid lines represent the model values (Eq. 3.30) from calculated diffusivities of the corresponding enzyme concentrations.

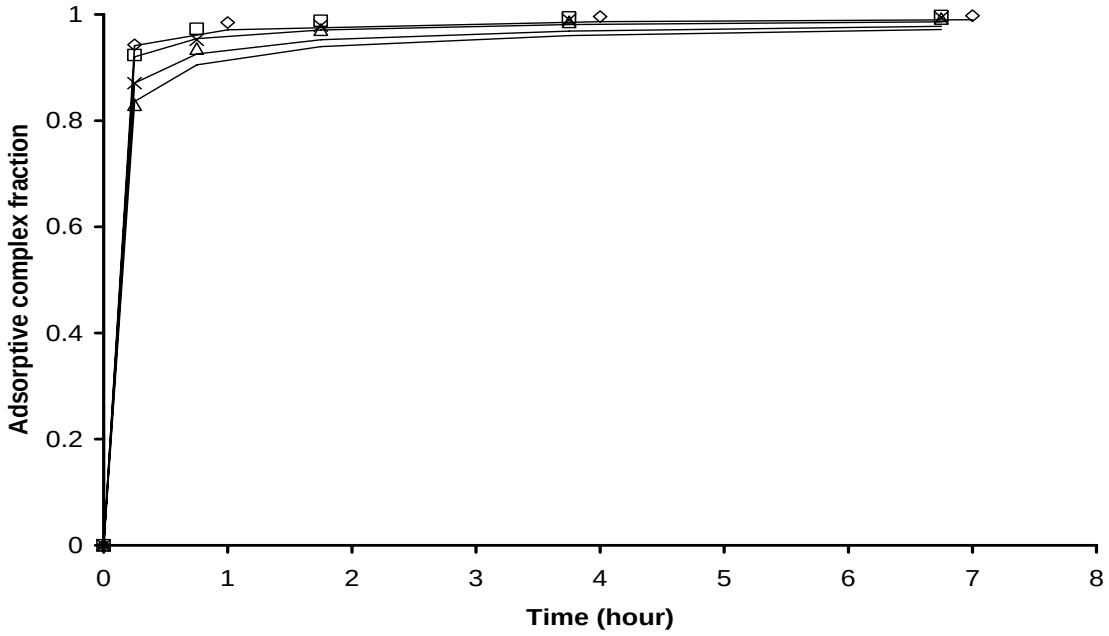

Fig. 3.8 Simulated enzyme complex fraction of Spezyme with time. Initial enzyme concentrations (g/l): □ 0.641, ◊ 1.28, Δ 2.55, and × 5.11. Solid lines represent the model values (Eq. 3.30) from calculated diffusivities of the corresponding enzyme concentrations.

which is greater than that of the dye, resulting in the slower diffusion rate.

3.6 Conclusions

Cotton gin waste, which is a lignocellulosic material, is a residue from the cotton ginning industry. It is potentially a raw material for the production of bioethanol. This study demonstrates that the carbohydrates in CGW can be converted into reducing sugars using steam-explosion pretreatment and enzymatic hydrolysis. Because of the huge mass of CGW produced by the USA cotton industry, the investigation points out a new way to produce bioethanol from industrial wastes as well as solve the waste disposal problem. The two-parameter model developed in this study can describe a wide range of change in sugar concentration with time, which is attributed to its expression of the natural logarithm relationship between the sugar concentration and time. The model provides a simple method to describe the kinetic behavior of enzymatic hydrolysis of insoluble substrate for industrial applications. The model was successfully used to fit the experimental data of enzymatic hydrolysis of cotton gin waste. This study also proposes a method based on a series expression from Fick's second law to estimate the diffusivity of an enzyme on an insoluble substrate.

References

Agblevor, F. A., Batz, S., and Trumbo, J. Composition and ethanol production potential of cotton gin residues. Applied Biochemistry and Biotechnology 105-108: 219-230 2003.

Beck, R. S., and Clements, D. L. Ethanol production from cotton gin trash. Proceedings of the symposium on: Cotton gin trash utilization alternatives, Texas Agricultural Experiment Service, Lubock, TX, p163–81 1982.

Bailey, C. J. Enzyme kinetics of cellulose hydrolysis. *Biochemical Journal*, 262, 1001-1002, 1989.

Brink, D. L. Making alcohol from cotton gin waste and cotton stalks. Proceedings of the symposium on: Cotton gin trash utilization alternatives, University of California Cooperative Extension, Hanford, CA, p.20-27 1981.

Crank, J. *The Mathematics of Diffusion*, 2nd Ed. University Press: Oxford, U. K. p. 78, 1975.

Etters, J. N. Diffusion equations made easy. Textile Chemist Colorist. 12: 140-145 1980.

Ghose. T. K. Measurement of cellulase activities. Pure and Applied Chemistry, 59 (2) 257-268, 1987.

Jeoh, T. and Agblevor, F. A. Characterization and fermentation of steam exploded cotton gin waste. Biomass and Bioenergy. 21 (2): 109-120 2001.

Levenspiel, O. *Chemical Reaction Engineering*, 2nd. John Wiley & Sons, Inc. p. 541-543, 1972.

Miller, G. L. Use of dinitrosalicylic acid reagent for determination of reducing sugar. Anal. Chem. 31: 426-428 1959.

Overend, R. P. and Chornet, E. Fractionation of lignocellulosics by steam-aqueous pretreatments. Philosophical Transactions of the Royal Society of London, 321: 523-536 1987.

Parnell C. B, Lepori W. A, and Capareda, S. C. Converting cotton gin trash into useable energy-technical and economic considerations. Proceedings Beltwide Cotton Conference, National Cotton Council of America, Memphis, TN, Vol. 2: p969-972 1991.

Chapter Four

Optimization of Enzyme Loading and Hydrolytic Time in the Hydrolysis of the Mixtures of Cotton Gin Waste and Recycled Paper Sludge for the Maximum Profit Rate*

4.1 Introduction

As discussed in Chapter Two, cotton gin waste (CGW) and recycled paper sludge (RPS) are two residues from the cotton and paper manufacturing industries. Both CGW and RPS contain about 50% or more cellulose and hemicellulose components [Lark et. al, 1997; Jeoh and Agblevor, 2001]. These polymers can be converted into monomeric sugars through hydrolysis, and these sugars can be used to produce ethanol and other high-value chemicals through fermentation.

The conversion of cotton gin waste to bio-fuel has been investigated by some researchers [Brink, 1981; Beck and Clements, 1982; Parnell, et. al, 1991; Jeoh and Agblevor, 2001; Agblevor et. al, 2003; Shen and Agblevor, 2008]. Ethanol production from RPS through cellulase hydrolysis and yeast fermentation also has been investigated by Lark et al. [1997]. However, there is no publication on the hydrolysis and ethanol production from the mixture of CGW and RPS. On the other hand, the barrier to commercial ethanol production from lignocellosic materials is that the process is not economical compared to other processes from sugar crop and starch materials. Therefore, the optimization of process parameters is important to improve the process economics. However, the process parameters, such as enzyme loading and hydrolytic time, in

*Jiacheng Shen and Foster A. Agblevor. Kinetics of enzymatic hydrolysis of steam exploded cotton gin waste. Chemical Engineering Communications. 195:9: 1107-1121, 2008.

enzymatic hydrolysis cannot be optimized by traditional methods described in Chapter Two because the conversion or sugar concentration increases monotonically with increasing enzyme loading and hydrolytic time in experimental ranges. There is no study in literature on how to solve the optimal problem of monotonic function in enzymatic hydrolysis. In this chapter, the optimization of enzyme loading and hydrolytic time in the hydrolysis of the mixtures of CGW and RPS for the maximum profit rate is reported.

4.2 Objectives

In this study, the objectives were

(1) To investigate the enzymatic hydrolytic kinetics of various mixtures of CGW and RPS, and optimize the ratio of the mixtures;

(2) To develop a novel model of enzymatic hydrolysis as a basis for profit rate models;

(3) To determine the values of the kinetic model parameters for the mixtures of CGW and RPS;

(4) To develop the profit rate models which include both the influencing hydrolytic and profit rate factors, and optimize enzyme loading and hydrolytic time for maximum profit rates.

4.3 Development of Enzymatic Hydrolysis Model

The assumptions of the model were:

(1) The enzymes of endo-β-1,4-glucanase, exo-β-1,4-cellobiohydrolase, and glycosidase were assumed to be a single enzyme that hydrolyzes the insoluble substrate into the reducing sugars.

(2) The structure of the insoluble substrate is assumed to be homogeneous, *i.e.* there was no distinction between amorphous and crystalline regions. This assumption is also in agreement with the requirement of Langmuir adsorption model.

(3) The enzyme deactivation was assumed to be a second order reaction, and the main factor influencing the hydrolysis rate.

The free enzymes (e) (g/l) in the suspension are adsorbed on the active sites on the surface of the insoluble substrate (C) (g/l) to form complexes. These complexes include the effective (Ce^*) (g/l) and ineffective ones (Ce^*_{in}) (g/l). The former produces reducing sugars, and the latter deactivates the enzyme. The two processes are expressed in the reactions below:

$$C + e \Leftrightarrow Ce^* \tag{4.1}$$

$$C + e \xrightarrow{k_3'} Ce^*_{in} \tag{4.2}$$

where the forward reaction in Eq (4.1) represents an adsorption of enzyme on the insoluble substrate, whose rate constant is k_1' (l/(g.h)), the backward reaction in Eq. (4.1) represents a desorption of enzyme from the insoluble substrate, whose rate constant is k_{-1}' (h^{-1}), and k_3' (l/(g.h)) is the enzyme deactivation rate constant. These effective complexes Ce^* in Eq. (1) produce reducing sugars G (g/l) and free enzymes e (Eq. (4.3)).

$$Ce^* \xrightarrow{k_2'} rG + e \tag{4.3}$$

where k_2' (h^{-1}) is the rate constant of sugar formation, and the constant r is the average conversion factor from cellulose and hemicellulose to sugars (in the following calculation, r is assumed to be 0.9 for conversion of glucan unit (MW 162) in cellulose to glucose (MW 180).

According to the mass action law, the reaction rate is a product of the nth power of the reactants. For simplification, the reactions in Eqs. (4.1) and (4.3) were assumed to be the first power of the reactants. Thus, the rate of the complex-formation from reactions (4.1) and (4.3) is given by:

$$\frac{dCe^*}{dt} = k_1^{'}C \times e - k_{-1}^{'}Ce^* - k_2^{'}Ce^* \tag{4.4}$$

Considering the substrate mass balance, the substrate concentration, C, is given by

$$C = C_0 - Ce^* - Ce_{in}^* - rG \tag{4.5}$$

where C_0 (g/l) is the initial substrate concentration. Substituting Eq. (4.5) into Eq. (4.4), it yields

$$\frac{dCe^*}{dt} = k_1^{'}\left(C_0 - Ce^* - Ce_{in}^* - rG\right)e - k_{-1}^{'}Ce^* - k_2^{'}Ce^* \tag{4.6}$$

Applying the quasi-steady state condition to Eq. (4.6), and assuming $Ce^*_{in} << C_0$, the complex concentration Ce^* is given by

$$Ce^* = \frac{\left(C_0 - rG\right)e}{K_e + e} \tag{4.7}$$

$$K_e = \frac{k_{-1}^{'} + k_2^{'}}{k_1^{'}} \tag{4.8}$$

where K_e (g/l) is the equilibrium constant.

From the enzyme mass balance, we have

$$e_0 = e + Ce^* + Ce_{in}^* \tag{4.9}$$

where e_0 is the initial enzyme concentration (g/l), and at the quasi-steady state condition, we have

$$\frac{dCe_{in}^{*}}{dt} = -\frac{de}{dt} \tag{4.10}$$

From assumption 3, the enzyme deactivation rate can be expressed in the following equation,

$$\frac{de}{dt} = -\frac{dCe_{in}^{*}}{dt} = -k_3^{'}e^2 \tag{4.11}$$

Integrating Eq. (4.11) with the boundary conditions e = e_0 at t = 0, and e = e at t = t, it produces

$$e = \frac{e_0}{1 + k_3^{'}e_0 t} \tag{4.12}$$

At any time after the onset of hydrolysis, the rate of the product-formation from reaction (4.3) is

$$\frac{d(rG)}{dt} = k_2^{'}Ce^{*} \tag{4.13}$$

Applying Eqs. (4.7) and (4.12) in Eq. (4.13), it becomes

$$\frac{d(rG)}{dt} = \frac{k_2^{'}(C_0 - rG)e_0}{K_e(1 + k_3^{'}e_0 t) + e_0} \tag{4.14}$$

Since $k_2^{'}$, C_0, e_0, $k_3^{'}$, and K_e are constants. Eq. (4.14) can be integrated with the boundary conditions G = 0 at t = 0, and G = G at t = t. Thus

$$G = \frac{C_0}{r}\left\{1 - \left[\frac{K_e + e_0}{K_e(k_3^{'}e_0 t + 1) + e_0}\right]^{b}\right\} \tag{4.15}$$

where the constant (dimensionless). (4.16)

Thus, the conversion, x, is defined as

$$x = \frac{C_0 - C}{C_0} = \frac{rG}{C_0} = 1 - \left[\frac{K_e + e_0}{K_e\left(k_3^{'} e_0 t + 1\right) + e_0} \right]^b \tag{4.17}$$

Eq. (4.17) is a three-parameter model. When $e_0 \to \infty$, x converges to a constant if t is constant.

$$x = \frac{C_0 - C}{C_0} = \frac{rG}{C_0} = 1 - \left(\frac{1}{K_e k_3^{'} t + 1} \right)^b \tag{4.18}$$

and when $t \to \infty$, x converges to the maximum conversion of 1.

From the experimental data of enzymatic hydrolysis in Chapter 4.5 Results and Discussion, it was found that Eq. (4.17) could fit each set of the experimental hydrolytic data for each initial enzyme concentration. However, when Eq. (4.17) was used to fit all the experimental data for four initial enzyme concentrations to obtain a set of values for K_e, $k_2^{'}$, and $k_3^{'}$, the predicted results deviated from the experimental data greatly.

To develop a profit rate model, we need a kinetic model in which a set of constants K_e, $k_2^{'}$, and $k_3^{'}$ can be used to correlate all the four sets of experimental data. It was noted that the values of constants K_e, $k_2^{'}$, and $k_3^{'}$ in Tables 4.1 and 4.2 were not monotonic, while the values of b increased monotonically with initial enzyme concentration. Hence, the constants of K_e and $k_3^{'}$ in the range of the four experimental enzyme concentrations were taken as the average values, $K_{e,ave}$ and $k^{'}_{3,ave}$ for the profit rate model, and the constant b was assumed to be linear with initial enzyme concentration as follows:

$$b = a_1 e_0 + a_2 \tag{4.19}$$

where a_1 and a_2 are constants determined by fitting all the experimental data of a mixture in the following formula:

$$\min \sum_{i=1}^{m} \sum_{j=1}^{n} w_i \left(x_{cij} - x_{ij} \right)^2 \tag{4.20}$$

where w is the weight determined by variance, x_c is the predicted conversion, x is the conversion in the experiments, m is the total number of initial enzyme concentration (here is 4), n is the total number of experimental points for an initial enzyme concentration (here is 11), and subscripts i and j denote the index numbers of initial enzyme concentration and the experimental points, respectively. Hence, Eq. (4.17) becomes

$$x = \frac{rG}{C_0} = 1 - \left[\frac{K_{e,ave} + e_0}{K_{e,ave}\left(k'_{3,ave} e_0 t + 1 \right) + e_0} \right]^{\left(a_1 e_0 + a_2 \right)} \tag{4.21}$$

4.4 Development of Profit Rate Models

Considering an enzymatic hydrolysis process with a feed recycle (Fig. 4.1) for reducing sugar production, and assuming that c_h ($/g substrate), c_f ($/g substrate), and c_p ($/g substrate) denote the costs of hydrolysis, feedstock, operation including feedstock handling, pretreatment, and steam production per treated unit weight of substrate, respectively, and c_e ($/g enzyme) denotes the enzyme cost in a sugar production process.

The sugar production cost s_{pc} ($/l hydrolytic volume) per unit reactor volume with respect to the initial enzyme concentration is given by

$$s_{pc} = C_0 x c_p + c_h C_0 + c_f x C_0 + e_0 c_e \tag{4.22}$$

where $C_0 c_f x$ is the substrate cost ($/l hydrolytic volume), $C_0 x c_p$ is the operating cost to reach a conversion x of substrate ($/l hydrolytic volume), $C_0 c_h$ is the hydrolytic cost

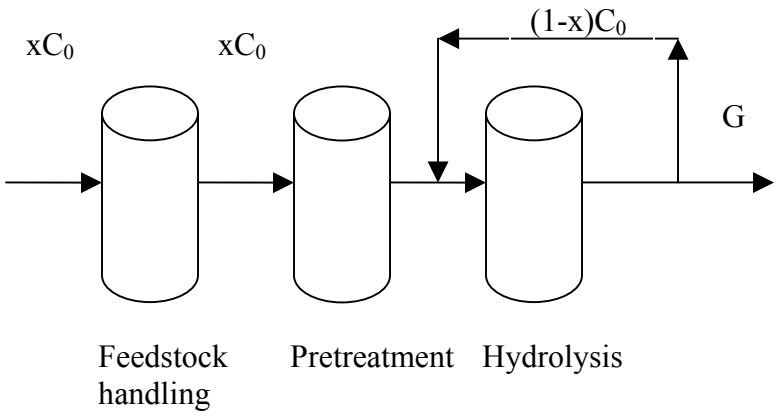

Fig. 4.1 Reducing sugar production with substrate recycle

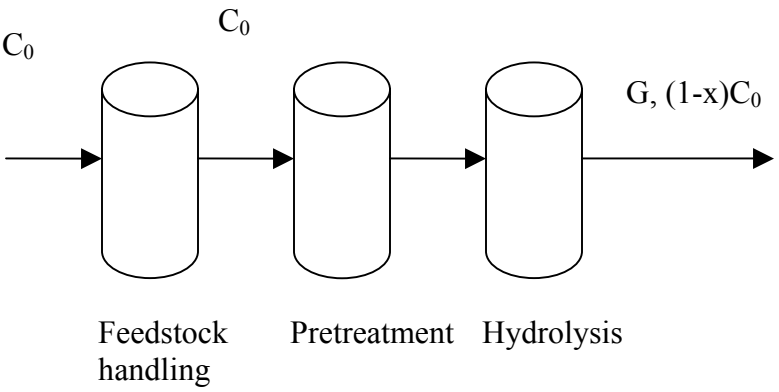

Fig. 4.2 Reducing sugar production without substrate recycle

($/l hydrolytic volume), and e_0c_e is the enzyme cost ($/l hydrolytic volume). Similarly, the sugar production cost for an enzymatic hydrolysis process without a feed recycle can be established as follows (Fig. 4.2),

$$s_{pc} = C_0\left(c_p + c_h\right) + c_f C_0 + e_0 c_e \tag{4.23}$$

The profit p_r ($/l hydrolytic volume) per unit reactor volume for the sugar production is given by

$$p_r = p_s - s_{pc} \tag{4.24}$$

where p_s is the market price of sugar ($/l hydrolytic volume). The market price of sugar should be equal to the mass of sugar G (= C_0x/r) (g glucose/l hydrolytic volume) multiplied by the market price c_s of a unit of sugar ($/g sugars). Eq. (4.24) becomes

$$p_r = \frac{c_s C_0 x}{r} - s_{pc} \tag{4.25}$$

Eq. (4.25) is based on a unit hydrolytic volume. Since sugar is not the final product in ethanol production, it is more convenient to express the costs of c_p, c_h, c_f, and c_s ($/g substrate) in Eq. (4.25) as c_p' c_h', c_f', and c_s' in terms of $ ethanol market price in unit volume of ethanol using the conversion factors r (g cellulose/g sugars), R_1 (l ethanol/g substrate), R_2 (g substrate/g cellulose), and R_3 (the fraction of sugar market price in ethanol market price):

$$\begin{aligned} & c_k\left[\frac{\$(production\ cost\ for\ unit\ k)}{g\ substrate}\right] \\ & = c_k'\left[\frac{\$(production\ cost\ for\ unit\ k)}{l\ ethanol}\right] R_1\left(\frac{l\ ethanol}{g\ substrate}\right) \end{aligned} \tag{4.26}$$

where the subscript k denotes subscripts p, h, and f, and

$$c_s\left[\frac{\$(sugar\ market\ price)}{g\ sugar}\right]=c_g^{'}\left[\frac{\$(ethanol\ market\ price)}{l\ ethanol}\right]R_1\left(\frac{l\ ethanol}{g\ substrate}\right)R_2 \left(\frac{g\ substrate}{g\ cellulose}\right)r\left(\frac{g\ cellulose}{g\ sugar}\right)R_3\left(\frac{\$\ sugar\ market\ price}{\$\ ethanol\ market\ price}\right) \tag{4.27}$$

Eq. (4.25) becomes

$$p_r=R_1C_0\left(c_s^{'}R_2R_3-c_p^{'}-c_f^{'}\right)\left\{1-\left[\frac{K_{e,ave}+e_0}{K_{e,ave}\left(k_{3,ave}^{'}e_0t+1\right)+e_0}\right]^{\left(a_1e_0+a_2\right)}\right\} -R_1C_0c_h^{'}-E_0c_e \tag{4.28}$$

The profit in Eq. (4.28) is a function of both the initial enzyme concentration and the hydrolytic time. After analyzing its partial derivate $\left(\frac{\partial p_r}{\partial t}\right)_{e_0}$ with respect to t, it was found that the maximum profit increased as the hydrolytic time increased. Thus, there was no optimal hydrolytic time, but only an optimal initial enzyme concentration. However, it was observed that the reducing sugar concentration at the initial hydrolytic period rose rapidly; while it increased slowly towards the end of the reaction period. If the hydrolysis is carried out in a short period of time, more hydrolytic cycles can be performed and more sugars can be produced within a certain period; but more enzyme will be consumed. This suggests that there are simultaneous optimal enzyme loading and hydrolytic time at which the profit from increased sugar production will be offset by the increased cost of enzyme. Therefore, the profit rate $p_r^{'}$ (profit per unit time) ($/l hydrolytic volume and time) can be derived from Eq. (4.28) as follows:

$$p_r^{'}=\frac{1}{t}\left\{\begin{array}{l} R_1C_0\left(c_s^{'}R_2R_3-c_p^{'}-c_f^{'}\right)\left\{1-\left[\frac{K_{e,ave}+e_0}{K_{e,ave}\left(k_{3,ave}^{'}e_0t+1\right)+e_0}\right]^{\left(a_1e_0+a_2\right)}\right\} \\ -R_1C_0c_h^{'}-e_0c_e \end{array}\right\} \tag{4.29}$$

where t (h) is hydrolytic time. Using the Nelder-Mead simplex search method for the maximum profit rate in Eq. (4.29), a set of optimal initial enzyme concentration e_{0op} and hydrolytic time t_{op} can be obtained at an ethanol market price $c_s^{'}$ for the known values of r, R_1, R_2, R_3, $c_p^{'}$, $c_h^{'}$, $c_f^{'}$, c_e, and C_0.

Similarly, a profit rate model $p_{rn}^{'}$ without feed recycle can be derived as follows:

$$p_{rn}^{'} = \frac{1}{t}\left\{\begin{array}{l} R_1 C_0\left(c_s^{'} R_2 R_3\right)\left\{1-\left[\dfrac{K_{e,ave}+e_0}{K_{e,ave}\left(k_{3,ave}^{'} e_0 t+1\right)+e_0}\right]^{\left(a_1 e_0+a_2\right)}\right\} \\ -R_1 C_0\left(c_f^{'}+c_p^{'}+c_h^{'}\right)-e_0 c_e \end{array}\right\} \tag{4.30}$$

The ratio, p_s, of profit rate and sugar production cost for recycle mode, and the ratio, p_{sn}, of profit rate and sugar production cost for non-recycle mode can be expressed as

$$p_s = \frac{p_r^{'}}{s_{pc}} \tag{4.31}$$

$$p_{sn} = \frac{p_{rn}^{'}}{s_{pc}} \tag{4.32}$$

4.5 Materials and Methods

4.5.1 Materials

Cotton gin waste and recycled paper sludge were obtained from the MidAtlantic Cotton Gin, Inc. (Emporia, VA), and International Paper (Frankin, VA), respectively. The cellulase enzyme Spezyme AO3117 was donated by Genencor International (Rochester, NY). The actual activity of the enzyme determined in our laboratory by a filter paper method was 29 Filter Paper Unit (FPU)/g [Ghose, 1987].

4.5.2 Methods

4.5.2.1 Pretreatment of materials

The two mixtures of CGW (80% and 75%) and RPS (20% and 25%) were pretreated by steam explosion for 2 minutes at 220^{o}C in a 25-l batch reactor located at the Thomas M. Brooks Forest Products Center, Blacksburg, VA. The severity factor ($\log(R_0)$) for the retention time and temperature was calculated to be 3.83.

4.5.2.2 Enzymatic hydrolysis

The mixtures of steam exploded CGW and RPS of 1.0 g (dry basis) were added to 250 ml flasks, and these flasks were sterilized in an autoclave at 121^{o}C for 1 hour. After that, 0.1 liter of 0.1 M sodium acetate buffer of pH 5.0 and the various quantities of enzyme (the initial enzyme concentrations were from 1.0 g/l (2.9 FPU/g dry substrate) to 6.0 g/l (17.4 FPU/g) were added to the flasks. The suspensions were hydrolyzed for 72 hours in a reciprocating shaker bath (Versa-Baths, Fisher Scientific) at 50°C and 80 rpm. Aliquots of 1 ml were taken from the suspension at various intervals. The samples were centrifuged at 6000 rpm for 5 minutes (Marathon-26km, Fisher Scientific). The experiments were repeated three times.

4.5.2.3 Analytical methods

The reducing sugar contents of the supernatants were determined using the dinitrosalicylic acid (DNS) method [Miller, 1959].

The acid-insoluble lignin and ash in the two mixtures of CGW and RPS were determined according to ASTM E1721-95 [1997] and ASTM E1755-95 [1997], respectively. The carbohydrate contents of the mixtures were measured according to ASTME1721-95 procedure [1997]. A filtrate of 5 ml after an autoclave cycle (60 minutes at 121^{o}C) and vacuum filtration was adjusted to a pH 4-5 using 4M sodium hydroxide, and the final volume of the filtrate was recorded. The reducing sugar content in the

filtrate was measured by DNS method [Miller, 1959]. The contents m_c (wt%) of the carbohydrate in the mixtures were calculated using the following equations.

$$m_c = \frac{0.087 C_c}{m_b} 100\% = \frac{0.087 \times 0.9 v_f C_s}{m_b v_i} 100\% \quad (4.33)$$

where C_c (g/l) is the carbohydrate concentration, C_s (g/l) is the reducing sugar concentration in the filtrate by DNS method, v_i (l) is the initial volume of the filtrate before pH adjustment and v_f (l) is the final volume of the filtrate after pH adjustment, the constant 0.9 is the conversion factor from cellulose to glucose, and m_b and the constant 0.087 are the sample weight and the volume of the autoclaved suspension in ASTM E1721-95 procedure [1997], respectively.

4.6 Results and Discussion

4.6.1 Compositions of the CGW/RPS mixtures

The compositions of the CGW/RPS mixtures are listed in Table 4.1. Although the CGW/RPS (80%/20%) mixture had a higher convertible carbohydrate than the CGW/RPS (75%/25%) mixture, the reducing sugar concentrations after enzymatic hydrolysis were lower than those for the CGW/RPS (75%/25%) mixture. The difference in the reducing sugar concentration may be related to the catalytic mechanism of hydrolysis. In the standard procedure of ASTM E1721-95 [1997], sulfuric acid was used, while enzyme was used in this experiment. Table 4.1 also indicates that with increasing RPS content in the mixtures, the ash contents of the mixtures increased. The higher ash content (20.3%) of the CGW/RPS (75%/25%) mixture suggested that it was not suitable to add a large fraction of RPS to the mixture.

4.6.2 Effects of initial enzyme concentration on the hydrolysis of the CGW/RPS mixtures

Effects of the initial concentration of Spezyme^{TM} (enzyme) on the hydrolysis of the two CGW/RPS mixtures are shown in Figs. 4.3 and 4.4. The conversions (reducing sugar concentrations) increased with increased residence time and initial enzyme concentration (enzyme loading). The conversion (reducing sugar concentration) for the CGW/RPS (75%/25%) mixture increased from 46.3% (2.55 g/l) to 73.8% (4.06 g/l), when the initial Spezyme enzyme loading was increased from 2.9 FPU/g dry substrate to 17.4 FPU/g dry substrate. The CGW/RPS (75%/25%) mixture had the higher conversion and sugar concentration than those of the CGW/RPS (80%/20%) mixture. The conversions of the mixtures in this study were somewhat lower than those of other feedstocks reported in literature. This may be attributed to: 1) Lignin contents in the feedstock: both CGW and RPS contain higher lignin contents. The feedstock containing a high lignin content required a high enzyme loading for hydrolysis. Pan et al. [Pan et al., 2005] observed that the required enzyme loading was proportional to the lignin content of feedstock. A 90% conversion of cellulose to glucose for the feedstock of organosolv pulping containing a 27.4% lignin needed an enzyme loading of 40 FPU/g cellulose, while it only needed 30 FPU/g cellulose for a lignin content of 18.4% to achieve similar conversion. 2) Ash contents: RPS had a high ash content, which could easily adsorb the enzyme in the liquid and make the enzyme lose its activity. Hence, a higher enzyme loading was required for the hydrolysis.

The conversion values were fitted in Eq. (4.17) using nonlinear regression (Figs. 4.3 and 4.4). The constants K_e, k_2' and k_3' determined from the fitting process are shown in Tables 4.1 and 4.2. The two predicted curves for the initial enzyme concentration of 10 g/l are also shown in Figs. 4.3 and 4.4, both of which indicate a good convergent

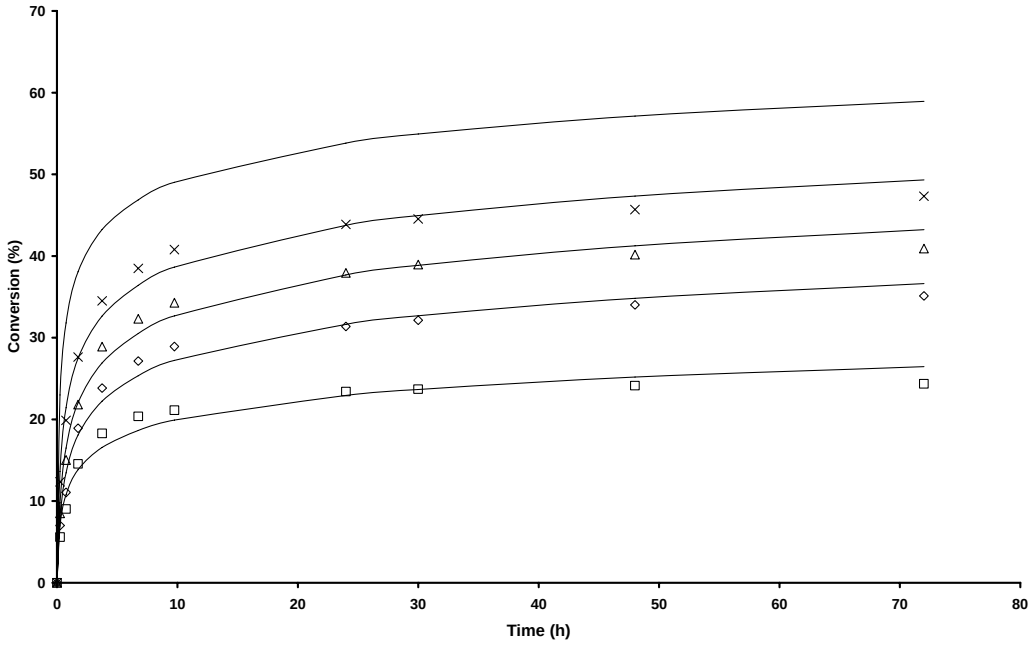

Fig. 4.3 Hydrolytic kinetics of CGW/RPS (80%/20%) mixture. Experimental conditions: mixture concentration 10 g (dry)/l, temperature 50°C, and 80 rpm. Initial enzyme concentrations (g/l): □ 1, ◊ 2, Δ 4, and × 6. Solid lines represent the model values (Eq. 4.17) of the corresponding enzyme concentrations and a curve of predicted 10 g/l.

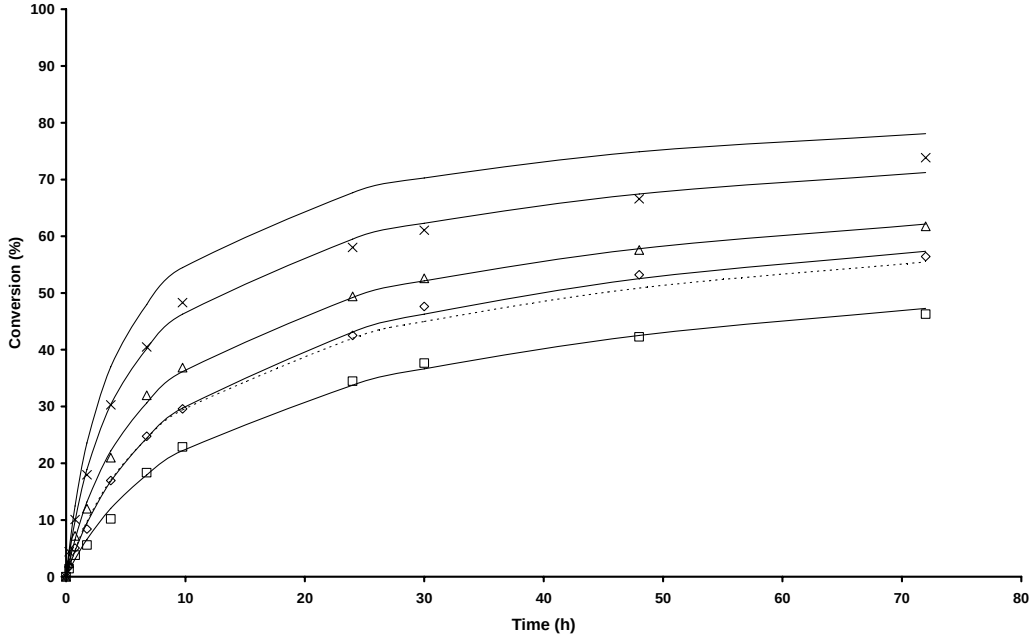

Fig. 4.4 Hydrolytic kinetics of CGW/RPS (75%/25%) mixture. Experimental conditions: mixture concentration 10 g (dry)/l, temperature 50°C, and 80 rpm. Initial enzyme concentrations (g/l): □ 1, ◊ 2, Δ 4, and × 6. Solid lines represent the model values (Eq. 4.17) of the corresponding enzyme concentrations and a curve of predicted 10 g/l. Dotted line represents the model value (Eq. 4.21) of 2 g/l.

characteristic. The constants K_e, k_2', and k_3' for the CGW/RPS (75%/25%) mixture were smaller than those for the CGW/RPS (80%/20%) mixture. The constant k_3' represents the enzyme deactivation; hence, the smaller the k_3', the lower the enzyme deactivation, which explains why the CGW/RPS (75%/25%) mixture produced the higher reducing sugar concentration. The constant K_e represents the ratio of the rate constant of complex-consumption and the rate constant of complex-formation (Eq. (4.8)), and the constant k_2' represents the reducing sugar formation rate. The smaller the K_e and k_2', the slower the complexes were consumed, and the slower the reducing sugar formation rate. It may be inferred that the complex consumption and product (sugar) formation of the CGW/RPS (75%/25%) mixture would be lower than those of the CGW/RPS (80%/20%) mixture. However, the experimental data showed that the reducing sugar concentration from the CGW/RPS (75%/25%) mixture was higher than that of the CGW/RPS (80%/20%). This may suggest that the hydrolytic rate was controlled by enzyme deactivation. In such a situation the enzyme deactivation rate controlled the hydrolytic rate in spite of the other reaction parameters.

4.6.3 Optimal enzyme loading and hydrolytic time

Galbe et al. [1997] made a technoeconomic evaluation for ethanol production from wood. According to their study: the operating cost of feedstock handling, pretreatment, and steam production was 22% (assuming 11% for steam explosion), the hydrolytic cost was 12.1%, the feedstock cost (wood) was 29.7%, and other operating costs after hydrolysis such as distillation etc. were 36.2%. Because CGW and RPS are wastes and have a lower price than that of wood, the feedstock cost was assumed to be 10%. The re-calculated distribution of costs is shown in Table 4.4. The average ethanol market price in

Table 4.1 Compositions of CGW/RPS mixtures (%)

CGW	Carbohydrate	Acid-lignin	Ash	Others
80	57.5	25.5	11.6	5.37
75	49.6	26.3	20.3	3.79

Table 4.2 Model parameters (Eq. 4.17) for the CGW/RPS (80%/20%) mixture

e_0 (g/l)	e_d (FPU/g)	K_e (g/l)	k_2' (l/h)	k_3' (1/(g.h))	b (-)
1	2.9	8.07	7.33	18.5	4.92E-2
2	5.8	6.04	2.75	5.57	8.16E-2
4	11.6	3.58	1.62	4.41	1.02E-1
6	17.4	3.72	2.33	5.34	1.16E-1
Average	-	5.35	3.50	8.45	8.73E-2

e_d The enzyme loading based on the dry substrate (FPU/g)

Table 4.3 Model parameters (Eq. 4.17) for the CGW/RPS (75%/25%) mixture

e_0 (g/l)	e_d (FPU/g)	K_e (g/l)	k_2' (l/h)	k_3' (1/(g.h))	b (-)
1	2.9	1.83	0.141	0.268	0.288
2	5.8	1.27	0.121	0.255	0.374
4	11.6	1.86	0.165	0.234	0.379
6	17.4	1.76	0.226	0.271	0.475
Average	-	1.68	0.163	0.257	0.379

e_d The enzyme loading based on the dry substrate (FPU/g)

Table 4.4 The operating costs of various unit operations

Name	ha	t	st	p	h	f	Other	Total
Cost (%)	1.49	16.7	9.21	27.4	15.1	12.5	45.0	100

ha, t, st, p, h, and f denote the handling unit, the pretreatment unit, the stream production unit, the operating unit, whose cost is the sum of handling, pretreatment and steam production units, the hydrolysis unit, and the feedstock, respectively.

Table 4.5 Model parameters (Eq. 4.21) for the CGW/RPS (75%/25%) mixture

CGW (%)	$K_{e,ave}$	$k'_{3,ave}$	a_1	a_2
75	1.68	0.257	3.45E-2	0.264

Table 4.6 The maximum profit rates at the optimal enzyme loadings and times in Figs. 4.5-4.8 (ethanol market price \$0.6/l)

C_0 (g/l)	e_{op} (g/l)	e_{op} (FPU/g)	t_{op} (h)	p_{rop}' (\$/l)	Deviation	p_r' drop
100 (non-rec.)	1.89	0.548	21.3	12.2E-5	20%	4.9%
20 (non-rec.)	0.355	0.517	81.1	0.577E-5	20%	6.3%
100 (rec.)	2.76	0.798	68.9	4.07E-5	20%	7.1%
20 (rec.)	0.404	0.585	326	0.153E-5	20%	8.3%

March 2007 was about 0.6 $/l [www.energy. 2007]. The ethanol production cost was 0.48 $/l with assumption of the ratio of production cost to market price as 0.8. This production cost was multiplied by the cost percentages in Table 4.4 to obtain the operating cost c_p, the hydrolytic cost c_h, and the feedstock cost c_f ($/l substrate). The yield R_1 of ethanol per gram of substrate was assumed as 3.58E-4 l ethanol/g substrate (= 85 gallon ethanol/900 kg dry substrate) [Solar Energy Institute, 1982]. The conversion factors R_2, R_3, and r were, respectively, assumed to be 0.496 (the convertible carbohydrate factor for the CGW/RPS (75%/25%) mixture in Table 4.1), 0.55 (the fraction of the sugar market price in the ethanol market price), and 0.9 (the conversion ratio of glucan unit in cellulose and glucose). It was reported that the enzyme production cost was between $0.30-$0.81/pound cellulase ($0.661-1.78/l cellulase) [Himmel et al., 1997]. We assumed an average cost of $1.22/l cellulase.

The experimental data for the CGW/RPS (75%/25%) mixture were fitted in Eq. (4.21) and the fitted constants a_1 and a_2 are listed in Table 4.5. A simulated curve for enzyme concentration of 2 g/l is displayed in Fig. 4.4. The fitted precision of Eq. (4.21) is less than that of Eq. (4.17) in Fig. 4.4. Using the optimal method, fminserach, of MATLAB (Appendix 1), a series of sets of the optimal initial enzyme concentration (loading) and time for the CGW/RPS (75%/25%) mixture and two operating modes were obtained for various ethanol market prices and initial substrate concentrations. These results are shown in Figs. 4.9-4.14.

To confirm that the profit rates obtained were maximum rather than minimum, both of which have same mathematical conditions, we examined the profit rate surface in 4 figures. Figs. 4.5 and 4.6 show the two surfaces of profit rates for the operating mode

with recycle at various initial enzyme concentrations and hydrolytic times for the ethanol market price $0.6/l, and the substrate concentrations at 100 g/l and 20 g/l, respectively. Figs. 4.7 and 4.8 are the two similar surfaces without recycle at the same conditions of Figs. 4.5 and 4.6. The maximum profit rates were 12.2E-5, 0.577E-5, 4.07E-5, and 0.153E-5 $/l hydrolytic volume at the optimal initial enzyme concentrations (loading) and hydrolytic times (0.548 FPU/g and 21.3 h, 0.517 FPU/g and 81.1 h, 0.798 FPU/g and 68.7 h, and 0.585 FPU/g and 326 h) for Figs 4.5-4.8, respectively. If loading and time dropped by 20% from the optimal levels for the four cases, profit rates would decrease by 4.9%, 6.3%, 7.1% and 8.3%, respectively (Table 4.6).

Figs. 4.9-4.11 indicate the optimal conditions in enzyme loadings, hydrolytic times, conversions, sugar production costs, profit rates, and ratios of profit rate and sugar production cost with various ethanol market prices for the CGW/RPS (75%/25%) mixture in two operating modes. At the same ethanol market price, the enzyme loadings, optimal hydrolytic times, conversions, and sugar production costs for recycle mode were lower than those for non-recycle mode. In contrast, the profit rates, and the ratio of profit rates and sugar production cost were higher. All the results suggested that the recycle mode was better than non-recycle mode. At the ethanol market price of $0.6/l, the profit rate, and the ratio of profit rate and sugar production cost with recycle were, respectively, 2.99 and 4.84 times those without recycle, respectively (calculated from Fig. 4.11). The required enzyme loading, hydrolytic time, conversion, and operating cost were 0.363, 0.309, 0.673 and 0.618 times of those without cycle, respectively (calculated from Figs. 4.9 and 4.10). It was also noted that when the ethanol market price increased, the

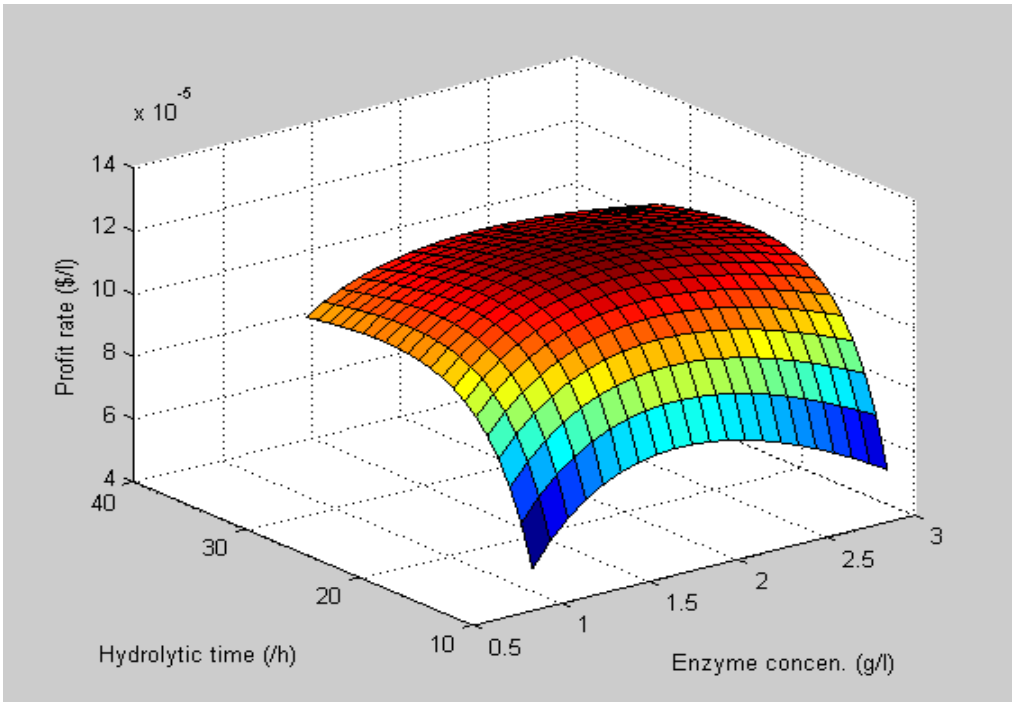

Fig. 4.5 Profit rate response surface with respect to the enzyme concentration and hydrolytic time for CGW/RPS (75%/25%) mixture. Conditions: recycle, C_0 = 100 g/l, and ethanol market price \$0.6/l.

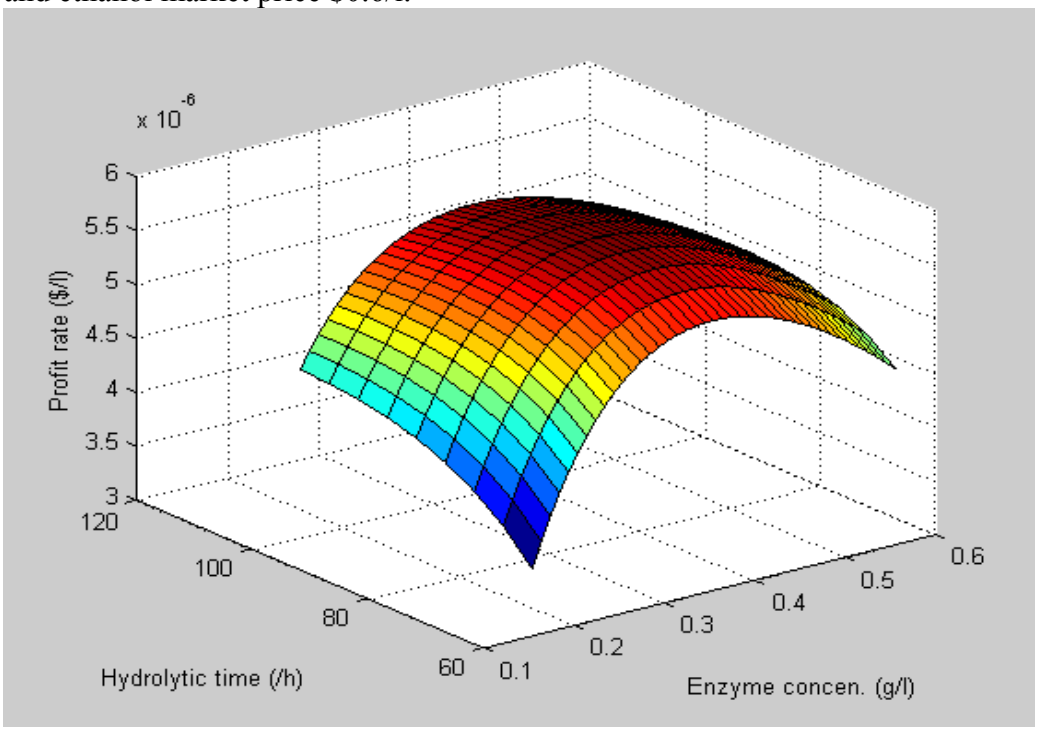

Fig. 4.6 Profit rate response surface with respect to the enzyme concentration and hydrolytic time for CGW/RPS (75%/25%) mixture. Conditions: recycle, C_0 = 20 g/l, and ethanol market price \$0.6/l.

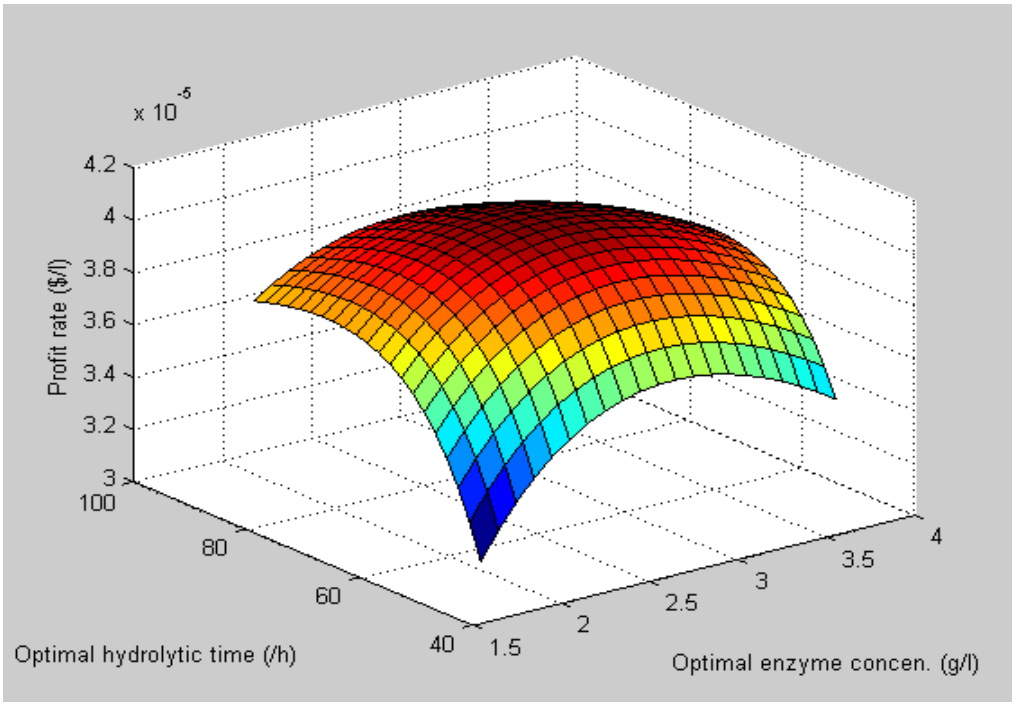

Fig. 4.7 Profit rate response surface with respect to the enzyme concentration and hydrolytic time for CGW/RPS (75%/25%) mixture. Conditions: non-recycle, C_0 = 100 g/l, and ethanol market price \$0.6/l.

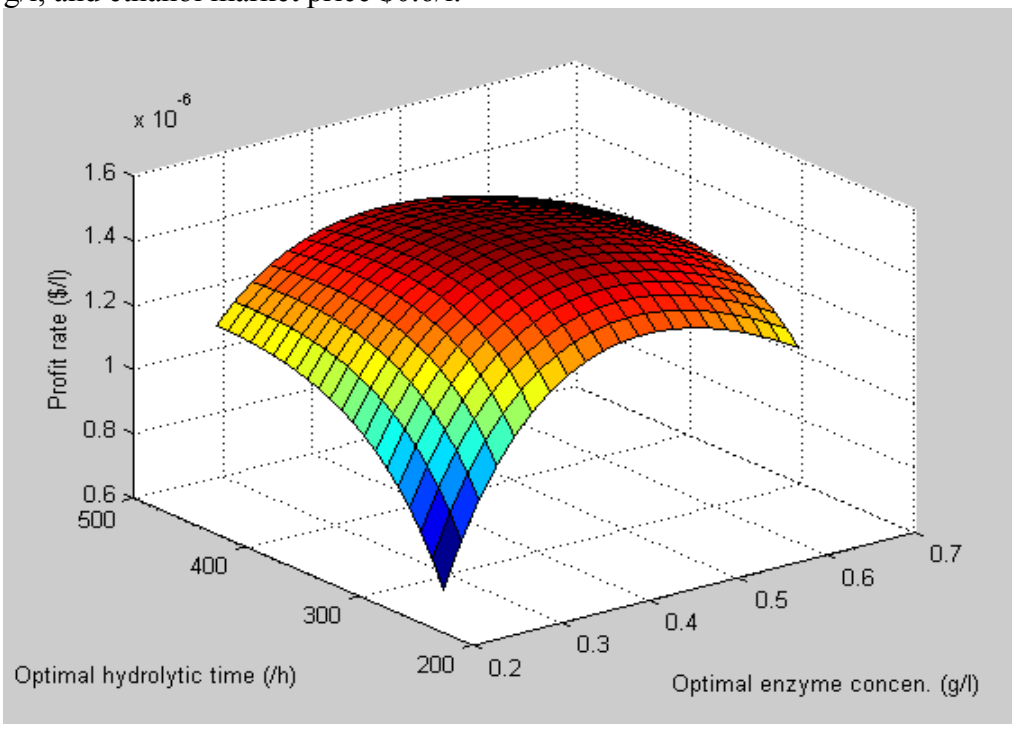

Fig. 4.8 Profit rate response surface with respect to the enzyme concentration and hydrolytic time for CGW/RPS (75%/25%) mixture. Conditions: non-recycle, C_0 = 20 g/l, and ethanol market price \$0.6/l.

allowable optimal initial enzyme loadings, profit rates, and the ratios of profit rate and sugar production cost also increased for both operating modes. For example, when the ethanol market price was double from 0.6 $/l to $1.2/l, the profit rates increased 9.17 and 18.5 times rather than 2 times with the adjustments of the optimal initial enzyme loading from 0.548 FPU/g and 0.798 FPU/g to 1.78 FPU/g and 2.54 FPU/g for the recycle and non-recycle modes, respectively (calculated from Fig. 4.11). The corresponding ratios of profit rate and sugar production cost were 5.57 and 11.8 times. This means that higher profit rate can be attained by adjusting the initial enzyme loading and hydrolytic time when the ethanol market price is up.

Figs. 4.12-4.14 indicate the optimal enzyme loadings, optimal hydrolytic times, conversions, sugar production costs, profit rates, and ratios of profit rate and sugar production cost with various substrate concentrations for the CGW/RPS (75%/25%) mixture at two operating modes. These figures also show that the recycle mode is better than the non-recycle mode. It was also found that with increase in the substrate concentration, the profit rate and the ratio of profit rate and sugar production cost quickly increased. The profit rate and the ratio of profit rate and sugar production cost at the substrate concentration 100 g/l were 9.69 and 4.06 times of those at the substrate concentration of 20 g/l for the recycle mode. This suggested that a high substrate concentration was an effective way to enhance the commercial competitiveness of ethanol production from lignocellulosic materials. Another finding was that with increase in the substrate concentration, the optimal enzyme loading increased instead of remaining constant. The optimal enzyme loadings were 0.517 FPU/g and 0.585 FPU/g at the substrate concentration of 20 g/l, but the optimal points shifted to 0.548 FPU/g and 0.802

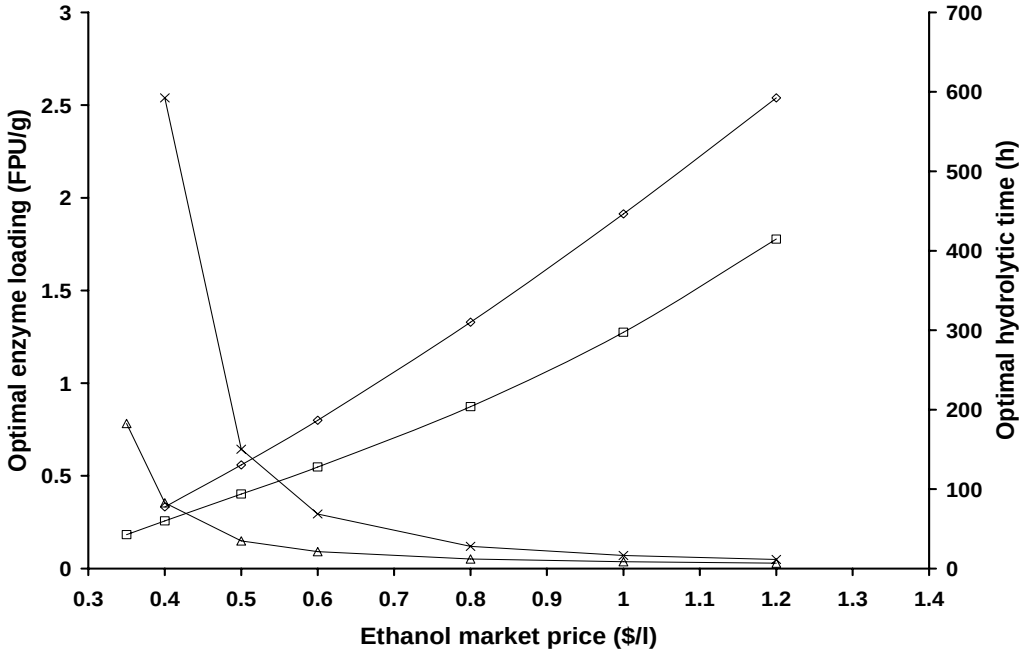

Fig. 4.9 Optimal initial enzyme loading e_{0op} and hydrolytic time t_{op} with ethanol market price for CGW/RPS (75%/25%) mixture. Conditions: mixture concentration 100 g/l. Recycle: e_{0op} □, t_{op} Δ, and non-recycle: e_{0op} ◊, t_{op} ×.

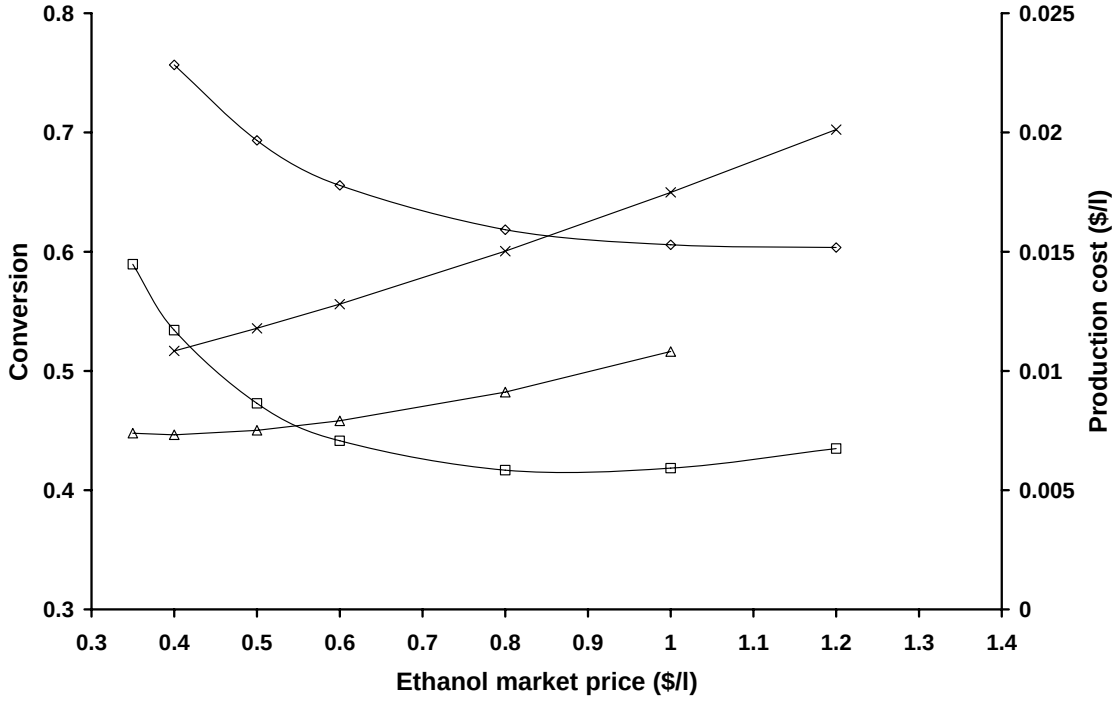

Fig. 4.10 Conversion x and sugar production cost s_{pc} with ethanol market price for CGW/RPS (75%/25%) mixture. Conditions: mixture concentration 100 g/l. Recycle: x □, s_{pc} Δ, and non-recycle: x ◊, s_{pc} ×.

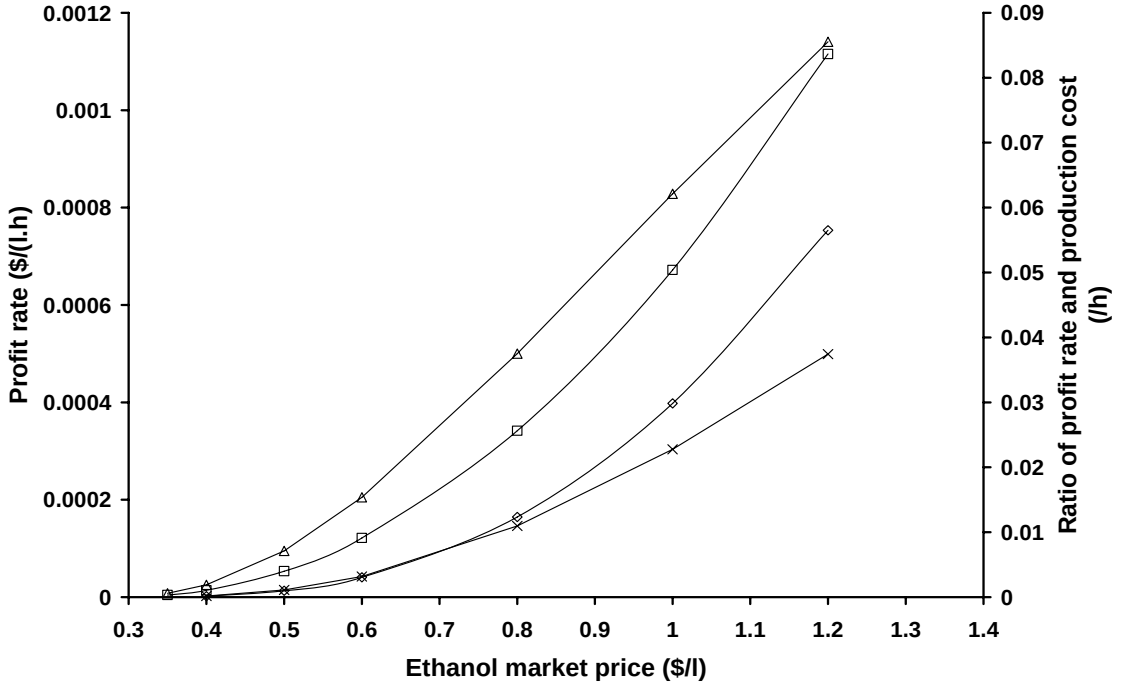

Fig. 4.11 Profit rate and ratio of profit rate to sugar production cost with ethanol market price for CGW/RPS (75%/25%) mixture. Conditions: mixture concentration 100 g/l. Recycle: p_r □, p_s Δ, and non-recycle: p_{rn} ◊, p_{sn} ×.

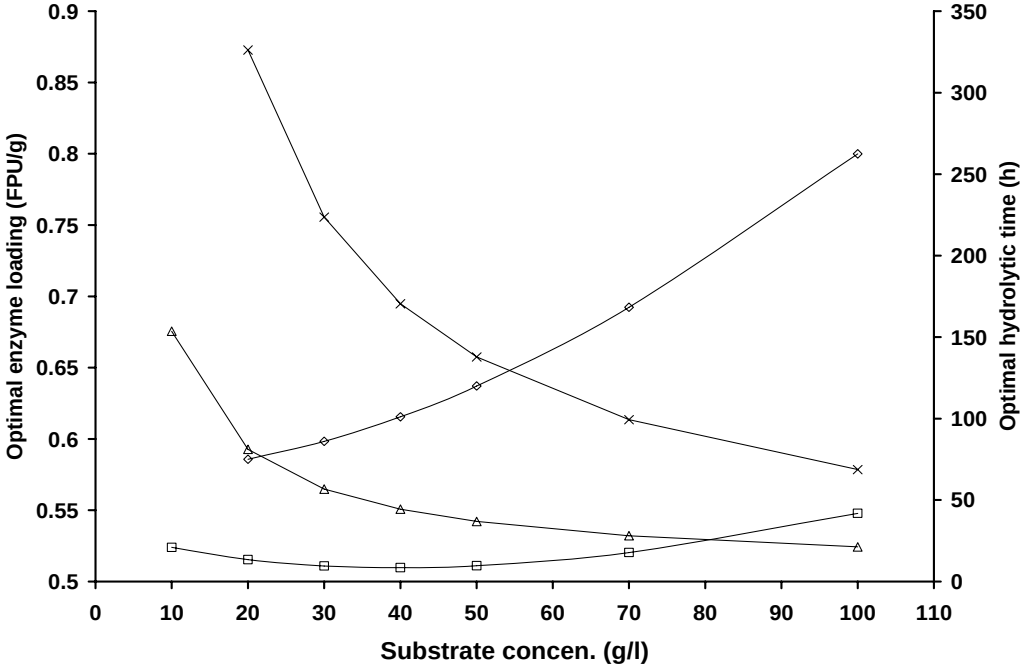

Fig. 4.12 Optimal initial enzyme loading e_{0op} and hydrolytic time t_{op} with initial substrate concentration for CGW/RPS (75%/25%) mixture. Conditions: ethanol market price $0.6/l. Recycle: e_{0op} □, t_{op} Δ, and non-recycle: e_{0op} ◊, t_{op} ×.

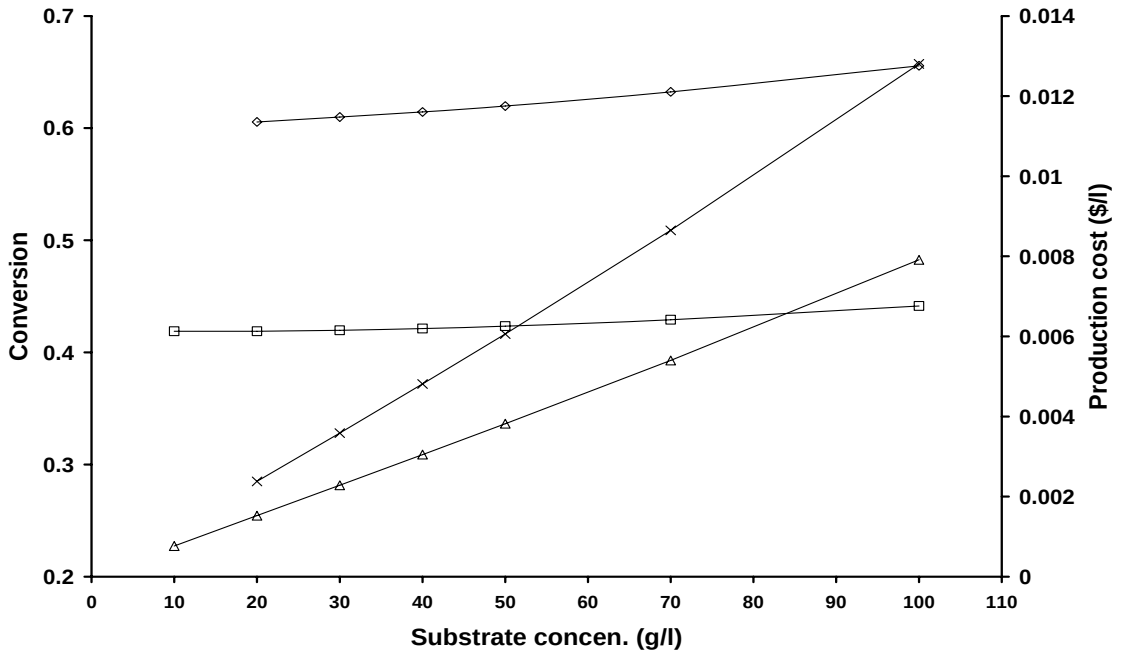

Fig. 4.13 Conversion x and sugar production cost s_{pc} with initial substrate concentration for CGW/RPS (75%/25%) mixture. Conditions: ethanol market price \$0.6/l. Recycle: x □, s_{pc} Δ, and non-recycle: x ◊, s_{pc} ×.

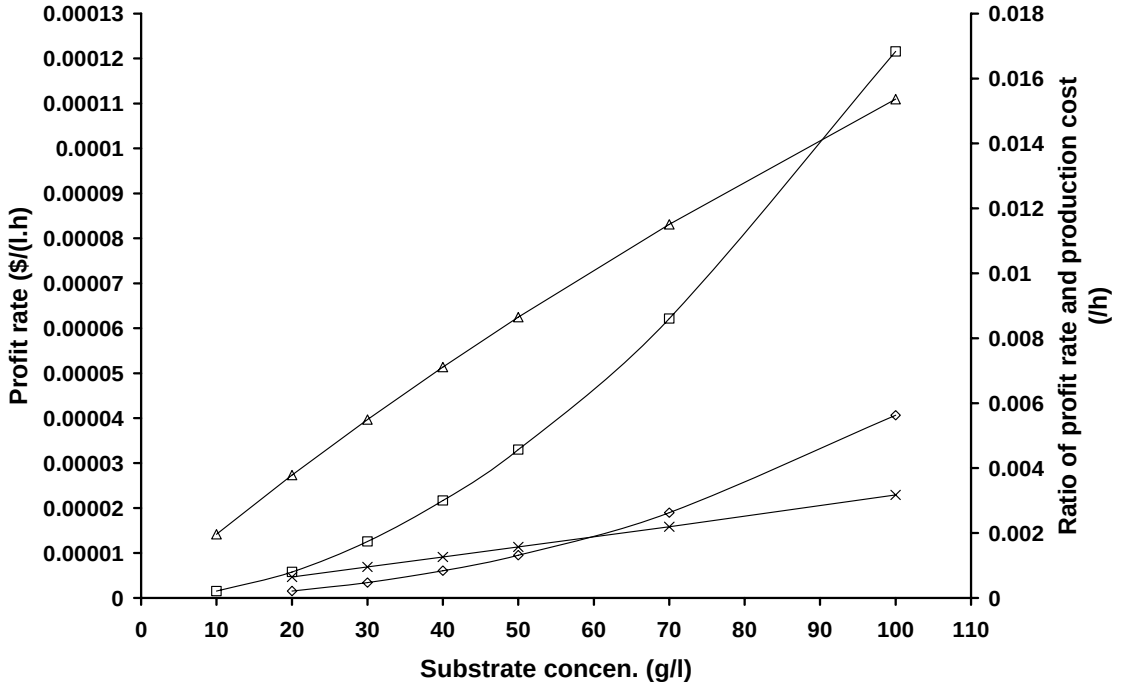

Fig. 4.14 Profit rate and ratio of profit rate to sugar production cost with initial substrate concentration for CGW/RPS (75%/25%) mixture. Conditions: ethanol market price \$0.6/l. Recycle: p_r' □, p_s Δ, and non-recycle: p_{rn}' ◊, p_{sn} ×.

FPU/g at the substrate concentration of 100 g/l for recycle and non-recycle modes, respectively. This fact is important for hydrolytic vessel scale-up. If the enzyme loading and time at a high substrate concentration are proportionally scale up from those at a low substrate concentration, the operating state at a high substrate concentration is no longer optimal like the operating state at a low substrate concentration. In the above example, when the substrate concentration increased five times, the optimal enzyme loading increased more than five times to maintain the optimal state. This means the optimal enzyme loading was not constant for the substrate concentration change.

Generally, the simulated results support the conclusion that enzyme hydrolysis should be performed with low enzyme loading, particularly for the recycle operating mode. However, the simulated data also indicated that the better profit rate could be obtained by increasing the enzyme loading if the ethanol market price increased. At a constant ethanol market price, using a high substrate concentration and a recycle process was two effective methods to increase the profit rate of ethanol production. In both cases of recycle and non-recycle, the conversions of feedstock were between 0.39 and 0.76 at the optimal enzyme loadings and hydrolytic times in this study. Therefore, it is not necessary to pursue a higher feedstock conversion, such as $x = 0.9$, because of the limitation of enzyme cost.

4.7 Conclusions

Cotton gin waste and recycled paper sludge, both of which contain cellulose and hemicelluloses, are the residues from the cotton and paper industries, respectively. They are potential raw materials for bioethanol production. In this study, the kinetic

experiments of hydrolysis showed that the reducing sugars could be produced from the CGW/RPS mixtures using enzyme Spezyme AO3117. It was concluded that the higher the initial enzyme concentration, the higher the conversion of the mixtures. The reducing sugar concentration and conversion of the CGW/RPS (75%/25%) mixture were higher than those of the CGW/RPS (80%/20%) mixture. The highest conversion of the former was 73.8% at enzyme loading of 17.4 FPU/g substrate for 72 hours hydrolysis. A three-parameter kinetic model assuming a second order enzyme deactivation rate was developed and its analytical expression was successfully applied to the hydrolytic experimental data of the mixtures to derive the model parameters. The two profit rate models, representing the operating modes with and without feedstock recycle, developed in this study were used to analyze the optimal enzyme loadings and hydrolytic times in hydrolysis for the maximum profit rate. The simulated results from the models showed that a high substrate concentration and a recycle operating mode were two effective methods to enhance the profit rate and the ratio of profit rate and sugar production cost in hydrolysis. The models were also used to predict the optimal enzyme loading and hydrolytic time for various ethanol market prices.

References

Agblevor, F. A., Batz, S., and Trumbo, J. Composition and ethanol production potential of cotton gin residues. Applied Biochemistry and Biotechnology 105-108: 219-230 2003.

ASTM E1721-95. Standard test method for determination of acid insoluble residues. In: Annual book of ASTM standards, American Society for Testing and Materials, West Conshohocken, PA. Vol. 11.05, p. 1238-1240, 1997.

ASTM E1755-95. Standard test method for determination of acid insoluble residues. In: Annual book of ASTM standards, American Society for Testing and Materials, West Conshohocken, PA. Vol. 11.05, p. 1252-1254, 1997.

Beck, R. S., and Clements, D. L. Ethanol production from cotton gin trash. Proceedings of the symposium on: Cotton gin trash utilization alternatives, Texas Agricultural Experiment Service, Lubock, TX, p163–81 1982.

Brink, D. L. Making alcohol from cotton gin waste and cotton stalks. Proceedings of the symposium on: Cotton gin trash utilization alternatives, University of California Cooperative Extension, Hanford, CA, p.20-27 1981.

Galbe, M., Larsson, M., Stenberg, K., Tengborg, T., and Zacch, G. Ethanolfrom wood: design and operation of a process development unit for technoeconomic process evaluation. Fules and Chemicals from Biomass edited by Saha BC, Woodward J. ACS symposium series 666. p. 110-129, 1997.

Ghose. T. K. Measurement of cellulase activities. Pure and Applied Chemistry, 59 (2) 257-268, 1987.

Himmel, M. E. Adney, W. S. Baker, J. O. Elander, R. McMillan, J. D. Nieves, R. A. Sheehan, J. J. Thomas, S. R. Yinzant, T. B. and Zhang, M. Advanced bioethanol production technology: a perspective. Fuels and Chemicals from Biomass edited by Saha, B. C., Woodward, J. ACS symposium series 666. p. 16, 1997.

Jeoh, T. and Agblevor, F. A. Characterization and fermentation of steam exploded cotton gin waste. Biomass and Bioenergy. 21 (2): 109-120 2001.

Lark, N., Xia, Y. K., Qin, C. G., Gong, C. S., and Tsao, G. T. Production of ethanol from recycled paper sludge using cellulase and yeast, Kluveromyces marxianus. Biomass & Bioenergy. 12 (2) 135-143, 1997.

Miller, G. L. Use of dinitrosalicylic acid reagent for determination of reducing sugar. Anal. Chem. 31: 426-428 1959.

Pan, X.J., Arato, C., Gilkes, N., Gregg, D., Mabee, W., Pye, K., Xiao, Z.Z., Zhang, X., and Saddler, J. Biorefining of softwoods using ethanol organosolv pulping: Preliminary evaluation of process streams for manufacture of fuel-grade ethanol and co-products. Biotechnology and Bioengineering. 90 (4), 473-481, 2005.

Shen, J., and Agblevor, F.A. Kinetics of enzymatic hydrolysis of steam exploded cotton gin waste. Chemical Engineering Communications. 195:9: 1107-1121, 2008.

Solar Energy Institute. Ethanol Fuels Reference Guide. A Division of Midwest Research Institute Operated for the U. S. Department of Energy. p. V, 1982.

www.energy.ca.gov/gasline/graphs/ethanol_10-years.htm, 2007.

Chapter Five

The Operable Model of Simultaneous Saccharification and Fermentation of Ethanol Production from Cellulose*

5.1 Introduction

As discussed in Chapter Two, simultaneous saccharification and fermentation (SSF) has several advantages over the separate hydrolysis and fermentation (SHF). Some mathematical models of SSF have also been proposed to predict the performance of SSF [Philippidis et al., 1992; Philippidis et al., 1993; South et al., 1995; Philippidis and Hatzis, 1997; Shin et al., 2006]. However, a common shortcoming of these studies is that the models have not been completely verified because the variation in microorganism concentration over time was not simulated. In addition, there is a problem in applying the Philippidis and Hatzis's model [1997] to experiments because measuring cellulose concentration in a suspension is often tedious, particularly when cellulose is in the biomass. Furthermore, Philippidis and Hatzis [1997] continuous SSF model is incorrect because the model does not include enzyme addition. In this chapter, the operable modeling of simultaneous saccharification and fermentation of ethanol production from cellulose is reported.

5.2 Objectives

In this study, the objectives were

* Jiacheng Shen and Foster A. Agblevor. The operable modeling of simultaneous saccharification and fermentation of ethanol production from cellulose. Submitted to Applied Biochemistry and Biotechnology.

(1) To develop the simple and operable SSF models for batch, continuous, and fed-batch processes. The models should have fewer than 10 parameters that can be determined by SSF experiments, while the models still represent the main mechanism of hydrolysis and fermentation;

(2) To estimate the model parameters from fitting the data of the four main components (cellobiose, glucose, cell and ethanol) in the SSF experiments;

(3) To predict the effects of continuous and fed-batch SSF operations based on the parameters obtained from the batch experiments.

5.3 Batch Operating Mode

Assumptions of the model are that:

(1) Cellulose is converted into glucose through cellobiose. Direct conversion of cellulose to glucose is negligible. This assumption was made because it was impossible to distinguish between directly converted glucose and indirectly converted glucose from cellulose in a culture containing cellulase enzymes. This assumption results in the following series of reactions:

$$\text{Cellulose} \xrightarrow{r_1} \text{Cellobiose} \xrightarrow{r_2} \text{Glucose} \qquad (5.1)$$

(2) According to the general principle of enzyme feedback inhibition in a series of enzyme reactions, the end product inhibits the first enzyme [Lehninger et al., 1993]. In the catalyzed products of a cellulase system, cellobiose and glucose are the products of endo-β-1,4-glucanase, exo-β-1,4-cellobiohydrolase and glycosidase, respectively. The

reaction rates r_1 (g/(l.h)) from cellulose to cellobiose and r_2 (g/(l.h)) from cellobiose to glucose during the hydrolysis are, respectively, expressed as

$$r_1 = \frac{k_1'' C}{1 + G/K_{1G} + B/K_{1B}} \tag{5.2}$$

$$r_2 = \frac{k_2 B}{1 + G/K_{2G}} \tag{5.33}$$

where B is the cellobiose concentration (g/l), G is the glucose concentration (g/l), C is the cellulose concentration (g/l), k_1'' is the variable associated with enzyme deactivation (h^{-1}), k_2 is the specific rate constant of cellobiose hydrolysis to glucose (h^{-1}), K_{1G} and K_{1B} are the inhibitory constants of glucose and cellobiose to the endo-β-1,4-glucanase and exo-β-1,4-cellobiohydrolase (g/l), respectively, and K_{2G} is the inhibitory constant of glucose to the glycosidase (g/l). Both r_1 and r_2 are enzymatic catalytic reactions. In principle, catalyst should not be included in a macro-kinetic rate equation because catalyst does not change its mass when it takes part in the chemical reaction. However, enzyme deactivation occurs during the hydrolysis: Cellulase enzyme, which mainly consists of endo-β-1,4-glucanase, exo-β-1,4-cellobiohydrolase and glycosidase, deactivation proceeds through the following catalytic mechanism: endo-β-1,4-glucanase and exo-β-1,4-cellobiohydrolase are first adsorbed on the surface of insoluble substrate (cellulose) to form complexes. These may be the effective complex and ineffective complex. The former further produces the cellobiose and free enzyme, and the latter deactivates endo-β-1,4-glucanase and exo-β-1,4-cellobiohydrolase. Glycosidase catalyzes the cellobiose into glucose in liquid phase. Therefore, the effect of enzyme deactivation can be included in the variable k_1'', which can be expressed as the product of the specific rate constant k_1 and enzyme concentration:

$$k_1^{''} = k_1 e \tag{5.4}$$

Substituting Eq. (5.4) into Eq. (5.2) produces

$$r_1 = \frac{k_1 eC}{1 + G/K_{1G} + B/K_{1B}} \tag{5.5}$$

where e is the enzyme concentration (g/l), and k_1 is the specific rate constant of cellulose hydrolysis to cellobiose (l/(g.h)). Because no solid-liquid reaction occurs for the glycosidase in cellulase, glycosidase deactivation can be negligible.

(3) The cell growth follows the Monod model. The reaction rates r_X (g/(l.h)) and r_G (g/(l.h)) of cell and glucose can be expressed as

$$r_X = \mu X = \frac{\mu_m XG}{K_G + G} \tag{5.6}$$

$$r_G = \frac{r_X}{Y_{X/G}} + mX \tag{5.7}$$

where μ is the specific cell growth rate (h^{-1}), μ_m is the maximum specific cell growth rate (h^{-1}), m is the maintenance coefficient for endogenous metabolism of the microorganisms (h^{-1}), K_G is the glucose saturation constant for microbial growth (g/l), X is the cell concentration (g/l), and $Y_{X/G}$ is the yield coefficient of cell mass on the glucose (g/g). In Eq. (5.6), the cell death is negligible because it was found that there was no great improvement in fitting precision for these equations if the rate constant of cell death was included into Eq. (5.6).

(4) The product (ethanol) formation associated with the cell growth can be represented as

$$\text{Glucose} \xrightarrow{r_X,\ r_G,\ r_E} \text{Ethanol} + \text{Cell} + CO_2 \tag{5.8}$$

The reaction rate r_E (g/(l.h)) of ethanol can be expressed as

$$r_E = \frac{k_4' r_X}{Y_{X/E}} = \frac{k_4 r_X}{Y_{X/G}} \tag{5.9}$$

where $k_4 = k_4' Y_{G/E}$ is the product formation coefficient associated with cell growth (dimensionless), $Y_{G/E}$ is the conversion factor of glucose to ethanol (g/g), $Y_{X/E}$, and $Y_{X/G}$ are the yield coefficients of cell on ethanol, and cell on glucose (g/g), respectively.

(5) The enzyme deactivation is caused by the ineffective adsorption of endo-β-1,4-glucanase and exo-β-1,4-cellobiohydrolase on the solid substrate. These assumptions result in the following reaction,

$$C + e_e \xrightarrow{k_3} Ce_{ein}^* \tag{5.10}$$

where e_e is the endo-β-1,4-glucanase and exo-β-1,4-cellobiohydrolase concentration (g/l), Ce_{ein}^* is the ineffective complex formed by the enzymes and substrate (g/l), and k_3 is the specific rate constant of enzyme deactivation (l/(g.h)). The ineffective complex formation rate is assumed to be a second order reaction, which can be expressed as

$$\frac{dCe_{ein}^*}{dt} = -\frac{de_e}{dt} = k_3 e_e^2 \tag{5.11}$$

where t is the residence time (h) because the experimental data of enzymatic hydrolysis showed that a second order enzyme deactivation can describe enzymatic hydrolysis better than a first order reaction. In industrial applications, because the total enzyme concentration e (g/l) is often used and the total enzyme concentration is proportional to the endo-β-1,4-glucanase and exo-β-1,4-cellobiohydrolase concentrations, the endo-β-1,4-glucanase and exo-β-1,4-cellobiohydrolase concentrations can be expressed in terms of the total enzyme concentration,

$$e_e = fe \tag{5.12}$$

where f is the proportionality constant. Hence, Eq. (5.9) becomes

$$\frac{deC_{in}^{*}}{dt} = -\frac{de}{dt} = k_3^{'} e^2 \tag{5.13}$$

where the constant $k_3^{'} = k_3 f$ (l/(g.h)). The integration of Eq. (5.13) with the boundary conditions $e = e_0$ at $t = 0$ and $e = e$ at $t = t$ is

$$e = \frac{e_0}{1 + k_3^{'} e_0 t} \tag{5.14}$$

When $t \rightarrow$ infinite, $e \rightarrow 0$.

(6) The effects of external and internal mass transfers on the enzyme reaction and microorganism metabolic processes can be neglected based on the assumptions that 1) mixing was perfect so that there was no concentration gradient between the substrate and bulk liquid; 2) the cellulose particles were sufficiently small so that there was no concentration gradient in the interior. This assumption implies that the SSF kinetics is only dependent on time, which can be expressed as a series of ordinary differential equations as shown below.

The overall change rate in cellobiose concentration can be expressed as

$$\frac{dB}{dt} = \frac{r_1}{0.947} - r_2 = \frac{k_1 eC}{0.947\left(1 + G/K_{1G} + B/K_{1B}\right)} - \frac{k_2 B}{1 + G/K_{2G}} \tag{5.15}$$

where t is the residence time (h), and 0.947 is the conversion factor of two glucan units in cellulose to cellobiose.

Eq. (5.15) combined with Eq. (5.14) produces

$$\frac{dB}{dt} = \frac{r_1}{0.947} - r_2 = \left[\frac{k_1 C}{0.947\left(1 + G/K_{1G} + B/K_{1B}\right)}\right]\left(\frac{e_0}{1 + e_0 k_3^{'} t}\right) - \frac{k_2 B}{1 + G/K_{2G}} \tag{5.16}$$

The overall change rates in glucose, cell, and ethanol concentrations are, respectively, expressed as

$$\frac{dG}{dt} = \frac{r_2}{0.95} - r_G = \frac{k_2 B}{0.95\left(1 + G / K_{2G}\right)} - \frac{\mu_m XG}{\left(K_G + G\right)Y_{X/G}} - mX \tag{5.17}$$

$$\frac{dX}{dt} = \frac{\mu_m XG}{K_G + G} \tag{5.18}$$

$$\frac{dE}{dt} = \frac{k_4 \mu_m XG}{\left(K_G + G\right)Y_{X/G}} \tag{5.19}$$

where 0.95 is the conversion factor of cellobiose to two glucose molecules.

The equations (5.16-5.19) can be used in principle to simulate the concentration changes of cellobiose, glucose, cell mass, and ethanol with respect to time. However, to make the equations operable, the cellulose concentration should be stated in terms of the other soluble concentrations because the measurement of cellulose concentration, as solid particles in suspension, in Eq. (5.16) is tedious. Assuming negligible by-product formation, the mass balance on cellulose can be expressed in terms of cellobiose, glucose, ethanol, and cell in the culture as follows,

$$C = C_0 - 0.9G - 0.947B - 0.9E/0.511 - 1.137\left(X - X_0\right) \tag{5.20}$$

where C_0 is the initial cellulose concentration (g/l), X_0 is the initial cell concentration (g/l), the constant 0.9 is the conversion factor of a glucan unit in cellulose to glucose, 0.511 is the inverse conversion factor of glucose to ethanol, and the constant 1.137 is the conversion factor of cellulose consumed to produce yeast (g cellulose/g dry cell) assuming the molecular formula of the yeast, *Saccharomyces cerevisiae*, to be $CH_{1.74}N_{0.2}O_{0.45}$ during anaerobic fermentation of glucose [Shuler and Kargi, 2002].

Furthermore, it was noted that the cellobiose concentration in our SSF experiments approached zero (Fig. 1). Therefore, the term B/K_{1B} in Eq. (5.19) can be negligible.

Substituting Eq. (5.20) into Eq. (5.16) produces

$$\frac{dB}{dt} = \frac{r_1}{0.947} - r_2 = \frac{k_1\left[C_0 - 0.9G - 0.947B - 0.9E/0.511 - 1.137\left(X - X_0\right)\right]}{0.947\left(1 + G/K_{1G}\right)} \left(\frac{e_0}{1 + k_3' e_0 t}\right) - \frac{k_2 B}{1 + G/K_{2G}} \tag{5.21}$$

Eqs. (5.21, 5.17-5.19) combined with the initial conditions $C = C_0$, $e = e_0$, $X = X_0$, $G = 0$, and $B = 0$ at time $t = 0$ can describe the concentration changes of cellobiose, glucose, cell, and ethanol with respect to time. The parameters k_1, k_2, k_3', k_4, K_G, K_{1G}, K_{2G}, m, and μ_m were determined using a MATLAB fitting program (Appendix 2).

5.4 Continuous Operating Mode (CSTR)

In the continuous operation, the substrate (cellulose) is continuously fed into the culture at a flow rate F, and the outflow containing ethanol, residual cellulose, cellobiose, glucose, cell, and enzyme exits continuously at the same flow rate F. The overall change rate of cellobiose concentration can be expressed as

$$\frac{dB}{dt} = \frac{r_1}{0.947} - r_2 - DB + DB_1 \tag{5.22}$$

where $D = F/V$ is the dilution rate (h^{-1}), F is the feed rate (l/h), V is the liquid volume in reactor (l), and B_1 is the convertible cellobiose concentration from the reaction r_1 in the continuous operation, which is equal to

$$B_1 = \frac{C_1 - C}{0.947} \tag{5.23}$$

where C_1 is the cellulose concentration (g/l) in the feed flow. Substituting Eq. (5.23) into Eq. (5.22) produces

$$\frac{dB}{dt} = \frac{r_1}{0.947} - r_2 + \frac{D(C_1 - C)}{0.947} - DB \tag{5.24}$$

Substituting Eqs. (5.3, 5.5, 5.20) into Eq. (5.24) produces

$$\begin{aligned}\frac{dB}{dt} &= \frac{k_1 e\left[C_0 - 0.9G - 0.947B - 0.9E/0.511 - 1.137(X - X_0)\right]}{0.947(1 + G/K_{1G})} - DB \\ &+ \frac{D}{0.947}\left\{C_1 - \left[C_0 - 0.9G - 0.947B - 0.9E/0.511 - 1.137(X - X_0)\right]\right\} - \frac{k_2 B}{1 + G/K_{2G}}\end{aligned} \tag{5.25}$$

Similarly, the overall reaction rate of glucose, the production rate of cell, the production rate of ethanol, and the rate of enzyme deactivation are, respectively, expressed as

$$\frac{dG}{dt} = \frac{r_2}{0.95} - r_G - DG = \frac{k_2 B}{0.95(1 + G/K_{2G})} - \frac{\mu_m XG}{(K_G + G)Y_{X/G}} - mX - DG \tag{5.26}$$

$$\frac{dX}{dt} = \frac{\mu_m XG}{K_G + G} - DX \tag{5.27}$$

$$\frac{dE}{dt} = \frac{k_4 \mu_m XG}{(K_G + G)Y_{X/G}} - DE \tag{5.28}$$

$$\frac{de}{dt} = -k_3' e^2 + D(e_0 - e) \tag{5.29}$$

5.5 Fed-batch Operating Mode

In a fed-batch operation, the substrate (cellulose) is continuously fed into the culture at a flow rate F (usually a constant rate), but no outflow exits from the reactor. In such a situation, the culture volume (V) in the reactor is not constant, but increases at the rate F.

The overall rate $dC^{'}/dt$ (g/h) of change of cellulose mass and the rate $dB^{'}/dt$ of change of cellobiose mass in the culture of fed-batch operation can be, respectively, expressed as

$$\frac{dB^{'}}{dt} = \frac{Vr_1}{0.947} - Vr_2 + FB_1 \tag{5.30}$$

where B_1 is the cellobiose concentration from the reaction r_1 in the fed-batch operation, which is equal to

$$B_1 = \frac{C_1}{0.947} \tag{5.31}$$

Substituting Eq. (5.31) into Eq. (5.30) produces

$$\frac{dB^{'}}{dt} = V\left(\frac{r_1}{0.947} - r_2\right) + \frac{FC_1}{0.947} \tag{5.32}$$

However,

$$\frac{dB^{'}}{dt} = \frac{d(VB)}{dt} = B\frac{dV}{dt} + V\frac{dB}{dt} \tag{5.33}$$

The rate dB/dt (g/h) of change of cellobiose concentration is

$$\frac{dB}{dt} = \left(\frac{r_1}{0.947} - r_2\right) + \frac{DC_1}{0.947} - DB \tag{5.34}$$

Substituting Eqs. (5.3, 5.5, 5.20) into Eq. (5.34) produces

$$\begin{aligned}\frac{dB}{dt} &= \frac{DC_1}{0.947} - DB \\ &+ \left\{\left[\frac{k_1 e\left(C_0 - 0.9G - 0.947B - 0.9E/0.511 - 1.137\left(X - X_0\right)\right)}{0.947\left(1 + G/K_{1G}\right)} - \frac{k_2 B}{1 + G/K_{2G}}\right]\right\}\end{aligned} \tag{5.35}$$

Similarly, the overall change rates (g/(l.h)) of glucose, cell, ethanol, and enzyme concentrations can be, respectively, expressed as

$$\frac{dG}{dt} = \left(\frac{r_2}{0.95} - r_G \right) - \frac{GF}{V}$$
$$= \left[\frac{k_2 B}{0.95(1 + G / K_{2G})} - \frac{\mu_m XG}{Y_{X/G}(K_G + G)} - mX \right] - DG \tag{5.36}$$

$$\frac{dX}{dt} = \frac{\mu_m XG}{K_G + G} - DX \tag{5.37}$$

$$\frac{dE}{dt} = \frac{k_4 \mu_m XG}{(K_G + G) Y_{X/G}} - DE \tag{5.38}$$

$$\frac{de}{dt} = -k_3' e^2 + De_0 - De \tag{5.39}$$

The change rate of culture volume is expressed as

$$\frac{dV}{dt} = F \tag{5.40}$$

It is noted that the dilution rate D for a fed-batch operation varies with time, while in the continuous operation D is a constant. The total masses (g/l) of cellobiose B', glucose G', cell X', ethanol E', and enzyme e' in the culture can be calculated by the corresponding concentrations B, G, X, E, and e multiplying the culture volume.

5.6 Materials and Methods

5.6.1 Materials

The following materials were used in the SSF experiments: microcrystalline cellulose (Avicel PH 101), Novozymes enzyme NS50052 (Novozymes, North America, Inc. Franklinton, NC), and *Saccharomyces cerevisiae*. The enzyme activity determined by the filter paper method was 97 FPU/g [Ghose, 1987]. The initial enzyme concentration used in the experiments was 4 g/l (9.7 FPU/g substrate).

The inoculation medium for *S. cerevisiae* was YM broth, which contained 0.3% yeast extract, 0.3% malt extract, 0.5% peptone, and 1.0% glucose. The fermentation medium contained 0.3% yeast extract, 0.25 g/l $(NH_4)_2HPO_4$, and 0.025 g/l $M_gSO_47H_2O$.

5.6.2 Methods

5.6.2.1 Preparation of Inoculum

Fresh colonies of *S. cerevisiae* from agar plates were inoculated in 500 ml Erlenmeyer flasks containing 200 ml YM medium with concentration 21 g/l. The cultures were grown in a shaker bath at 35°C and 200 rpm. The cells were harvested after 18 hours, at which time the optical density (OD) at 600 nm of the cells in the medium was greater than 0.35 after 10:1 dilution. The cells were centrifuged at 6000 rpm for 5 minutes under sterile condition, the supernatants were decanted, and the remaining solid was re-suspended in 50 ml of deionized sterile water. The washing operation was repeated three times. Finally, the cells were stored in 10 ml of deionized sterile water in the refrigerator until the time they were utilized for the fermentation.

5.6.2.2 Simultaneous saccharification and fermentation

The simultaneous saccharification and fermentation experiments were conducted in a DCU3, quad 1-liter fermenter (B. Braun Biotech International). The fermentation medium was composed of 0.5 l citric acid buffer (0.05 M, pH 4.8), 20 g Avicel PH 101, and 2.0 g Novozymes enzyme. The medium was initially inoculated with 0.15 g (dry weight) *S. cerevisiae*. The fermentation temperature was maintained at 36^{o}C, and a pH of 4.8 was maintained by automatic addition of either 2M hydrochloric acid or 2M sodium hydroxide solution during the SSF period. The agitation rate was constant at 300 rpm.

Two ml aliquots of the broth were taken periodically and prepared for analysis as described below.

5.6.2.3 Differential centrifugation sedimentation for separation of cellulose particles and yeast from the broth

Because the Avicel cellulose particles were mixed with the cell mass, direct measurement of cell concentration using spectrophotometric method was not possible. Thus, the substrate should be first separated from the broth by centrifugation. The aliquot was first centrifuged at 500 rpm for 5 minutes, which caused only the Avicel particles to settle out because of their higher density than that of the yeast cells. The mixture was decanted, and the supernatant containing the cells and medium was centrifuged again at 6000 rpm for 5 minutes. This second centrifugation caused the yeast cells to settle out. The supernatant was then decanted and prepared for HPLC analysis by filtering through 0.2 μm syringe filter.

5.6.2.4 Analytical methods

The wet cells from the second centrifugation were dry at 105^{o}C for 24 hours and weighed. The cellobiose, glucose, and ethanol concentrations were determined using Shimadzu 10A HPLC instrument (Shimadzu, Scientific Inc. Kyoto, Japan) equipped with an RI detector, and an auto-sampler (SIL-20AC). A carbohydrate column (7.8 X 300 mm, BP-100 H^{+}, 802 Benson Polymeric Inc., Reno, NV) was used for analysis. The column temperature was 60^{o}C, and the mobile phase was 0.0025 M H_2SO_4 with a flow rate of 0.6 ml/min. The working mode of HPLC was isocratic. The identities of the components were authenticated by comparing their retention times with those of pure compounds (Sigma-Aldrich, St. Louis, MO).

5.7 Results and Discussion

5.7.1 Batch SSF experiment and simulation

The SSF kinetic data of cellobiose, glucose, ethanol, and cell concentrations with respect to time are shown in Fig. 5.1. The ethanol concentration increased rapidly within the first 30 hours, and then leveled off until 48 hours. After 48 hours, the ethanol concentration slightly decreased probably because of the microbial conversion of ethanol into organic acids. The cellobiose and glucose concentrations peaked during the initial period (Fig. 5.1), because both cellobiose and glucose were the intermediates in a series of reactions from cellulose to ethanol. It is well known that the intermediate in a series of reactions often has a maximum concentration during the reaction course [Levenspiel, 1999]. Furthermore, because the rate of enzymatic hydrolysis of cellulose at the high enzyme concentration was fast, and the rate of ethanol production at the low cell concentration was slow during this period, both factors caused the accumulations of cellobiose and glucose. It was concluded that the ethanol production in the initial period was controlled by cell growth. After several hours, the cellobiose and glucose concentrations quickly decreased, and approached zero because of the fast cell growth and the decrease in the effective enzyme concentration. The process was then controlled by the enzymatic hydrolysis. Furthermore, the experiment showed that the optimal ethanol productivity for the SSF at 48 hours was about 0.292 g/(l.h), and the maximum ethanol concentration was about 14 g/l, which was equal to a theoretical ethanol yield of 61.8% calculated from the following equation:

$$Y_{th} = \frac{0.9E}{0.511C_0}100\,\% \tag{5.41}$$

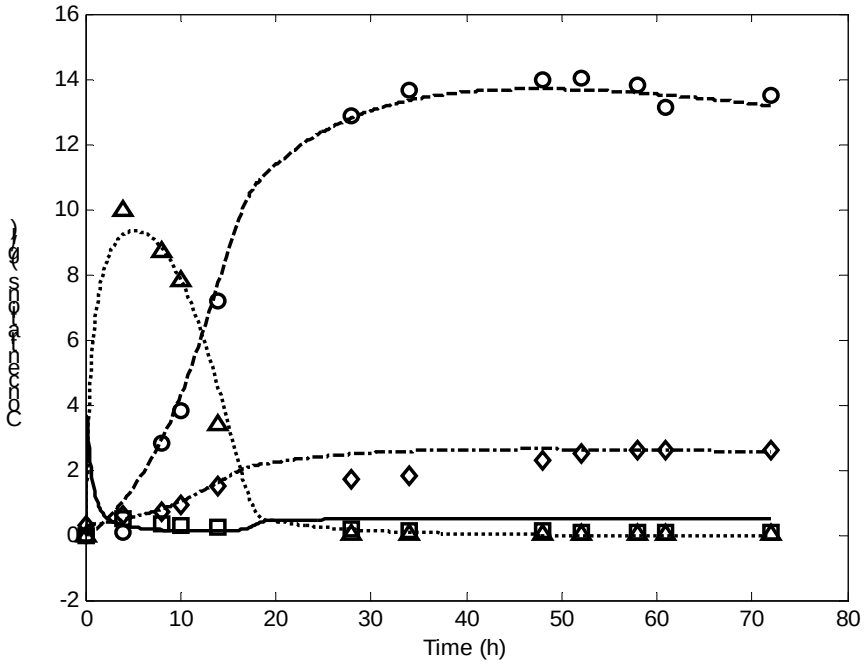

Fig. 5.1 The experimental points (signs) and simulated curves (lines) of cellobiose (□, solid), glucose (Δ, dot), ethanol (o, dash) and cell (◊,dash-dot) concentrations with time in the batch operation. Conditions: C_0 = 40 g/l, X_0 = 0.3 g/l, e_0 = 4 g/l, and $G_0 = B_0 = E_0$ = 0.

Table 5.1 The parameter values, confidence intervals, and percentages of CIs to values

Parameter	k_1 (l/(g.h))	k_2 h^{-1}	k_3' l/(g.h)	k_4 (-)	K_{1G} g/l	K_{2G} g/l	K_G g/l	m h^{-1}	μ_m h^{-1}
Value	0.6096	3.202	0.0997	3.024	0.1768	16.25	3.399	0.6420	0.1768
CI (±)	0.0281	0.0259	0.0056	0.1723	0.0091	0.0479	0.0073	0.0010	0.0006
PCI %	4.6	0.81	5.6	5.7	5.1	0.29	0.21	0.16	0.34

PCI: percentages of CIs to parametric values

This theoretical ethanol yield was similar to other experimental and industrial data [Zhu et al, 2006; Kosaric and Vardar-Sukan, 2001], but lower than 90% stated as the ideal yield [Ohgren et al. 2007; Glazer and Nikaido, 1995]. This may be because the cellulose in the SSF process had not been completely hydrolyzed due to the sub-optimal operating temperature and some by-products were produced. Another explanation may be that the carbon source required for the yeast growth was not included in the reaction equation:

$$C_6 H_{12}O_6 = 2C_2H_5OH + 2CO_2 \tag{5.42}$$

which is the basis for the theoretical yield.

The experimental values for the cellobiose, glucose, ethanol, and cell concentrations with respect to residence time were fitted in Eqs. (5.21, 5.17-5.19) at the corresponding initial conditions (C_0 = 40 g/l, X_0 = 0.3 g/l, G_0 = 0, B_0 = 0, e_0 = 4 g/l, and $Y_{X/G}$ = 0.515). $Y_{X/S}$ was determined from the experiment on *S. cerevisiae* growth on glucose. The parameters k_1, k_2, k_3', k_4, K_{1G}, K_{2G}, K_G, m, and μ_m in these equations were calculated using the MATLAB lsqnonlin method. These parametric values, their 95% confidence intervals (CI), and the percentages of CIs to the parametric values are listed in Table 5.1, and the simulated curves are shown in Fig. 5.1. The percentages of CIs to the parametric values range from 0.16-5.7%. From Fig. 5.1, we can see that the cellobiose concentration with time increased slightly in the later part of the SSF, which may imply that the conversion of cellobiose to glucose declined due to glycosidase deactivation. In Figure 5.1, the maximum cellobiose concentration was lower than the maximum glucose concentration, and the cellobiose maximum occurred earlier than the glucose maximum. This implied that the reaction from cellulose to cellobiose is a rate-controlling step because the reaction rate from cellobiose to glucose was faster than that from cellulose to

cellobiose. The value k_1e_0 ($0.61\times4 = 2.44\ h^{-1}$) of r_1 at the initial time is smaller than the rate constants k_2 ($3.20\ h^{-1}$) (Table 5.1) of r_2, but was greater than $\mu = \mu_m G/(K_G + G) = 0$ of r_X, which indicated that at the initial time, the conversion of cellulose to ethanol was controlled by cell growth. However, the enzymatic conversion of cellulose to cellobiose became the rate-controlling step as the glucose concentration increased (μ increased). The simulated data of the cell concentrations in Fig. 5.1 deviated from the experimental data between 20 and 40 hours of SSF, compared to the deviations from the other experimental points beyond the range between 20 and 40 hours. It appears that the increase in cell concentrations in the simulated curve between 20-40 hours was polynomial, while the experimental data was linear pattern. The deviation was probably because Eq. (5.4) is based on the first order kinetics for cell concentration (μX), which implies an exponential growth of cells in the presence of sufficient growth-limiting substrate. However, the cell growth in the SSF process was substrate limitation because of insufficient sugar supply from the slow reaction rate of enzymatic hydrolysis for cellulose. Therefore, the experimental cell growth was slower than the exponential growth expected from theory.

5.7.2 The effects of the initial conditions on ethanol production

The parametric constants obtained from the batch experimental data were used to estimate the effects of the initial conditions (the initial cellulose, cell, and enzyme concentrations) on ethanol production using Eqs (5.21, 5.17-5.19) (Figs. 5.2-5.4). The effects of the three initial cellulose concentrations (20, 40, and 80 g/l) on glucose, cell, and ethanol concentrations are shown in Fig. 5.2. When the initial cellulose concentration was doubled from 20 g/l to 40 g/l, and from 40 g/l to 80 g/l, the corresponding ethanol and cell concentrations almost doubled. The highest ethanol and cell concentrations were

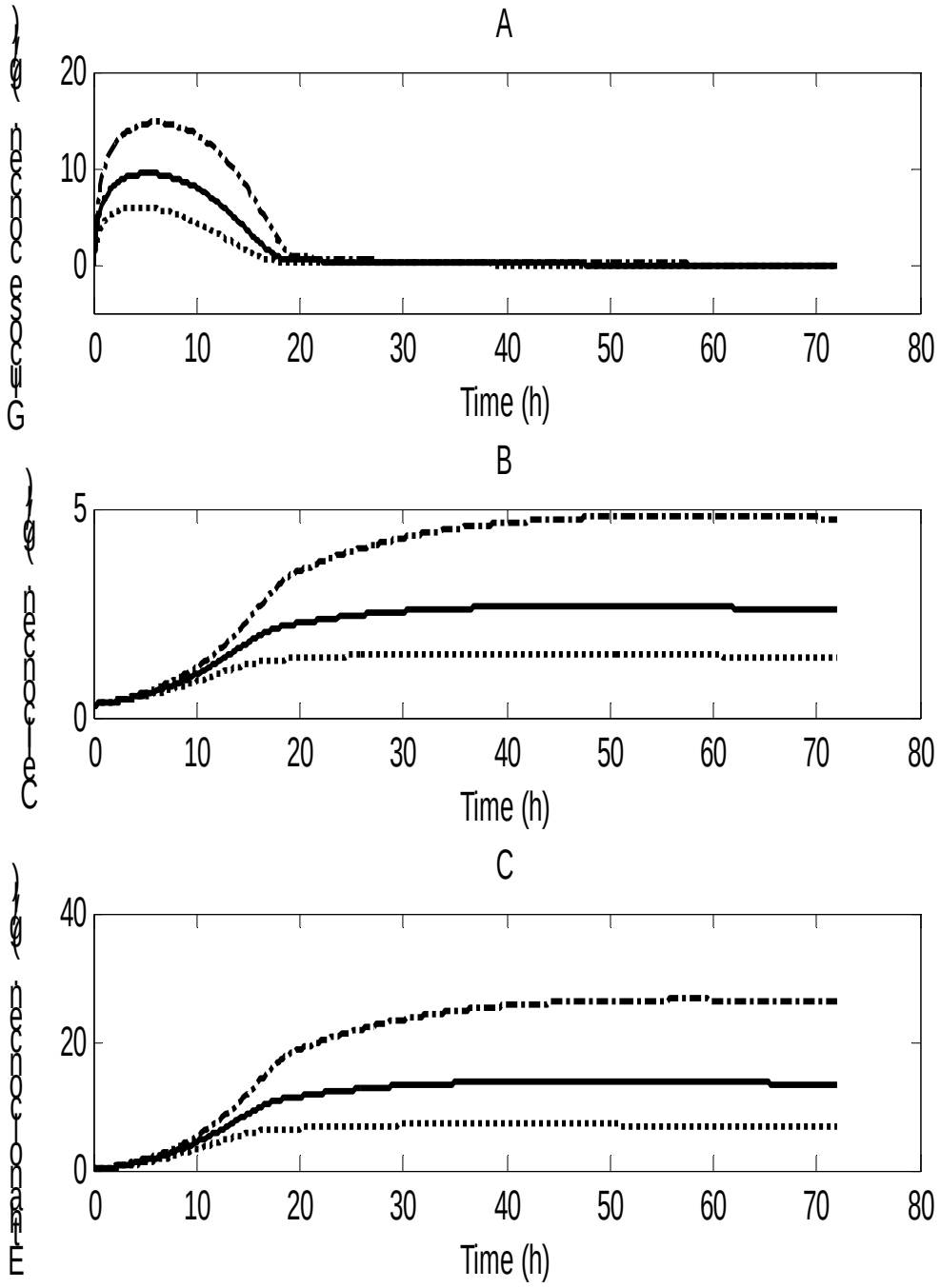

Fig. 5.2 The simulated glucose (A), cell (B), and ethanol (C) concentration curves (lines) with time at three cellulose concentrations: 20 g/l (dot), 40 g/l (solid), and 80 g/l (dash-dot) in the batch operation. Conditions: $X_0 = 0.3$ g/l, $e_0 = 4$ g/l, and $G_0 = B_0 = E_0 = 0$.

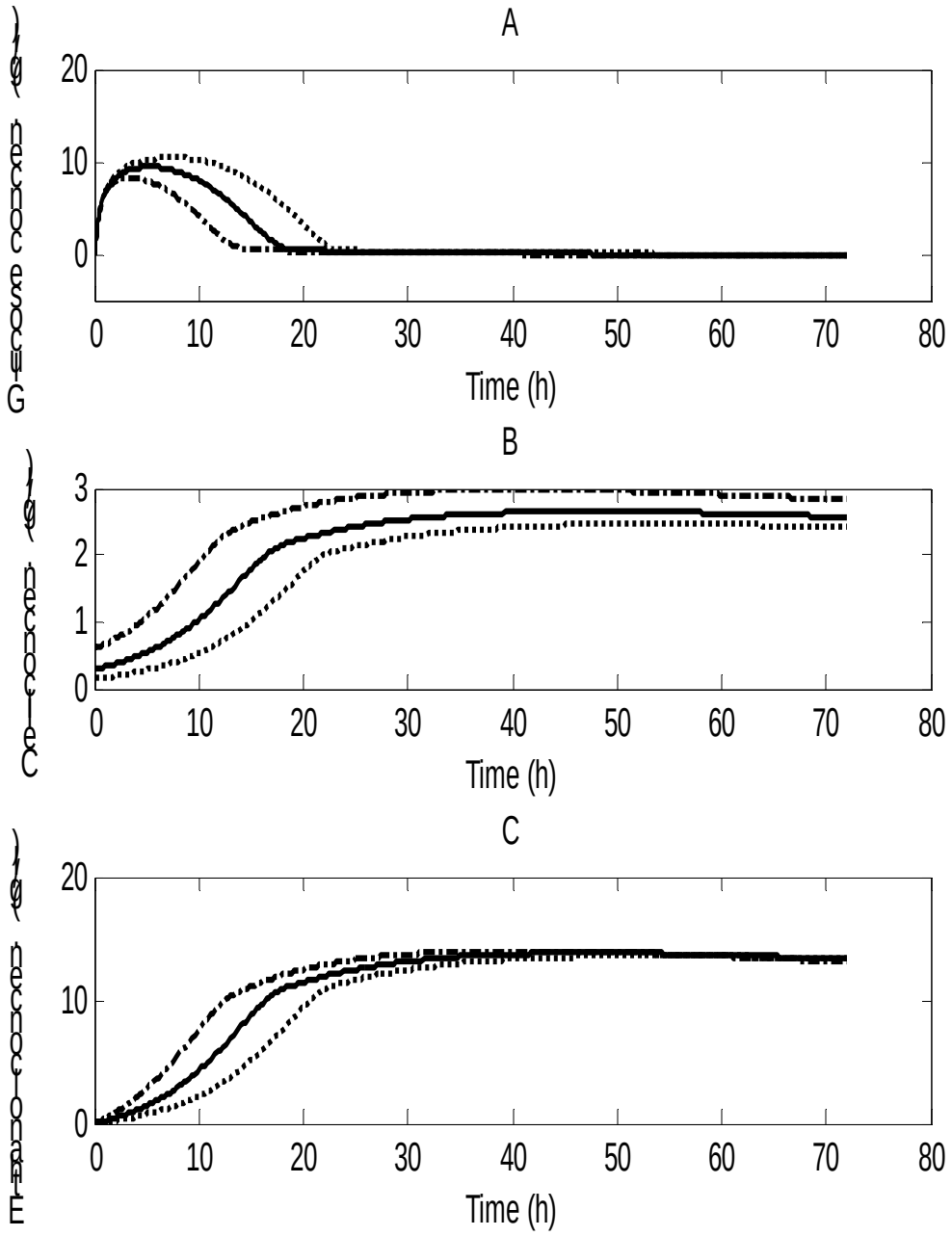

Fig. 5.3 The simulated glucose (A), cell (B), and ethanol (C) concentration curves (lines) with time at three initial cell concentrations: 0.15 g/l (dot), 0.3 g/l (solid), and 0.6 g/l (dash-dot) in the batch operation. Conditions: C_0 = 40 g/l, e_0 = 4 g/l, and $G_0 = B_0 = E_0 = 0$.

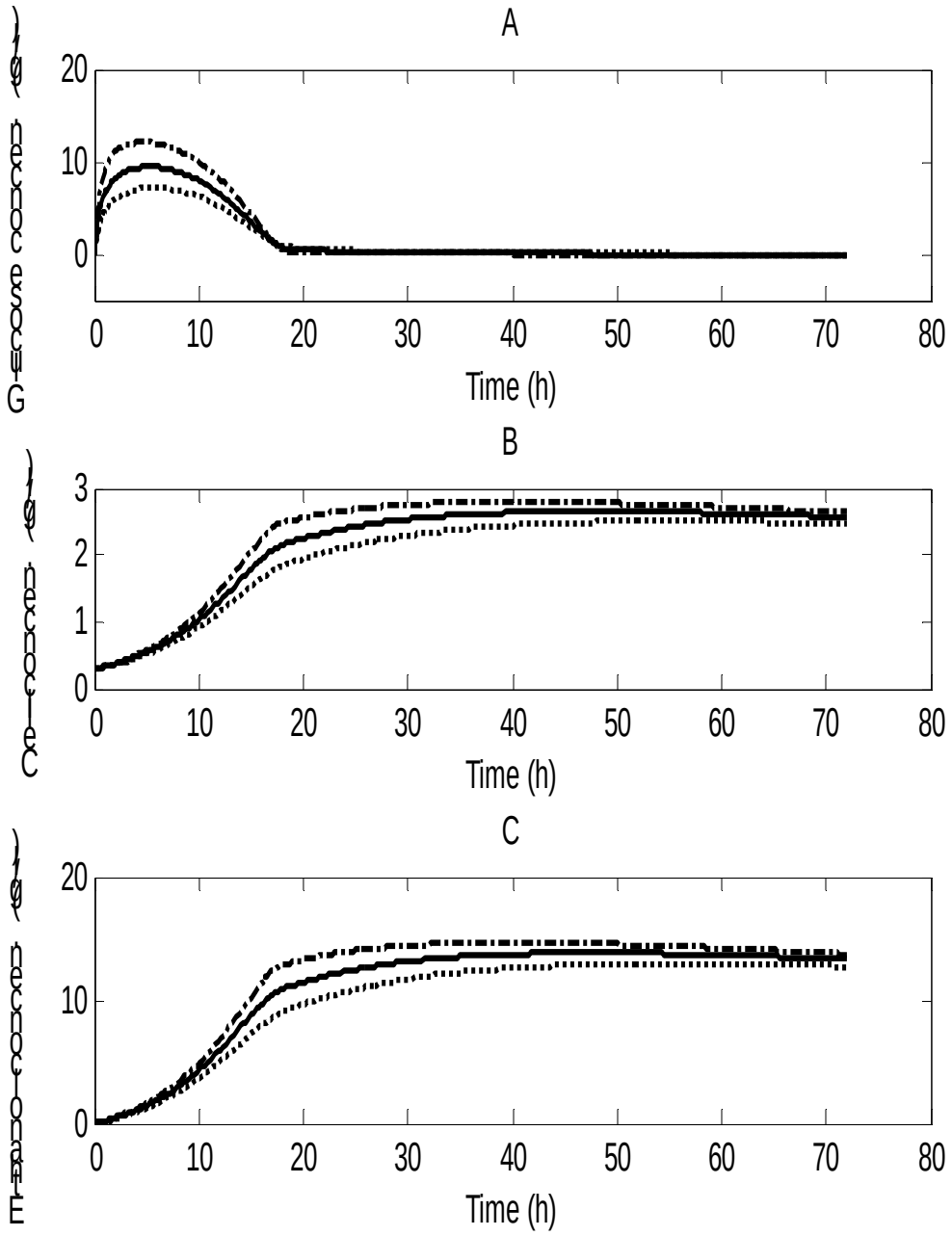

Fig. 5.4 The simulated glucose (A) cell (B), and ethanol (C) concentration curves (lines) with time at three initial enzyme concentrations: 2 g/l (dot), 4 g/l (solid), and 8 g/l (dash-dot) in the batch operation. Conditions: $C_0 = 40$ g/l, $X_0 = 0.3$ g/l, and $G_0 = B_0 = E_0 = 0$.

about 26 g/l and 4.8 g/l, respectively, for the initial cellulose concentration of 80 g/l. This suggested that the initial cellulose concentration was the main factor influencing the amount of ethanol produced. In addition, both the glucose concentration and the time to achieve the maximum concentration increased with increase in initial cellulose concentration. However, the residual glucose concentrations at the end of fermentation were similar for the three initial cellulose concentrations (Fig. 5.2).

The effects of the three initial cell concentrations (0.15, 0.3, and 0.6 g/l) on glucose, cell, and ethanol concentrations are shown in Fig. 5.3. The initial cell concentration did not have any major effect on the final ethanol concentration. Within the first 55 hours of the SSF process, the ethanol concentration for the initial cell concentration of 0.6 g/l was slightly higher than those of 0.3 g/l and 0.15 g/l. However, after 55 hours, the ethanol concentration for the initial cell concentration of 0.6 g/l was lower than those for 0.3 g/l and 0.15 g/l, because some ethanol was utilized by the cells. For example, the final cell concentration was 2.8 g/l for the initial cell concentration of 0.6 g/l, compared to 2.6 g/l and 2.4 g/l for the initial cell concentrations 0.3 g/l and 0.15 g/l, respectively, in Fig. 5.3B. In contrast, the highest glucose concentration for the initial cell concentration 0.6 g/l was lower than those for 0.3 g/l and 0.15 g/l, and the time at which the maximum glucose concentration occurred for the initial cell concentration 0.6 g/l was earlier than those for 0.3 g/l and 0.15 g/l. These can be attributed to the faster consumption of glucose at the higher cell concentration.

Fig. 5.4 shows the effects of the three initial enzyme concentrations (2, 4, and 8 g/l) on glucose, cell, and ethanol concentrations. When the initial enzyme concentration was increased from 2 g/l to 8 g/l, both the cell and ethanol concentrations increased (Fig.

5.4B, C). The maximum glucose concentration was higher with increase in the initial enzyme concentration for the same initial cellulose concentration. The time required to attain the maximum glucose concentration at the initial enzyme concentration 8 g/l was shorter than those at the other initial enzyme concentrations. The final glucose concentrations were almost the same for all three initial enzyme concentrations (Fig. 5.4A). This pattern reflects the basic property of catalysts: catalysts can increase the reaction rate, but cannot change the chemical equilibrium. In summary for the batch SSF process, the initial cellulose concentration is the most important factor in ethanol production, followed by the initial enzyme and cell concentrations.

5.7.3 Simulation of continuous operation

The variations in glucose, cell, and ethanol concentrations over time at various dilution rates in the continuous operation are shown in Fig. 5.5. From these graphs, we can see that the model indicates a basic property of the continuous operation: the concentrations of the three components approached constant values at the steady state with increasing residence time. When the dilution rate was increased, the time to reach the steady state of the system increased. However, when the dilution rate approached the washout point ($D = 0.08\ h^{-1}$), the steady state of the system immediately reached the point at which both the cell and ethanol concentrations were very low. At the steady state, the highest ethanol concentration was about 12.2 g/l at the dilution rate $0.01\ h^{-1}$ (Fig. 5.5C). This value was slightly lower than that in the batch experiment (14 g/l) because 1) the highest ethanol concentration was dependent on the dilution rate. The smaller the dilution rate, the higher the ethanol concentration; 2) the cellulose concentration C_1 (20 g/l) in the feed flow was lower than that in the batch experiment C_0 (40 g/l). Fig. 5.6 shows the

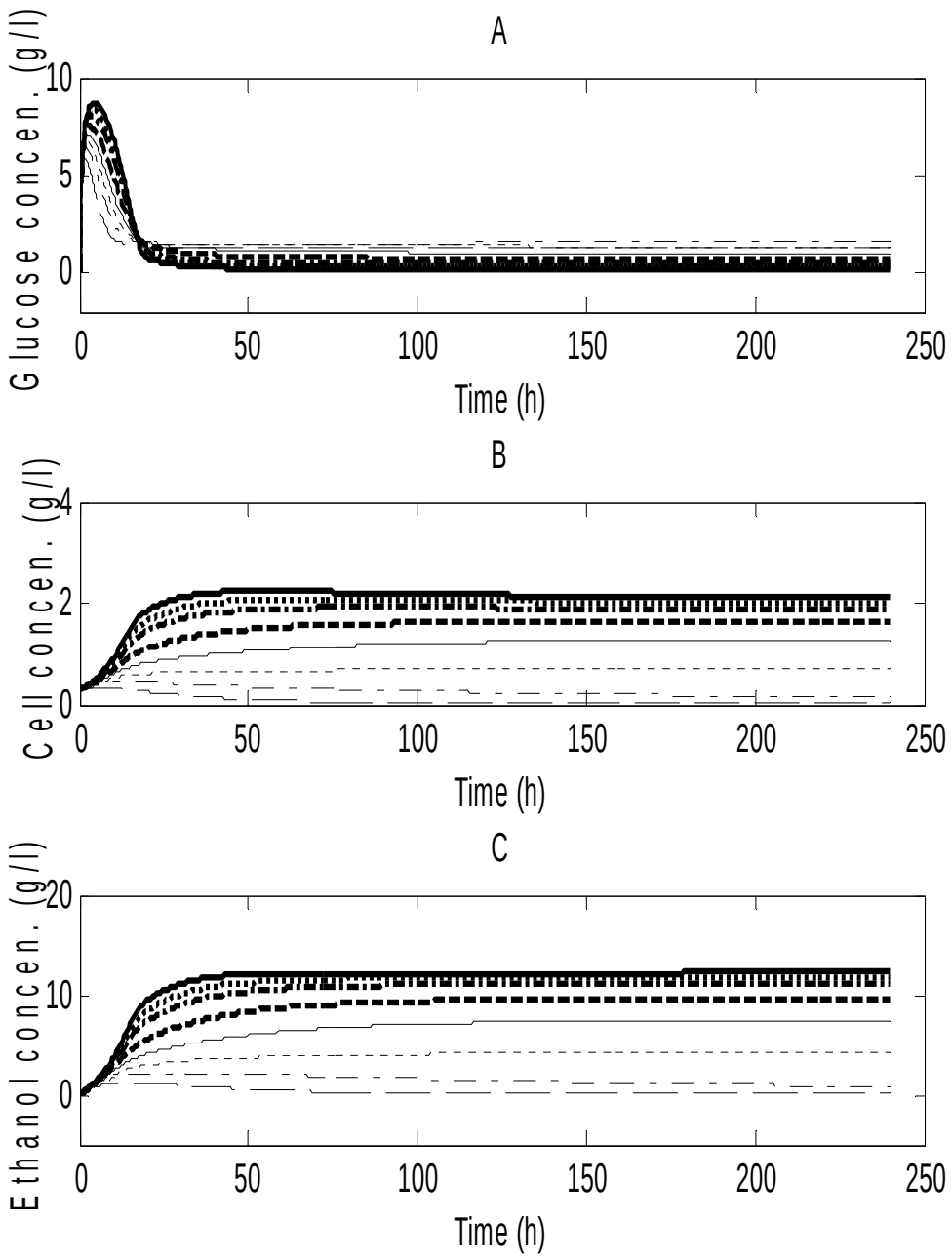

Fig. 5.5 The simulated glucose (A), cell (B), and ethanol (C) concentration curves (lines) with time at eight dilution rates: 0.01 /h (thick, solid), 0.015 /h (thick, dot), 0.02 /h (thick, dash-dot), 0.03 /h (thick, dash), 0.04 /h (fine, solid), 0.05 /h (fine, dot), 0.06 /h (fine, dash-dot), and 0.08 /h (fine, dash) in the continuous operation. Conditions: $C_0 = 40$ g/l, $C_1 = 20$ g/l, $X_0 = 0.3$ g/l, $e_0 = 4$ g/l, $e_1 = 1$ g/l, and $G_0 = B_0 = E_0 = 0$.

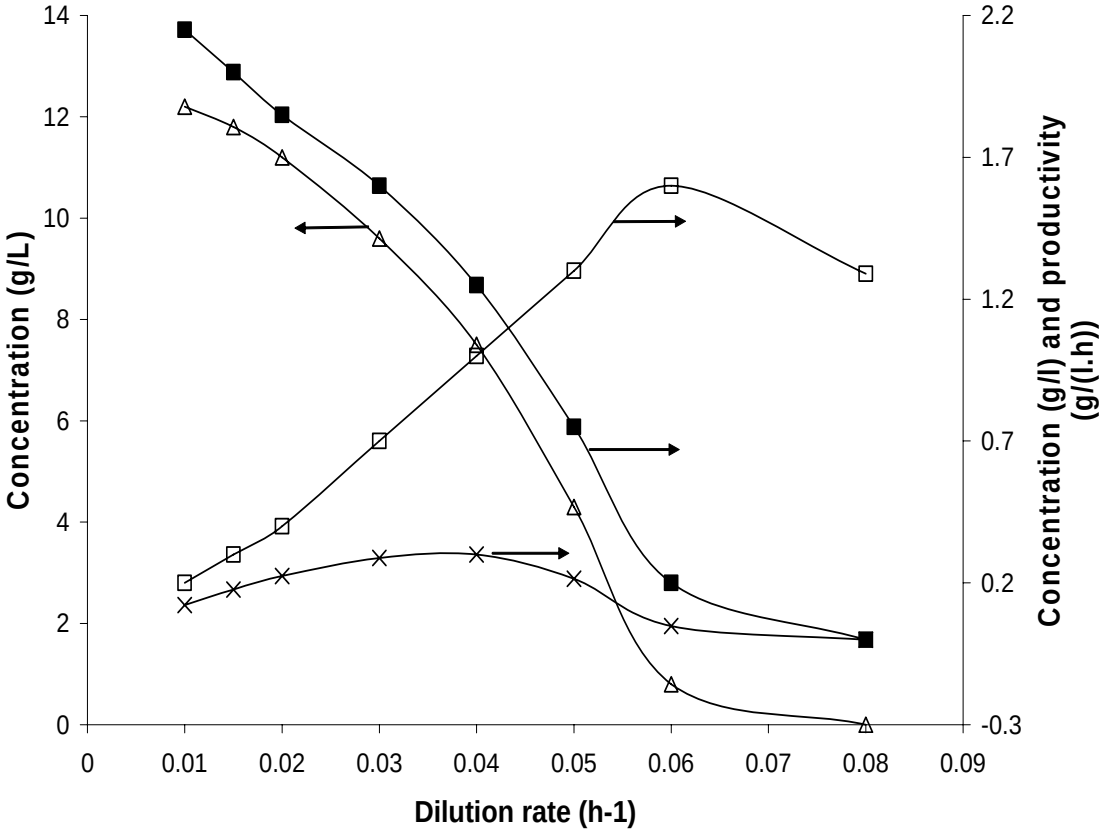

Fig. 5.6 The glucose, cell, and ethanol concentrations and productivity with dilution rate in the continuous operation. Glucose (□), cell (■), ethanol (Δ), and productivity (x). Conditions: $C_0 = 40$ g/l, $C_1 = 20$ g/l, $X_0 = 0.3$ g/l, $e_0 = 4$ g/l, $e_1 = 1$ g/l, and $G_0 = B_0 = E_0 = 0$.

glucose, cell, and ethanol concentrations as well as productivity (DE) at the steady state for various dilution rates. When the dilution rate was increased, the ethanol and cell concentrations decreased, whereas the glucose concentration increased to a maximum at the dilution rate 0.06 h^{-1}. The ethanol productivity increased with increased dilution rate until a maximum value (about 0.3 g/(l.h)) was attained at a dilution rate of 0.04 h^{-1}, and rapidly decreased to zero at a washout point. These observations about ethanol, cell, and productivity showed that the general principle of chemostat operation is applicable to the complicated situation of SSF [Blanch and Clark, 1996; Stanburg et al., 1995]. It should be noted that the glucose was an intermediate rather than an initial reactant. Therefore, its concentration did not decrease monotonically with increasing dilution rate.

5.7.4 Simulation of fed-batch operation

The variations in the concentrations of glucose, cell, and ethanol with time at the three feed flow rates (0.01, 0.02 and 0.03 l/h) in the fed-batch operation are shown in Fig. 5.7 (initial culture volume V_0 = 1 l, and cellulose concentration in the feed C_1 = 20 g/l). The corresponding variations of masses with time are presented in Fig. 5.8. The ethanol and cell concentrations quickly increased to a maximum within 20 hours. After 25 hours, the glucose and ethanol concentrations at the three flow rates were silimar (Fig. 5.7A and C), but there was a slight difference in cell concentrations (Fig. 5.7B), both of which resulted from the dilution effect of increasing the culture volume. Furthermore, the cell, ethanol, and glucose concentrations at the three feed flow rates were approximately constant after 30 hours (Fig. 5.7). This observation showed that the process achieved a quasi-steady state for the fed-batch operation when the substrate concentration in the feed was much greater than that in the culture [Pirt, 1979]. It is interesting to note that the cell

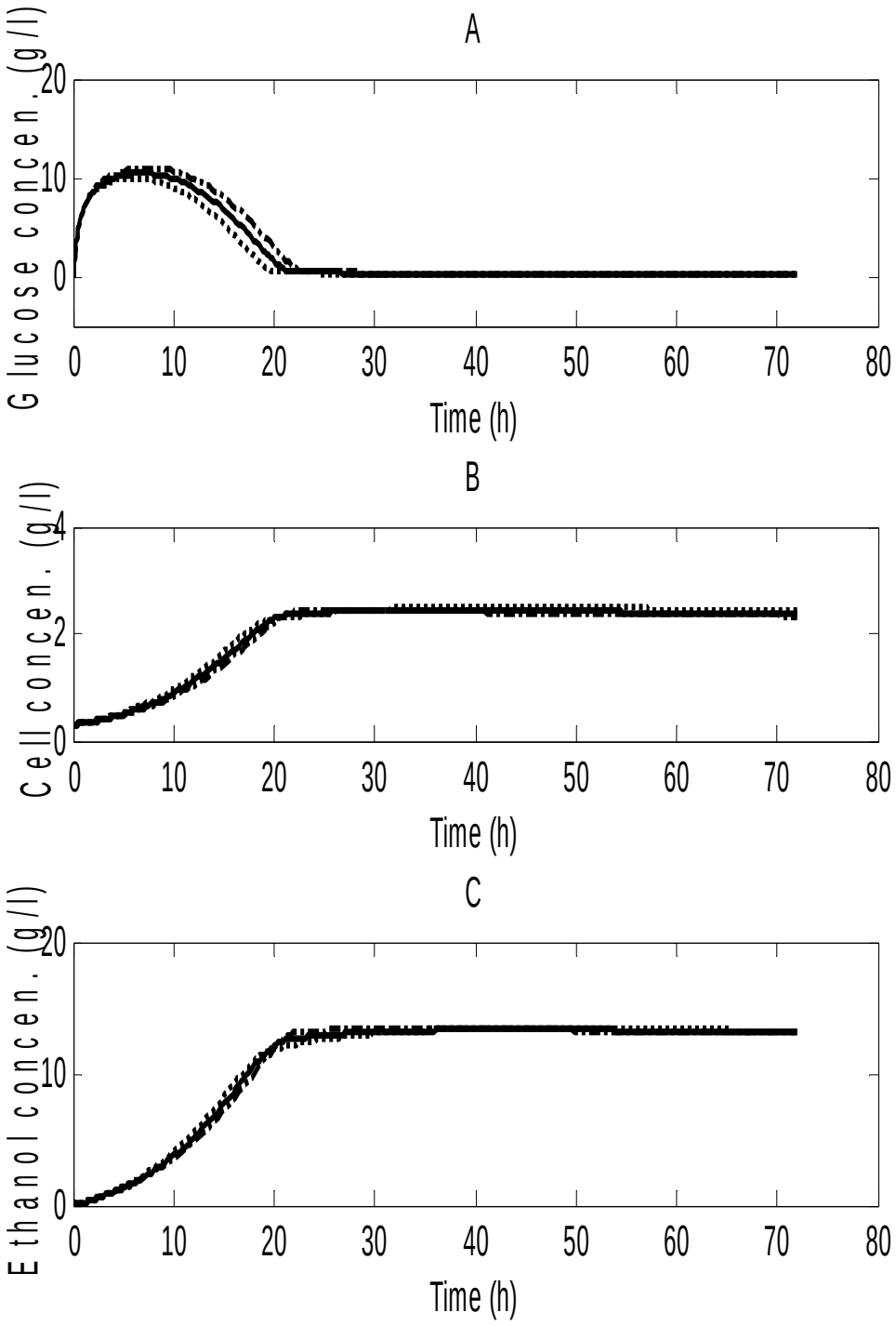

Fig. 5.7 The simulated glucose (A), cell (B), and ethanol (C) concentration curves (lines) with time at three flow rates: 0.01 l/h (dot), 0.02 l/h (solid), and 0.03 h/l (dash-dot) in the fed-batch operation. Conditions: C_0 = 40 g/l, C_1 = 20 g/l, e_0 = 4 g/l, e_1 = 1 g/l, X_0 = 0.3 g/l, V_0 = 1 l and $G_0 = B_0 = E_0 = 0$.

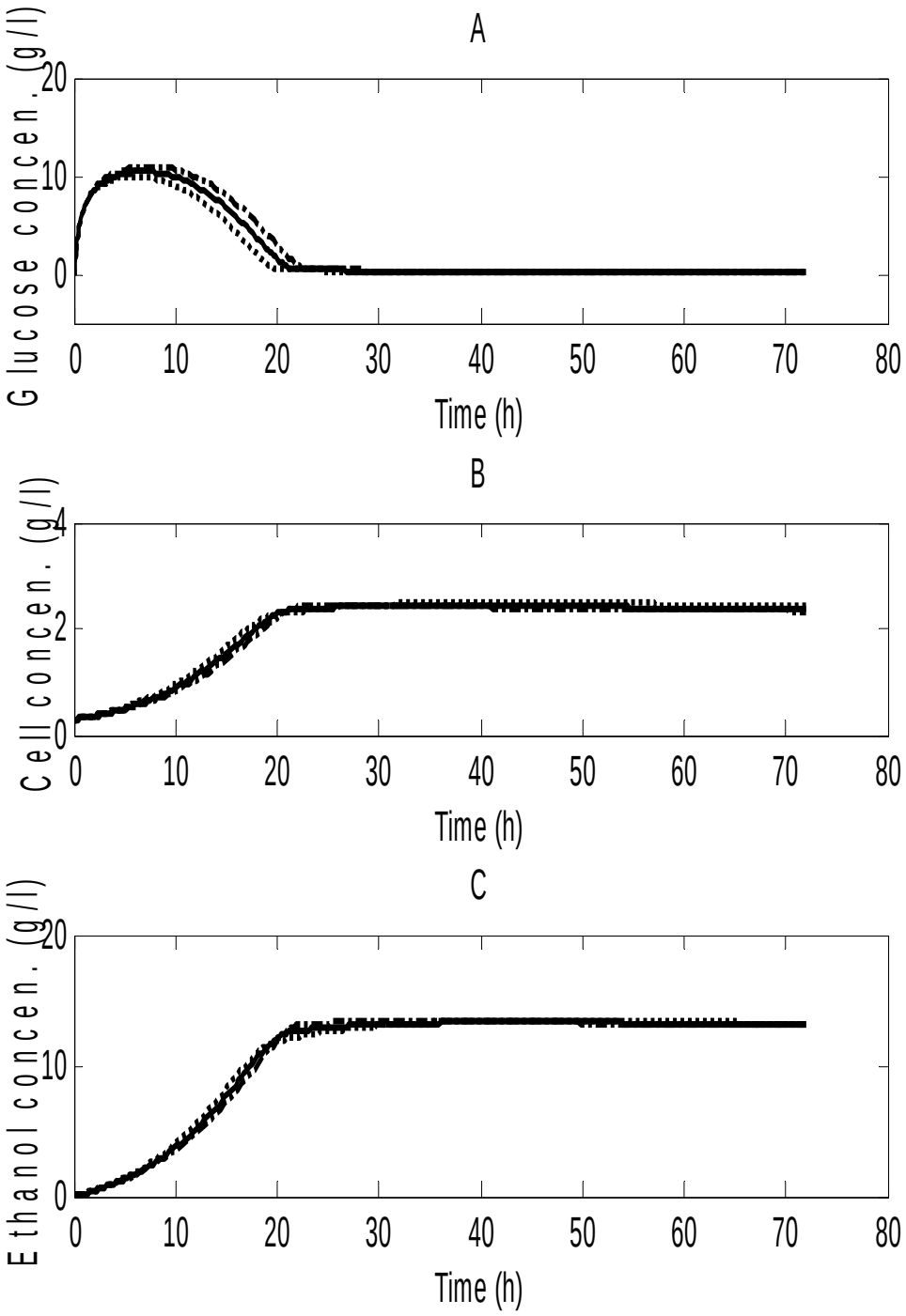

Fig. 5.8 The simulated glucose (A), cell (B), and ethanol (C) mass curves (lines) with time at three flow rates: 0.01 l/h (dot), 0.02 l/h (solid), and 0.03 h/l (dash-dot) in the fed-batch operation. Conditions as the same as Fig. 5.7.

and ethanol masses in the culture for the fed-batch operation greatly increased to about 7.5 g and 42 g, respectively, compared to the cell mass of 2.2 g and the ethanol mass of 14 g in the batch experiment.

5.8 Conclusions

Simultaneous saccharification and fermentation of ethanol production from lignocellulosic materials is a more advanced operating mode than separate hydrolysis and fermentation. The proposed model of the SSF process consists of the four ordinary differential equations to describe the changes in cellobiose, glucose, microorganism, and ethanol concentrations with respect to residence time. The model can be used to fit the experimental data for the four main components in the SSF process of ethanol production without additional experiments. The simulation of the batch experiments of ethanol produced from Avicel PH 101 indicated that the initial cellulose concentration was the main factor influencing the amount of ethanol produced; the initial enzyme and yeast concentrations had minor influences on ethanol production. Extended models for the continuous and fed-batch operations were also developed based on the batch model. Both models can be used to predict the dynamics of the continuous and fed-batch SSF operations of ethanol production based on the parameters obtained from the batch experiments. The simulated fed-batch operation showed a higher ethanol mass than the batch operation. The simulation also showed that there was an optimal dilution rate for the maximum productivity of ethanol in the SSF continuous mode. These models provide a basis for simulating and scaling up the SSF process.

References

Blanch, H. W. and Clark, D. S. *Biochemical Engineering*. Marcel Dekker, Inc. New York, NY. p 290, 1996.

Ghose. T. K. Measurement of cellulase activities. Pure and Applied Chemistry, 59 (2) 257-268, 1987.

Glazer, A. N., and Nikaido, H. Microbial Biotechnology W. H. Freedom and Company, New York. p. 366, 1995.

Kosaric, N., and Vardar-Sukan, F. Potential source of energy and chemical products in *The Biotechnology of Ethanol* edited by Roehr, M. WILEY-VCH Verlag GmbH, D-69469. p. 180, 2001.

Lehninger, A. L., Nelson, D. L., and Cox, M. M. *Principles of Biochemistry*, 2nd, Worth Publishers Inc. p. 229, 1993.

Levenspiel, O. *Chemical Reaction Engineering*, 3rd. John Wiley & Sons, Inc. p. 171, 1999.

Ohgren, K., Bura, R., Lesnicki, G., Saddler, J., and Zacchi, G. A comparison between simultaneous saccharification and fermentation and separate hydrolysis and fermentation using steam-pretreated corn stover. Process Biochemistry. 42 (5), 834-839, 2007.

Philippidis G. P., Hatzis C. Biochemical engineering analysis of critical process factors in the biomass to ethanol technology. Biotechnology Progress 13 (3): 222-231, 1997.

Philippidis G. P., Spindler, D. D. and Wyman, C. E. Mathematical modeling of cellulose conversion to ethanol by the simultaneous saccharification and fermentation process. Applied Biochemistry and Biotechnology. 34-5: 543-556, 1992.

Philippidis G. P., Smith, T. K., and Wyman, C. E. Study of the enzymatic hydrolysis of cellulose for production of fuel ethanol by simultaneous saccharification and fermentation process. Biot4echnology and Bioengineering 41 (9): 846-853, 1993.

Pirt, S.J. Fed-batch culture of microbes. Annals of the New York Academy of Sciences. Vol. 326, 119-125, 1979.

Shuler, M. L., and Kargi, F. *Bioprocess Engineering*. 2Ed, Prentice Hall PTR. p. 217, 2002.

South, C. R., Hogsett, D. A. L., and Lynd, L. R. Modeling simultaneous saccarification and fermentation of lignocellulose to ethanol in batch and continuous reactors. Enzyme and Microbial Technology. 17 (9), 797-803, 1995.

Stanburg, P. F., Whitaker, A., and Hall, S. J. *Principles of Fermentation Technology*, 2nd, Elserier Science Ltd. p. 23, 1995.

Zhu, S. D., Wu, Y. X., Zhao, Y. F., Tu, S. Y., and Xue, Y. P. Fed-batch simultaneous saccharification and fermentation of microwave/acid/alkali/H2O2 pretreated rice straw for production of ethanol. Chemical Engineering Communications. 193 (5), 639-648, 2006.

Chapter Six

Modeling Semi-simultaneous Saccharification and Fermentation of Ethanol Production from Cellulose*

6.1 Introduction

As discussed in Chapter Two, there are two common operating modes for the production of bioethanol from lignocellulosic materials: separate hydrolysis and fermentation (SHF), and simultaneous saccharification and fermentation (SSF). SSF generally has the higher productivity (ethanol produced per unit mass of dry feedstock per unit time (g/(g.h)) than SHF, because SSF has shorter operating time. However, for the yield (ethanol produced per unit mass of dried feedstock (g/g)), there is no consensus conclusion about which method is better. Semi-simultaneous saccharification and fermentation (SSSF), which consists of a pre-hydrolysis and a SSF, is an operating mode between SSF and SHF. SSSF is expected to have higher productivity and yield than both SSF and SHF. The difference between SSSF and SHF is that the substrate is not removed in SSSF so that it is continuously hydrolyzed by enzyme during the entire period, while the substrate is separated from the hydrolysate after hydrolysis in case of SHF. The difference between SSSF and SSF is that SSSF has a pre-hydrolysis. In this chapter, the modeling semi-simultaneous saccharification and fermentation of ethanol production from cellulose is reported.

*****Jiacheng Shen and Foster A. Agblevor. Modeling semi-simultaneous saccharification and fermentation of ethanol production from cellulose. Submitted to Biomass & Bioenergy.

6.2 Objectives

In this study, the objectives were

(1) To demonstrate the advantages of SSSF process in yield and productivity of ethanol production over SHF and SSF processes;

(2) To develop SSSF models for the batch, continuous, and fed-batch operations. The models will describe the variations in both the main component and by-product concentrations;

(3) To estimate the model parameters from fitting the data in the SSSF experiments;

(4) To predict the effects of continuous and fed-batch SSSF operations based on the parameters obtained from the batch experiments.

6.3 Batch Operating Mode

Following the enzymatic reaction mechanism from cellulose to glucose in Chapter 5.2 (Eq. (5.1)),

$$\text{Cellulose} \xrightarrow{r_1} \text{Cellobiose} \xrightarrow{r_2} \text{Glucose} \qquad (5.1)$$

the reaction rate r_1 (g/(l.h)) from cellulose to cellobiose during its hydrolysis can be expressed as

$$r_1 = \frac{k_1 eC}{1 + G/K_{1G} + B/K_{1B}} \qquad (5.5)$$

and the reaction rate r_2 (g/(l.h)) from cellobiose to glucose during its hydrolysis can be expressed as

$$r_2 = \frac{k_2 B}{1 + G / K_{2G}} \tag{5.3}$$

The reaction of product (ethanol) formation associated with the cell growth in Chapter 5.2 is

$$\text{Glucose} \xrightarrow{r_X,\ r_G,\ r_E} \text{Ethanol} + \text{Cell} + CO_2 \tag{5.8}$$

In Chapter 5.6, it was found that a first order reaction

$$r_X = \mu X = \frac{\mu_m XG}{K_G + G} \tag{5.6}$$

overestimated the actual cell growth in SSF because of limitation of carbon supply [Shen and Agblevor, 2008a]. In this study, the cell growth is assumed proportional to n orders of cell concentration, where n is constant to be determined by a fitting program. Therefore, the reaction rates r_X (g/(l.h)) and r_G (g/(l.h)) of cell and glucose can be, respectively, expressed as

$$r_X = \mu X^n = \frac{\mu_m X^n G}{K_G + G} \tag{6.1}$$

$$r_G = \frac{r_X}{Y_{X/G}} + mX^n \tag{6.2}$$

where μ is the specific cell growth rate constant $((l/g)^{n-1}h^{-1})$, μ_m is the maximum specific cell growth rate constant $((l/g)^{n-1}h^{-1})$, m is the maintenance coefficient for endogenous metabolism of the microorganisms $((l/g)^{n-1}h^{-1})$, K_G is the glucose saturation constant for the microbial growth (g/l), X is the cell concentration (g/l), and $Y_{X/G}$ is the yield coefficient of cell mass on the glucose (g/g).

The reaction rate r_E (g/(l.h)) of ethanol formation can be expressed as

$$r_E = k_4'' r_X \tag{6.3}$$

where k_4'' is the product formation coefficient associated with cell growth (dimensionless).

The by-product reactions are considered parallel with the main reaction (5.1). The reaction rate r_{Gl}, r_A, and r_L (g/(l.h)) of glycerol, acetic acid, and lactic acid can be, respectively, expressed as

$$r_{Gl} = k_5 r_X \tag{6.4}$$

$$r_A = k_6 r_X \tag{6.5}$$

$$r_L = k_7 r_X \tag{6.6}$$

where k_5, k_6, k_7 are the coefficients of glycerol, acetic acid, and lactic acid formations associated with cell growth (dimensionless), respectively.

The enzyme deactivation is caused by the ineffective adsorption of endo-β-1,4-glucanase and exo-β-1,4-cellobiohydrolase on the solid substrate (Chapter 5.2). Its integration with the boundary conditions $e = e_0$ at $t = 0$ and $e = e$ at $t = t$ can be expressed as (Chapter 5.2)

$$e = \frac{e_0}{1 + k_3' e_0 t} \tag{5.14}$$

The overall change rate of cellobiose concentration is expressed as

$$\frac{dB}{dt} = \frac{r_1}{0.947} - r_2 = \frac{k_1 e C}{0.947\left(1 + G/K_{1G} + B/K_{1B}\right)} - \frac{k_2 B}{1 + G/K_{2G}} \tag{6.7}$$

where 0.947 is the conversion factor of two glucan units in cellulose to cellobiose.

Eq. (6.7) combined with Eq. (5.14) and the term B/K_{1B} was negligible because of approximate zero cellobiose concentration in Fig. 6.3 and 6.4 produces

$$\frac{dB}{dt} = \frac{r_1}{0.947} - r_2 = \left[\frac{k_1 C}{0.947\left(1 + G/K_{1G}\right)}\right]\left(\frac{e_0}{1 + e_0 k_3' t}\right) - \frac{k_2 B}{1 + G/K_{2G}} \tag{6.8}$$

The overall change rates of glucose, cell, and ethanol concentrations are, respectively, expressed as

$$\frac{dG}{dt} = \frac{r_2}{0.95} - r_G = \frac{k_2 B}{0.95\left(1 + G/K_{2G}\right)} - \frac{\mu_m X^n G}{\left(K_G + G\right) Y_{X/G}} - mX^n \tag{6.9}$$

$$\frac{dX}{dt} = \frac{\mu_m X^n G}{K_G + G} \tag{6.10}$$

$$\frac{dE}{dt} = \frac{k_4'' \mu_m X^n G}{\left(K_G + G\right)} \tag{6.11}$$

where the constant 0.95 is the conversion factor of a cellobiose to two glucose molecules.

The overall change rates of glycerol, acetic, and lactic acid concentrations are, respectively, expressed as

$$\frac{dG_l}{dt} = \frac{k_5 \mu_m X^n G_l}{K_G + G} \tag{6.12}$$

$$\frac{dA}{dt} = \frac{k_6 \mu_m X^n A}{K_G + G} \tag{6.13}$$

$$\frac{dL}{dt} = \frac{k_7 \mu_m X^n L}{K_G + G} \tag{6.14}$$

where G_l, A and L are the concentrations (g/l) of glycerol, acetic acid, and lactic acid, respectively.

The equations (6.8-6.14) can be used in principle to simulate the concentration changes of cellobiose, glucose, cell mass, and ethanol as well as the by-products of

glycerol, acetic acid, and lactic acid with respect to time. However, to make the equations operable, the cellulose concentration should be stated in terms of the other soluble concentrations because the measurement of cellulose concentration of Eq. (6.8) is tedious, particularly when the carbohydrates are in biomass using the standard procedures ASTM E1721-95 [1997] and ASTM E1755-95 [1997]. The mass balance on cellulose can be expressed in terms of cellobiose, glucose, ethanol, cell, glycerol, acetic acid, and lactic acid in the culture as follows,

$$C = C_0 - 0.9G - 0.947B - 0.9E/0.511 - 1.137\left(X - X_1\right) - G_l/1.022 - A/1 - L/1 \quad (6.15)$$

where C_0 is the initial cellulose concentration (g/l), X_1 is the initial cell concentration (g/l) during the SSF period, the constant 0.9 is the conversion factor of a glucan unit in cellulose to glucose, the constant 0.511 is the inverse conversion factor of glucose to ethanol, and the constants 1.022, 1, and 1 are, respectively, the conversion factors (g/g) of glucose to glycerol, glucose to acetic acid, and glucose to lactic acid. The constant 1.137 is the conversion factor of cellulose consumed to produce yeast (g cellulose/g dry cell) assuming the molecular formula of the yeast *Saccharomyces cerevisiae* to be $CH_{1.74}N_{0.2}O_{0.45}$ during anaerobic fermentation of glucose [Shuler and Kargi, 2002].

Substituting Eq. (6.15) into Eq. (6.8) produces

$$\frac{dB}{dt} = \frac{r_1}{0.947} - r_2 = \frac{k_1}{0.947\left(1 + G/K_{1G}\right)}\left[C_0 - 0.9G - 0.947B - 0.9E/0.511 - 1.137\left(X - X_1\right) - G_l/1.022 - A - L\right]\left(\frac{e_0}{1 + k_3' e_0 t}\right) - \frac{k_2 B}{1 + G/K_{2G}} \quad (6.16)$$

Eq. (6.16, 6.9-6.14) combined with the initial conditions $C = C_1$, $e = e_1$, $G = G_1$, $B = B_1$, $X = X_1$, and $G_l = A = L = 0$ at time $t = 0$ in SSF period can describe the concentration changes of cellobiose, glucose, cell, ethanol, and by-products with respect to time. The parameters k_1, k_2, k_3', k_4'', k_5, k_6, k_7, K_G, K_{1G}, K_{2G}, m, and μ_m were determined using a MATLAB fitting program.

6.4 Continuous Operating Mode (CSTR)

In the continuous operation, the substrate (cellulose) is continuously fed into the culture at a flow rate F, and the outflow containing ethanol, residual cellulose, cellobiose, glucose, cell, by-products, and enzyme exits continuously at the same flow rate F. To achieve SSSF process in a continuous operation, two reactors are required: one is used for the pre-hydrolysis; another for SSF process (Fig. 6.1). The major differences between SSSF and SHF when operation is in the continuous operation though both have two reactors: 1) in the second phase of SSSF, the hydrolysis and fermentation are performed simultaneously, while in SHF, only fermentation is performed because the residual feedstock is removed; 2) the pre-hydrolytic time in the first reactor is shorter for the SSSF than the SHF.

The overall change rate of cellobiose concentrations can be expressed as

$$\frac{dB}{dt} = \frac{r_1}{0.947} - r_2 + D(B_1 - B) + \frac{D(C_1 - C)}{0.947} \tag{6.17}$$

where B_1 is the cellobiose concentrations (g/l) entering the fermenter R_2, $D = F/V_2$ is the dilution rate (h^{-1}), F is the feed flow rate (l/h), and V_2 is the liquid volume in fermenter R_2 (l). The last term of right hand in Eq. (6.17) represents the convertible cellulose concentration in the feed flow entering the fermenter R_2.

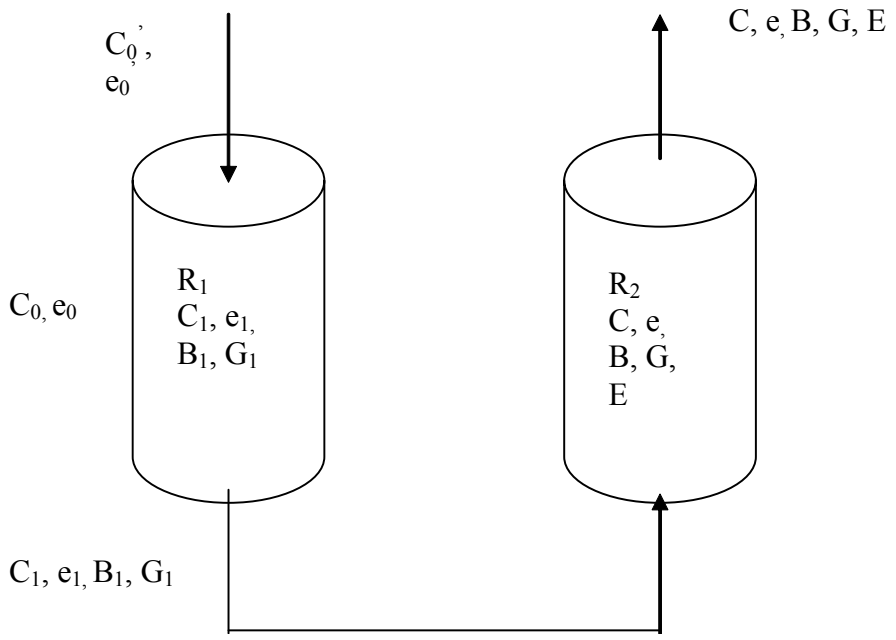

Fig. 6.1 A diagram of continuous operation for SSSF

Substituting Eqs. (5.3, 5.5, 6.15) into Eq. (6.17) produces

$$\frac{dB}{dt} = \frac{k_1 e\left[C_0 - 0.9G - 0.947B - 0.9E/0.511 - 1.137\left(X - X_1\right) - G_l/1.022 - A - L\right]}{0.947\left(1 + G/K_{1G}\right)}$$
$$- \frac{k_2 B}{1 + G/K_{2G}} + D\left(B_1 - B\right)$$
$$+ \frac{D}{0.947}\left\{C_1 - \left[C_0 - 0.9G - 0.947B - 0.9E/0.511 - 1.137\left(X - X_1\right) - G_l/1.022 - A - L\right]\right\} \tag{6.18}$$

Similarly, the overall change rates of glucose, cell, ethanol, by-product, and enzyme concentrations are, respectively, expressed as

$$\frac{dG}{dt} = \frac{r_2}{0.95} - r_G + D\left(G_1 - G\right)$$
$$= \frac{k_2 B}{0.95\left(1 + G/K_{2G}\right)} - \frac{\mu_m X^n G}{\left(K_G + G\right)Y_{X/G}} - mX^n + D\left(G_1 - G\right) \tag{6.19}$$

$$\frac{dX}{dt} = \frac{\mu_m X^n G}{K_G + G} - DX \tag{6.20}$$

$$\frac{dE}{dt} = \frac{k_4'' \mu_m X^n G}{(K_G + G)} - DE \tag{6.21}$$

$$\frac{dG_l}{dt} = \frac{k_5 \mu_m X^n G}{K_G + G} - DG_l \tag{6.22}$$

$$\frac{dA}{dt} = \frac{k_6 \mu_m X^n G}{K_G + G} - DA \tag{6.23}$$

$$\frac{dL}{dt} = \frac{k_7 \mu_m X^n G}{K_G + G} - DL \tag{6.24}$$

$$\frac{de}{dt} = -k_3' e^2 + D(e_1 - e) \tag{6.25}$$

where G_1 and e_1 are the glucose and enzyme concentrations (g/l) entering in fermenter R_2.

6.5 Fed-batch Operating Mode

In a fed-batch operation, the substrate (cellulose) is continuously fed into the culture at a flow rate F, but no outflow exits from the reactor. The flow rate is either constant or increase linearly or exponentially with time. In such a situation, the culture volume (V_2) is not constant, but increases at the rate F. The overall change rate dB'/dt of cellobiose mass in the culture can be expressed as,

$$\frac{dB'}{dt} = \frac{V_2 r_1}{0.947} - V_2 r_2 + FB_1 + F\frac{C_1}{0.947} \tag{6.26}$$

where B_1 is the cellobiose concentrations (g/l) entering in fermenter R_2. The last term of right hand in Eq. (6.26) represents the convertible cellulose concentration in the feed flow entering the fermenter R_2.

However,

$$\frac{dB^{'}}{dt}=\frac{d\left(V_2B\right)}{dt}=B\frac{dV_2}{dt}+V_2\frac{dB}{dt} \tag{6.27}$$

The change rate dB/dt (g/h) of cellobiose concentration is

$$\frac{dB}{dt}=\frac{r_1}{0.947}-r_2+D\left(B_1-B\right) \tag{6.28}$$

Substituting Eq. (5.3, 5.5, 6.15) into Eq. (6.28) produces

$$\begin{aligned}\frac{dB}{dt}&=D\left(B_1-B\right)-\frac{k_2B}{1+G/K_{2G}}+\frac{DC_1}{0.947}\\&+\left\{\left[\frac{k_1e\left[C_0-0.9G-0.947B-0.9E/0.511-1.137\left(X-X_1\right)-G_l/10.22-A-L\right]}{0.947\left(1+G/K_{1G}\right)}\right]\right\}\end{aligned} \tag{6.29}$$

Similarly, the overall change rates (g/(l.h)) of glucose, cell, ethanol, by-product, and enzyme concentrations can be, respectively, expressed as

$$\begin{aligned}\frac{dG}{dt}&=\left(\frac{r_2}{0.95}-r_G\right)+\frac{F}{V_2}\left(G_1-G\right)\\&=\left[\frac{k_2B}{0.95\left(1+G/K\right)_{2G}}-\frac{\mu_mX^nG}{Y_{X/G}\left(K_G+G\right)}-mX^n\right]+D\left(G_1-G\right)\end{aligned} \tag{6.30}$$

$$\frac{dX}{dt}=\frac{\mu_mX^nG}{K_G+G}-DX \tag{6.31}$$

$$\frac{dE}{dt}=\frac{k_4^{"}\mu_mX^nG}{\left(K_G+G\right)}-DE \tag{6.32}$$

$$\frac{dG_l}{dt}=\frac{k_5\mu_mX^nG}{K_G+G}-DG_l \tag{6.33}$$

$$\frac{dA}{dt}=\frac{k_6\mu_mX^nG}{K_G+G}-DA \tag{6.34}$$

$$\frac{dL}{dt}=\frac{k_7\mu_mX^nG}{K_G+G}-DL \tag{6.35}$$

$$\frac{de}{dt} = -k_3^{'}e^2 + De_1 - De \tag{6.36}$$

The increasing rate of culture volume is

$$\frac{dV}{dt} = F \tag{6.37}$$

It is noted that the dilution rate D changes with time, unlike the continuous operation where D is a constant. The total masses (g/l) of cellobiose B', glucose G', cell X', ethanol E', and enzyme e' in the culture can be calculated by the corresponding concentrations B, G, X, E, and e multiplying the culture volume.

6.6 Materials and Methods

6.6.1 Materials

Materials are the same as Chapter 5.4.

6.6.2 Methods

6.6.2.1 Preparation of inoculum

Preparation of inoculum is the same as Chapter 5.4.

6.6.2.2 Semi-simultaneous saccharification and fermentation

The semi-simultaneous saccharification and fermentation experiments were conducted in a one liter Quad fermenter (B. Braun Biotech International DCU3). Four cases were studied: 1) 24-hour pre-hydrolysis + 48-hour SSF, referred to as SSSF 24; 2) 12-hour pre-hydrolysis + 60-hour SSF, referred to as SSSF 12; 3) 72-hour SSF; and 4) 48-hour hydrolysis + 24-hour fermentation (SHF). The experiments were conducted for 72 hours. The fermentation medium was composed of 0.5 l citric acid buffer (0.05 M, pH 4.8), 20 g microcrystalline cellulose (Avicel PH 101), and 2.0 g Novozymes enzyme

(NS50052). In the pre-hydrolysis phase, the medium temperature and pH were maintained at 50^{o}C, and 4.8, respectively. After 24 or 12-hour hydrolysis, the medium temperature was adjusted to 36^{o}C and maintained at this temperature during the SSF phase. About 0.15 g (dry weight) *S. cerevisiae* was inoculated into the medium. The pH of fermentation was maintained at 4.8 by automatic addition of either 2M hydrochloric acid or 2M sodium hydroxide solution during the SSF period. The agitation rate was constant at 300 rpm. Two ml aliquots of the broth were taken periodically and prepared for analysis. When SSF was performed, the temperature and pH were, respectively, maintained at 36^{o}C and 4.8 from start to the end of experiments. When SHF was performed, hydrolysis was conducted at the temperature 50^{o}C and pH 4.8 for 48 hours, and the solid biomass was separated from the hydrolysate. The hydrolysate was fermented at temperature 36^{o}C and pH 4.8 for 24 hours. The SSF and SHF data were used for comparison with those of SSSF. The experiments were triplicate.

6.6.2.3 Differential centrifugation sedimentation for separation of cellulose particles and cells from the broth

Separation of cell and cellulose particles from the broth is the same as Chapter 5.6.2.3.

6.6.2.4 Analytical methods

Analysis methods are the same as Chapter 5.6.2.4.

6.7 Results and Discussion

6.7.1 Cellulose pre-hydrolysis and simulation

The conversion of cellulose and the reducing sugar concentration within 24 hours are showed in Fig. 6.2. The conversion and reducing sugar concentration increased with hydrolytic time. The highest conversion and reducing sugar concentration were about 58% and 26 g/l in 24-hour hydrolysis, respectively. To correlate the conversion (or sugar concentration) with hydrolytic time, Shen and Agblevor [2008b] developed an enzymatic hydrolysis model with convergent property as follows:

The substrate conversion x was defined as

$$x = \frac{C_0 - C}{C_0} = \frac{rG}{C_0} = 1 - \left[\frac{K_e + e_0}{K_e\left(k_3^{'} e_0 t + 1\right) + e_0} \right]^b \tag{4.17}$$

where r is the average conversion factor from one glucan unit in cellulose to glucose (0.9), $k_3^{'}$ is the enzyme deactivation constant in the pre-hydrolysis phase (l(g.h)), K_e is adsorption equilibrium constant (g/l), and b is the dimensionless constant.

The curves in Fig. 6.2 are simulated results for conversion and sugar concentration using Eq. (4.17). The parametric values of the model (4.17) are shown in Table 6.1.

6.6.2 Batch SSSF experiments and simulation

The concentrations of cellobiose, glucose, ethanol, and cell with respect to time for the SSSF 24 and 12 experiments are shown in Figs. 6.3 and 6.4, respectively. The glycerol, acetic acid, lactic acid concentrations for SSSF 24 are shown in Fig. 6.5. The ethanol and by-product concentrations rapidly increased within 20 hours for SSSF 24, and then leveled off after 30 hours. The similar result of ethanol concentration was also observed in 40 and 60 hours for the SSSF 12. The glucose concentrations in SSSF 24 and 12 gradually decreased from the high initial concentrations with increasing time. The optimal ethanol productivity for the SSSF 24, SSSF 12, SSF, and SHF after 72-hour hydrolysis and fermentation were about 0.222 g/(l.h), 0.189 g/(l.h), 0.194 g/(l.h), and

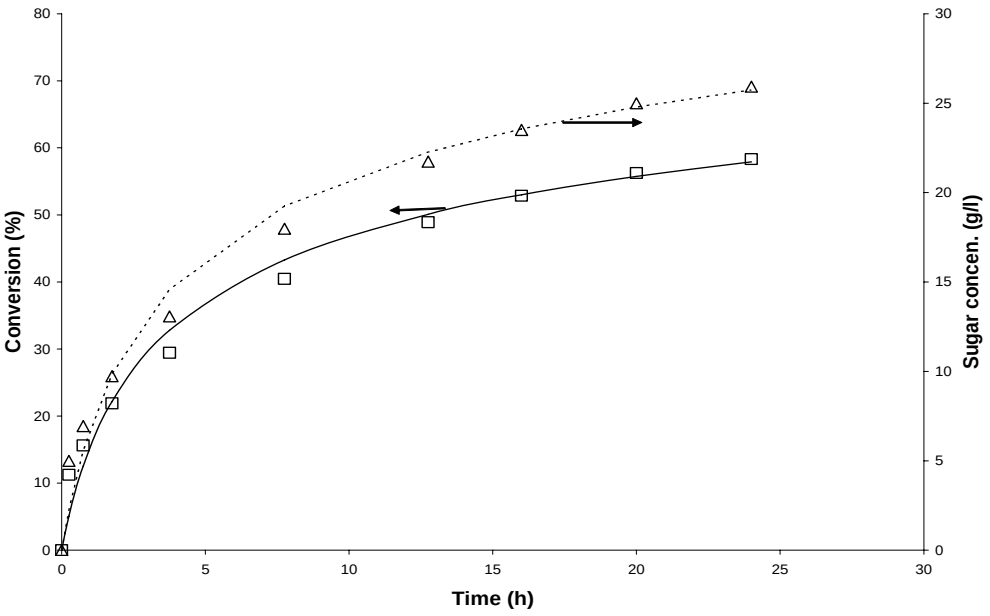

Fig. 6.2 The conversion of cellulose and reducing sugar concentration with time in the pre-hydrolysis phase. □, Δ experimental points. Solid and dash lines denote the model (4.17) values.

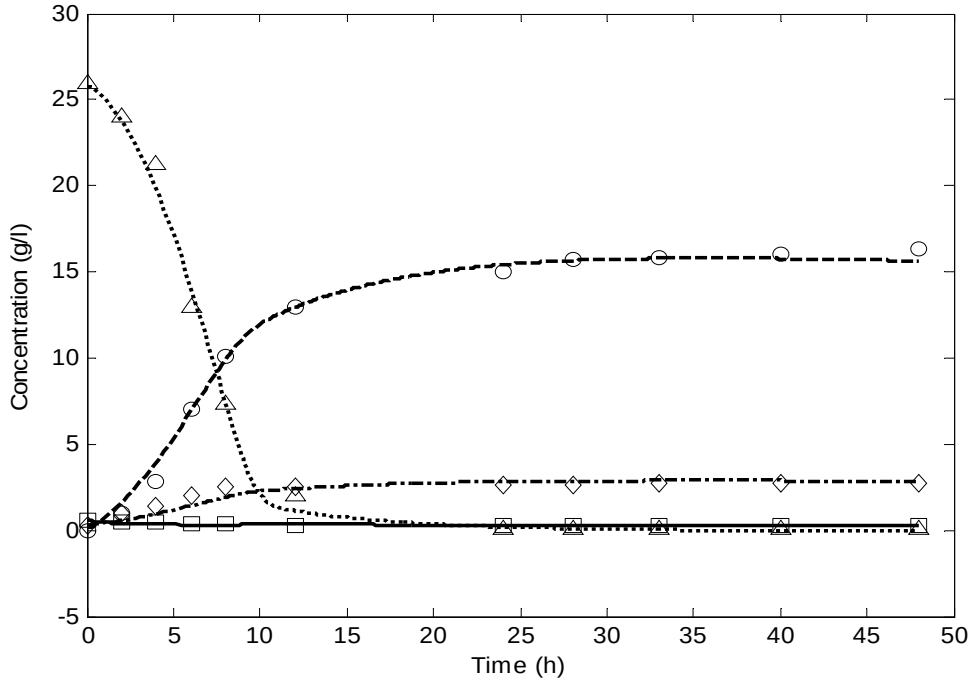

Fig. 6.3 The experimental points (signs) and simulated curves (lines) of cellobiose (□, solid), glucose (Δ, dot), ethanol (o, dash) and cell (◊, dash-dot) concentrations with time in the batch operation of SSSF 24. Conditions: $C_0 = 40$ g/l, $X_1 = 0.3$ g/l, $e_0 = 4$ g/l, $G_0 = B_0 = E_0 = 0$.

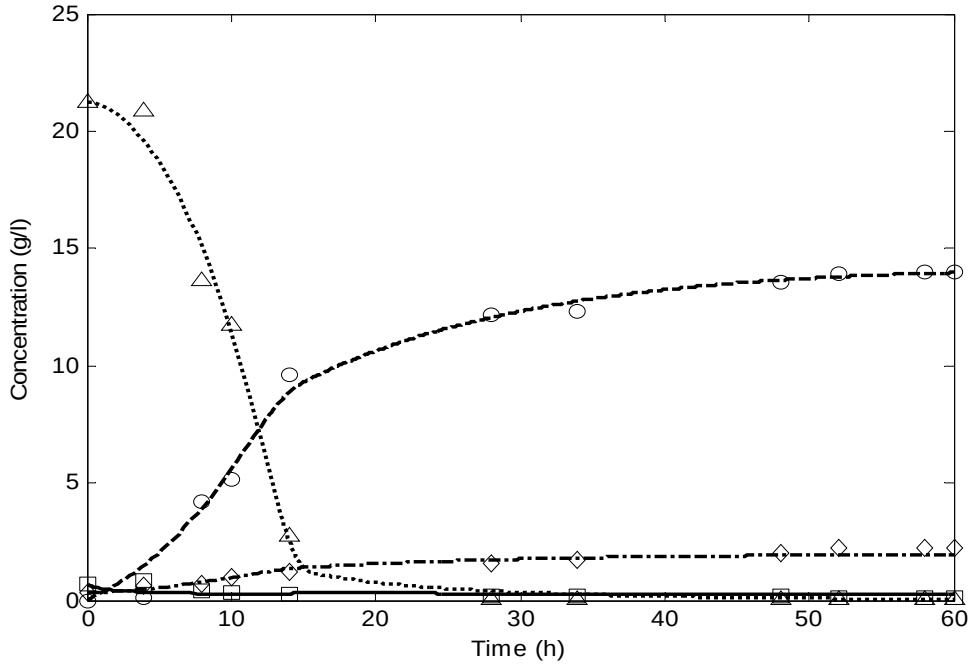

Fig. 6.4 The experimental points (signs) and simulated curves (lines) of cellobiose (□, solid), glucose (Δ, dot), ethanol (o, dash) and cell (◊, dash-dot) concentrations with time in the batch operation of SSSF 12. Conditions: C_0 = 40 g/l, X_1 = 0.3 g/l, e_0 = 4 g/l, G_0 = B_0 = E_0 = 0.

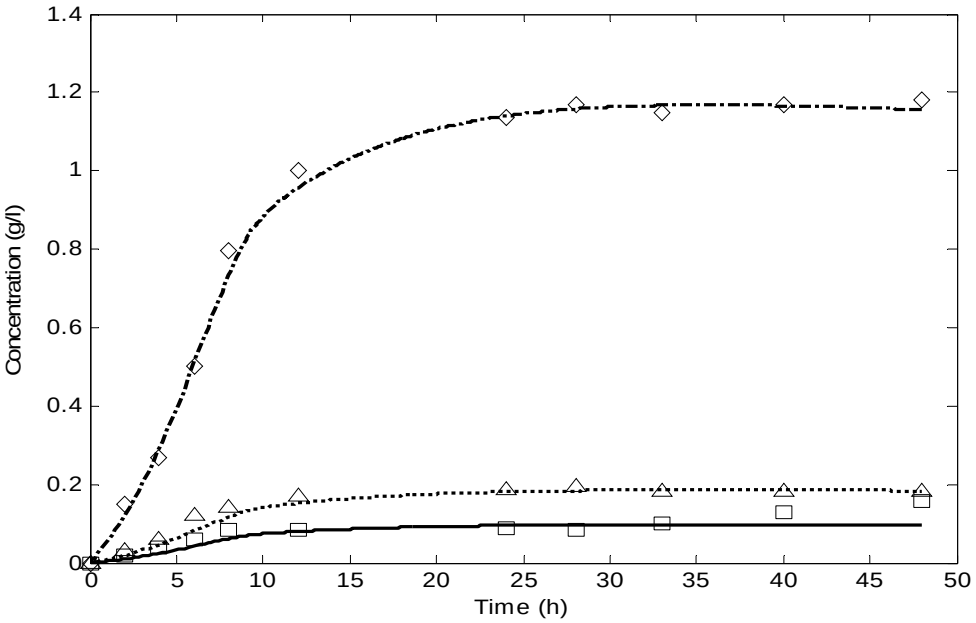

Fig. 6.5 The experimental points (signs) and simulated curves (lines) of acetic acid (□, solid), lactic acid (Δ, dot), and glycerol (◊, dash-dot) concentrations with time in the batch operation of SSS 24. Conditions are the same as Fig. 6.3.

Table 6.1 The parametric values in Eq. (4.17)

Parameter	K_e (g/l)	k_2' (l/h)	k_3' (l(g.h))	b (-)
Value	0.9975	0.2843	0.9837	0.2897

Table 6.2 A comparison of yields and productivities of ethanol for SSSF, SSF, and SHF

Name	SSSF 24	SSSF 12	SSF	SHF
Yield (%)	70.5	61.6	61.8	56.1
Productivity (g/(l.h)	0.222	0.189	0.194	0.176
Ethanol concen. (g/l)	16.0	14.0	14.0	12.7

Table 6.3 The parametric values in Eqs. (6.16, 6.9-6.14) for SSSF 24 and 12

Parameter	SSSF 24	SSSF 12
k_1 (l(g.h))	200	179
k_2 (h^{-1})	21.03	21.0
k_4'' (-)	3.148	4.36
k_5 (-)	0.0377	0.917
k_6 (-)	0.0718	0.940
k_7 (-)	0.4619	0.697
K_{1G} (g/l)	0.698	0.181
K_{2G} (g/l)	1.685	0.998
K_G (g/l)	9.847	7.802
m (h^{-1})	2.687	2.386
μ_m ($((l/g)^{n-1}h^{-1}$)	0.339	0.182
n (-)	0.699	1.130

0.176 g/(l.h), respectively. The corresponding maximum ethanol concentrations were about 16 g/l, 14 g/l, 14 g/l, and 12.7 g/l. These ethanol concentrations were equivalent to theoretical ethanol yields of 70.5%, 61.6%, 61.8%, and 56.1%. These results are summarized in Table 6.2. The theoretical ethanol yields were calculated using the following equation:

$$Y_{th} = \frac{0.9E}{0.511C_0}100\% \tag{6.38}$$

Another parameter used in SHF is the fermentation efficiency e_f (dimensionless) from sugar to ethanol, which is defined as

$$e_f = \frac{E}{0.511G_h}100\% \tag{6.39}$$

where G_h is the glucose concentration from hydrolysis (g/l). When the glucans in cellulose are completely converted into glucose ($C_0 = 0.9G_h$), the theoretical yield of SSF is equal to the fermentation efficiency. These theoretical ethanol yield were close to other experimental and industrial data [Zhu et al, 2006; Kosaric and Vardar-Sukan, 2001], but lower than the ideal yield of 76-90%, which included the carbon consumption for cell growth [Brown, 2003]. The theoretical yield, productivity, and ethanol concentration of SSSF 24 were higher than those for other operating modes. It can be concluded that SSSF can achieve higher yield and productivity than SSF and SHF when a suitable pre-hydrolysis time is selected.

The experimental values for the cellobiose, glucose, ethanol, cell, and by-product concentrations with respect to residence time can be fitted in Eqs. (6.16, 6.9-6.14) with the corresponding initial conditions (C_0 = 40 g/l, e_0 = 4 g/l, $Y_{X/G}$ = 0.515, X_1 = 0.3 g/l, G_1 = 25.92 g/l, B_1 = 0.5857 g/l for SSSF 24, but G_1 = 21.25 g/l, B_1 = 0.7015 g/l for SSSF

12). $Y_{X/S}$ was determined from the experiment on *S. cerevisiae* growth on glucose. The model parameters k_1, k_2, $k_3^{'}$, $k_4^{''}$, k_5, k_6, k_7, K_{1G}, K_{2G}, K_G, m, and μ_m in these equations can be obtained using the MATLAB lsqnonlin method. However, to reduce the number of fitted parameters and use the known enzyme deactivation constant $k_3^{'}$ obtained in the pre-hydrolysis phase, Eq. (6.16) was modified as follows:

$$\frac{dB}{dt} = \frac{r_1}{0.947} - r_2 = \frac{k_1}{0.947\left(1+G/K_{1G}\right)} \left[C_0 - 0.9G - 0.947B - 0.9E/0.511 - 1.137\left(X - X_1\right) - G_l/1.022 - A - L\right] \left[\frac{e_0}{1+k_3^{'}e_0\left(t+t_0\right)}\right] - \frac{k_2 B}{1+G/K_{2G}} \quad (6.40)$$

where t_0 is the time for the pre-hydrolysis (24 and 12 hours for SSSF 24 and 12, respectively) (h). This modification reduced the number of fitted parameters to 12. These parametric values are listed in Table 6.3. The simulated curves for SSSF 24 and 12 are shown in Figs. 6.3, 6.4, and 6.5, respectively. From Table 6.3, the inhibition constants K_{1G} and K_{2G} of SSSF 24 are greater than those for SSSF 12. This implies that SSSF 24 has less enzyme inhibition than SSSF 12 because the greater K_{1G} and K_{2G}, the greater the enzyme inhibition, which may be one of the reasons why SSSF 24 is more effective than SSSF 12. It is noted that because Eq. (6.1) was a non-linear reaction, the simulated curves of the cell concentrations fitted for the experimental points were better than those of SSF where the simulated curve of cell concentration deviated from the experimental data between 20 and 40 hours of SSF [Shen and Agblevor, 2008a].

6.7.3 The rate-controlling step in SSSF process

Eqs. (6.40, 6.9-6.14) are the rate expressions of cellobiose, glucose, cell, ethanol, and by-products. When the constants in these equations were determined, the reaction rates can be calculated. Figs. 6.6 and 6.7, respectively, show the rates for SSSF 24 and 12.

From the figures, the reaction rates of cellobiose, cell, and ethanol are positive, while the glucose reaction rate was negative because the glucose concentration gradually decreased from the initial high concentration accumulated in the pre-hydrolysis phase. During the first hour (Figs. 6.6 and 6.7), the cell growth rate for SSSF 24 controlled the entire process because it had the smallest absolute reaction rate, whereas for SSSF 12 the cell grow rate was almost the same as the glucose consumption rate. After one hour, the cellobiose absolute reaction rates in the figures were smallest within 30 hours for SSSF 24 and 50 hours for SSSF 12. These suggested that there was a transition point where the rate-controlling step was changed from cell growth control to cellobiose reaction control in ethanol production of SSF. Furthermore, the rate-controlling period (30 hour) from cellulose to cellobiose for SSSF 24 was shorter than that (50 hours) for SSSF 12. This explains one of the reasons why the SSSF 24 is better than SSSF 12 from the kinetic view because the enzymatic reaction is slow and the longer rate-controlling period is unfavorable for ethanol production. The reaction rates of ethanol and glucose have the highest absolute values (Figs. 6.6 and 6.7), because in the initial period, the yeast concentration was low so that the ethanol formation rate was low; as the yeast multiplied, ethanol formation rate gradually increased; finally, the ethanol formation rate again reduced due to the substrate (sugars) depletion.

6.7.4 Simulation of continuous operation

The variations of glucose, cell, and ethanol concentrations over time at various dilution rates in the continuous operation for SSSF 24 and 12 are shown in Figs. 6.8 and 6.9, respectively. The curves show the dynamics of SSSF from unstable states to steady states: the three component concentrations approached constant values at steady state

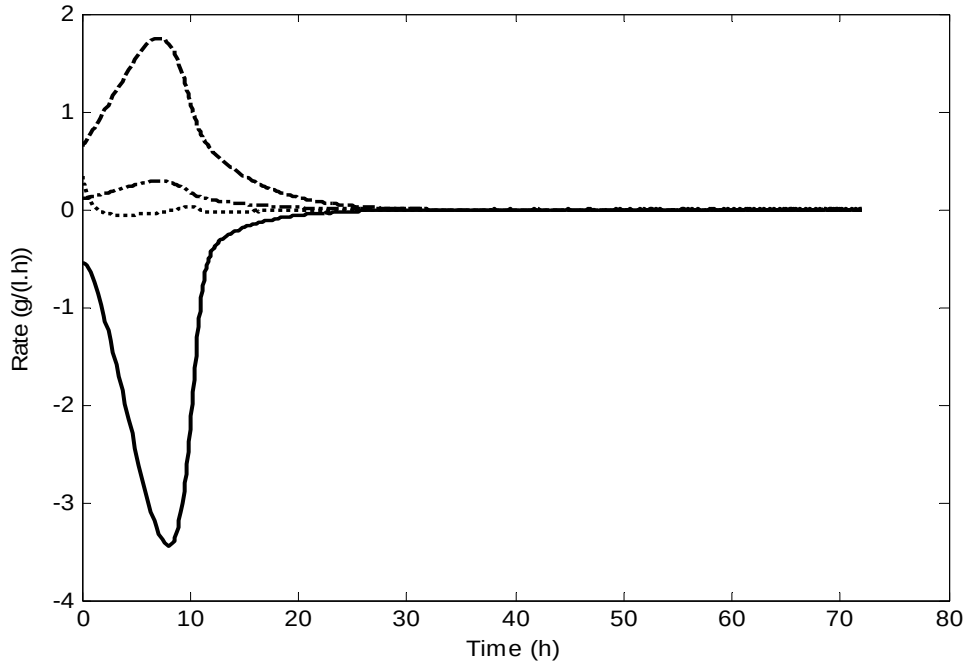

Fig. 6.6 The reaction rates of cellobiose (dot), glucose (solid), cell (dash-dot), and ethanol (dash) in the batch operation of SSSF 24. Conditions are the same as Fig. 6.3.

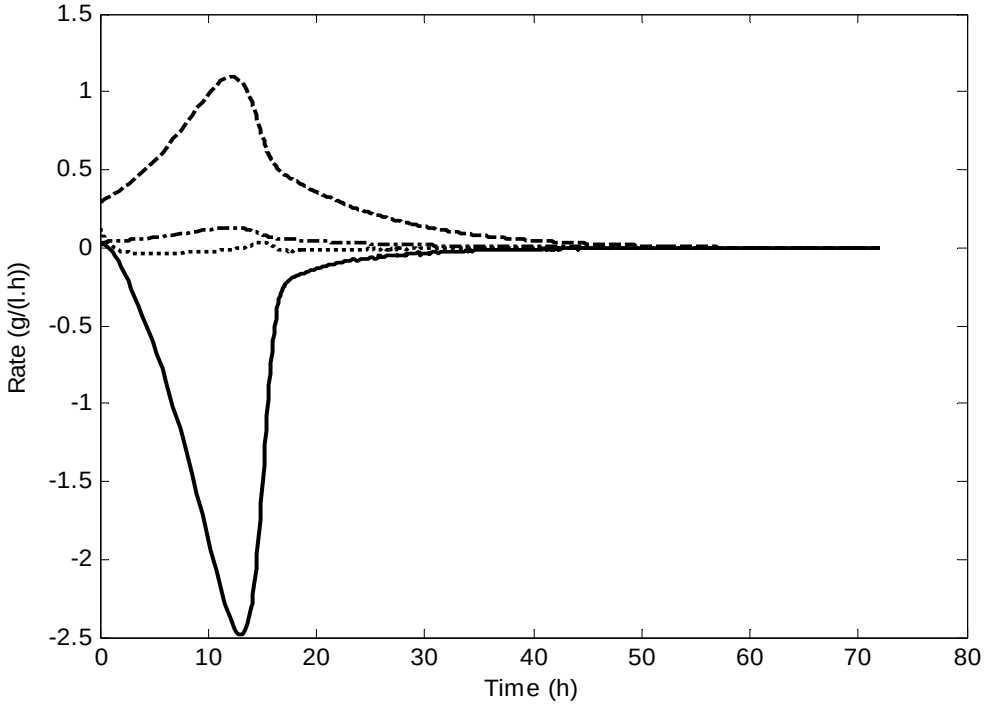

Fig. 6.7 The reaction rates of cellobiose (dot), glucose (solid), cell (dash-dot), and ethanol (dash) in the batch operation of SSSF 12. Conditions are the same as Fig. 6.4.

with increasing residence time. When the dilution rate was increased, the time to reach the steady state for the system increased. However, when the dilution rates approached the washout points (D = 0.4 h^{-1} and 0.12 h^{-1} for SSSF 24 and 12, respectively), the steady states of the systems immediately reached the washout points at which both the cell and ethanol concentrations were very low. At the steady state, the highest ethanol concentration was 17.5 g/l at the dilution rate 0.04 h^{-1} for SSSF 24 (Fig. 6.8B), while, for SSSF 12, the highest ethanol concentration was 15.9 g/l at the dilution rate 0.02 h^{-1} (Fig. 6.9B). The highest ethanol concentration depended on the dilution rate. The smaller the dilution rate, the higher the ethanol concentration. Figs. 6.10 and 6.11 show the glucose, cell, and ethanol concentrations as well as productivity (DE) of ethanol at the steady state for various dilution rates for SSSF 24 and 12. The ethanol and cell concentrations decreased as the dilution rate was increased. In contrast, the glucose concentrations initially increased with the dilution rate, however, above the dilution rate 0.3 h^{-1}, the glucose concentration for SSSF 24 leveled off. The ethanol productivities increased to the maximum values (1.5 g/(l.h) at the dilution rate of 0.16 h^{-1} for SSSF 24 and 0.88 g/(l.h) at the dilution rate of 0.08 h^{-1} for SSSF 12) with increased dilution rate, and then rapidly decreased to zero at the washout points (Figs. 6.10 and 6.11). These observations about ethanol, cell, and productivity showed that the general principle of chemostat operation is applicable to the complicated situation of SSSF [Blanch and Clark, 1996; Stanburg et al., 1995]. Although there is not a great difference in the highest ethanol concentration between SSSF 24 (17.5 g/l) and 12 (16 g/l), the ethanol productivity of SSSF 24 was 1.76 times that of SSSF 12 because the former was performed at the higher dilution rate than the latter.

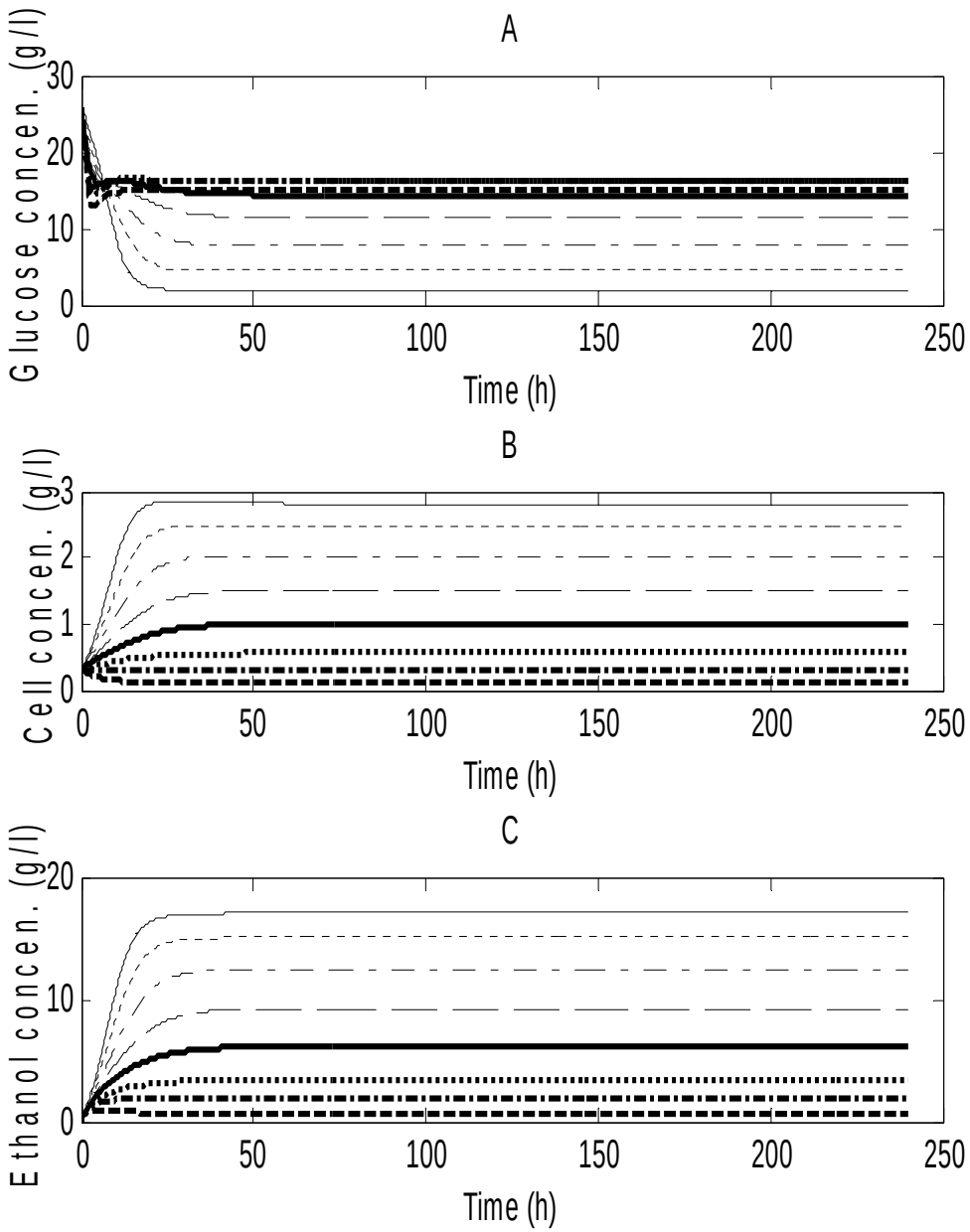

Fig. 6.8 The simulated glucose (A), cell (B), and ethanol (C) concentration curves (lines) with time at eight dilution rates: 0.04 /h (fine solid), 0.08 /h (fine dot), 0.12 /h (fine dash-dot), 0.16 /h (fine dash), 0.2 /h (thick solid), 0.25 /h (thick dot), 0.3 /h (thick dash-dot), and 0.4 /h (thick dash) in the continuous operation of SSSF 24. Conditions: $C_0 = 40$ g/l, $C_0' = 20$ g/l, $X_1 = 0.3$ g/l, $e_0 = 2$ g/l, $e_0' = 1$ g/l, and $G_0 = B_0 = E_0 = 0$.

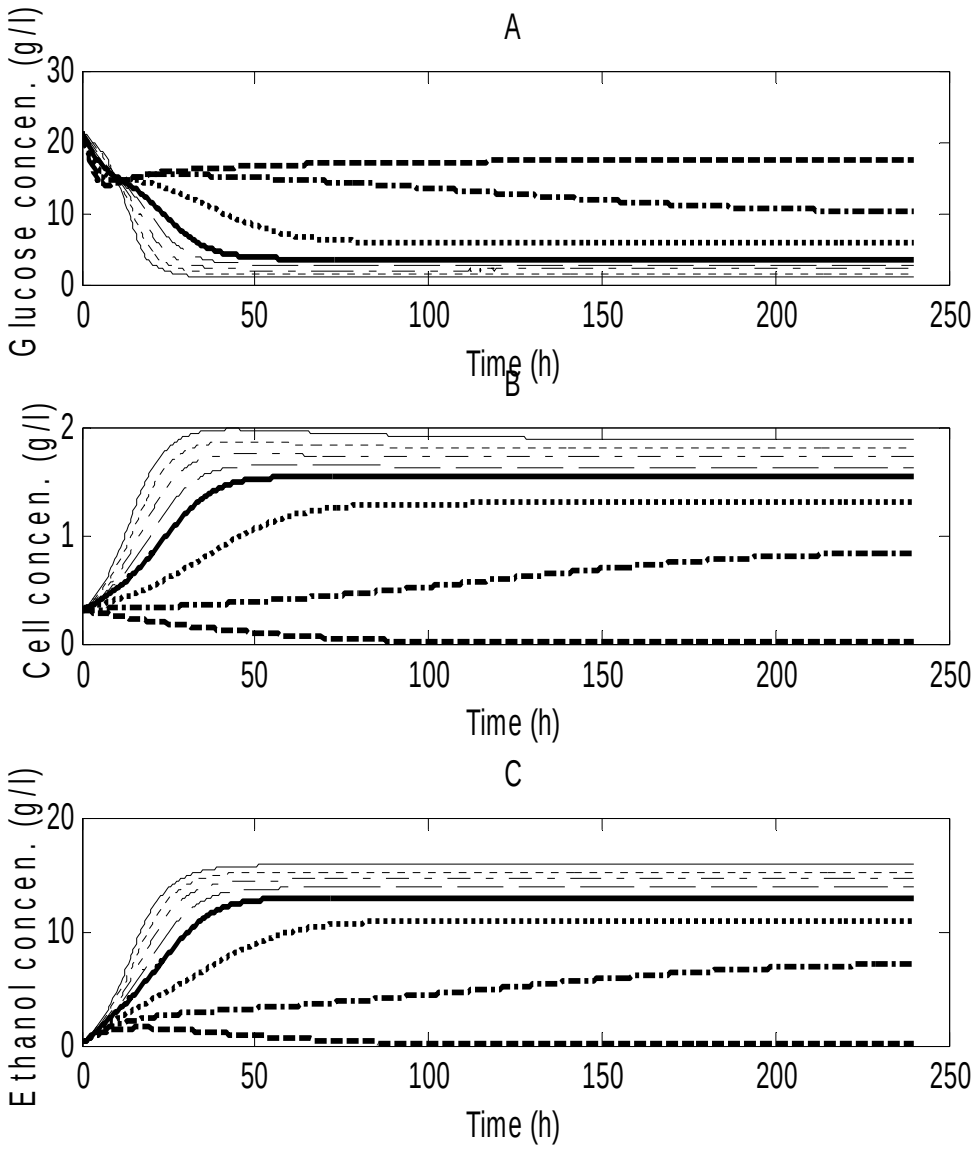

Fig. 6.9 The simulated glucose (A), cell (B), and ethanol (C) concentration curves (lines) with time at eight dilution rates: 0.02 /h (fine solid), 0.03 /h (fine dot), 0.04 /h (fine dash-dot), 0.05 /h (fine dash), 0.06 /h (thick solid), 0.08 /h (thick dot), 0.1 /h (thick dash-dot), and 0.12 /h (thick dash) in the continuous operation of SSSF 12. Conditions: $C_0 = 40$ g/l, $C_0' = 20$ g/l, $X_1 = 0.3$ g/l, $e_0 = 2$ g/l, $e_0' = 1$ g/l, and $G_0 = B_0 = E_0 = 0$.

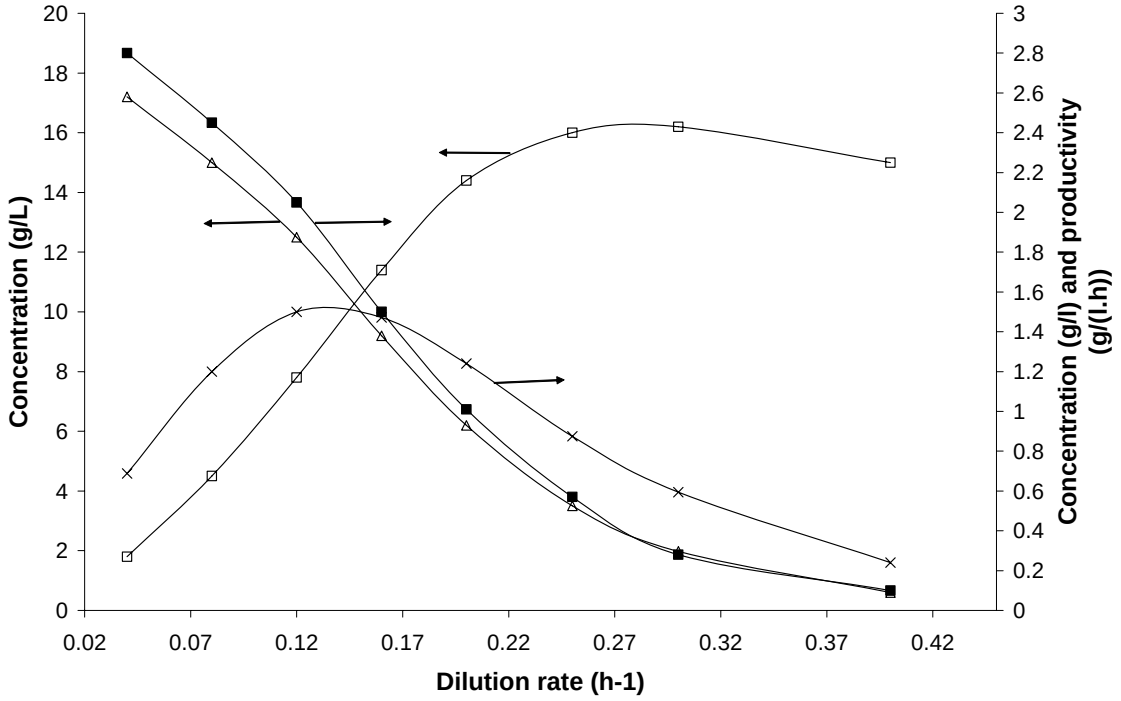

Fig. 6.10 The glucose, cell, and ethanol concentrations and productivity with dilution rate in the continuous operation of SSSF 24. Glucose (□), cell (■), ethanol (Δ), and productivity (x). Conditions are the same as Fig. 6.8.

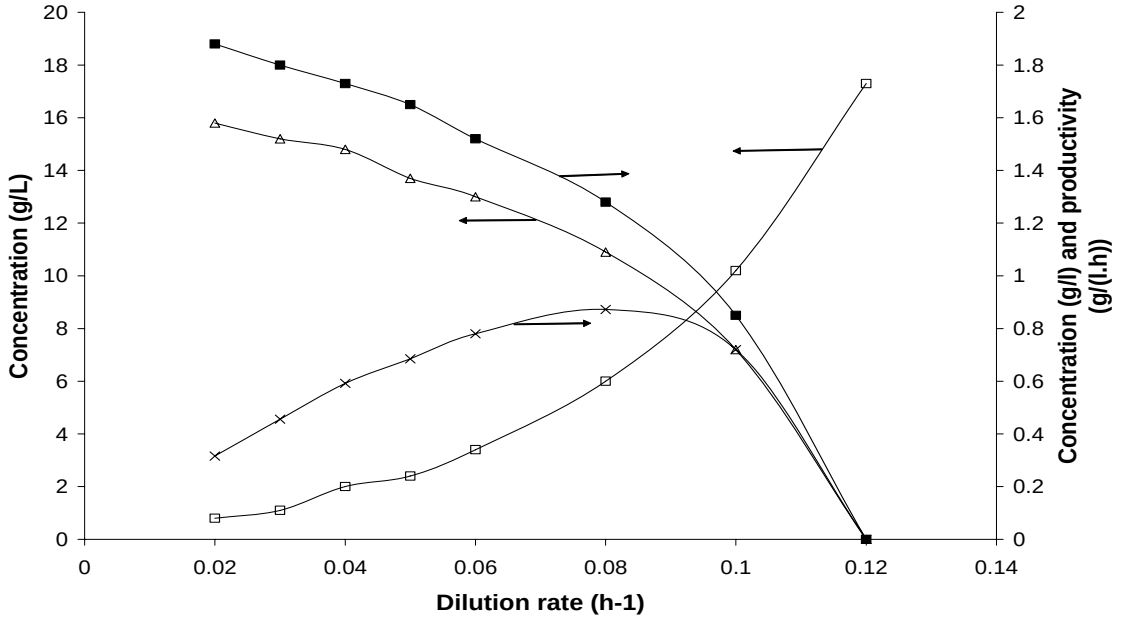

Fig. 6.11 The glucose, cell, and ethanol concentrations and productivity with dilution rate in the continuous operation of SSSF 12. Glucose (□), cell (■), ethanol (Δ), and productivity (x). Conditions are the same as Fig. 6.9.

6.7.5 Simulation of fed-batch operation

The variations in the concentrations of glucose, cell, and ethanol with time at the three constant feed flow rates (0.1, 0.2 and 0.3 l/h) in the fed-batch operation for SSSF 24 and 12 are shown in Figs. 6.12 and 6.14, respectively (initial culture volume V_1 = 1 l, and cellulose concentration in the feed $C_0^{'}$ = 20 g/l). The corresponding variations of masses with time are presented in Figs. 6.13 and 6.15. The ethanol and cell concentrations rapidly increased within 30 hours for SSSF 24 and within 50 hours for SSSF 12. After 50 fours for SSSF 24 and 70 hours for SSSF 12, the glucose, cell and ethanol concentrations at the three flow rates were similar (Figs. 6.12 and 6.14) at a quasi-steady state for the fed-batch operation because of the dilution effect of increasing the culture volume. The quasi-steady state for the fed-batch operation can be achieved when the substrate concentration in the feed flow is much greater than that in the culture [Pirt, 1979]. It is interesting to note that the cell and ethanol masses in the culture for the fed-batch operation greatly increased compared to those for batch operation. For example, the cells and ethanol masses were 47 g and 290 g for SSSF 24, and 32 g and 260 g for SSSF 12 at a flow rate 0.2 l/h, whereas the cells and ethanol masses were 2.6 g and 16 g in the batch experiment for SSSF 24, and 2 g and 14 g for SSSF 12. These values of ethanol concentration and mass also show that SSSF 24 is better than SSSF 12 in the fed-batch operation mode (Figs. 6.12C and 6.13C, and 6.14C and 6.15C).

It is well known that a constant feed rate is not an optimal operating mode for the fed-batch fermentation because the substrate consumption rate caused by microorganism increased exponentially as the substrate is sufficiently supplied. However, fed-batch operations are usually carried out by feeding the growth-limiting substrate continuously

at a constant flow rate into a bioreactor because this operation is simple and easily controlled, but the reaction rate will decrease with time since a constant feeding rate cannot compensate for the exponential rate of the substrate consumption. Therefore, the exponential fed-batch operation had been suggested for optimal operation of the bioreactor [Martin and Felsenfeld, 1964; Edwards et. al, 1970; Dunn and Mor, 1975; Lim et. al., 1977; Yamane and Shimizu, 1984]. Simulated results for the exponential fed-batch operation following Eq. (6.41) at the three initial flow rate (F_1 = 0.1, 0.2, and 0.3 l/h) with similar conditions of Figs. 6.12-6.15 are shown in Figs. 6.16-6.19.

The increasing rate of culture volume is given by

$$\frac{dV}{dt} = F_1 \exp(\mu_c t) \tag{6.41}$$

where μ_c is the constant associated with the maximum specific cell growth rate μ. μ_c can be calculated from Monod model at the initial glucose concentration.

$$\mu_c = \frac{\mu_m G_1}{K_G + G_1} \tag{6.42}$$

The values used in Figs 6.16-6.19 are 0.246 h^{-1} and 0.133 h^{-1} for SSSF 24 and 12, respectively. Although the final ethanol concentration for the exponential fed-batch was almost the same as that for the constant fed-batch, the predicted cells and ethanol masses were 210 g and 1300 g after 18 hours of SSSF 24, and 160 g and 1300 g after 30 hours of SSSF 12 at the initial flow rate 0.2 h^{-1}. The cell and ethanol masses were, respectively, 4.47 and 4.48 times those for 72 hours of SSSF 24, and 5.0 and 5.0 time those for 72 hours of SSSF 12 at the same constant flow rate. The systems also achieved quasi-steady states at 18 and 30 hours for SSSF 24 and 12, respectively. However, the

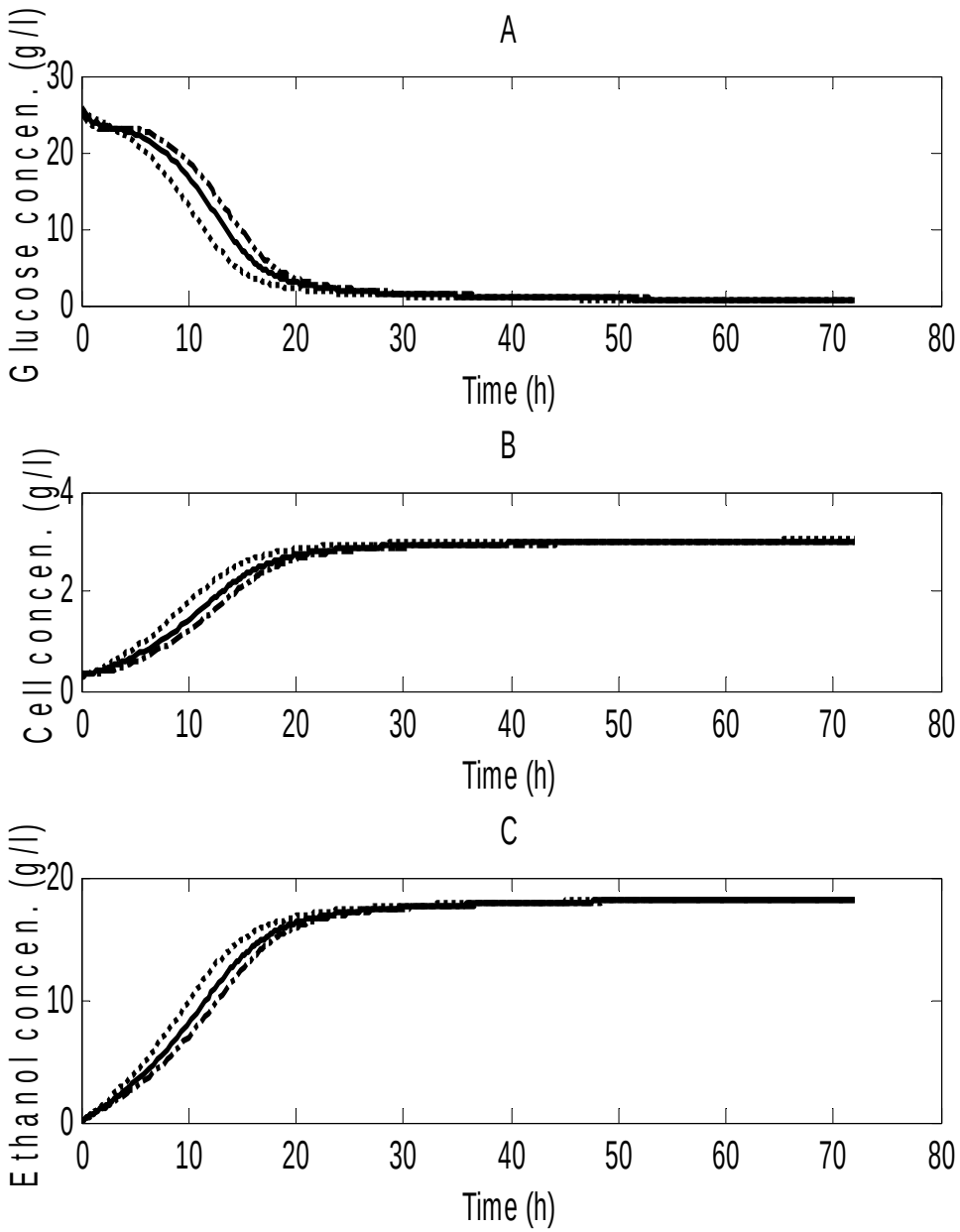

Fig. 6.12 The simulated glucose (A), cell (B), and ethanol (C) concentration curves (lines) with time at three flow rates: 0.1 l/h (dot), 0.2 l/h (solid), and 0.3 h/l (dash-dot) in the constant fed-batch operation of SSSF 24. Conditions: C_0 = 40 g/l, C_0' = 20 g/l, e_0 = 4 g/l, e_0' = 1 g/l, X_1 = 0.3 g/l, V_1 = 1 l and $G_0 = B_0 = E_0 = 0$.

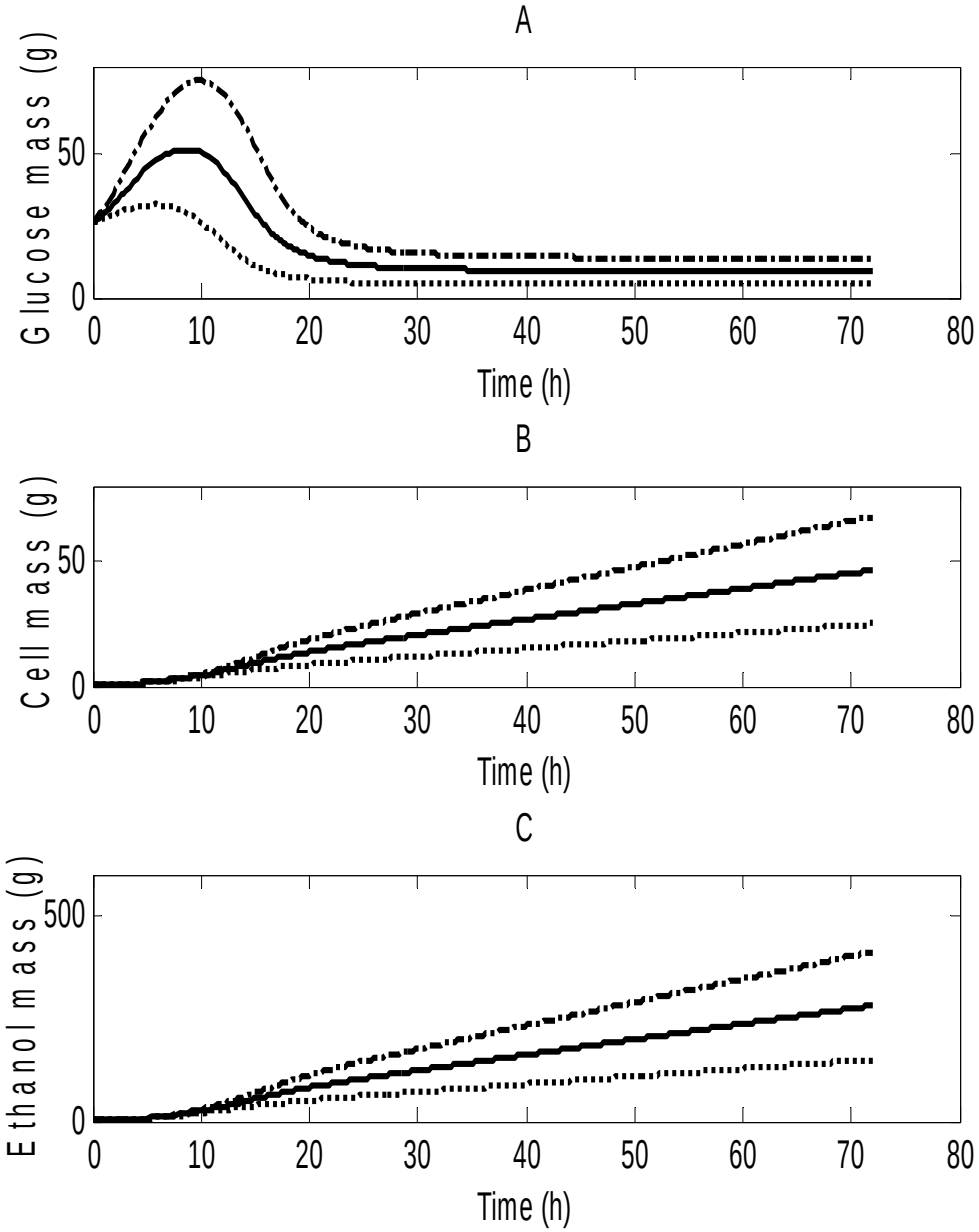

Fig. 6.13 The simulated glucose (A), cell (B), and ethanol (C) mass curves (lines) with time at three flow rates: 0.1 l/h (dot), 0.2 l/h (solid), and 0.3 h/l (dash-dot) in the constant fed-batch operation in SSSF 24. Conditions are the same as Fig. 6.12.

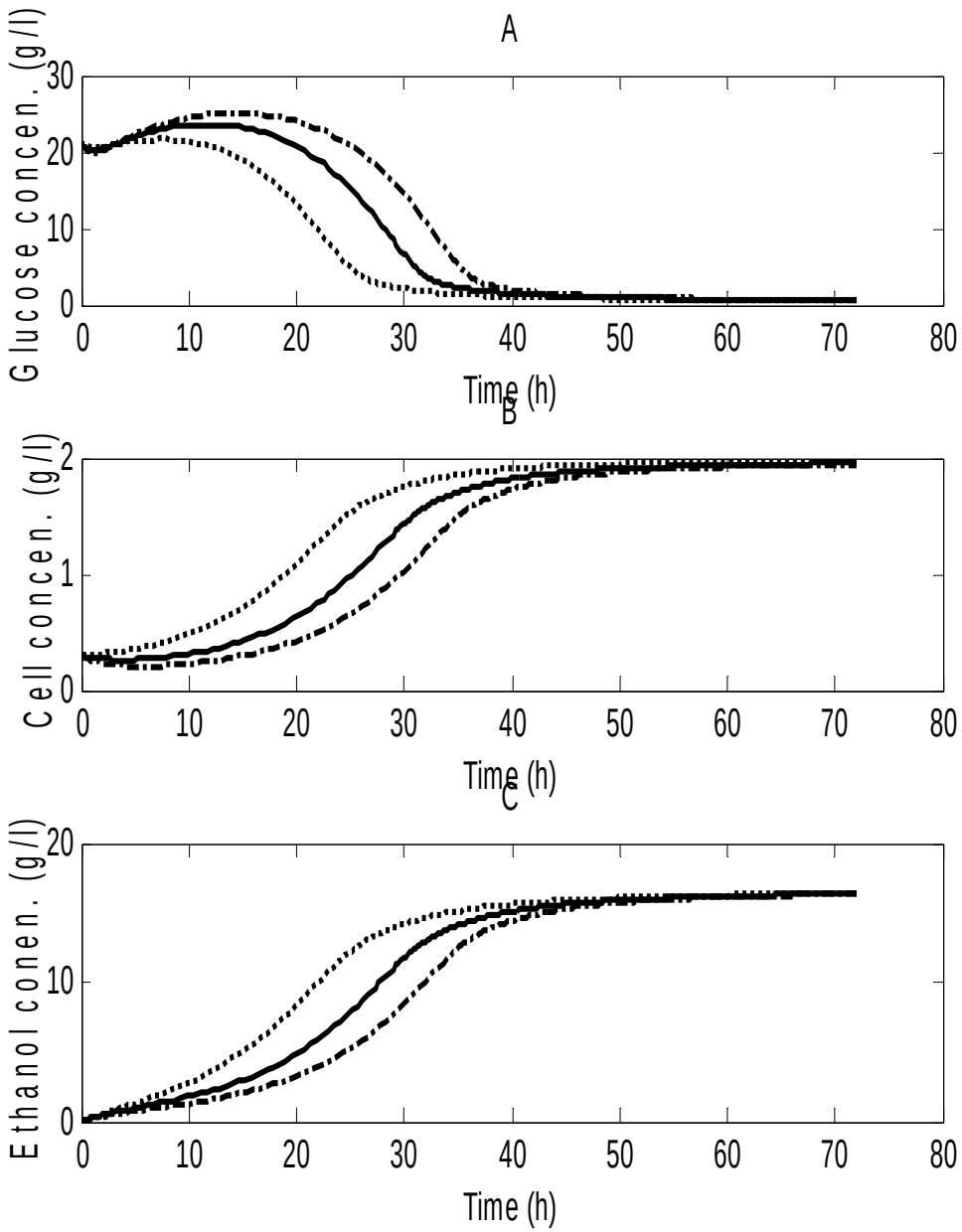

Fig. 6.14 The simulated glucose (A), cell (B), and ethanol (C) concentration curves (lines) with time at three flow rates: 0.1 l/h (dot), 0.2 l/h (solid), and 0.3 h/l (dash-dot) in the constant fed-batch operation of SSSF 12. Conditions: C_0 = 40 g/l, C_0' = 20 g/l, e_0 = 4 g/l, e_0' = 1 g/l, X_1 = 0.3 g/l, V_1 = 1 l and $G_0 = B_0 = E_0 = 0$.

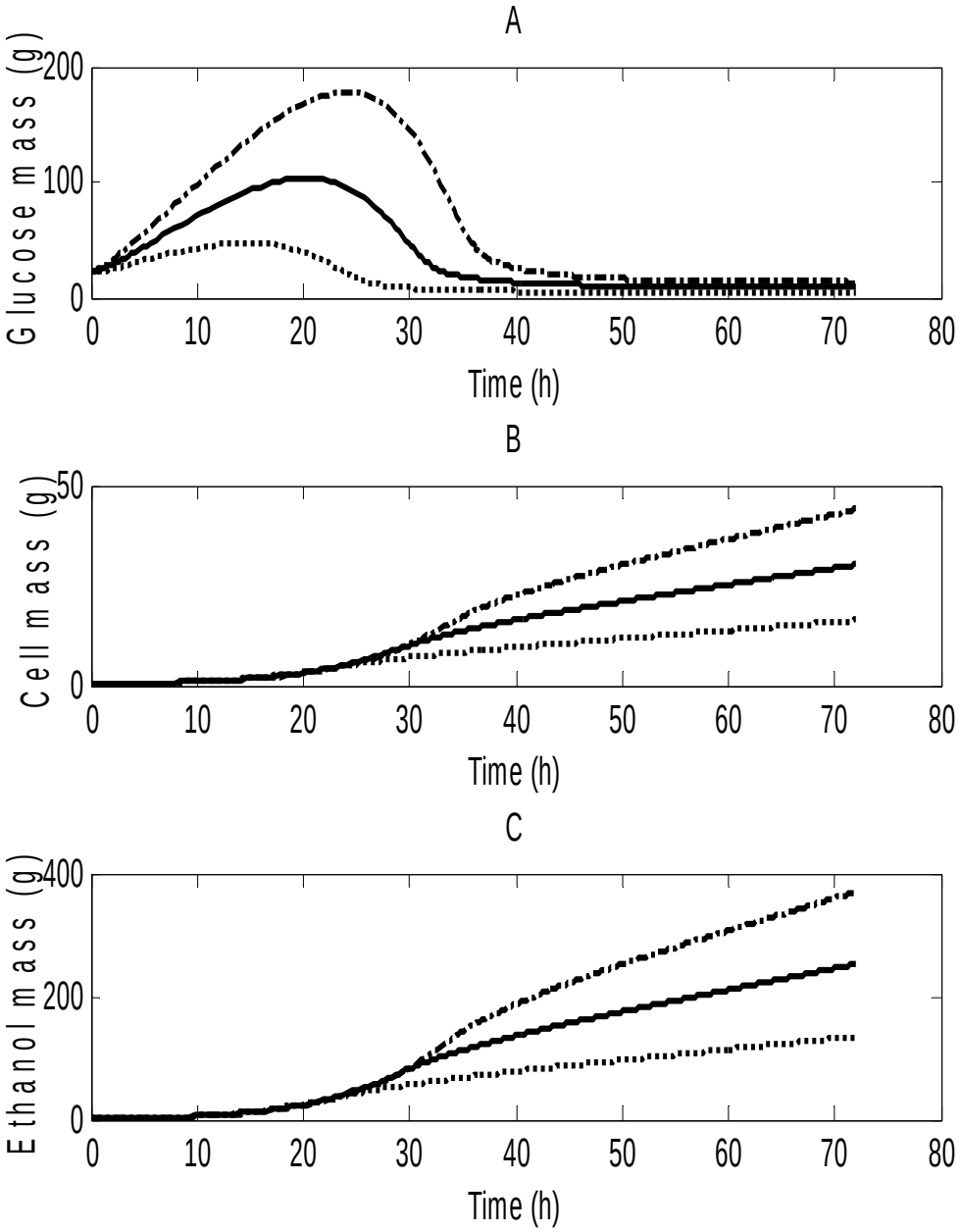

Fig. 6.15 The simulated glucose (A), cell (B), and ethanol (C) mass curves (lines) with time at three flow rates: 0.1 l/h (dot), 0.2 l/h (solid), and 0.3 h/l (dash-dot) in the constant fed-batch operation in SSSF 12. Conditions are the same as Fig. 6.14.

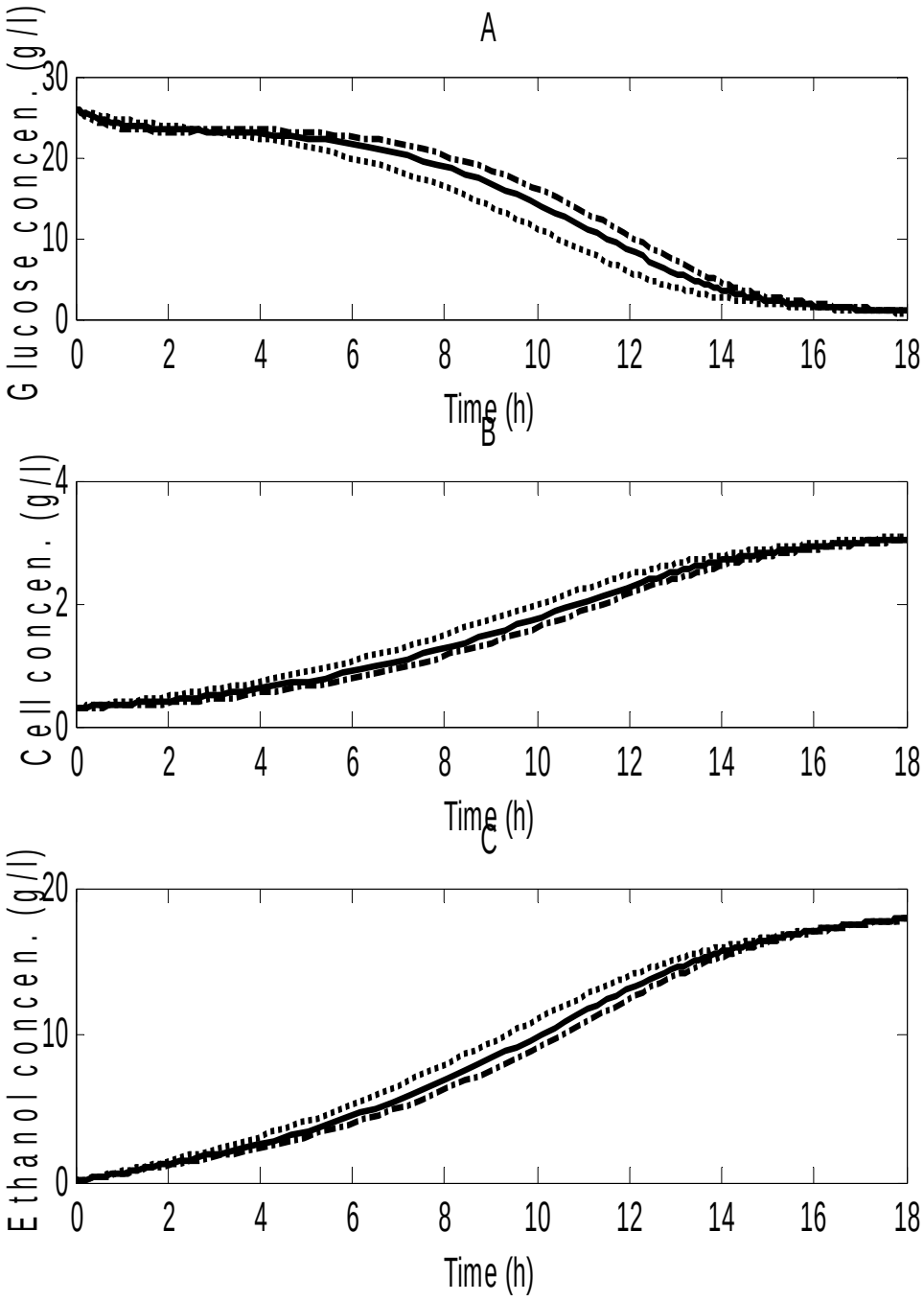

Fig. 6.16 The simulated glucose (A), cell (B), and ethanol (C) concentration curves (lines) with time at three initial flow rates: 0.1 l/h (dot), 0.2 l/h (solid), and 0.3 h/l (dash-dot) in the exponential fed-batch operation of SSSF 24. Conditions: C_0 = 40 g/l, C_0' = 20 g/l, e_0 = 4 g/l, e_0' = 1 g/l, X_1 = 0.3 g/l, V_1 = 1 l and $G_0 = B_0 = E_0 = 0$.

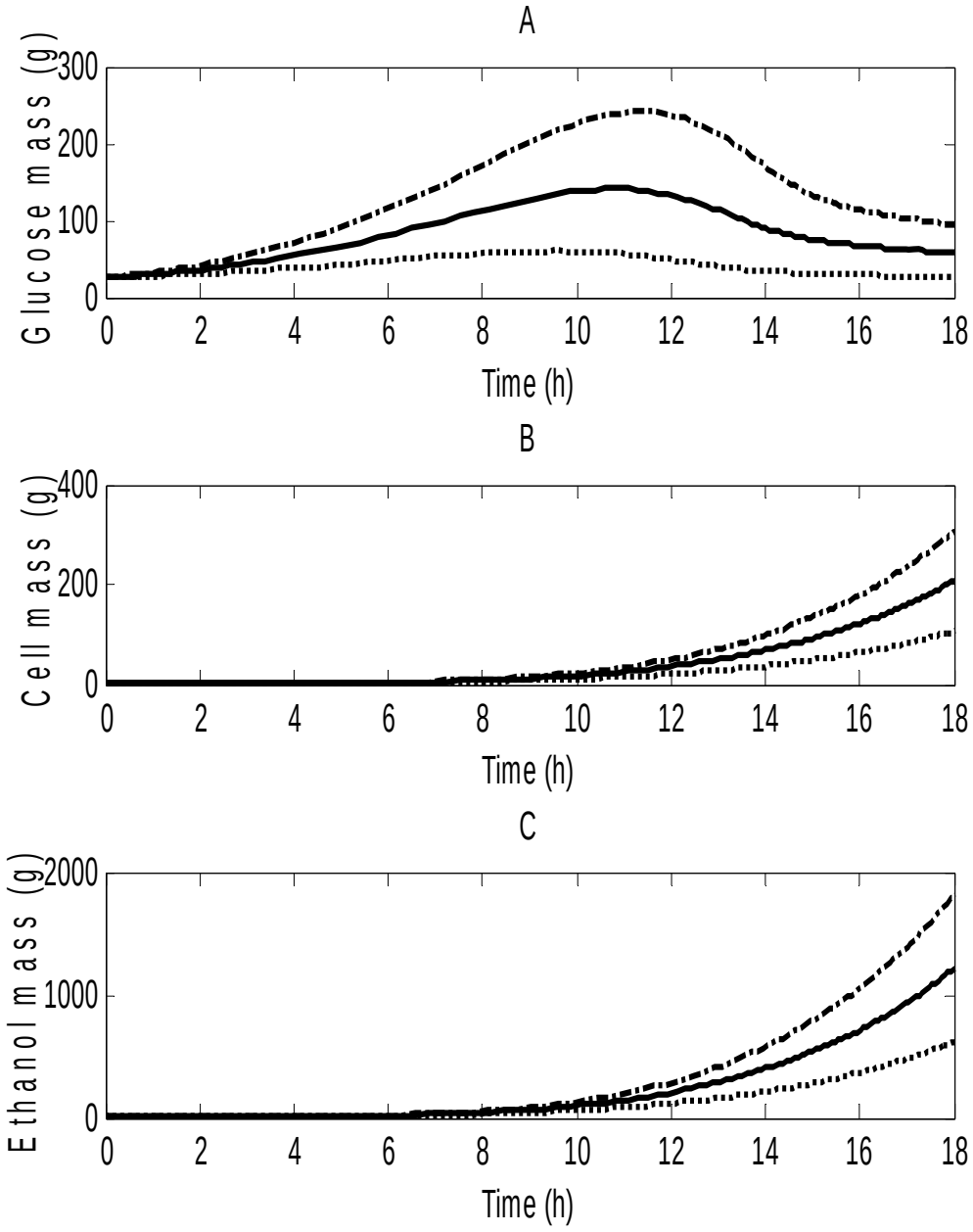

Fig. 6.17 The simulated glucose (A), cell (B), and ethanol (C) mass curves (lines) with time at three initial flow rates: 0.1 l/h (dot), 0.2 l/h (solid), and 0.3 h/l (dash-dot) in the exponential fed-batch operation of SSSF 24. Conditions are the same as Fig. 6.16.

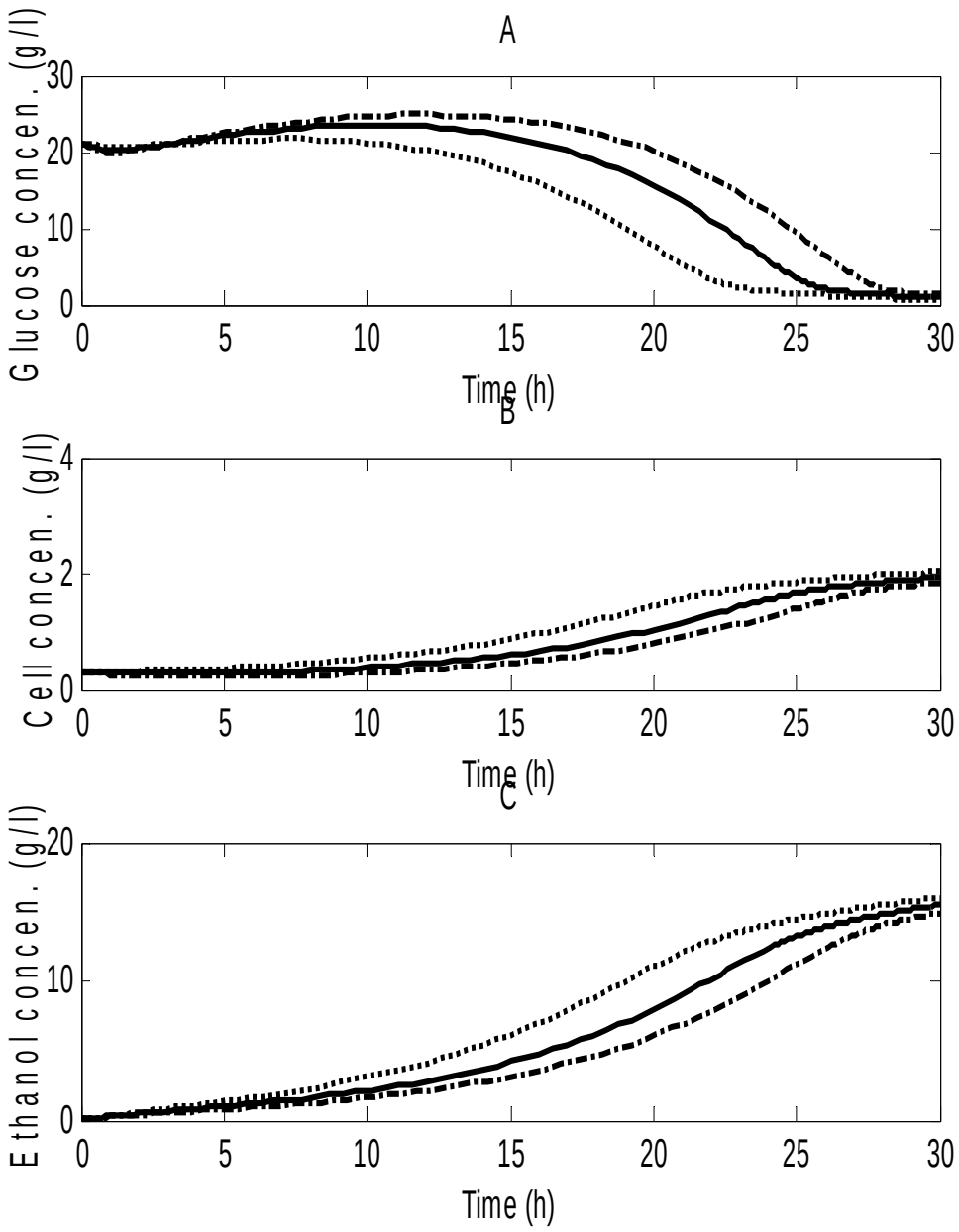

Fig. 6.18 The simulated glucose (A), cell (B), and ethanol (C) concentration curves (lines) with time at three initial flow rates: 0.1 l/h (dot), 0.2 l/h (solid), and 0.3 h/l (dash-dot) in the exponential fed-batch operation of SSSF 12. Conditions: C_0 = 40 g/l, $C_0^{'}$ = 20 g/l, e_0 = 4 g/l, $e_0^{'}$ = 1 g/l, X_1 = 0.3 g/l, V_1 = 1 l and $G_0 = B_0 = E_0 = 0$.

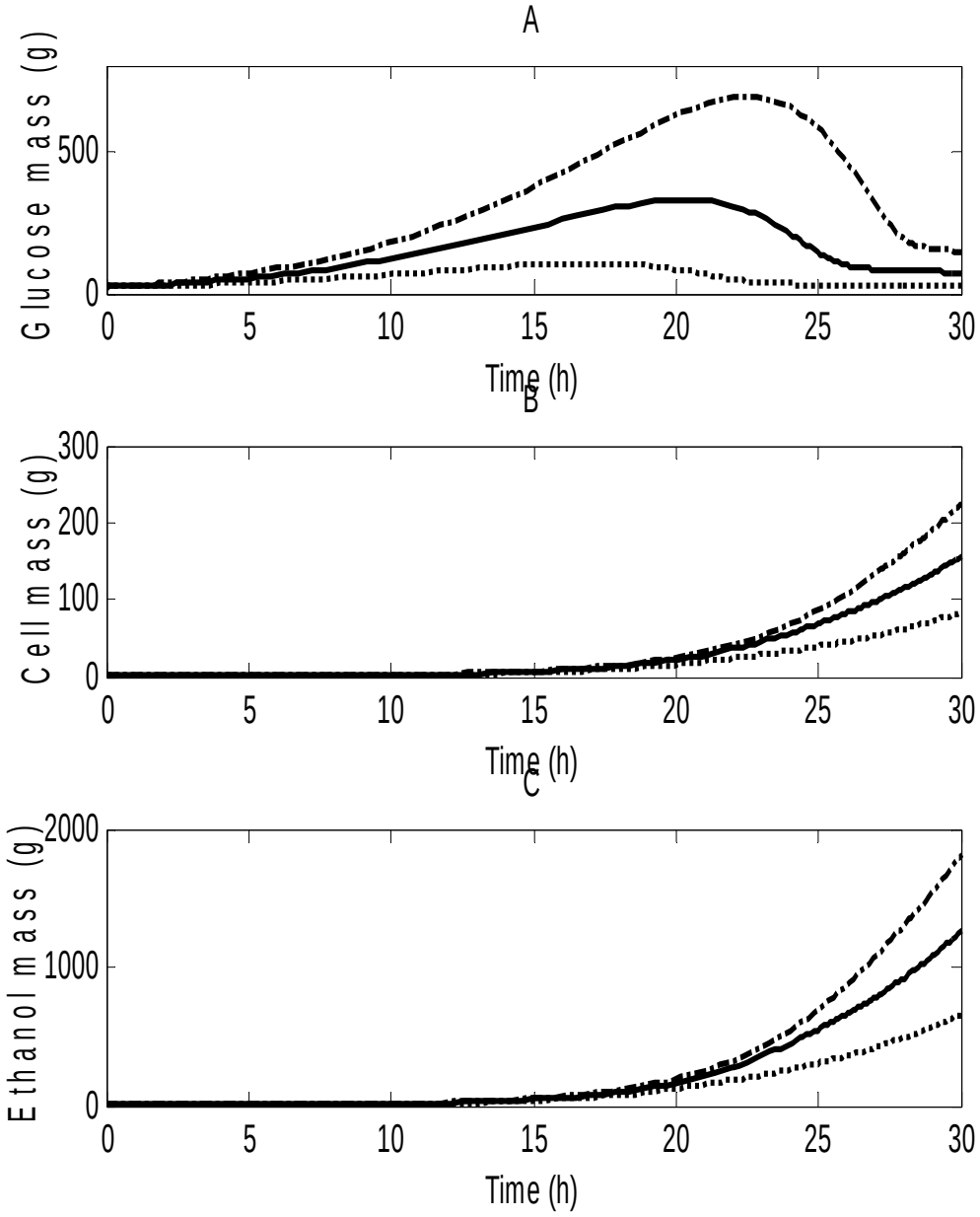

Fig. 6.19 The simulated glucose (A), cell (B), and ethanol (C) mass curves (lines) with time at three initial flow rates: 0.1 l/h (dot), 0.2 l/h (solid), and 0.3 h/l (dash-dot) in the exponential fed-batch operation of SSSF 12. Conditions are the same as Fig. 6.18.

exponential fed-batch cannot be operated for a long period because the culture volume increases rapidly.

6.8 Conclusions

Semi-simultaneous saccharification and fermentation of ethanol production is an operating mode between SSF and SHF. It consists of a pre-hydrolysis and a SSF. The batch experiments of SSSF for ethanol production using cellulose showed that SSSF can achieve the higher yield and productivity of ethanol than SSF and SHF when a suitable pre-hydrolytic time is selected. The SSSF model, comprising the seven ordinary differential equations, which describe the concentration changes of cellobiose, glucose, microorganism, ethanol, glycerol, acetic acid, and lactic acid with respect to residence time, was developed and validated. Extended SSSF models for the continuous and fed-batch operations were also developed from the batch model. Both models can be used to predict the dynamics of the continuous and fed-batch SSSF operations of ethanol production using the parameters obtained from batch experiments. The simulation also showed that there was an optimal dilution rate for the maximum productivity of ethanol in the continuous SSSF mode. The productivity of SSSF 24 was higher than that of SSSF 12. The simulated fed-batch operation with the exponential increasing flow rate produced much better effect on ethanol production than the constant fed-batch operation and the batch operation. These models provide a basis for simulating and scaling up the SSSF process.

References

ASTM E1721-95. Standard test method for determination of acid insoluble residues. In: Annual book of ASTM standards, American Society for Testing and Materials, West Conshohocken, PA. Vol. 11.05, p. 1238-1240, 1997.

ASTM E1755-95. Standard test method for determination of acid insoluble residues. In: Annual book of ASTM standards, American Society for Testing and Materials, West Conshohocken, PA. Vol. 11.05, p. 1252-1254, 1997.

Blanch, H. W. and Clark, D. S. *Biochemical Engineering*. Marcel Dekker, Inc. New York, NY. p 290, 1996.

Brown, R. C. Biorenewable Resources. Iowa State Press, Ames, Iowa. p. 160, 2003.

Dunn, I. J., and Mor, J. R. Variable-volume conituous cultivation. Biotechnology and Bioengineering. 17: 1805-1822, 1975.

Edwards, V. H., Gottschalk, M. J., Noojin III, A., Tuthill, L. B., and Tannahill, A. L. Extended culture: the growth of candida utilis at controlled acetate concentrations. Biotechnology and Bioengineering. 12: 975-999, 1970.

Kosaric, N., and Vardar-Sukan, F. Potential source of energy and chemical products in *The Biotechnology of Ethanol* edited by Roehr, M. WILEY-VCH Verlag GmbH, D-69469. p. 180, 2001.

Lim, H.C., Chen, B.J., and Creagan, C. C. An analysis of extended and exponentially-fed-batch cultures. Biotechnology and Bioengineering. 21: 425-433, 1977.

Martin, R. G., and Felsenfeld, G. A. A new device for controlling the growth rate of microorganisms: the exponential gradient generator. Anal. Biochem., 91: 43-53, 1964.

Shen, J., and Agblevor, F.A. The operable modeling of simultaneous saccharification and fermentation of ethanol production from cellulose. Submitted. 2008a.

Shen, J., and Agblevor, F.A. Optimization of enzyme loading and hydrolytic time in the hydrolysis of the mixtures of cotton gin waste and recycled paper sludge for the maximum profit rate. Biochemical Engineering Journal. 41: 241-250, 2008b.

Shuler, M. L., and Kargi, F. *Bioprocess Engineering*. 2Ed, Prentice Hall PTR. p. 217, 2002.

Stanburg, P. F., Whitaker, A., and Hall, S. J. *Principles of Fermentation Technology*, 2nd, Elserier Science Ltd. p. 23, 1995.

Yamane, T., and Shimizu, S. Fed-batch techniques in microbial processes in Advances in biochemical Engineering/Biotechnology, Edited by Fiechter, A. Sringer-Verlag Berlin, Heidelberg, Vol. 30, p147-194, 1984.

Zhu, S. D., Wu, Y. X., Zhao, Y. F., Tu, S. Y., and Xue, Y. P. Fed-batch simultaneous saccharification and fermentation of microwave/acid/alkali/H2O2 pretreated rice straw for production of ethanol. Chemical Engineering Communications. 193 (5), 639-648, 2006.

Chapter Seven

Ethanol Production from the Mixture of Cotton Gin Waste and Recycled Paper Sludge using Semi-simultaneous Saccharification and Fermentation*

7.1 Introduction

Cotton gin waste (CGW) and recycled paper sludge (RPS), both of which can be potentially used for bioethanol production, are two residues from the cotton and paper manufacturing industries. As discussed in Chapter Two, ethanol production from individual CGW and RPS has been investigated. However, there is no publication on ethanol production from the mixture of CGW and RPS. On the other hand, Shen and Agblevor [2008a] have developed a novel operating mode of semi-simultaneous saccharification and fermentation (SSSF), which includes a pre-hydrolysis phase and a SSF phase. The study on ethanol production from microcrystalline cellulose (Avicel PH 101) showed that SSSF could achieve both higher ethanol productivity and yield than SSF and SHF when an optimal pre-hydrolysis period was selected. Meanwhile, an operable SSF model was also developed [Shen and Agblevor, 2008b], which consists of four ordinary differential equations that describes the variations in concentrations of the four main components (cellobiose, glucose, ethanol, and cell). The model has been successfully applied to ethanol production from Avicel PH 101. However, the model was not applied to ethanol production from a real biomass. In this chapter, the ethanol

*Jiacheng Shen and Foster A. Agblevor. Ethanol production from the mixture of cotton gin west and recycled paper sludge using semi-simultaneous saccharification and fermentation. Submitted to Applied Biochemistry and Biotechnology.

production from the mixture of cotton gin waste and recycled paper sludge using the semi-simultaneous saccharification and fermentation method is reported.

7.2 Objectives

In this study, the objectives were

(1) To investigate the effect of pre-hydrolysis time on ethanol productivity and yield during the SSSF of CGW/RPS mixture;

(2) To investigate the effect of other factors, such as enzyme loading, substrate concentration, and severity factor, on ethanol production during the SSSF of CGW/RPS mixture;

(3) To apply the SSF model to the kinetic data from the mixture of CGW and RPS, and determine the model parameters.

7.3 Materials and Methods

7.3.1 Materials

Cotton gin waste (CGW) and recycled paper sludge (RPS) were obtained from the MidAtlantic Cotton Gin, Inc. (Emporia, VA), and International Paper (Frankin, VA), respectively. They were thoroughly mixed to form the mixture of 75 wt% CGW and 25 wt% RPS. The Novozymes enzyme NS50052 used in the experiments was donated by Novozymes, North America, Inc. (Franklinton, NC). The actual activity of the enzyme determined in our laboratory by a filter paper method was 97 Filter Paper Unit (FPU)/g [Ghose, 1987]. The initial enzyme concentrations used in the experiments were 4 and 8 g/l (the corresponding enzyme loadings were 9.7 and 18.4 FPU/g substrate). The

inoculation medium for *S. cerevisiae* was YM broth, which contained 0.3% yeast extract, 0.3% malt extract, 0.5% peptone, and 1.0% glucose. The fermentation medium contained 0.3% yeast extract, 0.25 g/l $(NH_4)_2HPO_4$, and 0.025 g/l $M_gSO_47H_2O$.

7.3.2 Methods

7.3.2.1 Steam-exploded pretreatment for the mixture of CGW and RPS

The mixture of CGW (75 wt%) and RPS (25 wt%) was pretreated by steam explosion for 2 minutes at 220°C and 235°C in a 25-l batch reactor located at the Thomas M. Brooks Forest Products Center, Blacksburg, VA. The severity factor ($\log(R_0)$) for the retention time and temperatures were calculated to be 3.83 and 4.26, respectively. The steam-exploded mixture contained about 70% moisture.

7.3.2.2 Preparation of inoculum

Preparation of inoculum is the same as Chapter 5.6.2.1.

7.3.2.3 Semi-simultaneous saccharification and fermentation

The semi-simultaneous saccharification and fermentation experiments were conducted in a DCU3 quad one liter fermenter (B. Braun Biotech International). 20 g or 30 g (dry basis) of the steam exploded mixture of CGW and RPS were added to the fermenter containing 0.5 liter of citric acid buffer medium (0.05 M, pH 4.8), and the fermenter were sterilized in an autoclave at 121°C for 1 hour. After that, 2.0 or 4.0 g enzyme (the initial enzyme concentrations were 4.0 or 8.0 g/l) were added to the fermenters. In the pre-hydrolysis phase, the medium temperature and pH were maintained at 50°C, and 4.8, respectively. After 24 or 12-hour hydrolysis, the medium temperature was adjusted to 36°C and maintained at this temperature during the SSF phase. About 0.15 g (dry weight) *S. cerevisiae* was added into the medium. The pH of the fermentation

broth was maintained at 4.8 by automatic addition of either 2M hydrochloric acid or 2M sodium hydroxide solution during the SSF period. The agitation rate was constant at 300 rpm. Two ml aliquots of the broth were taken periodically and prepared for analysis as described below. The aliquots were centrifuged, and then the supernatants were decanted and prepared for HPLC analysis by filtering through 0.2 μm syringe filter. A set of SSF and SHF experiments were also conducted. When SSF (no pre-hydrolysis), was performed, the temperature and pH were, respectively, maintained at 36^{o}C and 4.8 from start to the end of experiments. When SHF was performed, hydrolysis was conducted at the temperature 50^{o}C and pH 4.8 for 48 hours, and the solid biomass was separated from the hydrolysate. The hydrolysate was fermented at temperature 36^{o}C and pH 4.8 for 24 hours. The SSF and SHF data were compared to those of SSSF. The experiments were run in triplicate.

7.3.2.4 Analytical methods

HPLC analytical methods for ethanol, sugars, and by-products, and the cell dry weight measurement were the same as described in Chapter 5.6.2.4.

The contents of the acid-insoluble lignin, carbohydrate and ash in the dry steam-exploded mixture of 75% CGW and 25% RPS, and the raw mixture were determined according to ASTM E1721-95 [1997] and ASTM E1755-95 [1997], respectively. The carbohydrate contents of the liquid fraction of the pretreated wet mixture were measured as follows: about 1 g wet steam-exploded mixture was suspended in 84 ml deionized water, and the suspension was stirred for 30 minutes to dissolve the soluble fractions into the water. Then, the suspension was centrifuged at 6000 rpm (10000 g-val.) for 10 minutes, and solid was removed. 3 ml 72% sulfuric acid was added to the supernatant to

form 4% dilute sulfuric acid solution. The solutions were sterilized in an autoclave at 121^{o}C for 1 hour. The samples were analyzed for various sugars by HPLC described above. These sugar concentrations were converted into the carbohydrate concentrations in the wet steam-exploded mixture, such as glucan and xylan, refereed to as w_{glw} and w_{xlw} (g/l), respectively, by the HPLC method described in Chapter 5.6.2.4, after 4% sulfuric acid treatment.

To distinguish the effect of the dilute sulfuric acid (4%) from the concentrated sulfuric acid (72%) on hydrolysis of the dry mixture in the procedure of ASTM E1721-95, some samples of the dry mixture were directly hydrolyzed by dilute sulfuric acid as follows: the dry sample in 84 ml deionized water was added 3 ml 72% sulfuric acid to form 4% dilute sulfuric acid solution. The suspensions containing the solid mixture were sterilized in the autoclave at 121^{o}C for 1 hour, and the carbohydrate compositions, such as glucan and xylan, refereed to as w_{gd} and w_{xd} (g/l), respectively, in the liquid fraction were analyzed.

7.4 Results and Discussion

7.4.1 Compositions of the mixture of CGW and RPS

The compositions of the raw mixture of 75% CGW and 25% RPS, the dry steam exploded fiber, and the wet steam exploded fiber (i. e. including the liquid fraction) are shown in Table 7.1. After steam explosion pretreatment, the glucan content in the mixture increased from 46.2% to 47.6%, and the lignin content increased from 23% to 28.7%. The xylan content decreased from 8.13% to 5.18%, and the ash content decreased from 19.4% to 7.17%. This was because at high temperature, xylan in hemicellulose could be

Table 7.1 The compositions of mixture of 75% CGW and 25% RPS

Composition	Glucan (%)	Xylan (%)	Lignin (%)	Ash (%)	Other (%)
Raw CGWRPS	46.2 (44.4^{+}, 1.82^{++})	8.13 (4.47^{+}, 3.67^{++})	23.0	19.4	3.34
DSECGWRPS	47.6	5.178	28.7	7.17	11.3
WSECGWRPS	47.7	5.183	28.6	7.15	11.3

DSECGWRPS dry steam-exploded CGW and RPS
WSECGWRPS wet steam-exploded CGW and RPS
+ Concentrated sulfuric acid contribution
++ Diluted sulfuric acid contribution

Table 7.2 The composition concentrations in the liquid fraction of the wet mixture of 75% CGW and 25% RPS, and in the liquid fraction of the dry steam-exploded mixture after 4% sulfuric acid treatment

Composition	Glucan (g/l)	Xylan (g/l)
w_{gd} and w_{xd}	1.50	10.1
w_{glw} and w_{xlw}	11.2	19.8

Table 7.3 Model parameters (Eq. 4.17) for the mixture of 75% CGW and 25% RPS

e_0 (g/l)	e_d (FPU/g)	K_e (g/l)	k_2' (l/h)	k_3' (1/h)	b (l/g)
4	9.7	0.50	0.128	0.407	0.63
8	19.4	0.838	0.275	0.817	0.402

e_d The enzyme loading based on the dry substrate (FPU/g)

Table 7.4 A comparison of yields and productivities of ethanol for SSSF, SSF, and SHF

Operating mode	SSSF 24	SSSF 12	SSF	SHF
Theoretical yield (%)	78.5	71.7	69.8	72.1
Yield (g/g substrate)	0.206	0.188	0.183	0.189
Productivity (g/(l.h)	0.094	0.086	0.084	0.086
Ethanol concen. (g/l)	6.75	6.17	6.02	6.19

Table 7.5 The parameter values, confidence intervals, and percentages of CIs to values

Parameter	e_0 = 4 g/l	CI (±)	PCI (%)	e_0 = 8 g/l	CI (±)	PCI (%)
k_1 (l(g.h))	0.289	0.0128	4.4	0.3	0.0058	1.9
k_2' (h^{-1})	2.9	0.0029	0.1	3.0	0.0005	0.02
k_3' l/(g.h)	0.0243	0.0082	34	0.02	0.0007	3.5
k_4 (-)	2.0	0.0167	0.84	1.4	0.001	0.07
K_{1G} (g/l)	0.039	0.0042	11	0.04	0.004	10
K_{2G} (g/l)	15.9	0.0859	0.54	15.0	0.0209	0.14
K_G (g/l)	3.0	0.0155	0.52	3.0	0.0047	0.16
m (h^{-1})	0.69	0.0306	4.4	0.6	0.0015	0.25
μ_m (h^{-1})	0.59	0.0132	2.2	0.6	0.0007	0.12

PCI: percentages of CIs to parametric values

decomposed by steam explosion, and released into the liquid fraction. The ash components, which included calcium oxide, calcium carbonate, and other inorganic ashes, also appeared to be released into the liquid fraction under steam explosion condition. However, the glucan and lignin in biomass were not decomposed even at high temperature. Therefore, the relative contents of glucan and lignin increased after steam explosion pretreatment because of the loss of the hemicellulose and ash. Similar observation has been reported by Jeoh and Agblevor [2001]. Table 7.1 also shows also shows the ratio, w_{it}, of i composition weight in the wet steam-exploded mixture to the weight of dry mixture, *i.e.*

$$w_{it} = \frac{w_i + w_{il}}{w}\% \tag{7.1}$$

where w_i is the weight of i composition in the dry mixture (g), w_{il} is the weight of i composition in the liquid fraction of the wet mixture (g), and w is the weight of dry mixture (g). It was found that the contributions of glucan (0.1 % in Table 1) and xylan (0.005 % in Table 7.1) in the liquid fraction of the wet mixture to the total glucan and xylan contents of the wet mixture were very small because glucan (1.5 g/l) and xylan (10.1 g/l) concentrations in liquid fraction were very low (Table 7.2). These values are lower than those reported for steam-pretreated corn stover [Ohgren et al., 2007], probably because 3% SO_2 was added to corn stover in the steam pretreatment of Ohgren's experiment, which made hydrolysis more effective. Table 7.2 also shows the glucan and xylan concentrations, w_{ild}, to be 11.2 g/l and 19.8 g/l, respectively. These values can be converted into percentages of glucan and xylan in the dry steam-exploded mixture after 4 % sulfuric acid treatment shown in Table 7.1 to distinguish between the effect of the concentrated and dilute sulfuric acids on the hydrolysis. The contributions of the

concentrated sulfuric acid in decomposition of the carbohydrate fraction during hydrolysis were 96.1% for glucan and 55.0% for xylan, while the contributions of dilute sulfuric acid were 3.9% for glucan and 45.0% for xylan. The greater contribution difference of glucan (92.2%) than that of xylan (10%) between the concentrated acid and dilute acid hydrolysis was because the hemicellulose (source of xylan) was easier decomposed than cellulose (source of glucan) with the dilute acid treatment.

7.4.2 Cellulose pre-hydrolysis and simulation

The conversion of cellulose and the reducing sugar concentration of the mixture of CGW and RPS at enzyme concentrations 4 g/l and 8 g/l within 24 hours are shown in Fig. 7.3. The conversion and reducing sugar concentration increased with hydrolytic time. The highest conversion and reducing sugar concentration were about 64.8% and 12.5 g/l for the initial enzyme concentration of 4 g/l, and 67.9% and 12.9 g/l for the initial enzyme concentration of 8 g/l. To correlate the conversion (or sugar concentration) with hydrolytic time, Shen and Agblevor [2008c] developed an enzymatic hydrolysis model with convergent property shown below:

The substrate conversion x is defined as

$$x = \frac{C_0 - C}{C_0} = \frac{rG}{C_0} = 1 - \left[\frac{K_e + e_0}{K_e\left(k_3' e_0 t + 1\right) + e_0} \right]^b \tag{4.17}$$

where r is the average conversion factor of one glucan unit in cellulose to glucose (0.9), k_3' is the enzyme deactivation constant in the pre-hydrolysis phase (g/l), and b is a fitted constant (dimensionless) (definition see Chapter 4.3).

The data in Fig. 7.1 included both the experimental and simulated results for conversion and sugar concentration using Eq. (4.17). The parametric values of model (4.17) are shown in Table 7.2. The constants K_e, k_2', and k_3' at the initial enzyme

concentration of 4 g/l were smaller than those at 8 g/l. The constant k_3' represents the enzyme deactivation; hence, the smaller the k_3', the lower the enzyme deactivation. At a higher enzyme concentration, the enzyme has more chance to be adsorbed on the lignin and loses its activity. Hence, k_3' has a larger value at a higher enzyme concentration. The constant k_2' represents the reducing sugar formation rate. At a high enzyme concentration, k_2' becomes larger due to the increased ethanol formation. The constant K_e represents the ratio of the rate constant of complex-consumption and the rate constant of complex-formation. The K_e value increase may result from the k_3' value increase.

7.4.3 The batch SSSF experiment and simulation

Four cases of batch SSSF, SSF, and SHF were studied: 1) 24-hour pre-hydrolysis + 48-hour SSF 48, referred to as SSSF 24; 2) 12-hour pre-hydrolysis + 60-hour SSF, referred to as SSSF 12; 3) 72-hour SSF, referred to as SSF, and 4) 48-hour hydrolysis + substrate separation + 24-hour fermentation (SHF). The experiments were conducted for a total of 72 hours. The xylose, glucose, and ethanol concentrations with respect to time for the SSSF 24, 12, and SSF experiments at the initial enzyme concentration of 4 g/l are shown in Figs. 7.2 through 7.4. In general, the ethanol concentration rapidly increased within the first 60, 45, and 48 hours for SSSF 24, 12, and SSF, respectively, and then slightly decreased for SSS 12 and SSF, which could be because of the formation of organic acids. For SSSF 24 and 12 the glucose concentrations gradually decreased from the higher initial values with increasing time. On the contrary, the glucose concentration in the SSF first increased because of the low cell concentration (the low ethanol production rate), and the high enzyme concentration, which resulted in the accumulation

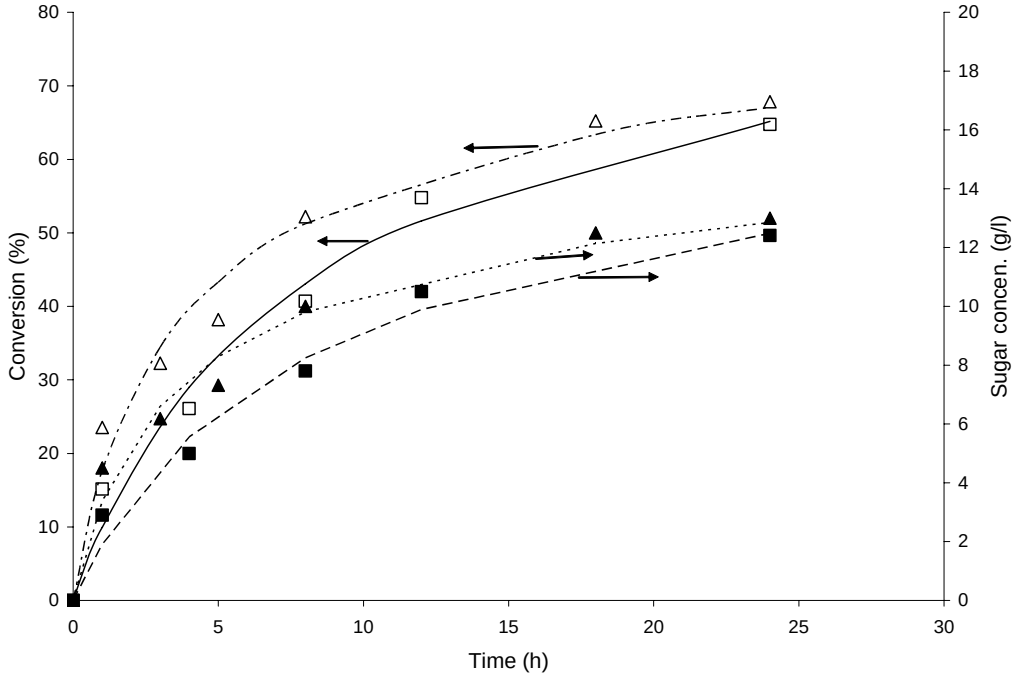

Fig. 7.1 The reducing sugar concentration and conversion of mixture with time in the pre-hydrolysis phase. Symbol: experimental points, line: model values □, ■: SSSF 24 at initial enzyme concentration 4 g/l, Δ, ▲: SSSF 12 at initial enzyme concentration 8 g/l.

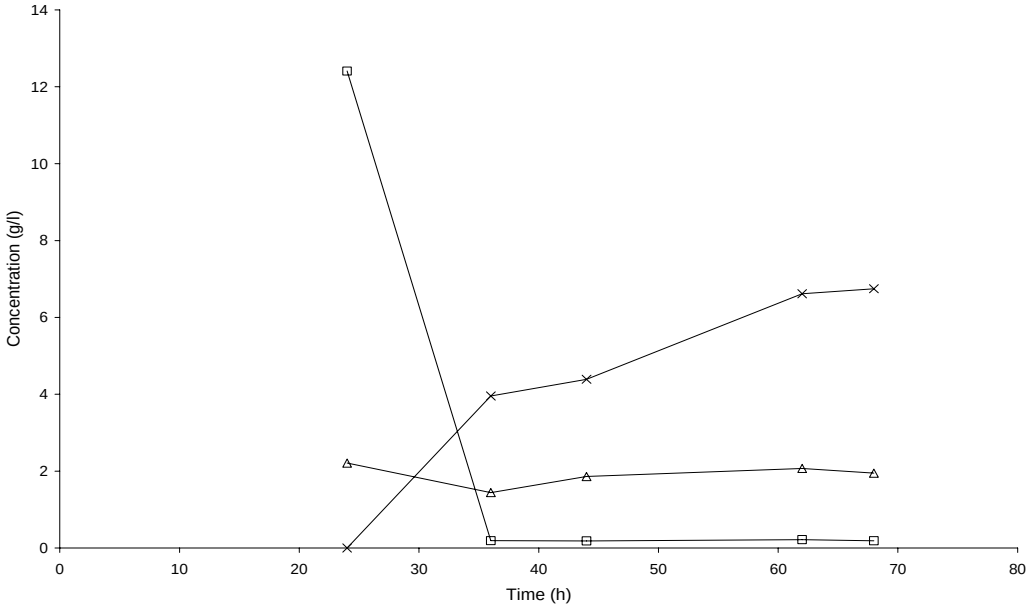

Fig. 7.2 The variation in concentrations of various compounds during the batch SSSF 24. The experimental points (signs): glucose (□), xylose (Δ) and ethanol (x). Conditions: C_0 = 19.2 g/l, X_1 = 0.3 g/l, e_0 = 4 g/l, $G_0 = B_0 = E_0 = 0$, the severity factor 4.23.

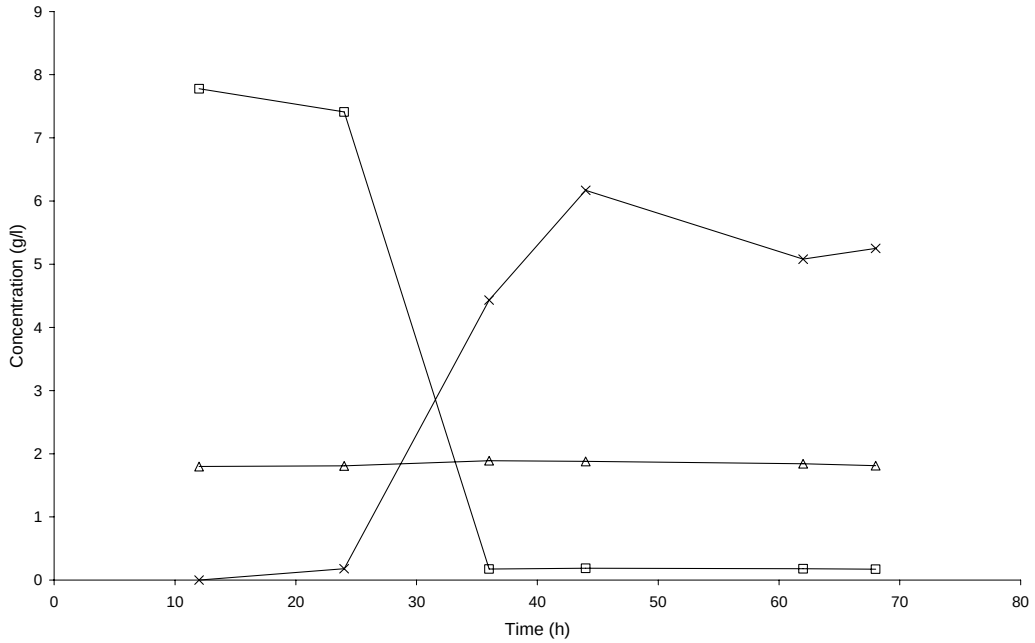

Fig. 7.3 The variation in concentrations of various compounds during the batch SSSF 14. The experimental points (signs): glucose (□), xylose (Δ) and ethanol (x). Conditions: C_0 = 19.2 g/l, X_1 = 0.3 g/l, e_0 = 4 g/l, $G_0 = B_0 = E_0 = 0$, the severity factor 4.23.

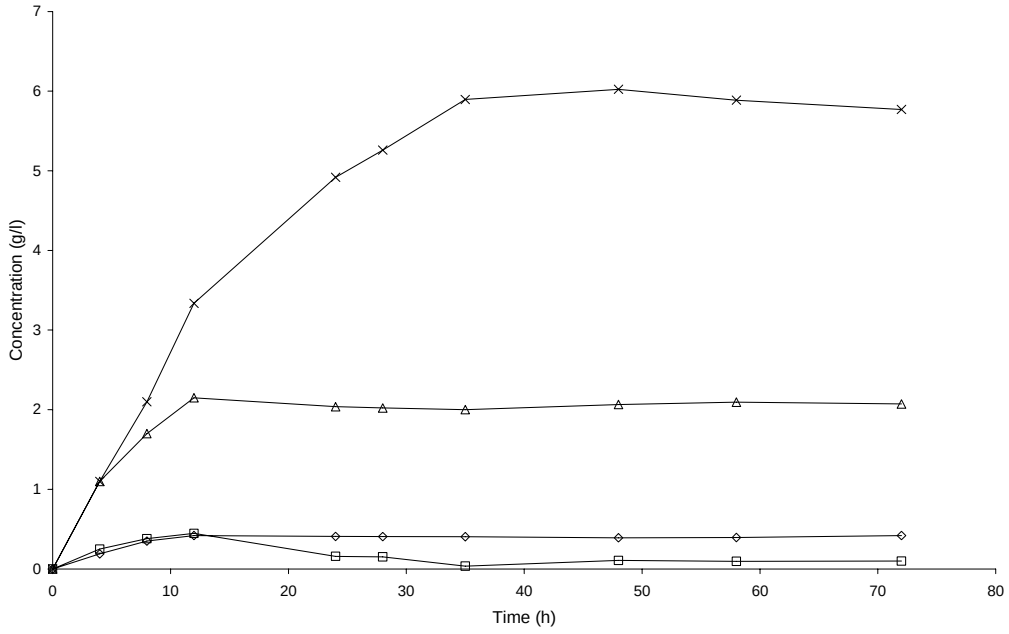

Fig. 7.4 The variation in concentrations of various compounds during the batch SSF. The experimental points (signs): glucose (□), xylose (Δ) ethanol (x), and cellobiose (◊). Conditions: C_0 = 19.2 g/l, X_1 = 0.3 g/l, e_0 = 4 g/l, $G_0 = B_0 = E_0 = 0$, the severity factor 4.23.

of glucose during the initial 12 hours. For all the three cases, the glucose concentration approached zero after 36 hours reaction. This was because the yeast grew exponentially due to the sufficient supply of growth-limiting substrate, and the glucose was quickly consumed. The xylose concentrations were roughly constant after pre-hydrolysis for SSSF 24 and 12, and after 12 hours for SSF because *S. cerevisiae* does not utilized pentoses. As mentioned previously, the steam-exploded mixture of CGW and RPS contained about 70% moisture. Therefore, the yield calculation should account for the culture volume increase due to the contribution of water from the mixture. The actual liquid volume was 0.61 l for substrate concentration 40 g/l at 0.5 l culture. Therefore, yield Y (g ethanol/g dry substrate) should be

$$Y = \frac{EV}{W} \tag{7.2}$$

where V is the actual culture volume (l), E is the ethanol concentration (g/l), and W is the substrate mass in the culture (g). The maximum ethanol concentration for SSSF 24, 12, SSF, and SHF were 6.75 g/l, 6.17 g/l, 6.02 g/l, and 6.19 g/l, and the maximum ethanol yields were 0.206, 0.188, 0.183, and 0.189, respectively. These yields were equal to a theoretical ethanol yield of 78.5%, 71.7%, 69.8%, and 72.1%, respectively, calculated using the following equation:

$$Y_{th} = \frac{0.9Y}{0.511G_r}100\,\% \tag{7.3}$$

where G_r is the glucan fraction in raw biomass. These theoretical ethanol yields were similar to other experimental and industrial data [Zhu et al., 2006; Kosaric and Vardar-Sukan, 2001], but the theoretical ethanol yields of SSSF 12, SSF, and SHF were lower than the ideal yield of 76-90%, which considered the carbon consumption for cell growth

[Brown, 2003]. The final ethanol productivity for the SSSF 24, 12, SSF, and SHF after 72-hour were about 0.094 g/(l.h), 0.086 g/(l.h), 0.084 g/(l.h), and 0.086 g/(l.h). The above ethanol yield, theoretical yields, and productivities show that SSSF 24 is more efficient than either SSSF 12, SSF, or SHF.

7.4.4 Parametric effects of on the ethanol production from the CGW and RPS mixtures

Figs. 7.4 and 7.7 show the glucose, xylose, and ethanol concentrations over time for SSF at two initial enzyme concentrations of 4 g/l and 8 g/l. Because more enzyme used in Fig. 7.7, the ethanol concentration quickly increased within initial 12 hours to 4.7 g/l, while the ethanol concentration in Fig. 7.4 at 12 hours was only 3.3 g/l. Similar results were observed for comparisons of Fig. 7.2 (4 g/l) and Fig. 7.5 (5.4 g/l) for 72 hours of SSSF 24, and Fig. 7.3 (4.6 g/l) and Fig. 7.6 (5 g/l) for 72 hours of SSSF 12 at the initial enzyme concentrations of 4 g/l and 8 g/l. The variations of glucose, xylose, and ethanol concentrations for SSSF 12 at the severity factor of 3.83 are shown in Fig. 7.8. Compared to Fig. 7.3 at the severity factor of 4.23, the ethanol concentration of the former was lower than that of the latter. This indicates that the greater severity factor, (which means higher temperature in the present study), was more favorable for ethanol production. The effect of substrate concentration on ethanol SSF production are shown in Fig. 7.4 (at substrate concentration 40 g/l) and Fig. 7.9 (at substrate concentration 60 g/l). The ethanol concentration in both figures were similar, which might result from in-perfected mixing at the high substrate concentration of 60 g/l. We observed that the agitation in the fermenter was not effective at the high substrate concentration 60 g/l. However, the theoretical yield (53.4%) and yield (0.145 g ethanol/g dry substrate) for substrate

concentration of 60 g/l were lower than those for substrate concentration of 40 g/l (67.5% and 0.184 g ethanol/g substrate).

7.4.5 Simulation of SSF ethanol production from the mixture of CGW and RPS

A mathematical model of SSF was developed by Shen and Agblevor [2008b] as shown below:

$$\frac{dB}{dt} = \frac{r_1}{0.947} - r_2 = \frac{k_1\left[C_0 - 0.9G - 0.947B - 0.9E/0.511 - 1.137\left(X - X_0\right)\right]}{0.947\left(1 + G/K_{1G}\right)} \left(\frac{e_0}{1 + k_3' e_0 t}\right) - \frac{k_2 B}{1 + G/K_{2G}} \tag{5.21}$$

$$\frac{dG}{dt} = \frac{r_2}{0.95} - r_G = \frac{k_2 B}{0.95\left(1 + G/K_{2G}\right)} - \frac{\mu_m XG}{\left(K_G + G\right)Y_{X/G}} - mX \tag{5.17}$$

$$\frac{dX}{dt} = \mu X = \frac{\mu_m XG}{K_G + G} \tag{5.18}$$

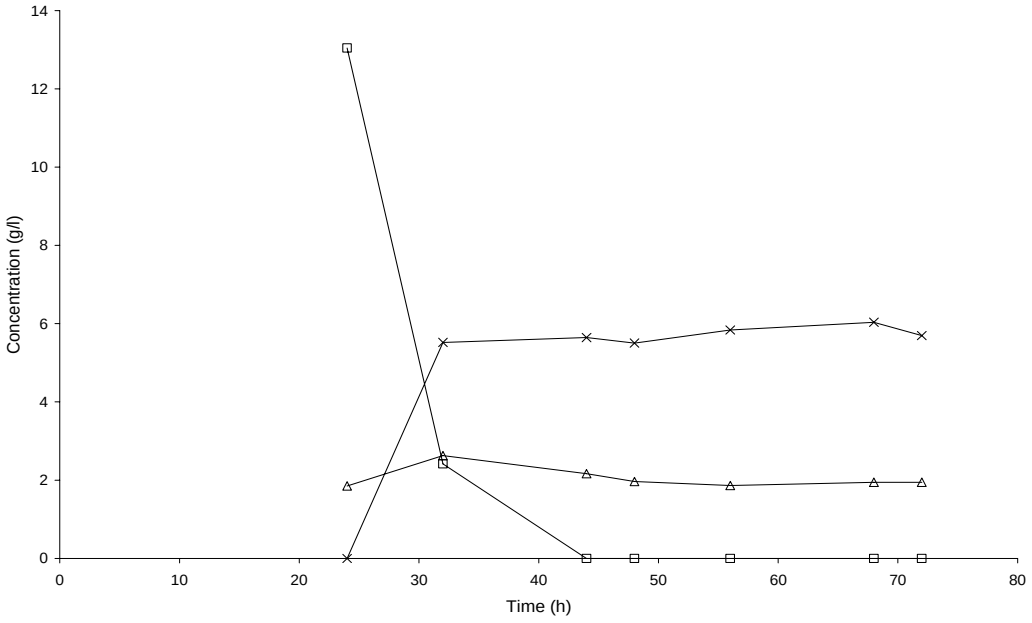

Fig. 7.5 The variation in concentrations of various compounds during the batch SSSF 24. The experimental points (signs): glucose (□), xylose (Δ) and ethanol (x). Conditions: C_0 = 19.2 g/l, X_1 = 0.3 g/l, e_0 = 8 g/l, $G_0 = B_0 = E_0 = 0$, the severity factor 4.23.

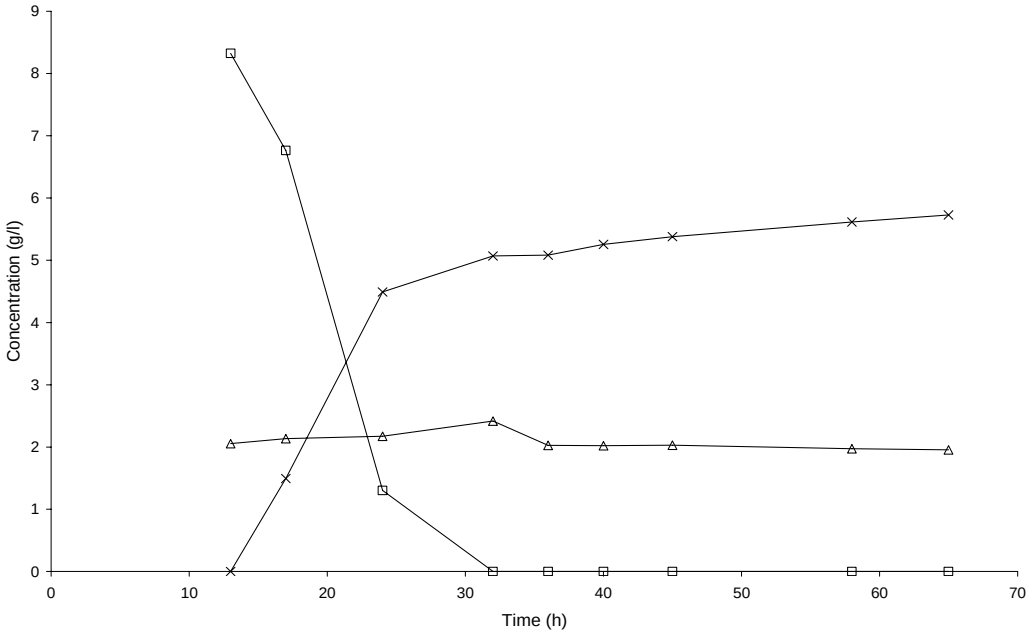

Fig. 7.6 The variation in concentrations of various compounds during the batch SSSF 12. The experimental points (signs): glucose (□), xylose (Δ) and ethanol (x). Conditions: C_0 = 19.2 g/l, X_1 = 0.3 g/l, e_0 = 8 g/l, $G_0 = B_0 = E_0 = 0$, the severity factor 4.23.

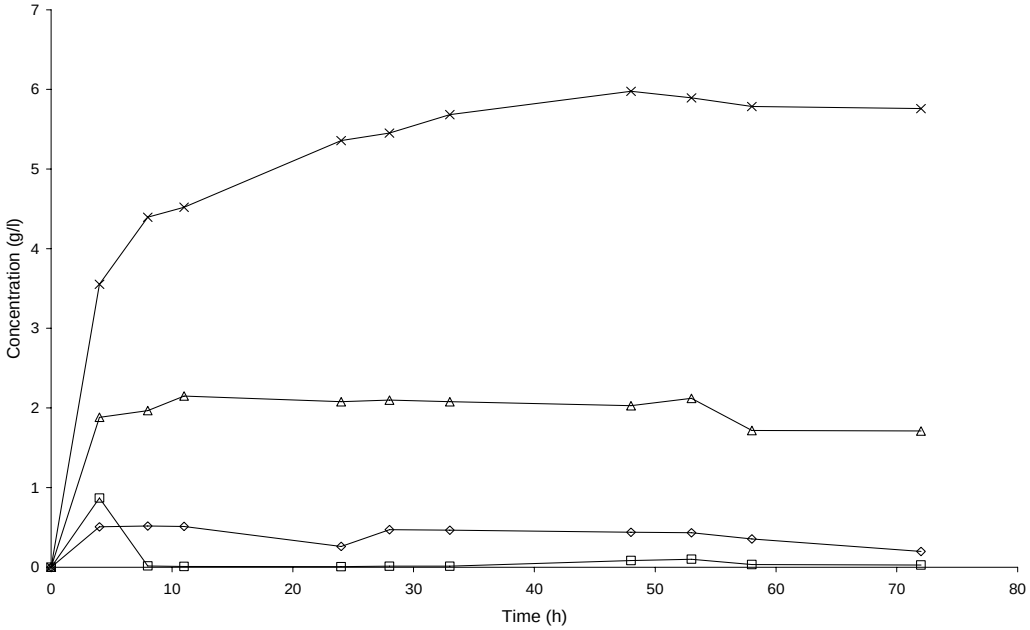

Fig. 7.7 The variation in concentrations of various compounds during the batch SSF. The experimental points (signs): glucose (□), xylose (Δ) ethanol (x), and cellobiose (◊). Conditions: C_0 = 19.2 g/l, X_1 = 0.3 g/l, e_0 = 8 g/l, $G_0 = B_0 = E_0 = 0$, the severity factor 4.23.

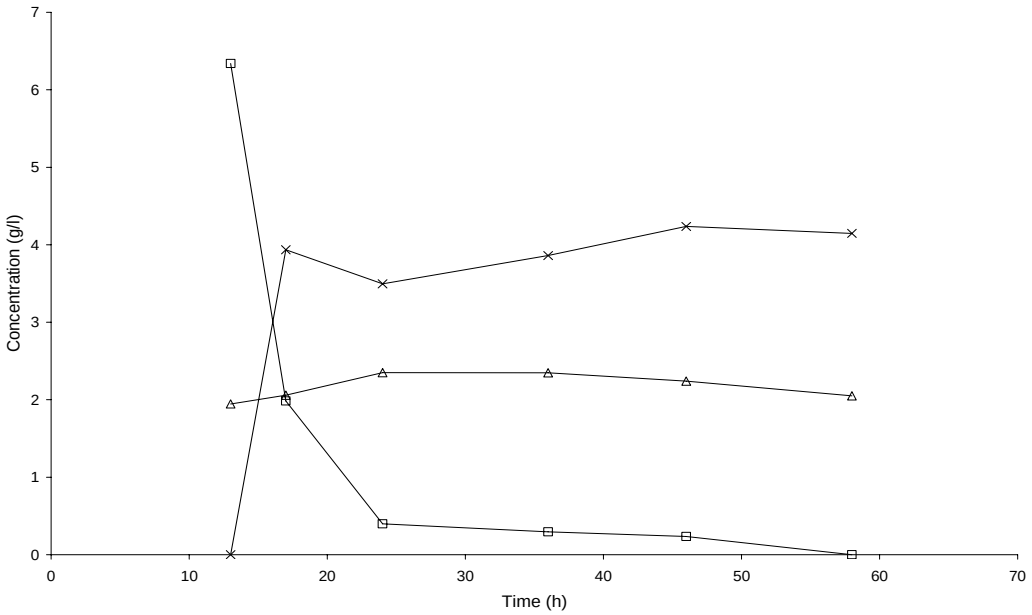

Fig. 7.8 The variation in concentrations of various compounds during the batch SSSF 12. The experimental points (signs): glucose (□), xylose (Δ) ethanol (x), and cellobiose (◊). Conditions: C_0 = 19.2 g/l, X_1 = 0.3 g/l, e_0 = 4 g/l, $G_0 = B_0 = E_0 = 0$, the severity factor 3.83.

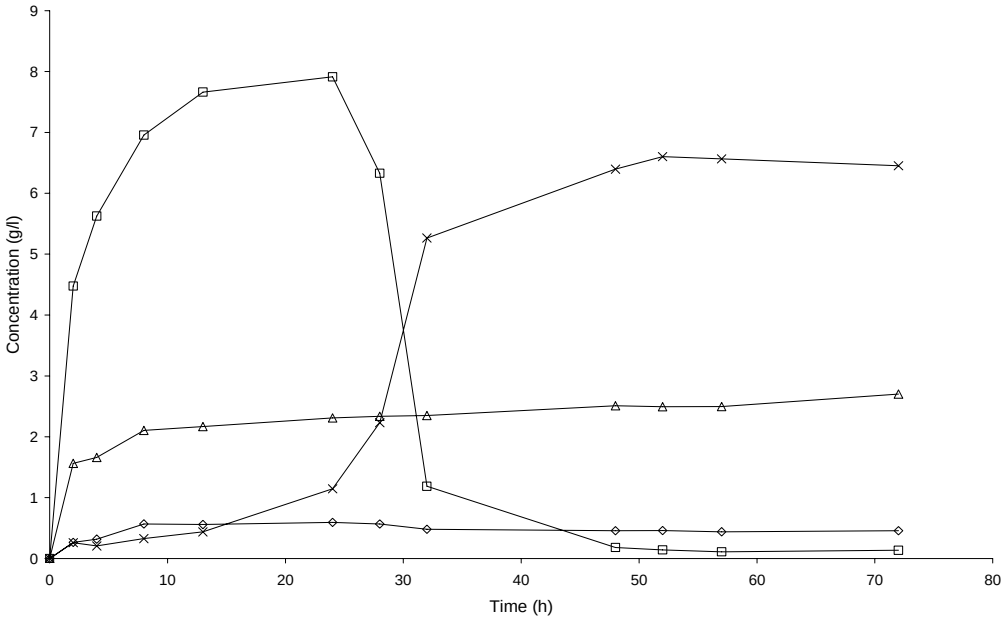

Fig. 7.9 The variation in concentrations of various compounds during the batch SSSF 12. The experimental points (signs): glucose (□), xylose (Δ) ethanol (x), and cellobiose (◊). Conditions: C_0 = 28.4 g/l, X_1 = 0.3 g/l, e_0 = 4 g/l, $G_0 = B_0 = E_0 = 0$, the severity factor 4.23.

$$\frac{dE}{dt} = \frac{k_4 \mu_m XG}{(K_G + G)Y_{X/G}} \tag{5.19}$$

Eqs. (5.21, 5.17-5.19) combined with the initial conditions of C = 19.2 g/l, e = 4 g/l or 8 g/l, X = 0.3 g/l, G = 0, and B = 0 at time t = 0 can describe the concentration changes of cellobiose, glucose, cell, and ethanol with respect to time. The parameters k_1, k_2, k_3', k_4, K_G, K_{1G}, K_{2G}, μ_m and m were determined using a MATLAB fitting program (the yeast concentrations with time were adopted from our previous study with similar experimental conditions [Shen and Agblevor, 2008c]). These parametric values, their 95% confidence intervals (CI), and the percentages of CIs to the parametric values (PCI) are listed in Table 7.5, and the simulated curves are shown in Figs. 7.10 and 7.11. From Figs. 7.10 and 7.11, we can see that the cellobiose concentration increased slightly in the later part of the SSF, which may imply that the conversion of cellobiose to glucose declined due to glycosidase deactivation. In both figures the maxima for the cellobiose concentration were lower than those of the glucose concentration, and the times for the maxima of the cellobiose were earlier than those of the glucose. This implied that the reaction from cellulose to cellobiose was a rate-controlling step because the reaction rate from cellobiose to glucose was faster than that from cellulose to cellobiose. The values of k_1e_0 (1.16 h^{-1} for the initial enzyme concentration 4 g/l and 2.4 h^{-1} for 8 g/l) of r_1 at the initial time are smaller than the rate constants k_2 (2.9 h^{-1} for the initial enzyme concentration 4 g/l and 3.0 h^{-1} for 8 g/l) of r_2 (Table 7.5), but are greater than $\mu = \mu_m G/(K_G + G) = 0$ of r_X. This indicated that initially the conversion of cellulose to ethanol was controlled by cell growth. However, the enzymatic conversion of cellulose to cellobiose would control the process as the glucose concentration increased (μ increased) at which the values of k_1e were less than k_2 and μ.

7.4.6 The rate-controlling step in SSF process

Eqs. (5.21, 5.17-5.19) are the rate expressions of cellobiose, glucose, cell, and ethanol. When the constants in these equations are determined by the MATLAB program, the reaction rates can be calculated to observe which is the rate-controlling step. Figs. 7.12 and 7.13 show the rates for SSF at the initial enzyme concentrations 4 and 8 g/l, respectively. From the figures, the reaction rates of cell and ethanol were positive because their concentrations gradually increased, while the glucose reaction rate gradually decreased from positive to negative. The cellobiose reaction rate sharply changed from a positive peak to a negative peak, because in the initial period the cellobiose reaction rate was faster due to the higher enzyme concentration. As the effective enzyme concentration decreased, the cellobiose concentration gradually decreased and the rate became negative. Within the initial two hours (Figs. 7.12 and 7.13), the cell growth rate controlled the entire SSF process because it had the smallest absolute reaction rate among all the absolute reaction rates. After two hours, the cellobiose in the figures had the smallest absolute reaction rate, which showed that the reaction from cellulose to cellobiose became the rate-controlling step for ethanol production. In addition, due to the higher enzyme concentration, the reaction rates of cellobiose and glucose in Fig. 7.13 were faster than those in Fig. 7.12. For example, the peak of the glucose reaction rate for the initial enzyme concentration 8 g/l is 4.2 g/(l.h), while for 4 g/l, the peak of the glucose reaction rate is 2.6 g/(l.h).

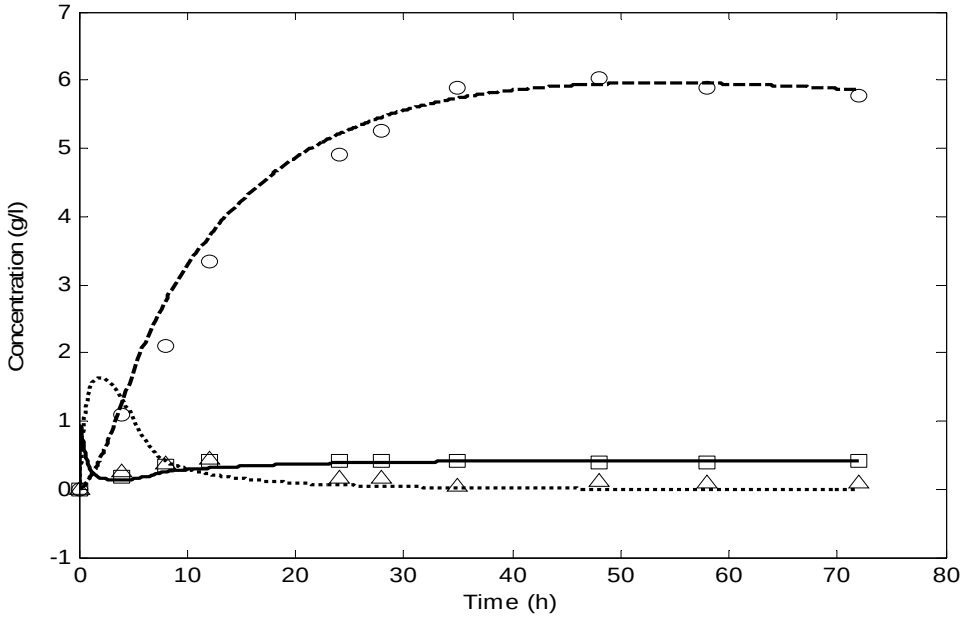

Fig. 7.10 The experimental points (signs) and simulated curves (lines) of cellobiose (□, solid), glucose (Δ, dot), and ethanol (o, dash) concentrations with time in the SSF. Conditions: C_0 = 19.2 g/l, X_0 = 0.3 g/l, e_0 = 4 g/l, and $G_0 = B_0 = E_0 = 0$.

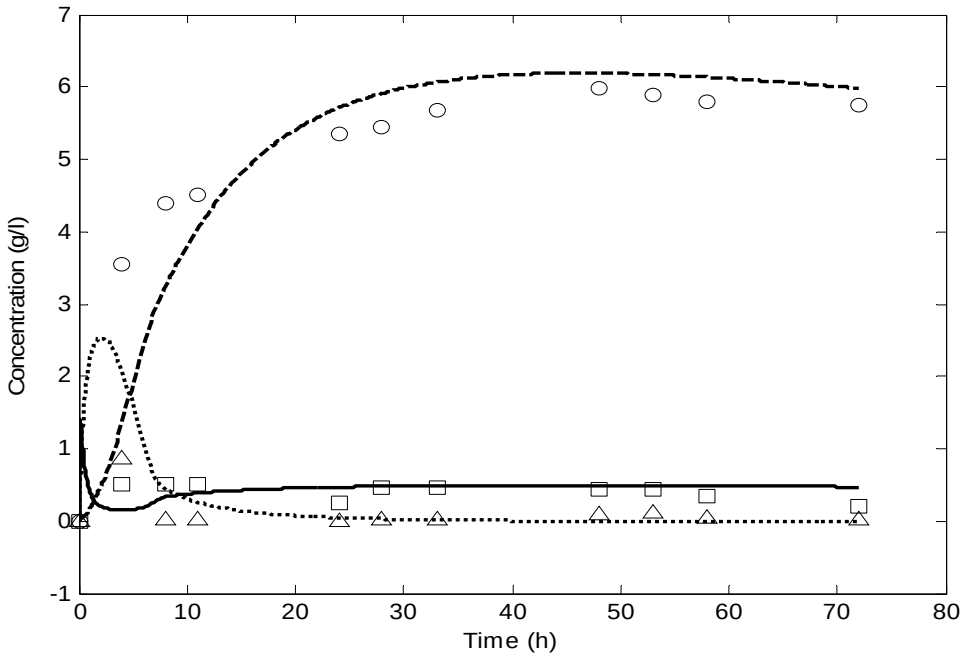

Fig. 7.11 The experimental points (signs) and simulated curves (lines) of cellobiose (□, solid), glucose (Δ, dot), and ethanol (o, dash) concentrations with time in the SSF. Conditions: C_0 = 19.2 g/l, X_0 = 0.3 g/l, e_0 = 8 g/l, and $G_0 = B_0 = E_0 = 0$.

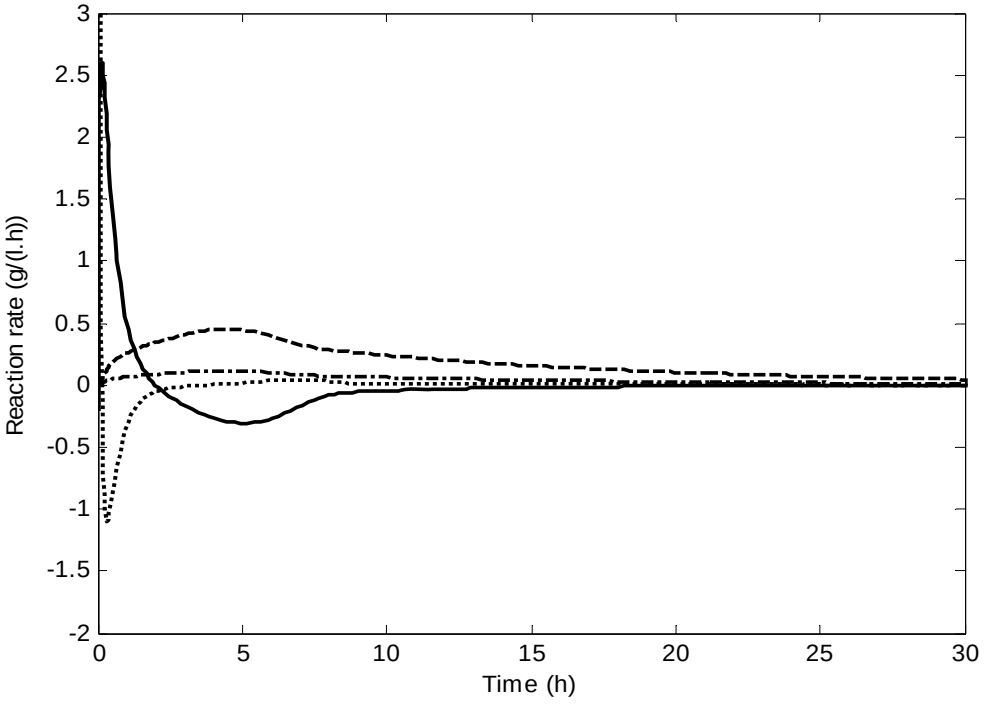

Fig. 7.12 The reaction rates of cellobiose (dot), glucose (solid), cell (dash-dot), and ethanol (dash) in the SSF. Conditions are the same as Fig. 7.10.

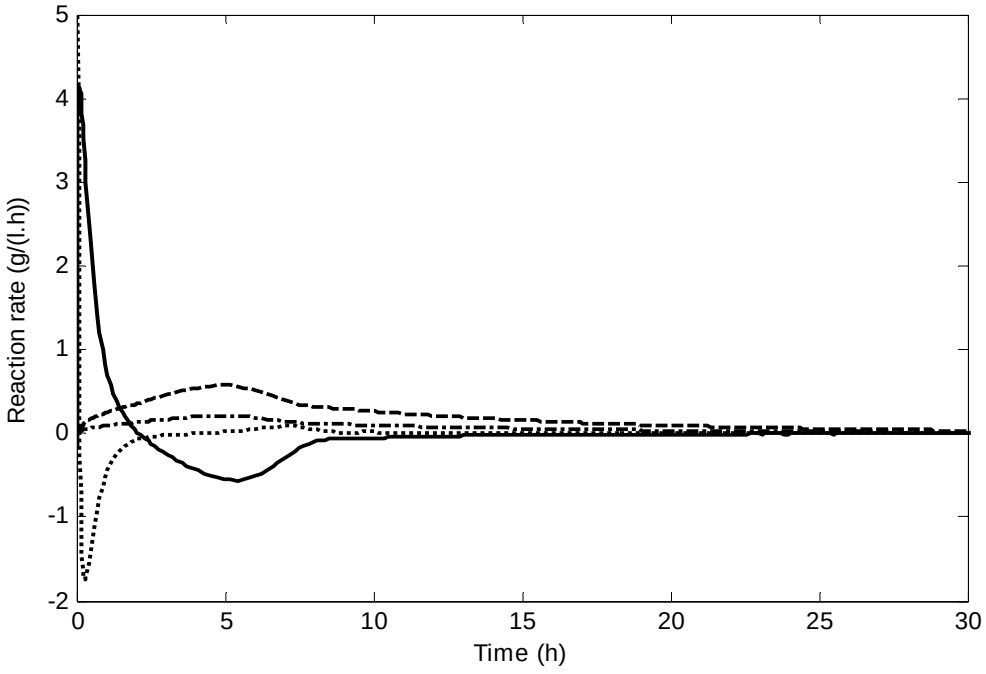

Fig. 7.13 The reaction rates of cellobiose (dot), glucose (solid), cell (dash-dot), and ethanol (dash) in the SSF. Conditions are the same as Fig. 7.11.

7. 5 Conclusions

In this study, semi-simultaneous saccharification and fermentation, consisting of a pre-hydrolysis and a SSF, was used to product ethanol from the steam-exploded mixture of 75 wt% CGW and 25 wt% RPS. The batch experiments showed that SSSF could produce higher ethanol concentration, yield, and productivity than SSF and SHF when the optimal pre-hydrolysis time was selected. It was concluded that the higher temperature of steam explosion enhanced the ethanol concentration, but the higher initial enzyme and substrate concentrations did not increase the ethanol concentration. The SSF model, which included the four ordinary differential equations for the description of concentration changes of cellobiose, glucose, microorganism, and ethanol with respect to residence time, was used to fit the experimental data for the four main components in the SSF process of ethanol production. This model showed good agreement between the experimental points and theoretical predictions.

References

ASTM E1721-95. Standard test method for determination of acid insoluble residues. In: Annual book of ASTM standards, American Society for Testing and Materials, West Conshohocken, PA. Vol. 11.05, p. 1238-1240, 1997.

ASTM E1755-95. Standard test method for determination of acid insoluble residues. In: Annual book of ASTM standards, American Society for Testing and Materials, West Conshohocken, PA. Vol. 11.05, p. 1252-1254, 1997.

Blanch, H. W. and Clark, D. S. *Biochemical Engineering*. Marcel Dekker, Inc. New York, NY. p 290, 1996.

Brown, R. C. Biorenewable Resources. Iowa State Press, Ames, Iowa. p. 160, 2003.

Ghose. T. K. Measurement of cellulase activities. Pure and Applied Chemistry, 59 (2) 257-268, 1987.
Jeoh, T. and Agblevor, F. A. Characterization and fermentation of steam exploded cotton gin waste. Biomass and Bioenergy. 21 (2): 109-120 2001.

Kosaric, N., and Vardar-Sukan, F. Potential source of energy and chemical products in *The Biotechnology of Ethanol* edited by Roehr, M. WILEY-VCH Verlag GmbH, D-69469. p. 180, 2001.

Ohgren, K., Bura, R., Lesnicki, G., Saddler, J., and Zacchi, G. A comparison between simultaneous saccharification and fermentation and separate hydrolysis and fermentation using steam-pretreated corn stover. Process Biochemistry. 42 (5), 834-839, 2007.

Shen, J., and Agblevor, F.A. Modeling semi-simultaneous saccharification and fermentation of ethanol production from cellulose. 2008a.

Shen, J., and Agblevor, F.A. Ethanol production from the mixture of cotton gin west and recycled paper sludge by semi-simultaneous saccharification and fermentation. 2008b.

Shen, J., and Agblevor, F.A. Optimization of enzyme loading and hydrolytic time in the hydrolysis of the mixtures of cotton gin waste and recycled paper sludge for the maximum profit rate. Biochemical Engineering Journal. 41: 241-250, 2008c.

Zhu, S. D., Wu, Y. X., Zhao, Y. F., Tu, S. Y., and Xue, Y. P. Fed-batch simultaneous saccharification and fermentation of microwave/acid/alkali/H2O2 pretreated rice straw for production of ethanol. Chemical Engineering Communications. 193 (5), 639-648, 2006.

Chapter Eight

Summary

Cotton gin waste (CGW) and recycled paper sludge (RPS) are residues from the cotton and paper industries, respectively. They contain cellulose and hemicelluloses, which are potential raw materials for bioethanol production. In this study, the kinetics of enzymatic hydrolysis of CGW and the mixtures of CGW and RPS using two enzymes (Spezyme AO3117 and Novozymes NS50052) were investigated. The experiments showed that the reducing sugars could be produced from the CGW and the mixtures of CGW and RPS after steam explosion and enzymatic hydrolysis of these materials. It was concluded that higher initial enzyme concentration increased the conversion of the materials. The reducing sugar concentration and conversion of the mixture of 75% CGW and 25% RPS were higher than those of the mixture of 80% CGW and 20% RPS. The highest conversion of the former was 73.8% at enzyme loading of 17.4 FPU/g substrate after 72 hours hydrolysis. A three-parameter kinetic model assuming a second order enzyme deactivation rate was developed and its analytical expression was successfully applied to the hydrolytic experimental data of the mixtures to derive the model parameters. The two profit rate models developed in this study, representing the operating modes with and without substrate recycle, were used to analyze the optimal enzyme loadings and hydrolytic times for the maximum profit rate. The simulated results from the models showed that a high substrate concentration and a recycle operating mode were the two effective methods to enhance the profit rate in ethanol production. The models can also be used to predict the optimal enzyme loading and hydrolytic time for various ethanol market prices.

Simultaneous saccharification and fermentation (SSF) of ethanol production from lignocellulosic materials is a more advanced operating mode than separate hydrolysis and fermentation (SHF). The model developed for the SSF process includes the four ordinary differential equations which describe changes in cellobiose, glucose, microorganism, and ethanol concentrations with respect to residence time. The model can be used to fit the experimental data for the four main components in the SSF process of ethanol production from microcrystalline cellulose (Avicel PH 101). Extended models for the continuous and fed-batch operations were also developed based on the batch model. Both models can be used to predict the dynamics of the continuous and fed-batch SSF operations using the parameters obtained from the batch experiments. The simulation also showed that there was an optimal dilution rate for the maximum productivity of ethanol in the continuous SSF operating mode. The model was also used for ethanol production from the mixture of 75 wt% CGW and 25 wt% RPS. The parameters of SSF model were determined through fitting the experimental data of the four main components in ethanol production. The simulations of reaction rates of cellobiose, glucose, cell, and ethanol using the model and the parameters from the experiments showed that there was a transition point where the rate-controlling step was changed from cell growth control in the initial several hours to cellobiose reaction control in ethanol production of SSF from pure cellulose and the mixture of 75% CGW and 25% RPS. These models provide a basis for simulating and scaling up the SSF process.

Semi-simultaneous saccharification and fermentation (SSSF) of ethanol production is an operating mode between SSF and SHF. It consists of two phases: pre-hydrolysis and SSF. The batch experiments showed that for a selected optimal pre-hydrolysis time, the

SSSF mode produced higher ethanol concentration, yield, and productivity than SSF and SHF. It was concluded that the higher temperature of steam explosion enhanced the ethanol concentration, but the higher initial enzyme concentration did not increase ethanol concentration.

Chapter Nine

Recommendations

Ethanol Production from Agricultural Residues by Semi-simultaneous Saccharification and Co-fermentation of *E. coli* KO11

Lignocellulosic materials, such as agricultural residues, are most abundant resources for ethanol production. Agricultural residues usually contain cellulose and hemicellulose. The hemicellulose is decomposed to form pentoses such as xylose. It is well known that pentose cannot be converted into mono-sugars by natural yeast Saccharomyces cerevisiae. Therefore, some recombinant microorganisms, such as *E. coli* KO11, have been produced to convert both hexoses and pentoses to sugars, refereed to as co-fermentation [Ohta et al., 1991]. The corresponding experiments about co-fermentation in SHF and SSF have been conducted [Moniruzzaman and Ingram, 1998; Kim et al., 2008]. However, semi-simultaneous saccharification and co-fermentation (SSSCF): a extend SSSF consisting of pre-hydrolysis + SSCF, has been not applied to ethanol production from agriculture residues.

The objectives of this study are (1) to investigate the effect of pre-hydrolysis time on ethanol productivity and yield in SSSCF operation; (2) to develop SSSCF models for the batch, continuous, and fed-batch operations; (3) to estimate the model parameters from fitting the data in the SSSCF experiments; and (4) to predict the effects of continuous and fed-batch SSSCF operations based on the parameters obtained from the batch experiments.

References

Kim, T. H. Taylor, F. and Hicks, K. B. Bioethanol production from barley hull using SAA (soaking in aqueous ammonia) pretreatment. Bioresource Technology. 99(13): 5694-5702, 2008.

Moniruzzaman, M. and Ingram, L. O. Ethanol production from dilute acid hydrolysate of rice hulls using genetically engineered Escherichia coli. Biotechnology Letters. 20(10): 943-947, 1998.

Ohta, K. Beall, D. S. Mejia, J. P. Shanmugam, K. T. and Ingram, L. O. Metabolic engineering of klebsiella-oxytoca M5A1 for ethanol-production from xylose and glucose. Applied and Environmental Microbiology. 57(10) 2810-2815, 1991.

Appendix 1 MATLAB Programs

1. MATLAB optimal program for enzyme loading and hydrolytic time

```
function f = cgwrps75peth(x)
ke=1.6795;
k2=0.2568;
a=0.03445;
b=0.2644;
c=1-((ke+x(1))/(ke*(k2*x(1)*x(2)+1)+x(1)))^(x(1)*a+b)
f1 = 0.399*0.48*c*0.0003575*100+0.00122*x(1)+0.1507*0.48*0.0003575*100
f=-(100*0.0003575/0.496*0.55*0.6*c-f1)/x(2)
```

2. MATLAB fitting program of SSF

```
function ssf0h
%
clear all
clc
global Kinetics
tspan = [0 4 8 10 14 28 34 48 52 58 61 72];
x0 = [0; 0; 0.3; 0];
k0 = [0.6096 3.2015 0.1768 16.2464 0.0997 0.1768 0.6420 3.3990 3.0236];
lb = [0  0  0  0  0  0  0  0 0];
ub = [100  100  100  100  100 100 100 100 100];
Kinetics =...
       [4       0.5072       9.992          0.6  0.1016
        8       0.3248       8.687          0.7  2.804
        10      0.3104       7.808          0.9  3.794
        14      0.2605       3.373          1.5  7.17
        28      0.1606       0.02543        1.7  12.86
        34      0.1548       0.02226        1.8  13.65
        48      0.1127       0.01042        2.3  13.96
        52      0.1038       0.01373        2.5  14.04
        58      0.08219      0.01409        2.6  13.84
        61      0.1051       0.01207        2.6  13.15
        72      0.08661      0.009153       2.6  13.5
        ];
    yexp = Kinetics(:,2:5);
%
[k,resnorm,residual,exitflag,output,lambda,jacobian] = ...
   lsqnonlin(@ObjFunc,k0,lb,ub,[],tspan,x0,yexp);
ci = nlparci(k,residual,jacobian);
fprintf('  Using lsqnonlin() estimats the parameters:\n')
fprintf('\tk1 = %.4f CI %.4f\n',k(1),ci(1,2)-k(1))
fprintf('\tk2 = %.4f CI %.4f\n',k(2),ci(2,2)-k(2))
fprintf('\tk3 = %.4f CI %.4f\n',k(3),ci(3,2)-k(3))
fprintf('\tk4 = %.4f CI %.4f\n',k(4),ci(4,2)-k(4))
```

```
fprintf('\tk5 = %.4f CI %.4f\n',k(5),ci(5,2)-k(5))
fprintf('\tk6 = %.4f CI %.4f\n',k(6),ci(6,2)-k(6))
fprintf('\tk7 = %.4f CI %.4f\n',k(7),ci(7,2)-k(7))
fprintf('\tk8 = %.4f CI %.4f\n',k(8),ci(8,2)-k(8))
fprintf('\tk9 = %.4f CI %.4f\n',k(9),ci(9,2)-k(9))
fprintf('  The sum of the squares is: %.1e\n\n',resnorm)
[t4 Xsim4] = ode45(@KineticsEqs,[0 72],x0,[],k);
ce=40-0.9*Xsim4(:, 2)-0.947*Xsim4(:, 1)-0.9*Xsim4(:, 4)/0.511-1.137*Xsim4(:,3);
t3=[0 4 8 10 14 28 34 48 52 58 61 72];
xs1=[0 0.5072 0.3248 0.3104 0.2605 0.1606 0.1548 0.1127 0.1038 0.08219 0.1051
0.08661];
xs2=[0 9.992 8.687 7.808 3.373 0.02543 0.02226 0.01042 0.01373 0.01409 0.01207
0.009153];
xs3=[0.3 0.6 0.7 0.9 1.5 1.7 1.8 2.3 2.5 2.6 2.6 2.6];
xs4=[0 0.1016 2.804 3.794 7.170 12.86 13.65 13.96 14.04 13.84 13.15 13.50];
xs5=40-0.9*xs2-0.947*xs1-0.9*xs4/0.511-1.137*xs3;
figure (1), plot (t4, Xsim4(:, 1), 'k-', t3, xs1, 'bs');
figure (2), plot (t4, Xsim4(:, 2), 'k:', t3, xs2, 'b^');
figure (3), plot (t4, Xsim4(:, 3), 'k-.', t3, xs3, 'bd');
figure (4), plot (t4, Xsim4(:, 4), 'k--', t3, xs4, 'bo');
figure (5), plot (t4, ce, 'r-', t3, xs5, 'bx');
figure (6), plot (t4, Xsim4(:, 1), 'k-', t3, xs1, 'bs', t4, Xsim4(:, 2), 'k:', t3, xs2, 'b^', t4,
Xsim4(:, 3), 'k-.', t3, xs3, 'bd', t4, Xsim4(:, 4), 'k--', t3, xs4, 'bo');
figure (7), plot (t4, ce, 'r-', t3, xs5, 'bx');
disp(t4);
disp(Xsim4(:, 1));
disp(Xsim4(:, 2));
disp(Xsim4(:, 3));
disp(Xsim4(:, 4));
% ------------------------------------------------------------------
function f = ObjFunc(k,tspan,x0,yexp)          %
[t Xsim] = ode45(@KineticsEqs,tspan,x0,[],k);
ysim(:,1) = Xsim(2:end,1);
ysim(:,2) = Xsim(2:end,2);
ysim(:,3) = Xsim(2:end,3);
ysim(:,4) = Xsim(2:end,4);
f = [ysim(:,1)-yexp(:,1); ysim(:,2)-yexp(:,2);  ysim(:,3)-yexp(:,3); ysim(:,4)-yexp(:,4)];
% ------------------------------------------------------------------
function dCdt = KineticsEqs(t,C,k)             %
dCAdt = 1.056*k(1)*(40-0.9*C(2)-0.947*C(1)-0.9*C(4)/0.511-
1.137*C(3))*4/(1+4*k(5)*t)/(1+C(2)/k(3))-k(2)*C(1)/(1+C(2)/k(4));
dCBdt = 1.053*k(2)*C(1)/(1+C(2)/k(4))-k(6)*C(3)*C(2)/0.515/(k(8)+C(2))-k(7)*C(3);
dCCdt = k(6)*C(3)*C(2)/(k(8)+C(2));
dCEdt = C(3)*k(6)*k(9)*C(2)/(k(8)+C(2))/0.515;
dCdt = [dCAdt; dCBdt; dCCdt; dCEdt];
```

Appendix 2 Experimental Equipment

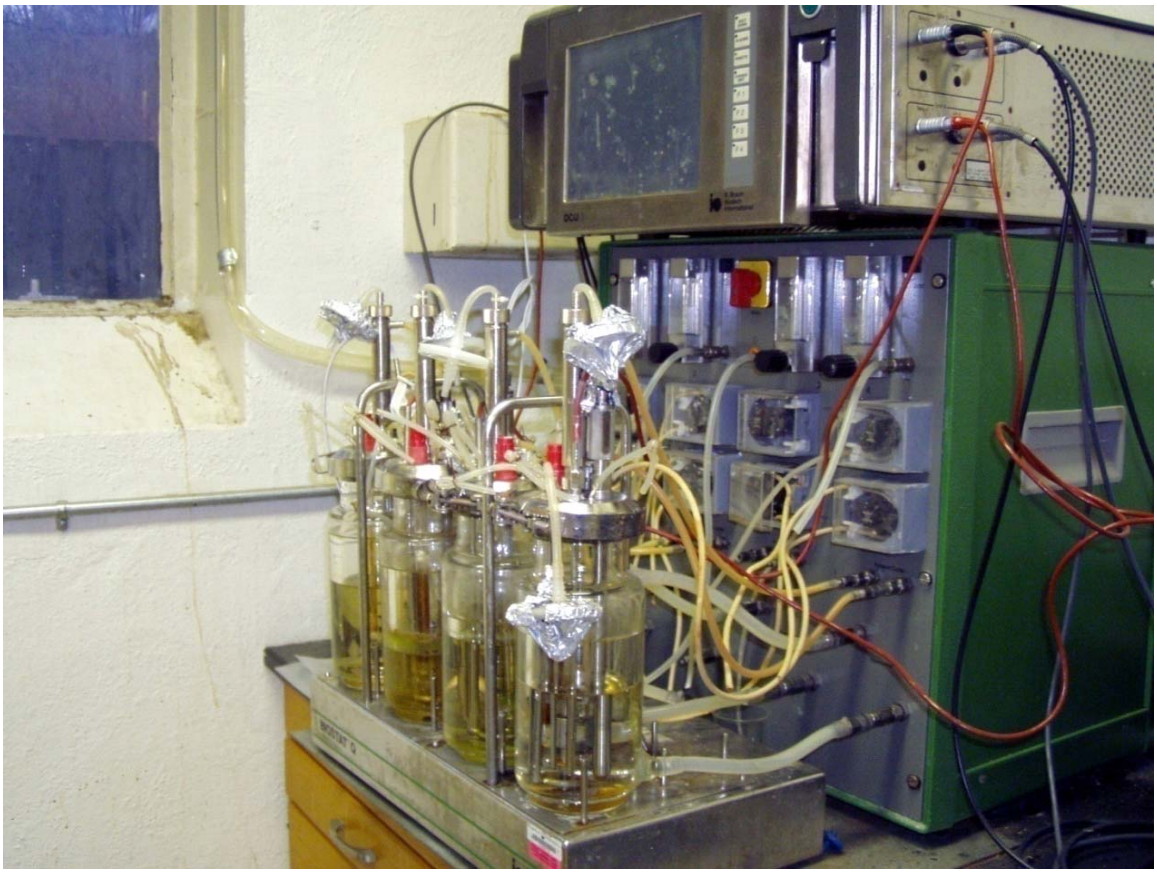

1 liter Fermenter

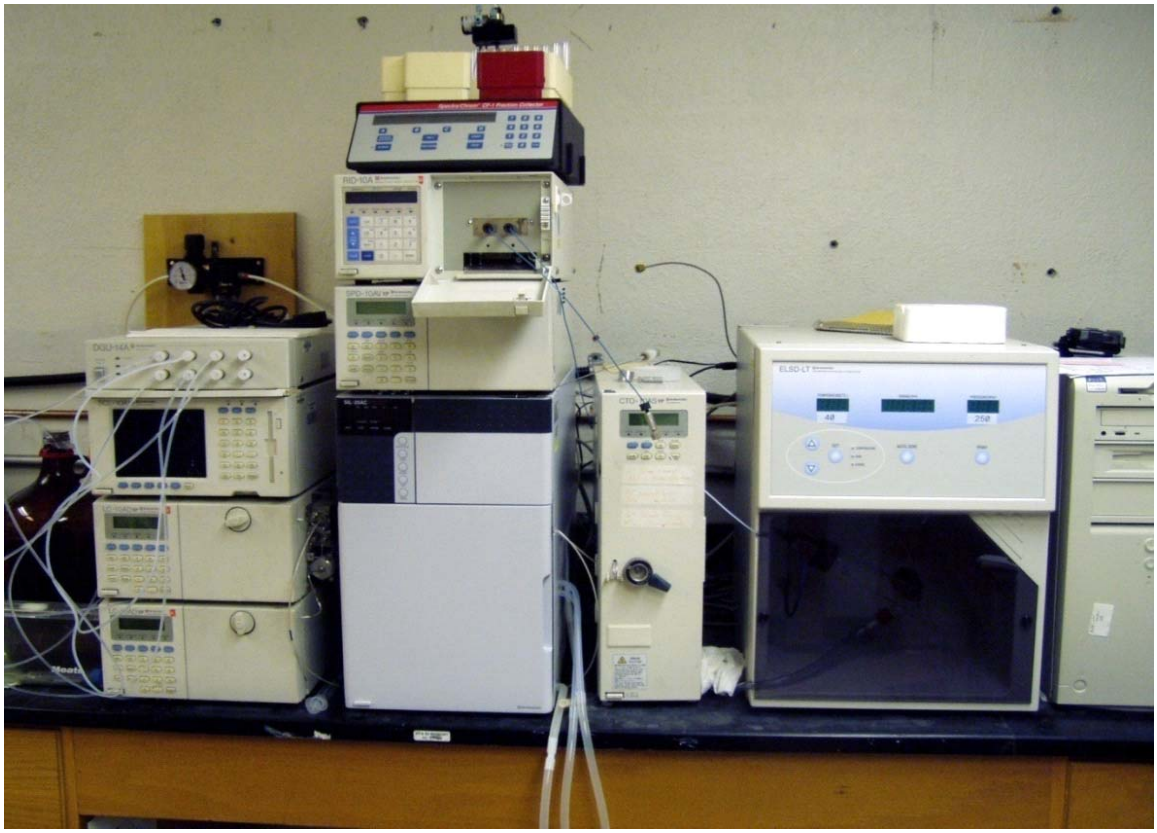

HPLC